THE UNIVERSITY OF HULL

Elucidation of the signalling mechanisms involved in TF-mediated apoptosis in endothelial cells

Thesis submitted to the University of Hull towards the degree of

Doctor of Philosophy

by

Ali Mahdi Ethaeb

September 2018

Abstract

Tissue factor (TF) is the main initiator of blood coagulation. In addition to its procoagulant property, TF has the ability to regulate various functions within cells including proliferation, angiogenesis and apoptosis. These outcomes appear to depend on the amount of TF with which the cell comes into contact with. In this study, human dermal blood endothelial cells (HDBEC) were transfected to express wild-type TF which is released following the activation of PAR2 in a normal physiological response. In addition, a model for the accumulation of TF in vascular disease and cancer was used by expressing a mutant form of TF (TF_{Ala253}-tGFP) which although expressed is not released by the cells and therefore it accumulates intracellularly. Initially, the phosphorylation of Src1 and Rac1 were monitored in order to determine any difference in phosphorylation patterns following PAR2 activation of cells. Phosphorylation of Src1, but not Rac1 was prolonged on expression of TF and was further enhanced on intracellular accumulation of TF. Therefore, the role of Src1 as a mediator of TF-induced apoptosis was examined next. Either inhibition of Src using $pp^{60c\text{-}src}$peptide, or suppression of Src1 expression using siRNA prevented the TF-induced p38 MAPK activation and subsequent cellular apoptosis. Following confirmation of the role of Src1 in this process, an attempt was then made to delineate upstream intermediaries involved in this pathway. By using an inhibitory antibody (AIIB2), β1-integrin was shown to participate in TF-induced Src1 activation. In contrast, prevention of Src1-FAK complex formation using FAK inhibitor-14 did not interfere with the TF-mediated Src1 activation, despite a clear reduction in Src1 phosphorylation. Furthermore, TF-induced apoptosis did not appear to require Src1-FAK binding. In conclusion, this study has established further steps in the pathway by which TF can induce cellular apoptosis, and suggests a mechanism by which the increased amount of TF during inflammation can have detrimental outcome on the vascular system.

Acknowledgment

I would like to thank my supervisor Dr Camille Ettelaie for her supervision, support and encouragement during the course of my PhD. I would also like to thank my second supervisor Prof. John Greenman for his help and advice. I will always be grateful to you for your support. My special thanks go to my parents for their continuous support, encouragement and inspiration throughout my PhD. I would also like to thank my sisters and their families. Your thoughts kept me strong and resolute in the achievement of my goals. I would like to thank my wife whose support and encouragement has taught me to be relentless throughout the years of studying for the PhD. It is my pleasure to express my thanks to the Iraqi Ministry of Higher Education and Scientific Research, the University of Wasit, and Iraqi Cultural Attachè in London for the scholarship and financial support of this research. I am very thankful to all my friends especially, Sophie, Yahya, Muhammed and Naima for their support and help. I also appreciate my children, Mishkat, Noran and Hasan who were always by my side and have grown up to be wonderful and understanding in this time. They never complained when I had to spend countless hours to focus on my work. You all make this achievement worth the while.

Ali

Publication and presentation

Parts of this work have been published as:

Ethaeb A, Greenman J, Ettelaie C. (2017) Characterisation of tissue factor-mediated molecular signalling mechanisms (poster). Presented at postgraduate student conference. University of Hull, UK.

Ethaeb A, Greenman J, Ettelaie C. (2017) Over-activation of Src1 mediates tissue factor-induced apoptosis in endothelial cells (poster). Presented at congress of the international society on thrombosis and haemostasis. Berlin, Germany.

Ethaeb A, Greenman J, Ettelaie C. (2017) Tissue factor induced endothelial cell apoptosis is mediated by Src1, FAK, and β1-integrin proteins (poster). Presented in BSHT Annual Scientific Meeting. University of Warwick, UK.

Ethaeb A, Greenman J, Ettelaie C. Over-activation of Src1 mediates tissue factor-induced apoptosis in endothelial cells (article in preparation)

To my parents

Thank you for supporting me all over my life

Table of content

Table of figures

Table of tables

List of Symbols and Abbreviations

α	Alpha
β	Beta
°C	Degrees centigrade
µ	Micro
%	Percentage
Ala	Alanine
A260	Absorption at 260 nm
A280	Absorption at 280 nm
ATP	Adenosine triphosphate
bp	Base pair
BSA	Bovine serum albumin
C	Cytosine
Ca^{+2}	Calcium
$CaCl_2$	Calcium chloride
Cdk	Cyclin dependent kinase
cDNA	Complementary deoxyribonucleic acid
CO_2	Carbon dioxide
dH_2O	Distilled water
DMEM	Dulbeco's modified essential medium
DMSO	Dimethyl sulphoxide
DNA	Deoxyribonucleic acid
E. coli	*Escherichia coli*
EDTA	Ethylenediaminetetraacetic acid
tGFP	Turbo green fluorescent protein
FCS	Foetal calf serum
FVII	Factor VII
FVIIa	Activated factor VII

FX	Factor X
FXa	Activated factor FX
g	Gram
g	Gravity
G	Guanine
GAPDH	Glyceraldehyde-3-phosphate dehydrogenase
Glycine	Gly
h	Hour
HCl	Hydrochloric acid
IL	Interleukin
JNK	c-Jun N-Terminal Kinase
Kb	Kilo base
L	Litre
M	Molar
m	Milli
mA	Milliamps
MAPK	Mitogen-activated protein kinase
MEK	Mitogen-activated protein kinase kinase
min	Minute
$MnCl_2$	Manganese chloride
mol	Mole
MPs	Microparticles
mRNA	Messenger ribonucleic acid
NaCl	Sodium chloride
NaOH	Sodium hydroxide
PAR	Protease activated receptor
PAR2-AP	Protease activated receptor2-activating peptide
PBS	Phosphate buffered saline

PCR	Polymerase chain reaction
RNA	Ribonucleic acid
RNase	Ribonuclease
rpm	Revolutions per minute
s	Second
SD	Standard deviation
SDS-PAGE	Sodium dodecyl sulphate polyacrylamide gel electrophoresis
SEM	Standard error of mean
SFKs	Src family kinases
siRNA	Short interfering RNA
T	Thymine
TBE	Tris borate-EDTA
TBST	Tris buffered saline tween 20
TEMED	N,N,N’,N’-Tetramethylethylenediamine
TF	Tissue factor
Tyr	Tyrosine
UV	Ultra violet
v/v	Volume to volume
w/v	Weight to volume

Chapter 1

General introduction

1.1 Introduction

There have been a number of studies which have established the relationship between thrombosis and cardiovascular disease which can cause morbidity and mortality in many chronic diseases. The release of procoagulant microvesicles from the diseased vascular tissues is a major factor that can give rise to thrombus formation in the blood vessels. Additionally, it is now well established that inflammation, diabetes, malignancy and even hypertension can induce the release of microvesicles. Importantly, it has been shown that microvesicles impair the vascular system exacerbating cardiovascular diseases particularly those involving endothelial cells damage (Chen et al, 2018; Preston et al, 2002; Sabatier et al, 2002; Tesselaar et al, 2007). The procoagulant activity of these microvesicles is derived from tissue factor (TF) which is present in the membrane of microvesicles (Davila et al, 2008). TF is known as the principal initiator of the coagulation mechanism (Tesselaar et al, 2007). Elevated level of TF positive microvesicles may be detected within the blood circulation during various pathophysiological conditions such as cancer, atherosclerosis and following injury or trauma (Bach & Moldow, 1997; Giesen et al, 1999; Hron et al, 2007; Simak et al, 2006; Thaler et al, 2012). In addition to coagulation, TF also has the ability to regulate various functions of endothelial cells including proliferation, angiogenesis, and apoptosis (Collier & Ettelaie, 2010; Ettelaie et al, 2011; Shai & Varon, 2011). This study has focused on the mechanism by which TF induces apoptosis and subsequent erosion of endothelial cells, which occurs during inflammatory conditions such as cancer and vascular disease.

1.1.1 Tissue factor

Tissue factor is also known as tissue thromboplastin, coagulation factor III, or CD142. A growing body of literature from various laboratories has demonstrated the importance of TF as the main initiator of blood coagulation (Bachli, 2000). A number of cell types, including skin epithelial cells, astrocytes and fibroblasts have been shown to express TF (Drake et al, 1989). TF is expressed in brain, lung, and kidney to control the bleeding (Erlich et al, 1999). In addition, cells of tunica adventitia and tunica intima within the blood vessel walls, and the cells of organ capsules express TF. This in turn creates haemostatic envelope which prevent the blood loss following the vasculature rupture (Fleck et al, 1990). Endothelial cells and circulating cells which are in direct contact with the blood do not express TF (Drake et al, 1989). Although, these cells have the ability to express TF following activation by cytokines during inflammation (Eisenreich & Rauch, 2010; Ruf & Edgington, 1994). In addition, macrophages express and release TF in response to lipopolysaccharide (LPS) (Imamura et al, 2002).

Under normal physiological conditions, TF-bearing microvesicles are not detected within blood circulation (Nemerson, 1988; Steffel et al, 2006). Following trauma or injury, endothelial cells can produce and release TF-bearing microvesicles into the bloodstream (Aird, 2007; Yau et al, 2015). However, TF may be detected within the circulation during various pathophysiological conditions such as cancer and cardiovascular complications and following injury and trauma (Bach & Moldow, 1997; Giesen et al, 1999; Simak et al, 2006; Thaler et al, 2012). Moreover, microvesicles with a high level of procoagulant activity have been reported to be released from cancer cell, particularly pancreatic and breast cancers (Gerotziafas et al, 2012; Zhang et al, 2017b).

In addition to its role in coagulation, the expression of TF in the visceral endoderm within the yolk sac has been shown. It has also been demonstrated that TF plays a vital role in the development of embryonic blood vessels (Carmeliet et al, 1996). Therefore, studies have indicated a pivotal role for TF in physiological non-haemostatic cell functions.

1.1.2 Tissue factor structure

The TF gene is located on chromosome 1 and is comprised of six exons separated by five introns (Mackman et al, 1989). TF genes have been reported to be present in 47 vertebrate genomes ranging from fishes to humans (Rallapalli et al, 2014). TF is a membrane glycoprotein of 47 kDa which is made up of a single chain consisting of 263 amino acids. The crystal structure of TF is analogous to the proteins of cytokine receptors family (class II), mainly the interferon γ receptor (Bazan, 1990). The structure of TF can be divided into three domains (Figure 1.1). A large extracellular N-terminal domain (residues 1-219), which is responsible for binding to factor VIIa. A hydrophobic transmembrane domain that crosses the membrane (residues 220-242) and connects the extracellular and cytoplasmic domains. A short cytoplasmic C-terminal (residues 243-263), which includes three serine residues and can be phosphorylated at serine 253 and 258 (Chu, 2011; Zioncheck et al, 1992). This domain has been suggested to be involved in signal transduction (Ruf et al, 1991; Spicer et al, 1987).

Figure 1.1 Schematic representation of the structural domains of TF

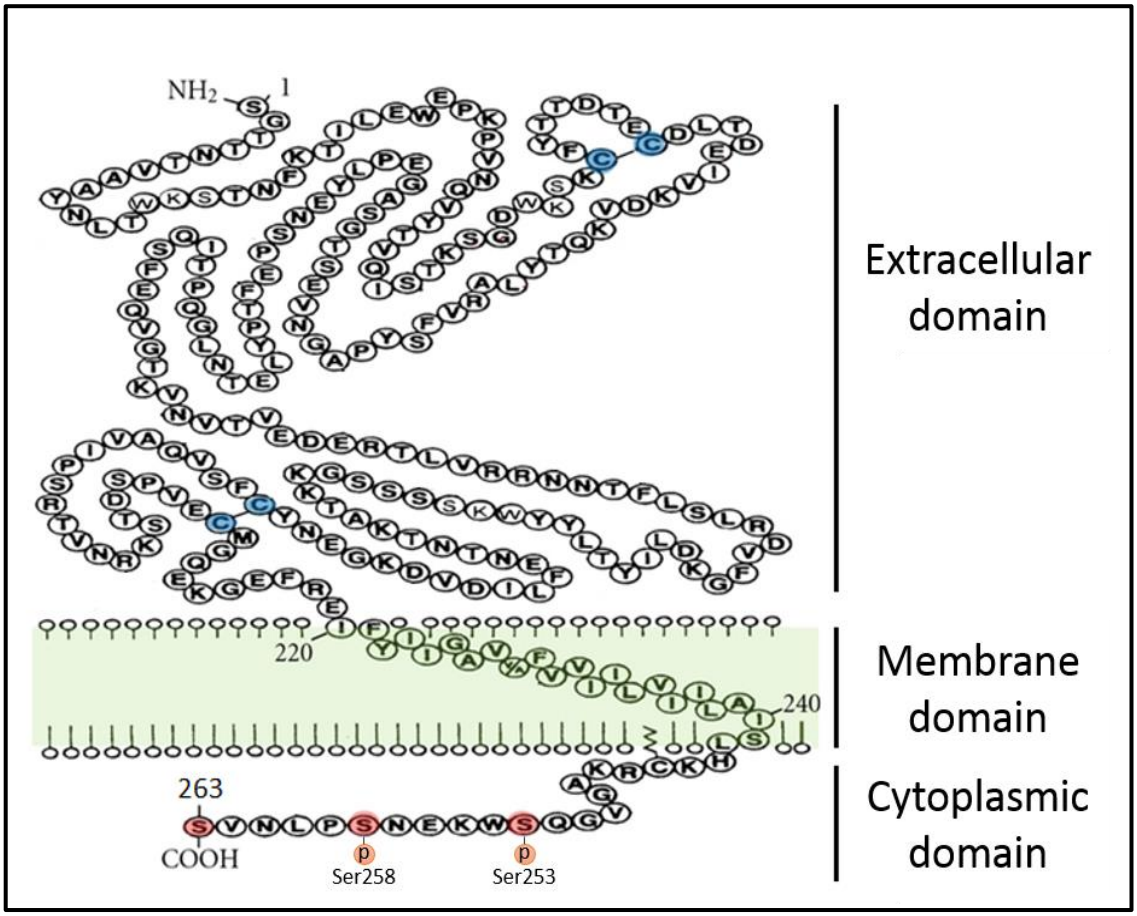

Human TF is a membrane glycoprotein made up of a single chain consisting of 263 amino acid. The structure is split into an extracellular domain (residues 1-219), a membrane-spanning domain (residues 220-242) and cytoplasmic tail (residues 243-263). The cytoplasmic domain contains three serine residues (red colour) but only serine 253 and 258 have been shown to undergo phosphorylation (adapted from Chu, 2011).

1.1.3 Tissue factor and coagulation

The coagulation cascade is formed of two pathways termed the intrinsic and the extrinsic pathways. These mechanisms act to activate a third pathway called the common pathway. As stated above, TF is the main initiator of the coagulation cascade (Figure 1.2). Various factors including collagen can activate the intrinsic pathway by the activation of factor XII (FXII) to activated FXIIa, which in turn activate factor XI (FXI) to activated FXIa. Activated FXIa then activate factor IX (FIX) to activated FIXa, which in turn activate factor X (FX) to activated FXa in the presence of activated FVIIIa (Mackman, 2009).

The exposure of TF to blood as a result of damage to blood vessels leads to the activation of the extrinsic pathway of coagulation (Egorina et al, 2008). The exposure of TF to the blood leads to the binding of extracellular domain of TF to circulating factor VII (FVII). This binding causes the activation of FVII to activated FVIIa and the formation of TF/FVIIa complex. The TF/FVIIa complex activates plasma zymogens factor IX (FIX) to activated FIXa and FX to activated FXa (Morrison & Jesty, 1984). FXa goes onto catalyse the conversion of prothrombin (FII) to thrombin (FIIa) (Esmon et al, 1974). As a consequence, thrombin causes the feedback process to activate factor VIII (FVIII) to activated FVIIIa and factor V (FV) to activated FVa to amplify the coagulation process. In addition, thrombin converts fibrinogen into fibrin monomers. The fibrin monomers aggregate and cross linked by another coagulation factor called FXIIIa, which itself is activated by thrombin. Additionally, thrombin a major platelet activator. Eventually, the aggregation of platelets together with insoluble fibrin clot make up the constituents of the haemostatic plug which prevents excessive blood loss and maintains vascular integrity.

Figure 1.2 The coagulation cascade and the role of TF in coagulation

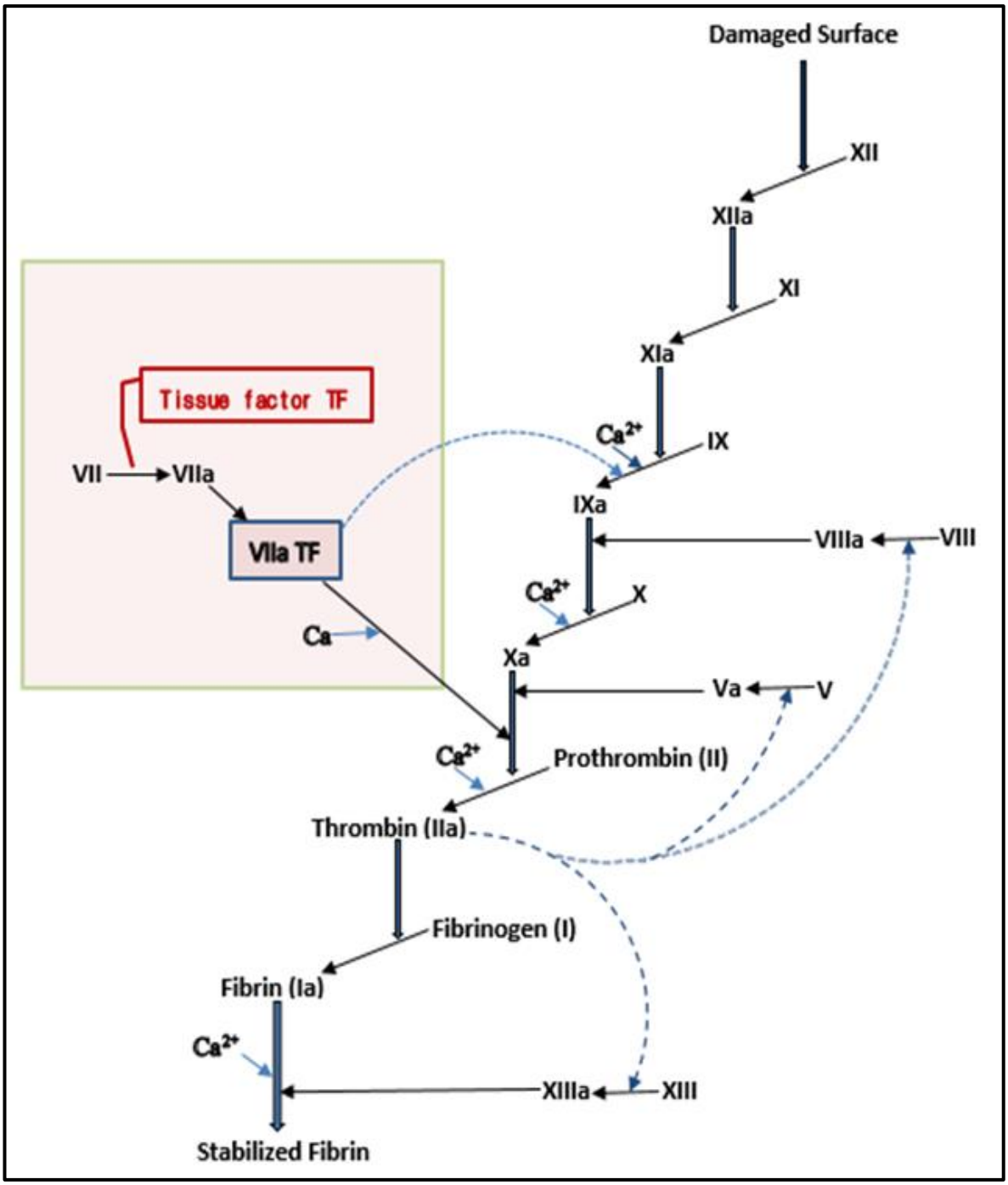

The coagulation cascade is formed of two pathways (intrinsic and extrinsic). TF binds FVIIa and activates extrinsic pathway. Intrinsic pathway can be activated by collagen. These mechanisms act to activate a third pathway (common pathway).

1.1.4 Tissue factor and cell signalling

In addition to its function in coagulation, TF has the ability to regulate cellular processes such as migration, proliferation (Hu et al, 2013) and apoptosis through intracellular signalling mechanisms (Pradier & Ettelaie, 2008; Pyo et al, 2004). Recently, it has been reported that the accumulation of TF within endothelial cells, either through increased expression, or by acquisition of TF from the bloodstream can promote cellular apoptosis through mechanisms mediated by p38 MAPK (ElKeeb et al, 2015). Previously, it was suggested that the cytoplasmic domain of TF is involved in signalling (Ruf & Mueller, 1999). Alternatively, TF/VIIa complex can activate PAR1 and PAR2 (Hjortoe et al, 2004; Hu et al, 2013). In fact, the interaction of TF with β1-integrin requires the formation of a complex with factor VIIa which can then activate PAR2, leading to subsequent pro-angiogenic and pro-migratory signals (Rothmeier et al, 2018). However, the interaction of TF with β1 and β3 integrins has recently been suggested to stimulate pro-angiogenic factors and to activate various signalling molecules including FAK and p38 MAPK (van den Berg et al, 2009). Therefore, the role of β-integrin in the mechanisms by which TF induce cellular apoptosis cannot be ruled out.

1.1.5 Microvesicles

Microvesicles (MVs) are referred to small vesicles with a diameter range between 0.1 μm and 1.0 μm depending on the cell origin. The microvesicles have a spherical shape and they can be isolated from blood plasma by ultracentrifugation at 10,000-20,000 *g* (Thery et al, 2009). Microvesicles are formed from the plasma membrane by direct budding into the extracellular space (Hugel et al, 2005). It has been reported that microvesicles can be released from the plasma

membrane of most of cell types during apoptosis and also following the activation of cells (Distler et al, 2005; Scholz et al, 2002). Low levels of circulating microvesicles have been detected in the blood under normal physiological conditions (Berckmans et al, 2001). In contrast, various diseases including inflammation and cardiovascular disease induce the production of high concentrations of microvesicles (Gyorgy et al, 2011; Habersberger et al, 2012; Loyer et al, 2014; Pan et al, 2016). Microvesicles can be produced by endothelial cells, platelets (Diehl et al, 2011; Stepien et al, 2012), cancer cells (Gerotziafas et al, 2012; Zhang et al, 2017b).

Microvesicle membranes are composed of a lipid bilayer which contain cytoplasmic and transmembrane proteins derived from their donor cell and can act as mediator of cell-to-cell communication (Figure 1.3) (Camussi et al, 2010; Thery et al, 2009). Therefore, microvesicles play an important role in cell processes through transfer these proteins, which can regulate cell signalling and induce endothelial cell dysfunction, inflammation and thrombosis (Habersberger et al, 2012; Jansen et al, 2013; Mause & Weber, 2010; Wang et al, 2013). Endothelial cells produce microvesicles as response to various stimuli including the activation of protease activated receptor 2 (PAR2) (Banfi et al, 2009; Coughlin & Camerer, 2003; Riewald & Ruf, 2003) and cytokines such as tumour necrosis factor-α (TNFα) (Combes et al, 1999; Peterson et al, 2008).

A number of studies have reported that tumour cell-derived microvesicles are highly procoagulant (Dvorak et al, 1981; Nomura et al, 2015). The main culprit of this activity is the exposure of TF, which together with phosphatidylserine can initiate the coagulation mechanism (Bastida et al, 1984; Hellum et al, 2012). Studies have also reported that cancer patients have increased risk of developing venous thromboembolism (VTE) due to the presence of high levels of TF-

containing tumour-derived microvesicles within blood circulation (Zwicker et al, 2009). Therefore, it was hypothesized that the TF-bearing microvesicles can cause further physiological process such as apoptosis.

Figure 1.3 The structure of a microvesicle

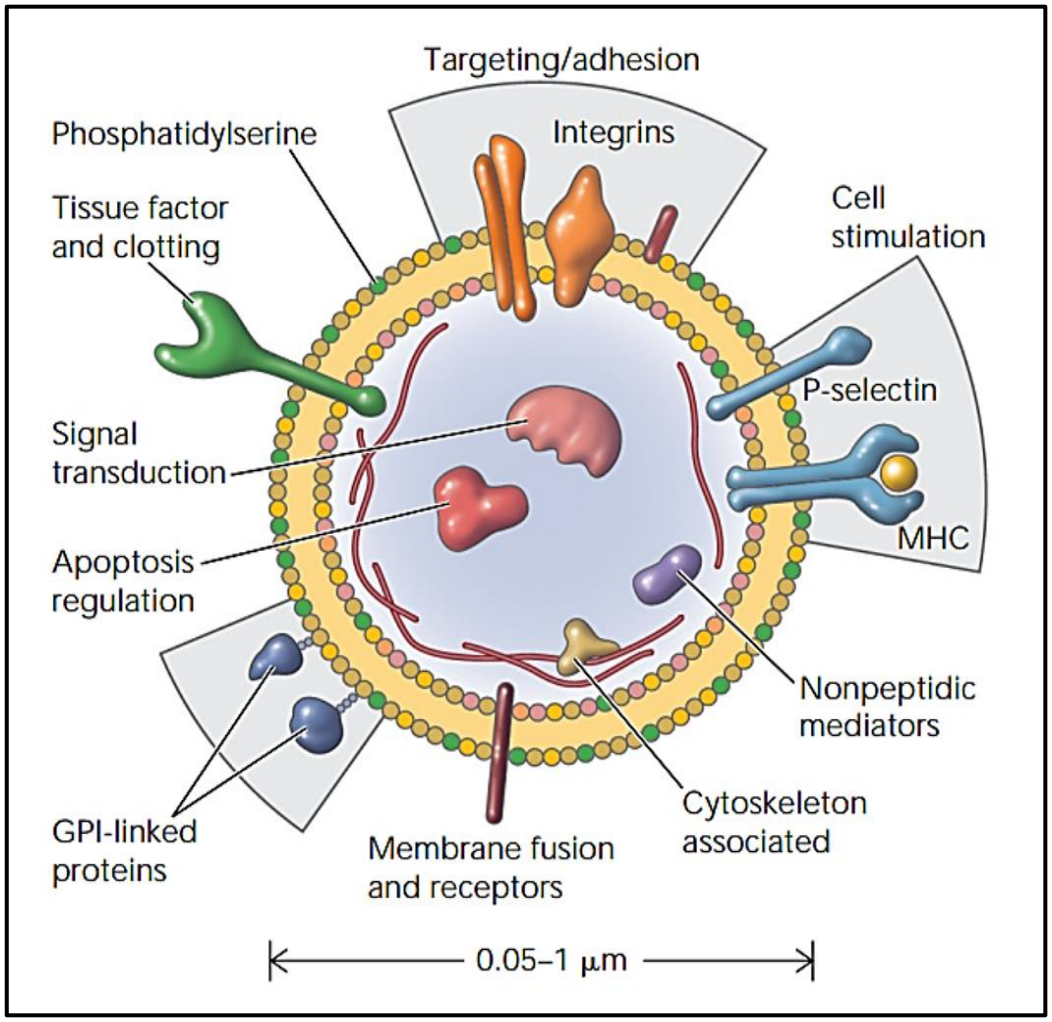

Microvesicles are formed from the plasma membrane by direct budding into the extracellular space. Microvesicles are composed of a lipid bilayer which contains cytoplasmic and transmembrane proteins derived from their original donor cell (Hugel et al, 2005).

1.1.6 Protease-activated receptor

Protease activated receptors (PARs) are a family of four G-protein coupled receptors (PAR1-PAR4). Vascular endothelial cells have been shown to express PAR1, PAR2 and PAR4 (Coughlin, 2000; Rezaie, 2014). PARs are activated by the cleavage of the receptors N-terminal through the action of proteases such as FXa, thrombin and trypsin (Figure 1.4) (Mackman, 2004; Major et al, 2003). This cleavage leads to the formation of a tethered ligand that binds to the main body of the receptor (Macfarlane et al, 2001) altering its shape which in turn induces the internal signal (Soh et al, 2010). FXa activates PAR1 and PAR2, while the TF/FVIIa complex activates PAR2 (Camerer et al, 2000; Riewald et al, 2001; Riewald & Ruf, 2001).

Studies have reported that PARs are involved in cell signalling that regulate cell physiology (El-Daly et al, 2014; Suen et al, 2014) and pathological conditions such as cancer cells migration and proliferation (Adams et al, 2011; Rothmeier & Ruf, 2012; Yang et al, 2015; Zhou et al, 2011). In addition, PAR2 has been detected in 72% of breast cancer cells as compared to 21% of normal breast cells (Su et al, 2009). Cancer cells also secret trypsin-like proteases that can activate PAR2 (Nystedt et al, 1995). Studies have shown that the signalling arising from PAR2 activation in cancer cells can promote the phosphorylation of the cytoplasmic domain of TF at Ser_{253}, which suggest that PAR2-dependent TF phosphorylation may regulate non-haemostatic functions including angiogenesis and migration (Ahamed & Ruf, 2004; Schaffner et al, 2010). In addition, TF phosphorylation at Ser_{253} through the activation of PAR2 results in the release of TF-bearing microvesicles which can cause blood coagulation (Collier & Ettelaie,

2011). Moreover, the treatment of endothelial cells with TF-bearing microvesicles prior to activation of PAR2 can result in either cellular apoptosis (ElKeeb et al, 2015) or proliferation (Pradier & Ettelaie, 2008) depending on the concentration of TF-bearing microvesicles. However, the signalling mechanisms by which the presence of TF in PAR2-activated cells need further investigation.

1.1.7 Endothelial cells

Endothelium is a single layer of cells that lines the interior surface of the vascular system and acts as a barrier between the bloodstream and the surrounding tissue (Galley & Webster, 2004). The main functions of endothelial cells are to maintain vascular tone and the anticoagulant properties of the vessels, but are also involved in processes including haemostasis, angiogenesis and inflammatory responses. Endothelial cells respond to hypoxia and high blood pressure by producing vasodilators including nitric oxide, which enhance the blood flow (Michiels, 2003). In addition, endothelial cells respond to tissue hypoxia and vascular endothelial growth factor (VEGF) produced by platelets, macrophages and tumour cells, which result in angiogenesis and vascular proliferation. Endothelial cells are also involved in restricting blood flow by producing vasoconstrictors such as endothelin (Michiels, 2003) or to limit the blood loss during injury.

Under normal physiological conditions, the endothelial cells prevent coagulation by expressing anticoagulant agents such as heparans and tissue factor pathway inhibitor (TFPI) (Aird, 2007; Michiels, 2003). However, many agents such as inflammatory cytokines (TNFα) have the ability to activate the endothelial cells (Combes et al, 1999; Pober, 2002). Activated endothelial cells are involved in

adhesion and inflammation (Cook-Mills & Deem, 2005). Once activated, endothelial cells express pro-inflammatory receptors such as intercellular adhesion molecule-1 (ICAM-1) and vascular cell adhesion molecule-1 (VCAM-1), to recruit leukocytes to the site of inflammation (Mesri & Altieri, 1999; Pober & Cotran, 1990). Endothelial cells also release TF-bearing microvesicles into the bloodstream following activation by cytokines (Eisenreich & Rauch, 2010; Ruf & Edgington, 1994). Since TF can promote endothelial cell apoptosis (ElKeeb et al, 2015), the investigation of the signalling pathway connecting TF to apoptosis may explain the denudation of endothelial cells that occurs during diseases.

Figure 1.4 The hierarchy of PAR activation by coagulation proteases

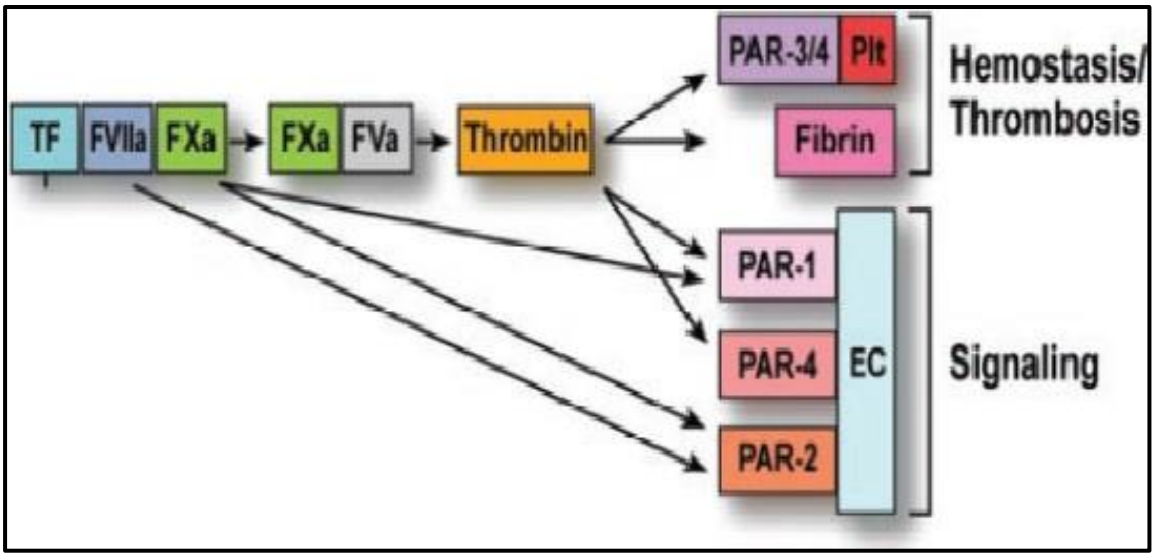

The activation of coagulation proteases together with TF results in the activation of signalling and coagulation. Various coagulation proteases have the ability to activate different PARs on endothelial cells (Mackman, 2004).

1.1.8 p38 MAPK signalling

p38 mitogen-activated protein kinases (MAPKs) is the stress-activated MAPK pathway and a member of a serine /threonine kinase family (Garcia-Gomez et al, 2012). p38 MAPK family consists of four isoform proteins p38α, p38β, p38γ, and p38δ, all of which have an apparent molecular weight of 38 kDa (Han et al, 1994). The four proteins share 60 % homology in their amino acid sequences. It has been reported that most cell types express p38α and p38β (Cuenda & Rousseau, 2007; Yasuda et al, 2011). However, p38γ is mainly detected in skeletal muscle while p38δ is expressed within the endocrine glands (Goedert et al, 1997). p38 MAPK is activated by the phosphorylation of Thr180 and Tyr182 residues. This activation occurs in response to different stress signals including cytokines such as IL-1β, DNA damage and lipopolysaccharide (LPS) stimulation (Raingeaud et al, 1995; Xiao et al, 2018). Upstream activators of p38 MAPK include the activated forms of Src1 (Watanabe et al, 2006; Watanabe et al, 2009), Rac1 (Coso et al, 1995; Puls et al, 1999) and TAK1 (Huth et al, 2017; Moriguchi et al, 1996; Wang et al, 1997). In addition, the activation of PAR2 can result in the phosphorylation of p38 MAPK (Enjoji et al, 2014).

It has been suggested that the level and/or duration of activation of p38 MAPK may determine the cellular response to this signal (Faust et al, 2012). Among these responses, the activation of p38 MAPK has been shown to promote cellular apoptosis (Cheng et al, 2017; ElKeeb et al, 2015). As mentioned in part 1.1.4, p38 MAPK has been shown to mediate apoptotic signalling mechanisms initiated by TF. Therefore, it is hypothesised that one or more of Src1, Rac1 and TAK1 proteins may act as mediator, connecting TF to p38 MAPK activation.

1.1.9 Src1

Src1 protein is a member of the Src family of kinases (SFKs) and has a molecular weight of 60 kDa. Src1 is a non-receptor tyrosine kinase which is encoded for by the proto-oncogene src (Byeon et al, 2012). Src1 is made of seven functional regions (Figure 1.5). The N-terminal domain is necessary for its localisation to the internal cytoplasmic surface of the membrane. Domain 2 (SH2) and domain 3 (SH3) allow Src1 to interact to phosphorylated tyrosine residues of different proteins. The linker domain that binds to SH3 domain when the protein is inactive. The kinase domain comprised of two lobes divided by catalytic cleft, which contain the activation loop. The activation loop harbour the auto-phosphorylation site (Tyr416) of Src1 (Guarino, 2010). C-terminal tail contains the negative regulatory site (Tyr527) (Boggon & Eck, 2004; Guarino, 2010; Roskoski, 2004). Src1 activity is controlled by the phosphorylation and de-phosphorylation of tyrosine residues within Src by protein kinases and phosphatase which result in structural changes in the Src1 protein (Hunter & Sefton, 1980; Xu et al, 1999) (Figure 1.6). Several studies have reported that in the inactive form of Src1, Tyr527 is phosphorylated and binds to the SH2 domain, while Tyr416 remains unphosphorylated. This produces a closed protein configuration with no kinase activity (Brown & Cooper, 1996; Johnson et al, 1996; Xu et al, 1999).

Following activation, Src1 regulates a number of cellular processes such as differentiation, proliferation and angiogenesis (Biscardi et al, 2000; Li et al, 2018b). For example, Src1 activation leads to downstream activation of p38 MAPK pathway and induce proliferation of synovial sarcoma cells (Watanabe et al, 2006; Watanabe et al, 2009). Additionally, Src1 has been shown to play a crucial role in cancer growth, progression, and metastasis (Gu & Gu, 2003; Parsons & Parsons, 2004).

Src1 has been shown to be a component of the focal adhesion complex (Wu et al, 2015). Studies have reported that β1-integrin has the ability to induce FAK auto-phosphorylation at Tyr397, which in turn binds to the SH2 domain of Src1 protein (Calalb et al, 1995; Schaller et al, 1994). As a result of Src1-FAK binding, the intramolecular interaction between the SH2 domain and the phospho Tyr527 in the C-terminal of Src1 is disrupted (Thomas & Brugge, 1997). This removal of the negative regulatory C-terminal creates an active conformation resulting in increased catalytic activity of Src1 (Schlaepfer et al, 1994). Subsequently, the activation loop is exposed which allows the phosphorylation of Src1 at Tyr416 (Guarino, 2010; Kleinschmidt & Schlaepfer, 2017). Therefore, the interaction of Src1 and FAK can induce Src1-mediated signalling (Schlaepfer et al, 2004).

It has been shown that Src1 can be activated by TF/FVIIa complex (Siegbahn et al, 2008). Therefore, a possible role for Src1 has been suggested in cellular apoptosis triggered by TF.

Figure 1.5 Structural domains of Src1 protein

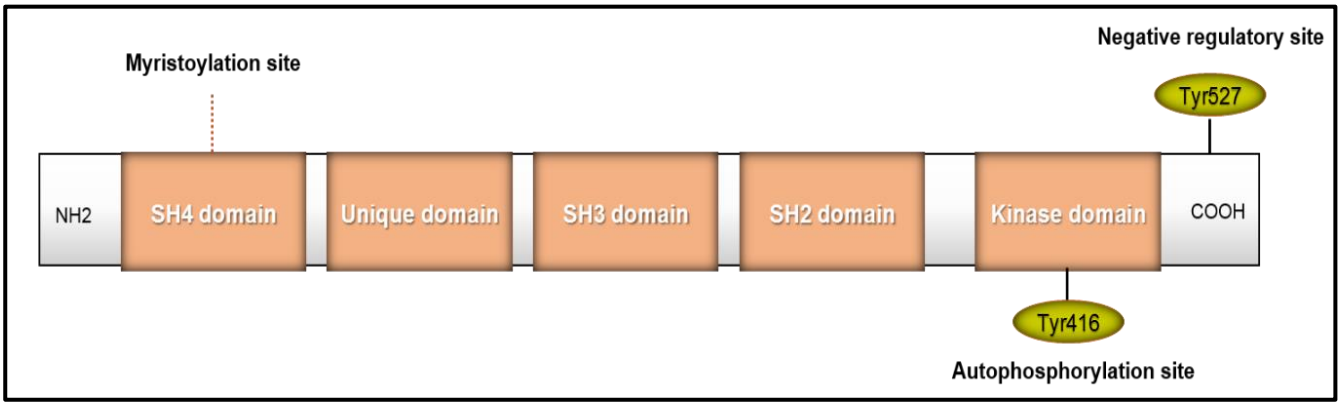

Src1 protein consists of seven functional domains: SH4 domain (Myristoylation site) is necessary for its localisation to the cytoplasmic membrane. The unique domain. SH3 and SH2 domains allow Src1 to interact with different proteins. The kinase domain contain the auto-phosphorylation site (Tyr416). C-terminal tail which contains negative regulatory site (Tyr527).

Figure 1.6 The structure and activation of Src1 protein

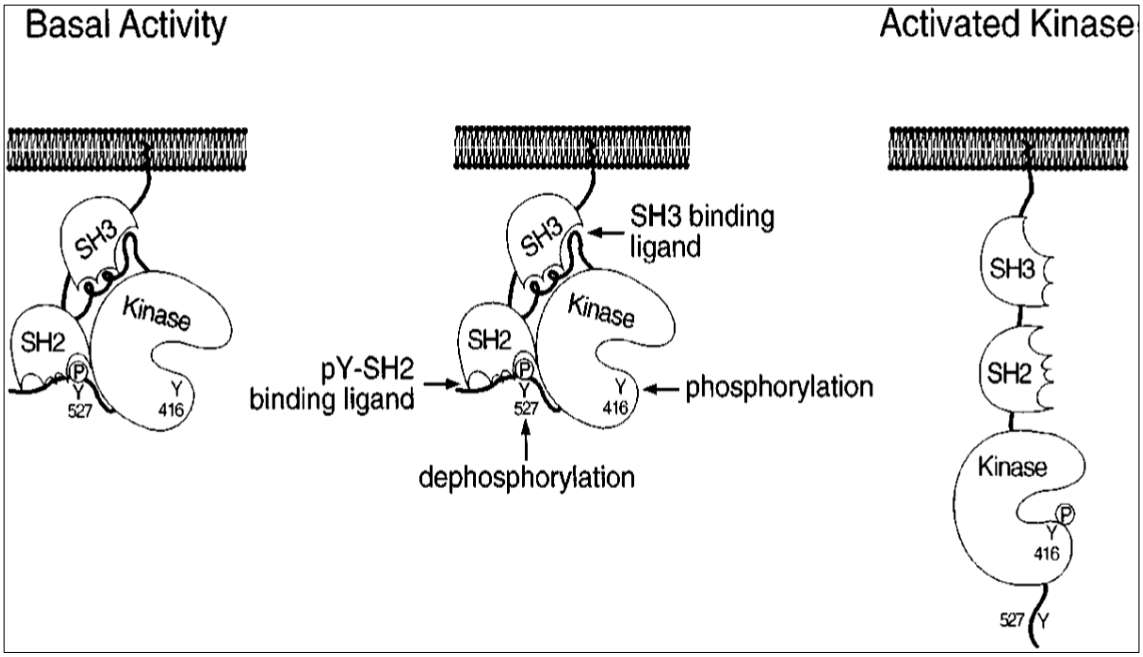

In the inactive form (left), Src1 is phosphorylated on tyrosine 527 (Tyr527) within the C-terminal which is connected to the SH2 domain, causing the closed configuration. The mechanism of Src1 activation involves the dephosphorylation of Tyr527 on C-terminal and the phosphorylation of Tyr416 within the kinase domain. Dephosphorylation of Tyr527 prevents its interaction with the SH2 domain, which creates an active conformation resulting in increased catalytic activity of Src1. Subsequently, the activation loop is exposed which allows the phosphorylation of Src1 at Tyr416 (Thomas & Brugge, 1997).

1.1.10 Rac1

Rac1 (ras-related C3 botulinum toxin substrate) is a member of small guanosine triphosphatase (GTPase) family which is related to ras-related proteins superfamily (Hall, 1994). Rac1 is a plasma membrane-associated GTP-binding protein that contains 192 amino acids. It has a molecular weight of 21 kDa and it is made up of four domains (Didsbury et al, 1989).

Rac1 is found in every eukaryotic cell (Aspenstrom et al, 2004; Boureux et al, 2007) and has been reported to play a crucial role in regulating cellular processes including migration, proliferation, phagocytosis, adhesion and apoptosis (Boissier & Huynh-Do, 2014; Kurdi et al, 2016; Leone et al, 2010; Wu et al, 2018). Rac1 influences gene transcription through a number of signalling pathways including the c-Jun N-terminal Kinase (JNK) and p38 MAPK pathway (Coso et al, 1995; Minden et al, 1995; Puls et al, 1999). Rac1 is activated by the phosphorylation of Ser71 (Kwon et al, 2000). In addition, previous studies have shown the ability of Src1 to activate Rac1 (Chiariello et al, 2001; Servitja et al, 2003). In relevance to the current study, it has been reported that the interaction of TF/FVIIa leads to the activation of Rac1 (Versteeg et al, 2000). Therefore, it is possible that Rac1 may be capable of relaying the signal initiated by TF, to the activation of p38 MAPK.

1.1.11 TAK1

TAK1 (TGF-beta-activated kinase 1) protein is also known as mitogen-activated protein kinase kinase kinase 7, MAP3K7 and MEKK7. TAK1 has been shown to be involved in inflammatory signalling pathways and many pro-inflammatory

cytokines and endotoxins such as interleukin-1 (IL-1) activate TAK1 (Irie et al, 2000; Ninomiya-Tsuji et al, 1999; Sakurai et al, 1999).

Three TAK1-binding proteins TAB1, TAB2, and TAB3 are required for TAK1 activation. The formation of the TAK1-TAB1-TAB2 complex or TAK1-TAB1-TAB3 complex results in the auto-phosphorylation of TAK1 (Cheung et al, 2004; Ishitani et al, 2003; Munoz-Sanjuan et al, 2002; Takaesu et al, 2000). The activation of TAK1 occurs through the interaction of TAB with the kinase domain of TAK1 (Shibuya et al, 1996). This interaction results in the auto-phosphorylation of TAK1, at Thr184 and Thr187 and a Ser192 in the kinase activation loop (Kishimoto et al, 2000; Ono et al, 2001; Sakurai et al, 2000). It has been suggested that the activation of TAK1 may also occur by integrin signalling and is mediated through the FAK/Src complex (Kim & Choi, 2012).

TAK1 has been shown to be associated with cellular processes including proliferation and apoptosis (Kim et al, 2009; Martin et al, 2011). In addition, it has been shown that TAK1 plays a crucial role in inflammation such as cancer (Melisi et al, 2011; Singh et al, 2012). TAK1 is reported to be activated by various stresses factors including osmotic shock and DNA damage (Dai et al, 2012; Hinz et al, 2010).

It has been known that TAK1 plays a crucial role in the activation of both c-Jun N-terminal Kinase (JNK) and p38 MAPK. These mechanisms are mediated through various MAPK kinases including MKK4 and MKK3/6 (Moriguchi et al, 1996; Ninomiya-Tsuji et al, 1999; Wang et al, 1997). In addition, TAK1 activation leads to downstream activation of p38 MAPK and can also lead to cellular apoptosis (Smith et al, 2012). Therefore, TAK1 is also a candidate as a mediator

of the signalling pathway connecting TF to p38 MAPK and subsequent cellular apoptosis in endothelial cells.

1.2 Hypothesis and Aims

The accumulation of TF within the endothelial cells has been reported to contribute to chronic pathological disorders such as cardiovascular disease. In addition, TF can induce cellular apoptosis through a mechanism that involves the activation of p38 MAPK. This study hypothesised that the accumulation of TF within the endothelial cells can cause the activation of p38 and subsequent cellular apoptosis, mediated by Src1, Rac1, TAK1, β1-integrin and FAK. To test this hypothesis, a model was used to identify and further elucidate the TF-induced apoptotic pathway. The aim of this study was to examine the signalling molecules that mediate TF-signalling resulting in the activation of p38 MAPK. The main objectives of the study were as follows.

- To investigate the phosphorylation patterns of Src1, Rac1 and TAK1 proteins following the activation of PAR2, in the presence and absence of TF.
- To confirm the role of Src1 protein as a mediator of TF-induced cellular apoptosis.
- To examine the role of β1-integrin and FAK protein in the activation of Src1 initiated by TF-signalling.

Chapter 2

Materials and methods

2.1 Materials

Ambion® by life technologies™

- Silencer® Select Pre-designed siRNA (SRC)
- Silencer® Select Pre-designed siRNA (NCOA1)
- Silencer® Select Negative Control #1 siRNA

Applied Biosystem, Warrington, UK

- Power SYBR Green RT-PCR mix

BD Bioscience, Oxford, UK

- Becton Ddickinson FACS Calibur flow cytometer
- CellQuest software version 3.3
- Falcon FACS tubes

BDH, Pool, UK

- SDS (sodium dodecyl sulphate)
- Glycerol
- Magnesium chloride
- Sodium acetate
- Sodium hydroxide

Bioline Ltd, London, UK

- Molecular grade agarose

Bio-rad, Hemel Hempstead, Hertfordshire, UK

- iCycler real-time thermal cycle
- Nitrocellulose membrane

BMG lab Tech, Offenburg, Germany

- POLAR star OPTIMA Plate reader

Cell Signalling Technologies, Leiden, The Netherland

- Rabbit anti-human phospho-FAK (Tyr397)
- Rabbit anti-human FAK
- Rabbit anti-human phospho-Rac1 antibody
- Rabbit anti-human Rac1/2/3 antibody
- Rabbit anti-human phospho-Src Family antibody
- Rabbit anti-human Src antibody
- Rabbit anti-human phospho-TAK1 antibody
- Rabbit anti-human TAK1 antibody
- Mouse anti-human phospho-p38 antibody
- Rabbit anti-human p38 antibody

Developmental Studies Hybridoma Bank University of Iowa, Iowa City, USA

- Rat anti-human Integrin beta-1 antibody (AIIB2)

Fermentas, Sankt Leon-Rot, Germany

- Multicolour broad range protein ladder (10-260 kDa)

Fisher scientific, Loughborough, Leicestershire, UK

- GeneRuler 1 kbp DNA ladder
- Lipofectamine™ RNAiMAX Transfection Reagent
- Glycine
- NaCl
- Tris Base
- DAPI (4′,6-diamidino-2-phenylindole), NucBlue™ Fixed Cell ReadyProbes™ Reagent

Flowgen Bioscience, Nottingham, UK

- Horizontal electrophoresis tank
- Proto FlowGel (acrylamide: bisacrylamide)
- Proto FlowGel, resolving buffer (1.5 M Tris-HCl (ph 8.8), 0.4% (w/v) SDS.)
- Proto FlowGel staking buffer

FMC Corporation, Philadelphia, USA

- SYBR Green I DNA stain

Gibco- Invitrogen Corporation, Paisley, UK

- Opti-MEM® I reduced serum medium
- TrypLE™ Select Enzyme (10X), no phenol red

Greiner Bio-One Ltd, Gloucestershire, UK

- 12 well culture plates, 25 and 75 cm^2 cell culture flasks

Hoefer, Inc, San Francisco, USA

- TE 50X protein transfer tank

http://imagej.nih.gov/ij/

- ImageJ program

LGC-ATCC, Teddington, UK

- MDA-MB-231 breast cancer cell line

Life Technology, Paisly, UK

- Endothelial cell serum-free medium
- Lipofectin reagent
- Lipofectamine® LTX & PLUS™ Reagent
- Lipofectamine® 2000 Reagent
- Lipofectamine™ 3000 Reagent

Lonza, Basel, Switzerland

- DMEM medium

Mirus Bio LLC, Madison, USA

- Trans IT® -LT1 transfection reagent
- Trans IT® -2020 transfection reagent

New England Biolab Inc, UK

- Q5 Site-Directed Mutagenesis Kit
- SOC outgrowth Medium

OriGene, Rockville, USA

- pCMV6-AC-TF-tGFP plasmid
- pCMV6-AC-tGFP plasmid

Promega Corporation, Southampton, UK

- Midipreps DNA purification system
- ProFluor® Src-Family Kinase Assay
- TBE Buffer; 0.9 M Tris-borate (pH 8.3), 25 mM EDTA
- TMB stabilised substrate for horse raddish peroxidase
- Western blue stabilised substrate for alkaline phosphatase

Promocell, Heidelberg, Germany

- Endothelial cell growth medium (MV)
- Endothelial cell growth supplement pack
- Foetal calf serum (FCS)
- Human coronary artery endothelial cells (HCAEC)
- Human dermal blood endothelial cells (HDBEC)

R&D Systems, Abingdon, UK

- *Escherichia coli* TB-1 strain

Santa Cruz Biotechnology, Heidelberg, Germany

- Donkey anti-goat alkaline phosphatase-conjugated antibody
- Goat-anti-GAPDH polyclonal IgG antibody
- Goat-anti-rabbit alkaline phosphatase-conjugated antibody

Scientific Lab Supplies, Nottingham, UK

- Magnitofection CombiMag reagent

Sigma Chemical Company, Poole, UK

- Ammonium persulphate
- Anisomycin
- Antibiotic antimycotic solution (Penicillin - Streptomycin - Neomycin Solution) (100X)
- Bovine serum albumin (BSA)
- Cycloheximide
- FAK Inhibitor-14 (1,2,4,5-benzenetetraamine tetrahydrochloride)
- Hydrogen peroxide solution (H_2O_2)
- Laemmli electrophoresis buffer
- N,N,N',N'-Tetramethylethylenediamine (TEMED)
- Phosphate buffered saline (PBS)
- PhosphoSafe™ Extraction Reagent (PhosphoSafe buffer)
- Powder microbial growth medium LB agar (Lennox)
- Powder microbial growth medium LB Broth (Luria Broth)
- proteinase-activated receptor 2-activating peptide (PAR2-AP)
- Trypsin/EDTA solution (1X)
- Tween 20

TCS Cellworks, Claydon, UK

- DMSO freeze medium

UVP LTD, Cambridge, UK

- 3 UV-transilluminator

WPA, Cambridge, UK

- UV-Visible spectrophotometer

- The Src1 inhibitor (pp$^{60c\text{-}src}$peptide TSTEPQpYQPGENL) and Src1 pseudo-inhibitor (TSTEPQWQPGENL) were gifts from Dr. Camille Ettelaie.

2.2 Methods

2.2.1 Cell culture

All the cell cultures were carried out in sterile conditions in a class II biological safety cabinet. Before starting the work, all the surfaces were cleaned using ethanol (75% v/v). All the media and reagents were warmed in a 37°C water bath for about 30 min before use. Only sterile plastic was used.

Three types of cells were used in this experiment:

a. Human breast cancer cell line (MDA-MB-231).
b. Human coronary artery endothelial cells (HCAEC).
c. Human dermal blood endothelial cells (HDBEC).

I. Culture of the MDA-MB-231 cell line

The MDA-MB-231 cell line was cultured in 75 cm^2 flasks in 10 ml of DMEM medium supplemented with 10% FCS (v/v). The cells were incubated at 37°C under 5% (v/v) CO_2. 2-3 ml of the media were replaced with fresh medium every 2 or 3 days while maintaining the total volume at 10 ml.

II. Culture of the primary cells (HCAEC and HDBEC)

HCAEC and HDBEC primary cells were cultured in 25 cm^2 flasks in 6 ml of complete endothelial medium that consisted of endothelial cell growth medium (MV), foetal calf serum (FCS) (5% v/v), endothelial cell growth supplement (0.004 ml/ml), epidermal growth factor (10 ng/ml), heparin (90 µg /ml) and hydrocortisone (0.2 µg/ml). The cells were cultured at 37°C under 5% CO_2. 2-3 ml of the media were replaced with fresh medium every 2 or 3 days while maintaining the total volume at 6 ml.

2.2.2 Subculturing, harvesting and counting the cells

When the cells were 80% confluent, the medium was removed from the flask and the cells were washed with 5 ml of sterile phosphate buffered saline (PBS) (pH 7.2) to remove traces of the serum and to maintain the correct pH. To detach the MDA-MB-231 cells, 2-3 ml of trypsin/EDTA solution was pipetted into the flask and incubated at 37ºC for 3-4 min. HCAEC and HDBEC were detached using 2-3 ml of TrypLE solution which was incubated at 37ºC for 3-4 min. The flask was then tapped firmly to release the cells. Complete media (2-3 ml) was then added to block the trypsin activity. To determine the number of cells, the cell suspension

(20 µl) was loaded into a haematocytometer and the number of cells in 1 mm^2 area counted. The number of cells was then calculated as:

Total number of cells in flask = number of cells counted per mm^2 x volume x 10,000

The cell suspension was transferred to a sterile tube and centrifuged at 2,400 *g* for 5 min at room temperature. The supernatant was poured off without disturbing the cell pellet and the cells were re-suspended in 2 ml of fresh medium. Aliquots of the cells were then placed in flasks or plates, as required.

2.2.3 Cryopreservation of cells

In order to cryopreserve the cells as stocks, the pelleted cells were re-suspended in 1 ml of DMSO freeze medium and 2 x 10^5 cells/ml were placed in each of the labelled cryovial. The vials were then transferred to a freezing chamber that contained isopropanol and were frozen at −70ºC overnight. This step ensures a gradual decrease in temperature (−1ºC/min) to retain the optimal viability of the cells. The cryovials were transferred to liquid nitrogen container on the following day for long-term storage. To start a new culture from frozen cells, cryovials containing the cells were defrosted in a 37ºC water bath for 1-2 min. The cells were then immediately transferred to flasks that contained warmed complete medium.

2.2.4 Adaptation of endothelial cells to serum-free medium

The complete endothelial culture medium used contained 5% (v/v) FCS which provides the essential nutrients required for cell maintenance and growth.

However, some of the studies aimed to examine the influence of the TF on signalling pathways and therefore need to use serum-reduced or serum-free medium. For these studies, HDBEC were cultured in a complete endothelial culture medium (MV) overnight and then gradually adapted to the serum-free medium by replacing the complete medium with 2% (v/v) FCS for 1 h which was then replaced with serum-free medium for another 1 h prior the experiments.

2.2.5 Activation of PAR2 and preparation of cell lysate

MDA-MB-231 cells, HCAEC or HDBEC (10^5/well) were cultured in 12-well plates in complete medium overnight. The medium was then removed, and the cells were washed with 1 ml of PBS and incubated for 30 to 60 min with 1 ml of serum-free medium. The cells were activated by the addition of the PAR2-agonist peptide (PAR2-AP) (SLIGKV-NH; 20 µM) to the medium and incubated up to 120 min. The medium was then removed and the cells were lysed using Laemmli electrophoresis buffer (4% SDS, 20% glycerol, 10% 2-mercaptoethanol, 0.004% bromophenol blue and 0.125 M Tris-HCl, pH 6.8). A pipette mechanically detach was used to the cells from the wells and to lyse the cells. The cell lysate samples were then boiled for 10 min to denature the proteins. The samples were analysed by western blots to detect the phosphorylation of specific proteins.

2.2.6 Estimation of protein concentration using the Bradford assay

To measure the protein concentration in the cell lysates, a standard curve was constructed by preparing a serial dilution of lipid-free BSA (0, 10, 20, 50, 100 and 200 µg/ml). The samples (cell lysate) and standards (10 µl) were placed

individually into 96-well plates and 200 µl of Bradford reagent (Bradford reagent stock diluted in dH_2O 3:2 v/v) was added to each well. Both the standards and samples were then incubated in a dark place at room temperature for 15 min. The absorption of the standards and samples was then measured at 584 nm using a plate reader (POLARstar OPTIMA plate reader). Based on the absorbance reading of the standards against protein concentrations, the standard curve was determined (Figure 2.1). The concentrations of the protein samples were then measured by using the equation from the standard curve.

2.2.7 SDS-polyacrylamide gel electrophoresis (SDS-PAGE)

The 12% (w/v) separating gel was prepared by mixing 4 ml acrylamide solution (30% (w/v) acrylamide, 0.8% (w/v) bisaacrylamide), 2.6 ml resolving buffer (1.5 M Tris-HCl pH 8.8, 0.4% (w/v) SDS), 3.3 ml de-ionised water and 100 µl ammonium persulphate (10% w/v). The solution was then gently mixed and 10 µl of N,N,N',N'-tetramethylethylenediamine (TEMED) added to start polymerisation. The solution was then poured in between the glass electrophoresis plates in a gel caster and covered with a layer of butanol (100%) and left to set for 1 h at room temperature. Once the gel was set, the butanol was removed and a 4% (w/v) stacking gel was prepared by mixing 0.65 ml of the acrylamide solution, 1.3 ml stacking buffer (0.5 M Tris-HCl pH 6.8, 0.4% (w/v) SDS), 3 ml de-ionised water and 100 µl ammonium persulphate (10% w/v). The solution was then gently mixed and 10 µl of N,N,N',N'-tetramethylethylenediamine (TEMED) was added. The solution was poured on top of the separating gel and an appropriate comb was inserted and allowed to set for about 1.5 h. The comb was then removed and the gel and glass plates placed in the electrophoresis tank. The electrophoresis

buffer (25 mM Tris-HCl pH 8.3, 192 mM glycine, 0.035% (w/v) SDS) was poured into the tank until it covered the gel. 5 µl of the molecular-weight protein markers (10-260 kDa) was loaded into the first well, and 20 µl of the pre-heated protein samples were loaded into the subsequent wells. Approximately 20 µg of protein lysate was loaded on the western blot. To separate the proteins, electrophoresis was carried out at 100 V until the line of blue dye reach the bottom.

2.2.8 Western blot analysis

Following electrophoresis, a transfer system was used to transfer the proteins onto a nitrocellulose membrane. Nitrocellulose membrane and blotting paper were prepared and soaked for 2 min in the transfer buffer (150 mM glycine, 20 mM Tris-HCl pH 8.3, 20 % (v/v) methanol), then the gel was gently positioned in between the nitrocellulose membrane and blotting paper. The gel, membrane and blotting papers were then placed in a holder and transferred to a transfer tank containing transfer buffer. The protein bands were transferred at 300 mA for 60 min at 4ºC. The nitrocellulose membrane was then blocked with TBST (20 mM Tris-HCl pH 8.0, 150 mM NaCl, 0.05 % (v/v) Tween 20) for 1 h with gentle shaking at room temperature. The membrane was then incubated overnight at 4ºC in primary antibody diluted in TBST (Table 2.1). The membrane was then washed three times (5 min each time) with TBST and incubated for 2 h with an appropriate secondary antibody diluted in TBST (Table 2.1) with gentle shaking at room temperature. The membrane was then washed three times with TBST and finally washed with dH_2O. The bands were developed with Western Blue-stabilised substrate for alkaline phosphatase and the images were recorded using a digital camera and the visualised bands analysed using the ImageJ program.

2.2.9 Preparation of the LB agar media plates

To prepare plates of agar media containing carbenicillin antibiotic, the LB agar powder (3.5 g) was dissolved in dH_2O (100 ml) and autoclaved. The agar media was then cooled down to 50°C and a carbenicillin (0.1 mg/ml) was added. To prepare the agar plates, 20 ml of LB agar was poured into a 75 mm Petri dish and left to solidify at room temperature in a sterile environment. The sealed plates were stored at 4°C until they were required.

2.2.10 Cryopreservation of the bacterial cells

A freezing solution was prepared by adding glycerol to LB broth media to give a final concentration of 20% (w/v). The freezing solution was mixed by vortexing and filtered through a 0.22-µm filter in order to sterilise the solution. Bacterial pellets were re-suspended in the appropriate amount of freezing medium, divided into 500 µl aliquots and transferred to Eppendorf tubes. The samples were frozen at −70ºC.

2.2.11 Bacterial cell culture

The LB broth powder (10 g) was dissolved in 400 ml of dH_2O to prepare the LB broth medium. The appropriate antibiotic (0.1 mg/ml carbenicillin) was then dissolved in the medium. 5-alpha competent *E. coli* containing a DNA plasmid (pCMV6-AC-TF-tGFP) was incubated in 100 ml of LB medium at 37ºC. On the following day, the medium was cooled to 4ºC and centrifuged for 15 min at 2500 *g* to pellet the bacteria.

Figure 2.1 Standard curve for the Bradford assay

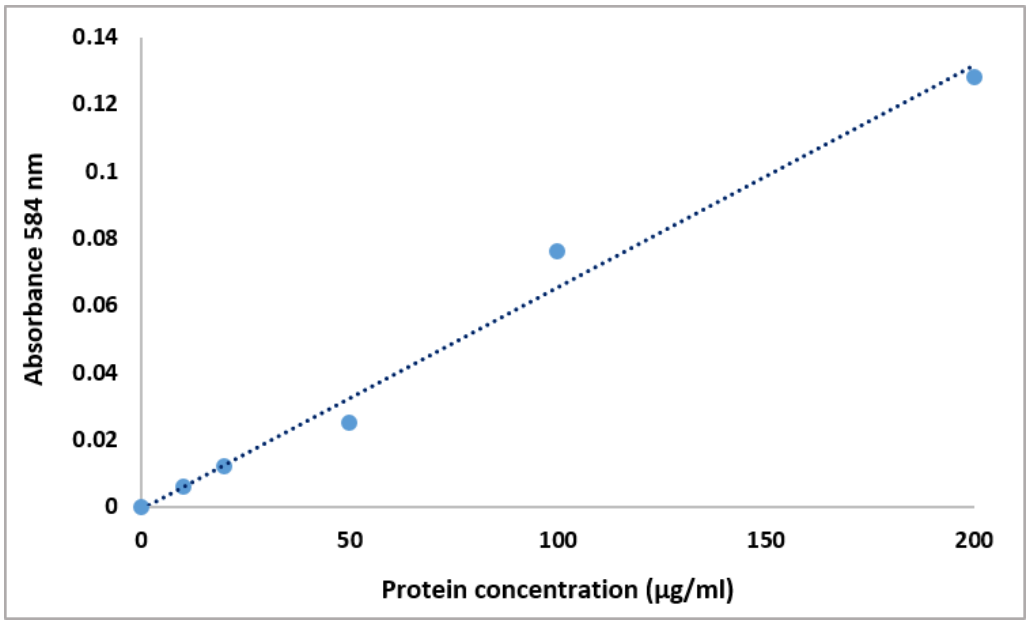

The standard curve was constructed using 0-200 µg/ml of the protein standards by diluting lipid-free BSA in dH2O. The standards (10 µl) were placed in 96-well plates and mixed with 200 µl of diluted Bradford reagent. The samples were then incubated in a dark place at room temperature for 15 min. The absorbance of the samples was then measured at 584 nm using a plate reader.

Table 2.1 Primary and secondary antibody dilutions used during the western blot procedure

Primary antibodies	Dilution antibodies: TBST (v/v)	Secondary antibodies	Dilution antibodies: TBST (v/v)
Rabbit anti-human Rac1/2/3 antibody	1:3000	Goat-anti-rabbit alkaline phosphatase-conjugated antibody	1:4000
Rabbit anti-human phospho-Rac1 antibody	1:3000	Goat-anti-rabbit alkaline phosphatase-conjugated antibody	1:4000
Rabbit anti-human Src antibody	1:3000	Goat-anti-rabbit alkaline phosphatase-conjugated antibody	1:4000
Rabbit anti-human phospho-Src family antibody	1:4000	Goat-anti-rabbit alkaline phosphatase-conjugated antibody	1:4000
Rabbit anti-human TAK1 antibody	1:3000	Goat-anti-rabbit alkaline phosphatase-conjugated antibody	1:4000
Rabbit anti-human phospho-TAK1 antibody	1:3000	Goat-anti-rabbit alkaline phosphatase-conjugated antibody	1:4000
Goat anti-human GAPDH antibody	1:5000	Donkey anti-goat alkaline phosphatase-conjugated antibody	1:5000

2.2.12 Isolation of plasmid DNA from bacteria using the Wizard plus Midiprep kit

Isolation of the plasmid DNA from the bacteria was carried out using the Wizard plus Midipreps DNA Purification system as follows. 3 ml of re-suspension buffer provided by the kit (50 mM Tris pH 7.5, 10 mM EDTA, 100 µg/ml RNase A) was used to re-suspend the bacterial pellet and transferred to a 20 ml tube. 3 ml of lysis buffer (0.2 M NaOH, 1 % SDS) was the added drop wise and the tube was gently inverted four times. 4 ml of neutralising buffer (1.32 M potassium acetate pH 4.8) was added to the tube with gentle mixed followed by centrifuging the mixture at 3000 *g* for 15 min to pellet the cell debris (genomic DNA?). The supernatant was then transferred into a 15 ml tube and centrifuged at 3000 *g* for a further 15 min to remove any remaining debris. Resin (10 ml) was added to the midiprep column followed by the supernatant. The mixture was cleared through the column using a vacuum. 20 ml of wash buffer (80 mM potassium acetate, 8.3 mM Tris-HCl pH 7.5, 40 µM EDTA, 55 % (v/v) ethanol) was added to wash the column and cleared through using a vacuum. The neck of the midiprep column was removed and the filter section (containing the resin) was transferred to a 1.5 ml microcentrifuge (Eppendorf) tube. The tube was then centrifuged at 12,000 *g* for 3 min to remove the residual wash buffer. The midiprep neck of the column was transferred to a new 1.5 ml Eppendorf tube and pre-warmed DNase-free water (300 µl) was added to the neck and incubated for 1 min at room temperature. To elute the plasmid, the Eppendorf tube was centrifuged for 2 min at 12,000 *g*. The neck of the column was removed and the eluted plasmid was centrifuged again to remove any resin fibres and the supernatant was moved to a new Eppendorf tube.

2.2.13 Ethanol precipitation of DNA

To remove any salts and endotoxins from the isolated plasmid DNA, the plasmid DNA was precipitated using ethanol. Sodium acetate (5 M) pH 5.2 (150 µl) and absolute ethanol (600 µl) were mixed with the DNA solution (150 µl) and the sample was incubated at −20°C for 30 min. The sample was then centrifuged at 12,000 *g* for 20 min in a microcentrifuge to pellet the DNA. The pellet was washed with 300 µl of ice-cold ethanol solution (75% (v/v)). The sample was then centrifuged at 12,000 *g* for a further 10 min. The supernatant was removed and the pellet was dried in a sterile environment for 10 min to remove any remaining ethanol. Finally, the pellet was re-suspended in nuclease-free water (150 µl) and the concentration of the plasmid DNA was measured to be used in subsequent studies.

2.2.14 Quantification of the concentration and purity of the isolated DNA

To determine the concentration of the eluted plasmid DNA, the sample was analysed by measuring the absorption of 1:10 dilution (v/v) of the DNA at 260 nm.

The DNA concentration (µg/ml) was calculated as:

DNA concentration (µg/ml) = Absorbance (260 nm) x 50 x dilution factor

The 260:280 ratio was measured to determine the purity of the DNA. A DNA sample with a ratio of above 1.3 was deemed to have sufficient purity.

2.2.15 Analysis of the plasmid DNA by agarose gel electrophoresis

The quality and purity of the plasmid DNA was examined by electrophoresis on a 0.5% (w/v) agarose gel. The gel was prepared by adding 0.25g of agarose to 50 ml of TBE buffer. A microwave oven was used to dissolve the agarose. The mixture was immediately poured into a pre-sealed gel tray, an appropriate comb was placed in the gel and it was allowed to solidify. DNA samples were prepared by adding 1 µl of SYBR Green I and 10 µl of loading buffer to 10 µl of the DNA sample. In addition, a DNA marker (10 µl) was mixed with 1 µl of SYBR Green I and the samples and markers were loaded into the wells. Electrophoresis was carried out at 100 V for around 1 h. and the bands were examined using a UV transilluminator.

2.2.16 Statistical analysis

The data represent the mean value of the number of experiments ± the standard deviation (SEM). The statistical analysis was carried out using the Statistical Package for the Social Sciences (SPSS) program. The one-way ANOVA procedure was used to determine significant differences in the variance when compared to the control.

Chapter 3

The influence of TF accumulation on Src1, Rac1 and TAK1 phosphorylation post PAR2 activation in endothelial cells

3.1 Introduction

Induction of protease-activated receptor 2 (PAR 2) leads to cellular activation and the release of tissue factor (TF) from the cell surface (Ettelaie et al, 2016). TF has been detected within the circulation during various pathophysiological conditions such as cancer, cardiovascular complications and following injury or trauma (Bach & Moldow, 1997; Giesen et al, 1999; Simak et al, 2006; Thaler et al, 2012). Recently, it has been reported that the accumulation of TF within endothelial cells can promote cellular apoptosis through mechanisms mediated through p38 MAPK signalling (ElKeeb et al, 2015). The main proteins capable of mediating the activation of p38 MAPK are the signalling molecules Src1, Rac1 and TAK1. In the first experimental chapter, the phosphorylation state of these proteins, following PAR2 activation was examined in endothelial cells and an attempt was made to clarify the possible roles of these proteins as signalling mediators during TF-p38 MAPK-induced apoptosis (Figure 3.1). Cells transfected to express Ala_{253}-substituted TF were used since this substitution results in the accumulation of TF within the cell, providing a reproducible model of TF accumulation that promotes cell apoptosis (ElKeeb et al, 2015). The data was compared to phosphorylation of Src1, Rac1 and TAK1 in cells expressing wild-type TF and cells expressing turbo GFP (pCMV6-AC-tGFP) as a control.

3.1.1 Aims

In this study, it is proposed that the activation of p38 MAPK following PAR2 induction is mediated through one, or a combination of the Src1, Rac1 and/or TAK1 proteins. In addition, it is suggested that the strength (magnitude and

length) of this signal is dependent on the presence or accumulation of TF within cells. Therefore, to examine these hypotheses, the phosphorylation of Src1, Rac1 and TAK1 following PAR2 activation was first measured over a period of time. After establishing the phosphorylation patterns in untransfected (HDBEC), comparisons were carried out in cells transfected to express wild-type TF, alanine-substituted TF or tGFP. Differences in the magnitude and length of Src1, Rac1 and TAK1 phosphorylation were examined. However, prior to the experiments, plasmids expressing TF with a Ser→Ala substitution at position 253 were prepared by site-directed mutagenesis. The transfection of the various plasmids using various transfection reagents was then optimised for maximal protein expression.

Figure 3.1 The proposed role of the Src1, Rac1 and TAK1 proteins in mediating TF-p38 MAPK signalling

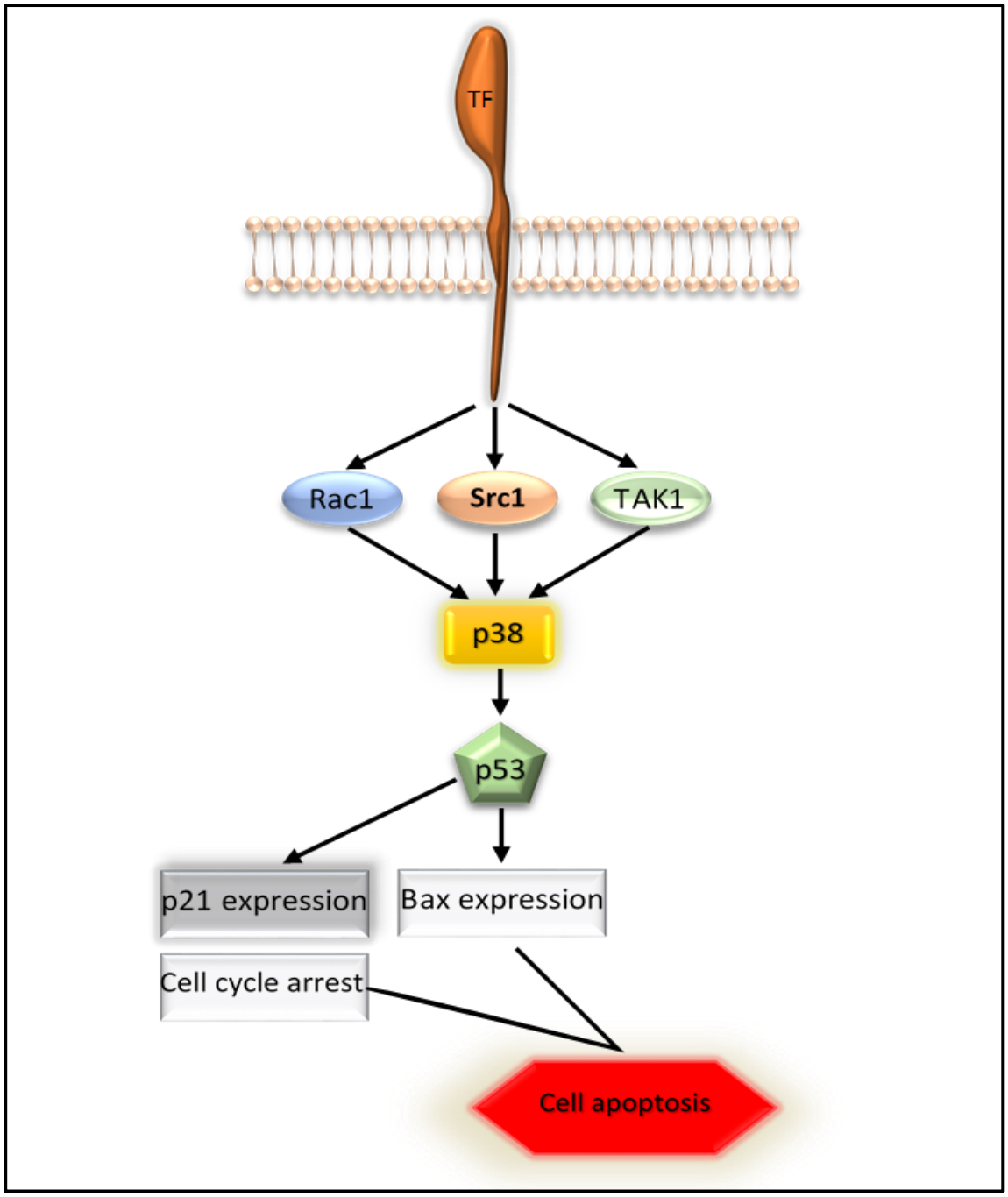

The accumulation of TF within endothelial cells stimulates cellular apoptosis through mechanisms mediated by p38 MAPK. Src1-, Rac1- and TAK1-signalling have been suggested as possible links between TF and p38 MAPK activation.

3.2 Methods

3.2.1 PCR-based DNA mutagenesis

The mammalian expression plasmid (pCMV6-AC-TF-tGFP) containing the wild-type TF (Figure 3.2) was isolated from an overnight culture of transformed 5-alpha competent *E. coli* bacteria using a midiprep isolation kit. PCR-based site-directed mutagenesis of the plasmid to alter Ser_{253} to Ala was performed using the Q5 Site-Directed Mutagenesis Kit. The PCR amplification was carried out using primers designed to introduce the desired mutation. A reaction mix was prepared containing Q5 hot-start high-fidelity master mix reagent (12.5 µl), a forward primer (0.5 µM), a reverse primer (0.5 µM), template DNA (final concentration 18 ng/µl) and nuclease-free water (9 µl).

Forward primer 5'-AGTGGGGCAGGCCTGGAAGGAGA

Reverse primer 5'-CCTGCCTTTCTACACTTG

A control was prepared containing 2 µl nuclease-free water with 1 µl of plasmid. The samples were transferred to the thermalcycler and the PCR carried out as shown in Table 3.1. Following amplification, a reaction mix was prepared using the PCR product (1 µl), 2X KLD reaction buffer (5 µl), 10X KLD enzyme mix (1 µl) and nuclease-free water (3 µl), mixed together and incubated for 5 min at room temperature. To transform the bacteria, 5 µl of the KLD mix was added to the tube of thawed 5-alpha competent *E. coli* bacteria (50 µl) and the tube was incubated on ice for 30 min. The cells were heat shocked at 42ºC for 30 s and then returned to the ice for 5 min. 950 µl of pre-warmed SOC outgrowth medium (2% vegetable peptone, 0.5% yeast extract, 10 mM NaCl, 2.5 mM KCl, 10 mM $MgCl_2$, 10 mM $MgSO_4$ and 20 mM glucose) was added to the mixture and incubated for 1 h at 37ºC. 20 µl of the bacterial suspension was spread on agar

media plates containing 0.1 mg/ml of carbenicillin and incubated overnight at 37ºC. Five individual bacterial colonies were picked out, transferred into LB broth media (10 ml) and incubated overnight at 37ºC with shaking. The samples were centrifuged for 15 min at 2500 *g* to pellet the bacteria. One part of each sample was used to make a bacteria stock while the second part was used to extract the plasmid using miniprep kit. Once the plasmid had been isolated, it was ready for sequencing to confirm the mutation.

Table 3.1 Conditions for PCR thermocycling

STEP	TEMP	TIME
Initial Denaturation	98°C	30 s
25 Cycles	98°C	10 s
	61°C	30 s
	72°C	2 min
Final Extension	72°C	2 min
Hold	4°C	

Figure 3.2 The pCMV6-AC-GFP mammalian plasmid used to express TF with a tGFP tag at the c-terminal

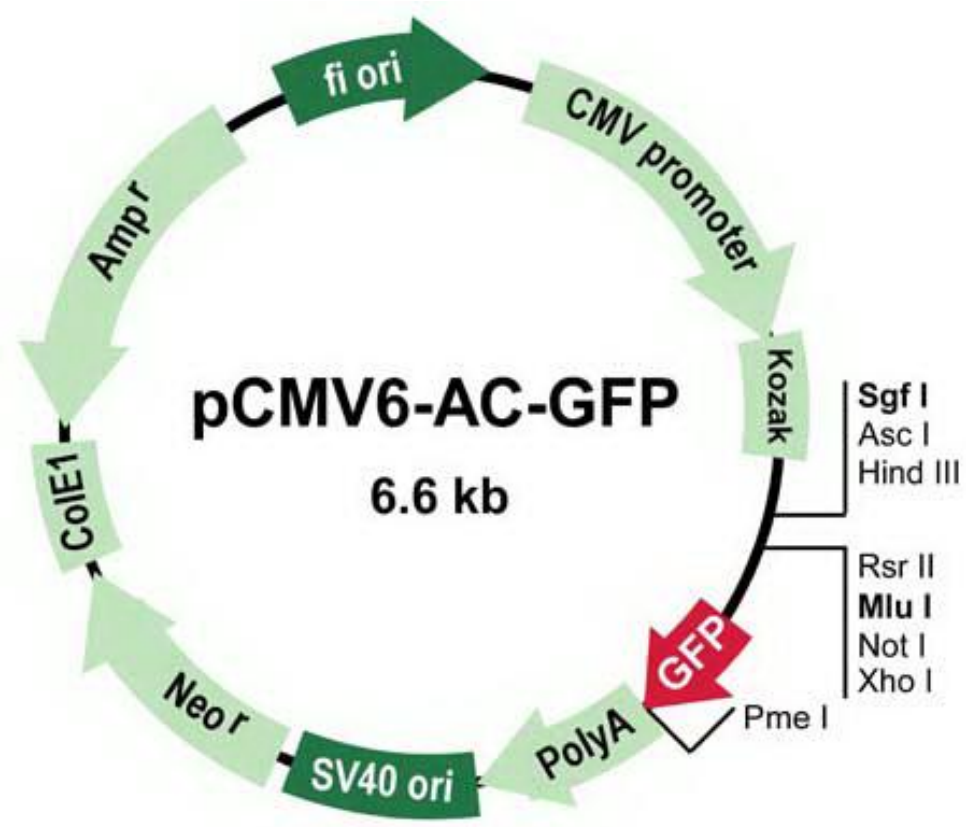

3.2.2 Transfection of HDBEC and HCAEC with plasmid DNA

To optimise the transfection procedure, the pCMV6-AC-tGFP plasmid was transfected into endothelial cells using a range of transfection reagents and the expression of tGFP was assessed by flow cytometry as described in 3.2.3.

3.2.2.1 Transfection of HDBEC and HCAEC using the Lipofectin transfection reagent

Endothelial cells (2 x 10^5/well) were seeded out in 6-well plates in 2 ml of complete MV media and incubated overnight. On the following day, the media was removed and the cells were washed with 1 ml of PBS. The cells were overlaid with Opti-MEM I-reduced serum medium (0.8 ml) and incubated for 1 h at 37ºC. The DNA-Lipofectin complex was prepared as follows:

A. Plasmid DNA solution: 1-2 µg of pCMV-AC-tGFP plasmid was diluted in 100 µl of Opti-MEM I-reduced serum medium and incubated at room temperature for 30-45 min.

B. Reagent solution: 10-20 µl of Lipofectin was diluted in 100 µl of Opti-MEM I-reduced serum medium and incubated at room temperature for 30 min.

The two solutions were gently mixed together and incubated at room temperature for 10-15 min. The DNA-Lipofectin complex was added to the cells and incubated at 37ºC for 5 h. Following the incubation, the media containing the DNA-Lipofectin complex was removed and the cells were washed with 1 ml of PBS. 2 ml of complete medium was then added, and the cells were incubated at 37ºC for 48 h.

3.2.2.2 Transfection of HDBEC and HCAEC using the TransIT®-LT1 transfection reagent and TransIT®-2020 transfection reagent

Two transfection reagents (TransIT-LT1 transfection reagent and TransIT-2020 transfection reagent) were used separately on HDBEC and on HCAEC. The cells (2 x 10^5/well) were seeded out in 6-well plates in 2 ml of complete MV medium and incubated overnight. The media was removed on the following day and the cells were washed with 1 ml of PBS. Fresh complete MV medium (1 ml) was then added to the cells and incubated for 1 h at 37ºC. The transfection reagent-DNA mixtures were prepared by gently mixing 100-250 µl of Opti-MEM I-reduced serum medium with1-2 µg of plasmid DNA and 2-5 µl of the transfection reagent (Trans IT-LT1 or Trans IT-2020). The mixtures were incubated for 25 min at room temperature. The mixtures were added drop wise to different areas of the wells and the plates were gently shaken. The cells were incubated at 37ºC for 48 h.

3.2.2.3 Reverse transfection using the TransIT®-2020 transfection reagent

To increase the transfection efficiency of endothelial cells, a variation of the above procedure was used (reverse transfection) which has been reported to produce higher rates of transfection (Fujita et al, 2007; Ziauddin & Sabatini, 2001). The plasmid DNA (2 µg) was diluted in 250 µl of Opti-MEM I-reduced serum medium. TransIT-2020 (5 µl) was then added to the plasmid-Opti-MEM mixture and incubated for 30 min at room temperature. The transfection reagent-DNA mixture (250 µl) was placed in each well of a 6-well plate. Endothelial cells (2 x 10^5/well) were suspended in 2 ml of complete medium and added to the wells, and then incubated for 24 h. The media was then replaced and incubated for a total of 48 h to allow for gene expression.

In addition, magnet-assisted transfection was used to attempt to improve the transfection efficiency. Following the preparation of the transfection reagent-DNA mixture, magnetic nanoparticles (1 µl; Magnitofection CombiMag) were added to the mixture and incubated for 20 min to allow for the association of DNA-magnetic particles. The final mixture was added drop wise to different areas of the wells and the plates were gently shaken. The plates were placed over a magnetic field for 20 min to draw the complex of DNA-magnetic particles towards the cells. Finally, the magnetic field was removed, and the procedure was completed, as previously described in section 3.2.2.2.

3.2.3 Determination of transfection efficiency by flow cytometry

To determine the efficiency of the cell-transfection procedure, HDBEC and HCAEC cells transfected with the pCMV-AC-tGFP mammalian expression vector. This plasmid encodes for the turbo green fluorescent protein (tGFP). The expression of tGFP in HDBEC and HCAEC was then measured by flow cytometry and compared against an untransfected set of cells. The cells were harvested and collected by centrifuge at 400 *g* for 15 min. The cells were suspended in PBS (300 µl) and transferred to polypropylene FACS tubes. The cells were analysed using a Becton Dickinson FACS-Calibur flow cytometer running the CellQuest software version 3.3. 10,000 events were recorded for each sample along with the intensity of the fluorescence. A gate was set to contain 3% of events from the control untransfected cells. The control cells were used to determine the amount of background fluorescence (auto-fluorescence) produced by untransfected cells. The percentage of transfected cells was then calculated and the mean cell fluorescence recorded.

3.2.4 Confirmation of the cell transfection by fluorescence microscopy

To confirm the transfection of the transfected cells, the cells were inspected using a fluorescence microscope (Zeiss Axio Vert.A1 fluorescence microscope). The transfections were carried out as previously described in section 3.2.2.2. Subsequently, the samples were washed twice with PBS, and were fixed using 4% (v/v) formaldehyde at room temperature for 20 min. The cells were then washed a further two times with PBS. To stain the nuclei, the cells were incubated with DAPI (5 µg/ml) for 5 min at room temperature. Finally, the cells were washed with PBS, and fluorescent imaging was carried out using a Zeiss Axio Vert.A1 fluorescence microscope with an AxioCam ICm1 camera attachment.

3.2.5 Optimisation of the western blot procedure to detect the phosphorylated and total Src1, Rac1 and TAK1 proteins

To detect the phosphorylated and total Src1, Rac1 and TAK1 proteins, MDA-MB-231 (2 x 10^5/well) and endothelial cells (HDBEC and HCAEC; 2 x 10^5/well) were seeded out in 6-well plates and incubated overnight. The cells were then lysed and the lysate was collected. The protein samples were then separated by SDS-PAGE and analysed using the western blot procedure, as described in section 2.2.8. Initially, the MDA-MB-231 cells were used to optimise the western blot protocol for each of the three proteins using antibodies for the total and phosphorylated proteins at the dilutions shown in Table 2.1. Once optimised, the procedures were employed to analyse these proteins in endothelial cells. The examination of TAK1 by western blot did not produce resolvable and was not continued further.

3.2.6 Time-course analysis of Src1 phosphorylation following PAR2 activation in transfected endothelial cells

To examine the role of TF on the activation time and phosphorylation status of Src1, sets of HDBEC (2 x 10^5/well) were seeded out in 6-well plates and incubated overnight. The cells were divided into four groups. Each group of cells was then either transfected as follows or used untransfected: The first group was transfected with the mutant plasmid pCMV6-AC-TF_{Ala253}-tGFP, the second group was transfected with the plasmid carrying wild-type TF pCMV6-AC-TF-tGFP and the third group was transfected with the pCMV6-AC-tGFP plasmid alone. All cells were permitted to express the respective proteins for 48 h. The cells were then activated by adding PAR2-AP (20 µM) at intervals up to 120 min. The cells were then lysed and the protein samples were separated by SDS-PAGE and analysed using the western blot procedure, as described in section 2.2.8. A quantitative analysis of the western blots was carried out using the ImageJ program and the amount of phospho Src1 was normalised against total Src1 at each interval.

3.2.7 Time-course analysis of Rac1 phosphorylation following cellular PAR2 activation in transfected cells

In addition to Src1, the samples were also used to examine the role of TF on the activation time and phosphorylation status of Rac1. The protein samples were separated by SDS-PAGE and analysed by western blot, as described in section 2.2.8. A quantitative analysis of the western blots was carried out using the ImageJ program and the amount of phospho Rac1 was normalised against total Rac1 at each time interval.

3.3 Results

3.3.1 PCR-based mutagenesis of wild-type tissue factor

Site-directed mutagenesis of the pCMV6-AC-TF-tGFP plasmid was carried out using the Q5 kit (New England Biolabs). The mutant plasmid was transformed into bacteria and spread on agar plates containing 0.1 mg/ml carbenicillin. Five separate colonies of bacteria were selected and propagated in Luria broth (LB). The plasmids were then extracted from these bacteria using a midiprep kit and analysed by agarose gel electrophoresis (Figure 3.3A). The concentration of the plasmid DNA was also measured, and the purity of the DNA was determined using a spectrophotometer (Figure 3.3B). The isolated plasmids were sequenced by Eurofins Genomics and two mutated clone sequences were found to contain the desired Ser_{253}→Ala mutation (Figure 3.4).

Once the sequence of the mutant plasmid was confirmed, samples of the bacteria carrying the plasmids encoding the mutant form of TF (samples 1 and 3), wild-type TF and tGFP were propagated and stored. Plasmids were extracted using midiprep. Finally, the plasmid samples were analysed by agarose gel electrophoresis (Figure 3.5A) and the quantity and purity of the DNA were determined using a spectrophotometer (Figure 3.5B) prior to use in endothelial cell transfection.

Figure 3.3 Analysis of the plasmids after mutagenesis

A)

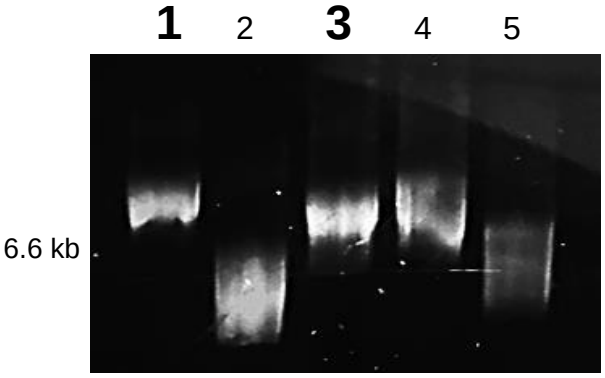

B)

	A260	A280	µg/ml	A260/A280 Ratio
1	0.123	0.068	61.5	1.809
2	0.307	0.174	153.5	1.764
3	0.262	0.149	131.0	1.758
4	0.155	0.084	77.5	1.845
5	0.152	0.082	76.0	1.854

pCMV6-AC-TF-tGFP plasmid was mutated using site-directed mutagenesis and transformed into *E. coli* bacteria. The bacteria were plated out and five colonies were isolated and the DNA extracted by midiprep. A) Micrograph of the agarose gel electrophoresis analyses of the five isolated plasmids (numbers 1 and 3 were positive for the desired mutation). B) Absorption values were measured at 260 nm and 280 nm and the concentration and purity of the plasmid DNA were calculated.

Figure 3.4 The sequence of the mutant form of the tissue factor (Ser$_{253}$→Ala)

TCAGGCACTACAAATACTGTGGCAGCATATAATTTAACTTGGAAATCAACTAA
TTTCAAGACAATTTTGGAGTGGGAACCCAAACCCGTCAATCAAGTCTACACTG
TTCAAATAAGCACTAAGTCAGGAGATTGGAAAAGCAAATGCTTTTACACAACA
GACACAGAGTGTGACCTCACCGACGAGATTGTGAAGGATGTGAAGCAGACGTA
CTTGGCACGGGTCTTCTCCTACCCGGCAGGGAATGTGGAGAGCACCGGTTCTG
CTGGGGAGCCTCTGTATGAGAACTCCCCAGAGTTCACACCTTACCTGGAGACA
AACCTCGGACAGCCAACAATTCAGAGTTTTGAACAGGTGGGAACAAAAGTGAA
TGTGACCGTAGAAGATGAACGGACTTTAGTCAGAACCAACAACAATTTAATAA
GCCTCCGGGATGTTTTTGGCAAGGACTTAATTTATACACTTTATTATTGGAAA
TCTTCAAGTTCAGGAAAGAAAACAGCCAAAACAAACACTAATGAGTTTTTGAT
TGATGTGGACAAAGGAGAAAACTACTGTTTCAGTGTTCAAGCAGTGATTCCCT
CGGGAACAGTTAACCGGAAGAGTACAGACAGCCCGGTAGAGTGTATGGGCCAG
GAGAAAGGGGAATTCAGAGAAATATTCTACATCATTGGAGCTGTGGTATTTGT
GGTCATCATCCTTGTCATCATCCTGGCTATATCTCTACACAAGTGTAGAAAGG
CAGG**AGTGGGGCAG**AGC**TGGAAGGAGA**ACTCCCCACTGAATGTTTCATAA

5'-**AGTGGGGCAGGCCTGGAAGGAGA** Ala253 forward primer.

5'-**CCTGCCTTTCTACACTTG** reverse primer

Figure 3.5 Analyses of the plasmids encoding the mutant TF, wild-type TF and tGFP

A)

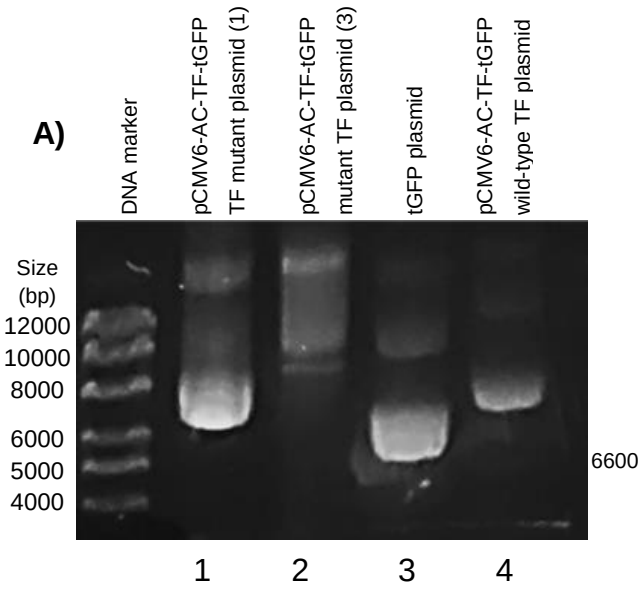

B)

	A260	A280	µg/ml	A260/A280 Ratio
1	1.185	0.856	592.5	1.384
2	0.471	0.287	235	1.641
3	1.472	0.853	736	1.726
4	1.95	1.15	975	1.696

Plasmids encoding the mutant form of TF (lanes 1 and 2), tGFP (lane 3) and wild-type TF (lane 4) were extracted from E. coli using midiprep and precipitated. The plasmids were then assessed using A) agarose gel electrophoresis and B) the quantity and the purity of the DNA samples were assessed. Measuring the absorption at 260 and 280 nm.

3.3.1.1 Examination of HDBEC and HCAEC transfection efficiency by Lipofectin, TransIT®-LT1 Transfection, and TransIT®-2020 reagents using flow cytometry

To optimise the transfection procedure for HDBEC and HCAEC, different transfection reagents (Lipofectin, Trans IT-2020 and Trans IT-LT1) were used to transfect a plasmid encoding for the tGFP protein into the endothelial cells. The number of transfected cells was then measured by flow cytometry and compared to that of untransfected cells in order to calculate the transfection efficiency.

Transfection of cells using Lipofectin showed a transfection efficiency of 2% with a mean fluorescence value of 55 (Figure 3.6). Due to the low percentage of transfection, other transfection reagents were proposed to achieve efficient transfection. Transfection of cells using TransIT-LT1 and TransIT-2020 transfection reagents showed a transfection percentages of 14% and 16% respectively with mean fluorescence of 137 and 93 respectively (Figure 3.6).

As part of the optimisation procedure, a different plasmid containing the mutant TF (pCMV6-AC-TF_{Ala253}-tGFP) was employed. In addition, a different amount of plasmid DNA (2.6 µg) was used to establish the optimal plasmid concentration for maximal transfection. Analyses of the transfection efficiencies found that Trans IT-2020 produced a transfection efficiency of 20% with a mean fluorescence value of 105.5, whilst in the same experiment, TransIT-LT1 produced a very poor transfection efficiency of only 1% (Figure 3.7).

Transfection of cells using the TransIT-2020 reagent produced the greatest transfection efficiency (18.13%) compared to the other two transfection reagents (Figure 3.7). However, the high level of the transfection reagent was found to be detrimental to the cells. Therefore, the remainder of the investigations were

carried out using the TransIT-2020 transfection reagent but with less of the plasmid (2 µg) and transfection reagent (5 µl) maintaining the ratio of DNA:transfection reagent. HDBEC (2 x 10^5/well) were seeded out in 6-well plates in complete MV medium and incubated overnight. The cells were then incubated with the transfection reagent-DNA complex (plasmid; 2 µg + TransIT-2020; 5 µl + Opti-MEM I; 250 µl) at 37ºC for 48 h. The final analyses of the transfection efficiency found that the highest transfection percentage was 31.4% with a mean fluorescence value of 103 (Figure 3.8).

Figure 3.6 Analysis of the transfection efficiency using the Lipofectin, TransIT®-LT1 and TransIT®-2020 transfection reagents

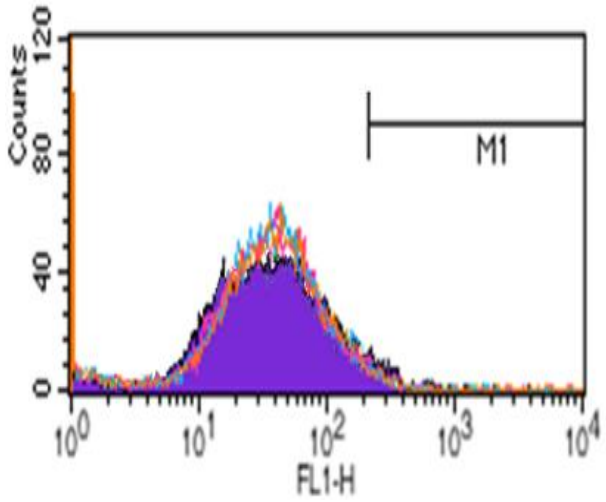

Untransfected EC (control).
Transfected cells using Lipofectin
Transfected cells using TransIT-2020.
Transfected cells using TransIT- LT1

HDBEC (2 x 10^5/well) were transfected with the tGFP (pCMV6-AC-tGFP) plasmid (2 µg) using the A) Lipofectin and B) TransIT-LT1 and TransIT-2020 transfection reagents (6 µl). Transfected cells were analysed using flow cytometry. 10,000 events were analysed for each sample. A gate (M1) encompassing 3% of the control sample (the solid purple area) was used to compare the fluorescence of the transfected cells with the untransfected control cells. The data is representative of four separate experiments.

Figure 3.7 Analysis of the transfection efficiency using the TransIT-LT1 and TransIT-2020 transfection reagents

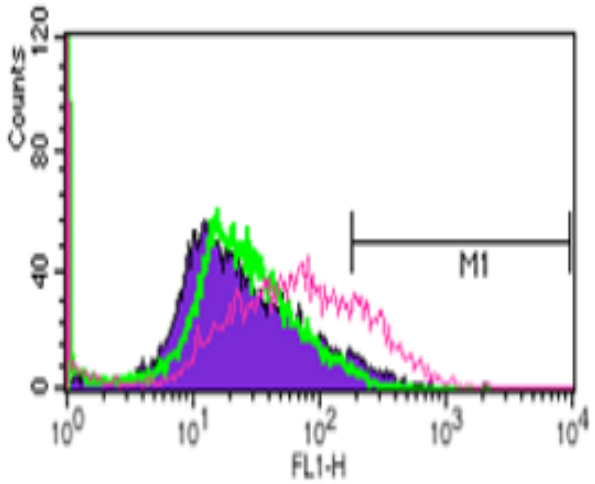

Untransfected cells (control)

Transfected cells using TransIT-2020. Transfected cells using TransIT- LT1

HCAEC (2 x 10^5/well) were transfected with 2.6 µg of the mutant form of the plasmid (pCMV6-AC-TF_{Ala253}-tGFP) using the TransIT-LT1 and TransIT-2020 transfection reagents (6 µl). The samples were incubated for 48 h to allow for protein expression. The transfected cells were analysed using flow cytometry and 10,000 events were examined for each sample. A gate (M1) was set to include 3% of cells (the solid purple area) and was used to compare the fluorescence of the transfected samples. The data is representative of two separate experiments.

Figure 3.8 Analysis of the transfection efficiency using the TransIT-2020 transfection reagent

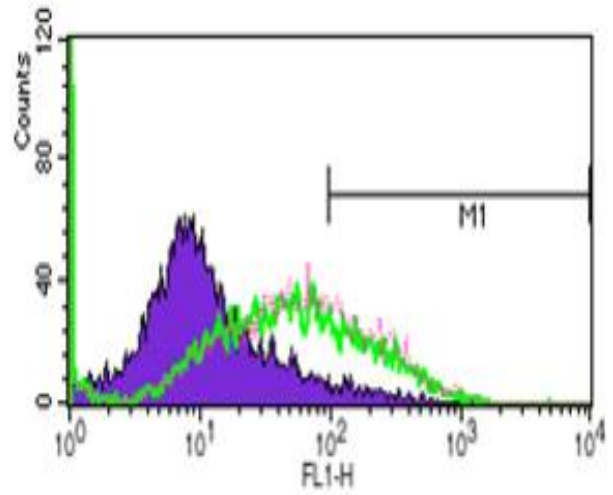

Untransfected cells (control)

Transfected cells (duplicates)

HDBEC (2 x 10^5/well) were transfected with 2 µg of the mutant form of TF (pCMV6-AC-TF_{Ala253}-tGFP) using the TransIT-2020 transfection reagent (5 µl). The samples were incubated for 48 h to allow for protein expression. The transfected cells were analysed using flow cytometry and 10,000 events were examined for each sample. A gate (M1) was set to include 3% of cells (the solid purple area) and was used to compare the fluorescence of the transfected samples. The data is representative of two separate experiments.

Reverse transfection was attempted to further improve the transfection efficiency. 100 µl of transfection reagent-plasmid mixture (1 µg plasmid (pCMV6-AC-TF_{Ala253}-tGFP) and 2.5 µl of TransIT-2020 in 100 µl of Opti-MEM I) was added to each well in a 12-well plate and HDBEC (2 x 10^5/well) were dispersed in 1 ml of complete medium and incubated for 48 h to allow for gene expression. The analyses of the cells showed a lower level of transfection at 22.5% (mean fluorescence value = 98.39) compared with the forward transfection procedure (Figure 3.9A).

In addition, magnet-assisted transfection was used to try and improve the transfection efficiency. Magnetic nanoparticles (1 µl) was added to the transfection reagent-plasmid mixture and then incubated for 20 min. The complex was then added to HDBEC (2 x 10^5/well) and the culture plates were placed on a magnetic plate for 20 min. The inclusion of the magnetic nanoparticles did not result in a significant increase in transfection levels (percentage transfection = 34.25%; mean fluorescence = 135.48) compared to the level of transfection (27.83%) with a mean fluorescence of 118.02 in transfected samples without the magnetic nanoparticles (Figure 3.9B).

Figure 3.9 Analysis of the transfection efficiency using reverse transfection and magnetic-assisted transfection

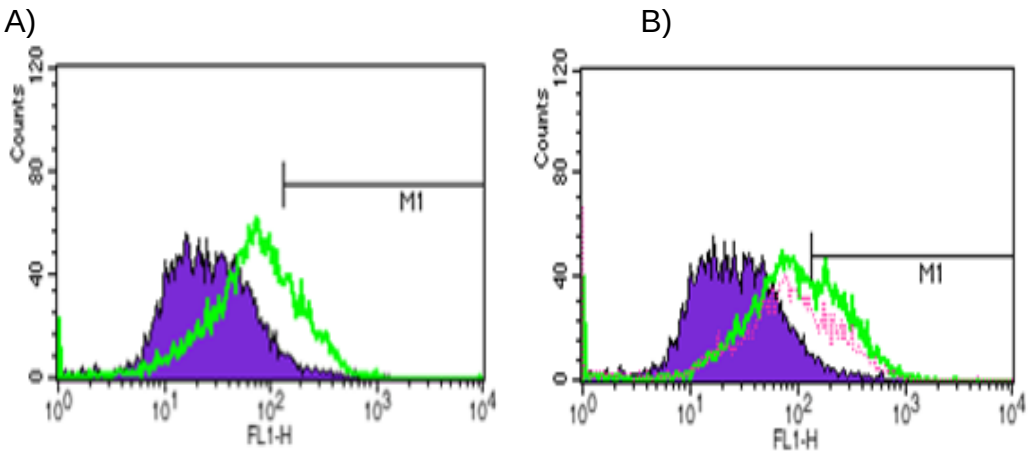

A) Reverse transfection was carried out using 100 µl of the transfection reagent-plasmid (pCMV6-AC-TF_{Ala253}-tGFP) mixture, which was placed in each well. HDBEC (2 x 10^5/well) were dispersed in 1 ml of complete medium and incubated for 24 h. The media was then replaced and incubated for a further 24 h to allow for gene expression.

B) Magnet-assisted transfection was carried out in the presence (green line) and absence (pink line) of the magnetic nanoparticles in the transfection reagent-plasmid mixture. The complex was added to the cultured HDBEC and the culture plate was placed on a magnetic plate for 20 min. The cells were incubated for 48 h to allow for gene expression. The transfected cells were analysed using flow cytometry and 10,000 events were examined for each sample. A gate (M1) was set to include 3% of the control cells (the solid purple area) and was used to compare the fluorescence of the transfected samples. The data is representative of two separate experiments.

3.3.2 Analysis the transfection efficiency using the TransIT®-2020 reagent in low-passage HDBEC

It has been proposed that a low cell passage rate passages (<5 passages) may improve the transfection efficiency (McCoy et al, 2010). Therefore, passage 4 cells were used in the next part of the optimisation experiment. HDBEC (2 x 10^5/well) were seeded out in 6-well plates in complete MV medium and incubated overnight. The cells were then incubated with the transfection reagent-DNA complex (pCMV-AC-tGFP (2 µg) + TransIT-2020 (5 µl) + Opti-MEM I (250 µl)) at 37ºC for 48 h. The final analyses of the transfection efficiency using flow cytometry showed a mean transfection percentage of 61% with a mean fluorescence value of 153 (Figure 3.10). This optimised transfection procedure was employed to transfect the HDBEC in subsequent studies.

3.3.3 Examination of HDBEC transfection by fluorescence microscopy

To confirm the transfection of endothelial cells, HDBEC (3 x 10^4/well) were seeded out in 48-well plates in 1 ml of complete MV medium and incubated overnight. The cells were transfected using the Trans IT-2020 transfection reagent to express tGFP and were incubated at 37ºC for 48 h. The analyses of green fluorescence by fluorescent microscopy showed that a majority of cells were expressing the green fluorescent protein (Figure 3.11).

Figure 3.10 Transfection of HDBEC using the TransIT-2020 reagent

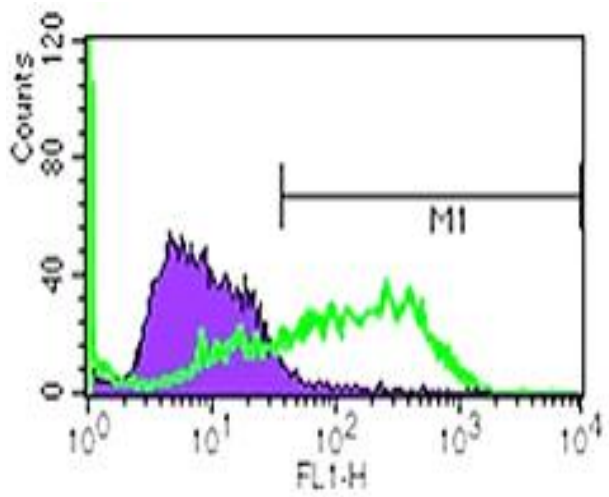

Untransfected cells (control).

Transfected cells.

Passage 4 HDBEC (2 x 10^5/well) were transfected with the pCMV6-AC-tGFP plasmid (2 µg) using the TransIT-2020 transfection reagent (5 µl). The samples were incubated for 48 h to allow for protein expression. The transfected cells were analysed using flow cytometry and 10,000 events were examined for each sample. A gate (M1) was set to include 3% of cells (the solid purple area) and was used to compare the fluorescence of the transfected samples. The data is representative of three separate experiments.

Figure 3.11 Examination of transfected HDBEC by fluorescence microscopy

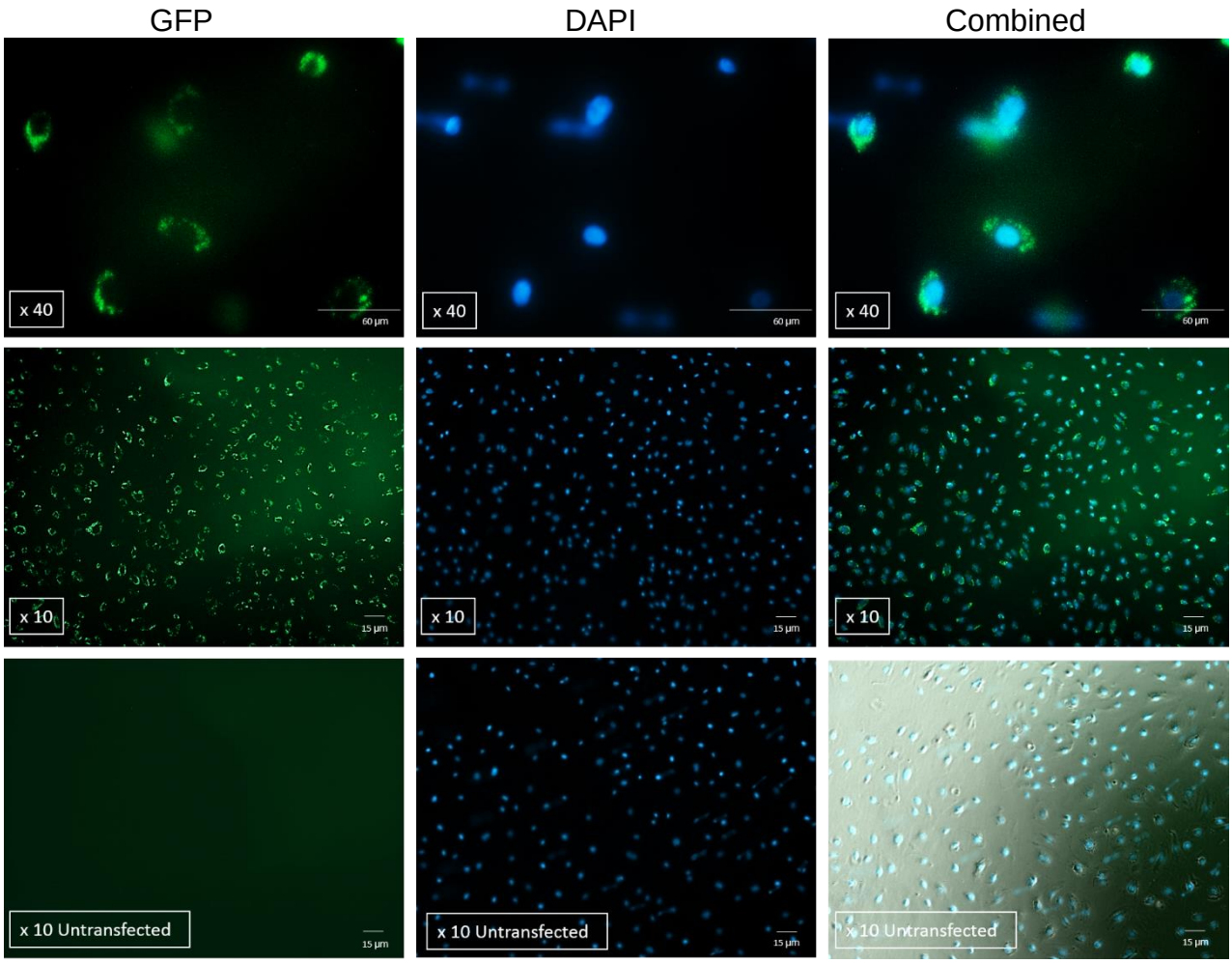

HDBEC (3 x 10^4/well) were transfected with the pCMV6-AC-tGFP plasmid (2 µg) using the TransIT-2020 transfection reagent (5 µl). The samples were incubated for 48 h to allow for protein expression. The transfected cells were washed with PBS and fixed using 4% (v/v) formaldehyde at room temperature for 20 min. Cells were then incubated with DAPI (5 µg/ml) for 5 min at room temperature to stain the nucleus. Finally, the cells were inspected using a fluorescence microscope. The data is representative of three experiments. (Magnification x 10 and 40).

3.3.4 Detection of the Src1, Rac1 and TAK1 proteins using western blotting

Western blot analysis was used to detect the total and phosphorylated Src1, Rac1 and TAK1 proteins. To optimise the western blot protocol, the human breast cancer cell line, MDA-MB-231 (2 x 10^5/well) was cultured in 6-well plates and incubated overnight. The cells were then lysed, collected and analysed by western blotting. Clear bands were obtained from the preliminary analysis using western blotting for the total proteins, but the bands were faint for phospho-TAK1 (Figure 3.12).

Following the optimisation of the western blot procedure for each of the three proteins in MDA-MB-231, the phosphorylation of Src1, Rac1 and TAK1 in HDBEC and HCAEC was examined using the same procedure of the western blot, it was possible to produce blots of sufficiently good quality for total and phosphorylated Src1 and Rac1 in HDBEC (Figure 3.13) for use in further experiments. However, the examination of TAK1 phosphorylation in HDBEC or HCAEC did not produce bands that were adequately resolved, and therefore, the examination of TAK1 phosphorylation was discontinued (Figure 3.14).

Figure 3.12 Examination of the phosphorylation of the Src1, Rac1, and TAK1 proteins in MDA-MB-231 cells

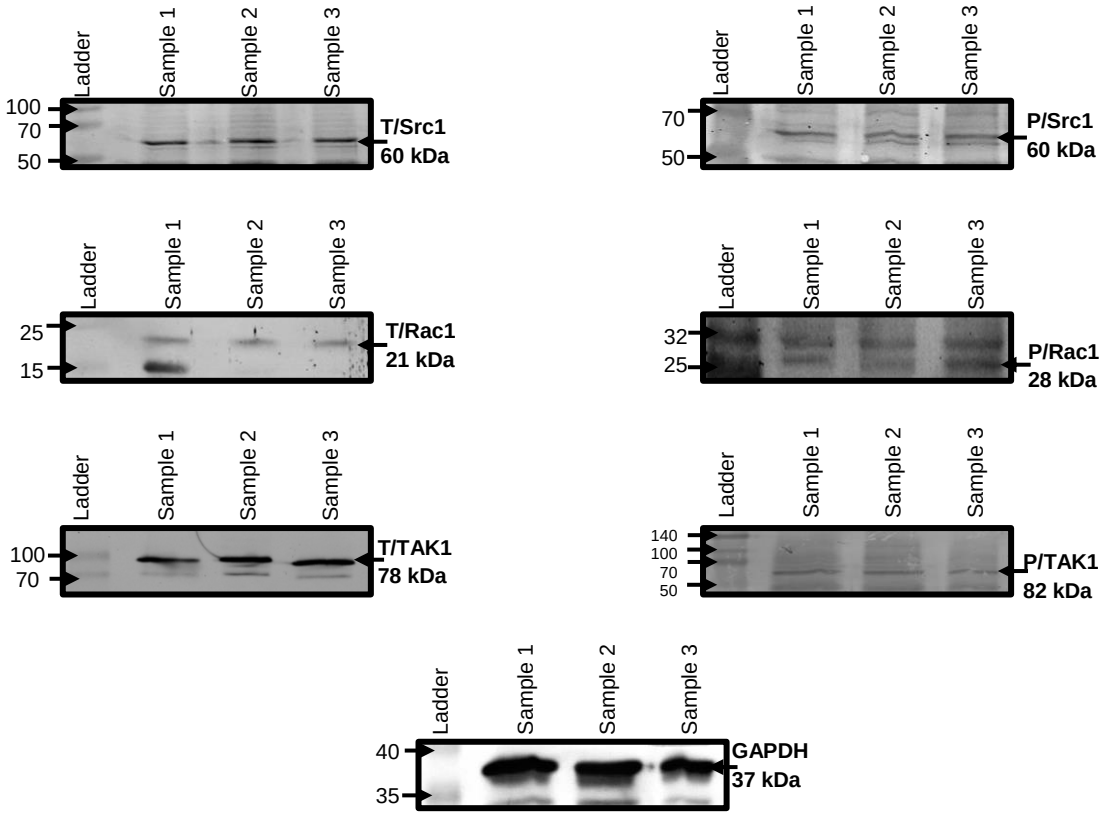

MDA-MB-231 (2 x 10^5/well) were seeded out in 6-well plates and incubated overnight. The cells were then lysed and collected. Western blot analysis was carried out using antibodies to determine the total and phosphorylated Src1, Rac1 and TAK1 proteins (n=3 independent experiments labelled as samples 1-3 on the micrographs).

Figure 3.13 Examination of the phosphorylation of the Src1 and Rac1 proteins in HDBEC

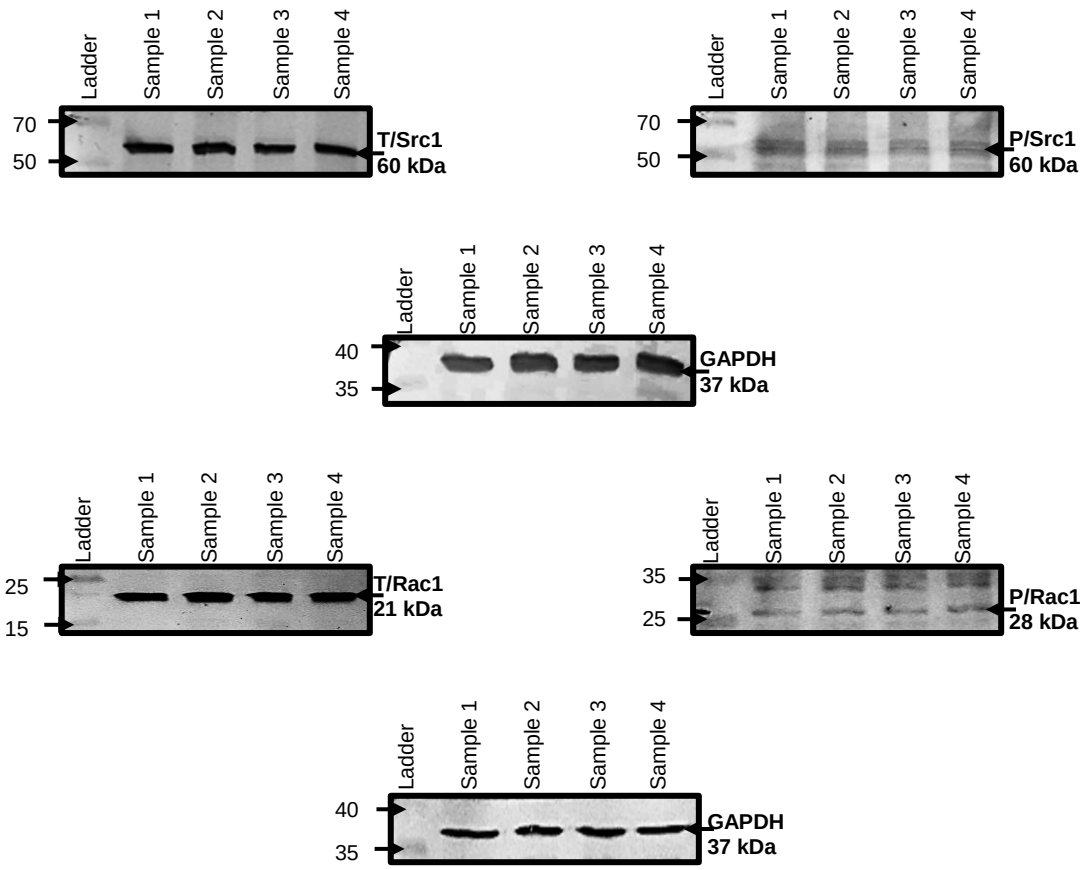

HDBEC (2 x 10^5/well) were seeded out in 6-well plates and incubated overnight. The cells were then lysed and collected. Western blot analysis was carried out using antibodies for the total and phosphorylated Src1 and Rac1 proteins (n=4 independent experiments labelled as samples 1-4 on the micrographs).

Figure 3.14 Examination of the TAK1 protein bands in HDBEC and HCAEC

A) HDBEC

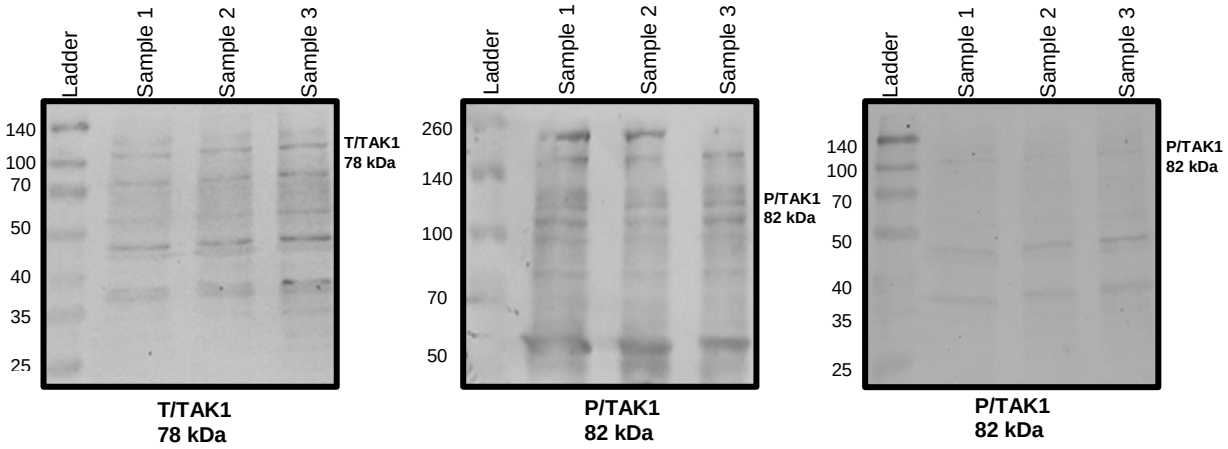

B) HCAEC

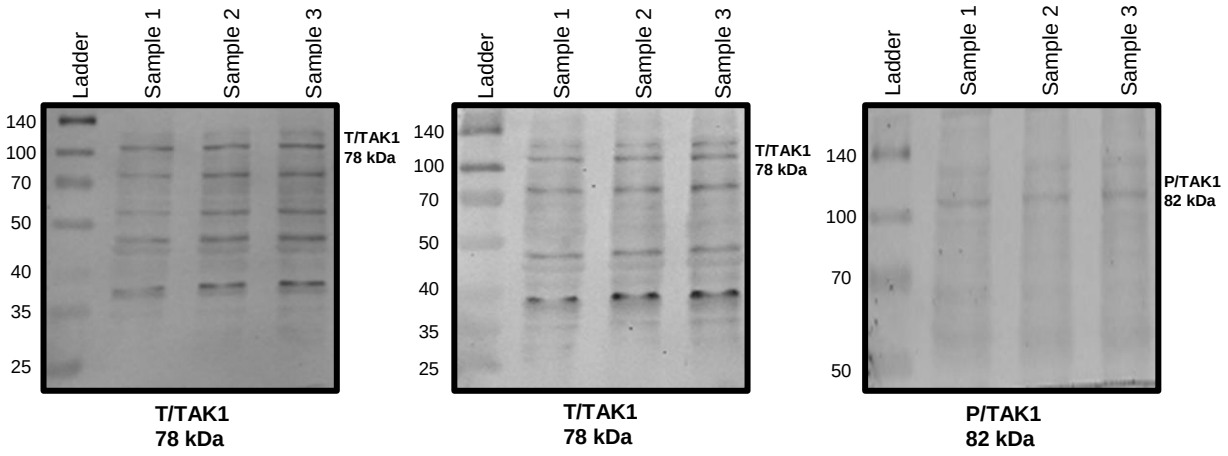

HDBEC and HCAEC (2 x 10^5/well) were seeded in 6-well plates and incubated overnight. The cells were then lysed and collected. Western blot analysis was carried out using antibodies for total (T/TAK1) and phosphorylated TAK1 (P/TAK1) in A) HDBEC and B) HCAEC (n=3 independent experiments labelled as samples 1-3 on the micrographs).

3.3.5 Examination of Src1 phosphorylation following PAR2 activation in transfected cells

To assess the effect of TF on the phosphorylation state of Src1 in HDBEC, four sets of cells were transfected as following with plasmids: A) the first set was transfected with the mutant pCMV6-AC-TF_{Ala253}-tGFP plasmid; B) the second set was transfected with the wild-type pCMV6-AC-TF-tGFP plasmid; C) the third set was transfected with the pCMV6-AC-tGFP plasmid; and D) the fourth set was left untransfected. The cells were activated using PAR2-AP (20 µM) for up to 120 min and then lysed. The protein samples were separated by 12% (w/v) SDS-PAGE. The samples were then transferred to a nitrocellulose membrane and probed using the anti-phospho-Src (pTyr416) family and anti-Src antibodies. The bands were quantified using the ImageJ program and the ratio of Src1 phosphorylation was normalised against the total Src1 at each interval. The results of the four groups were as follows:

A) Expression of the mutant form of TF in HDBEC resulted in a peak phosphorylation values with a higher magnitude at 80 and 100 min following the activation of PAR2 (Figure 3.15).

B) The second set of cells expressing the wild type TF showed no clear peak, although a small increase in phosphorylation was seen at 100 min following the activation of PAR2 (Figure 3.16).

C) The third set of cells expressing tGFP also showed no clear peak, although a small increase in the phosphorylation value was seen at 60 and 80 min following the activation of PAR2 (Figure 3.17).

D) The fourth untransfected set produced a phosphorylation peak at 60 min following the activation of PAR2 (Figure 3.18).

Figure 3.15 Time-course analysis of the phosphorylation of Src1 in HDBEC transfected to express TF_{Ala253}-tGFP

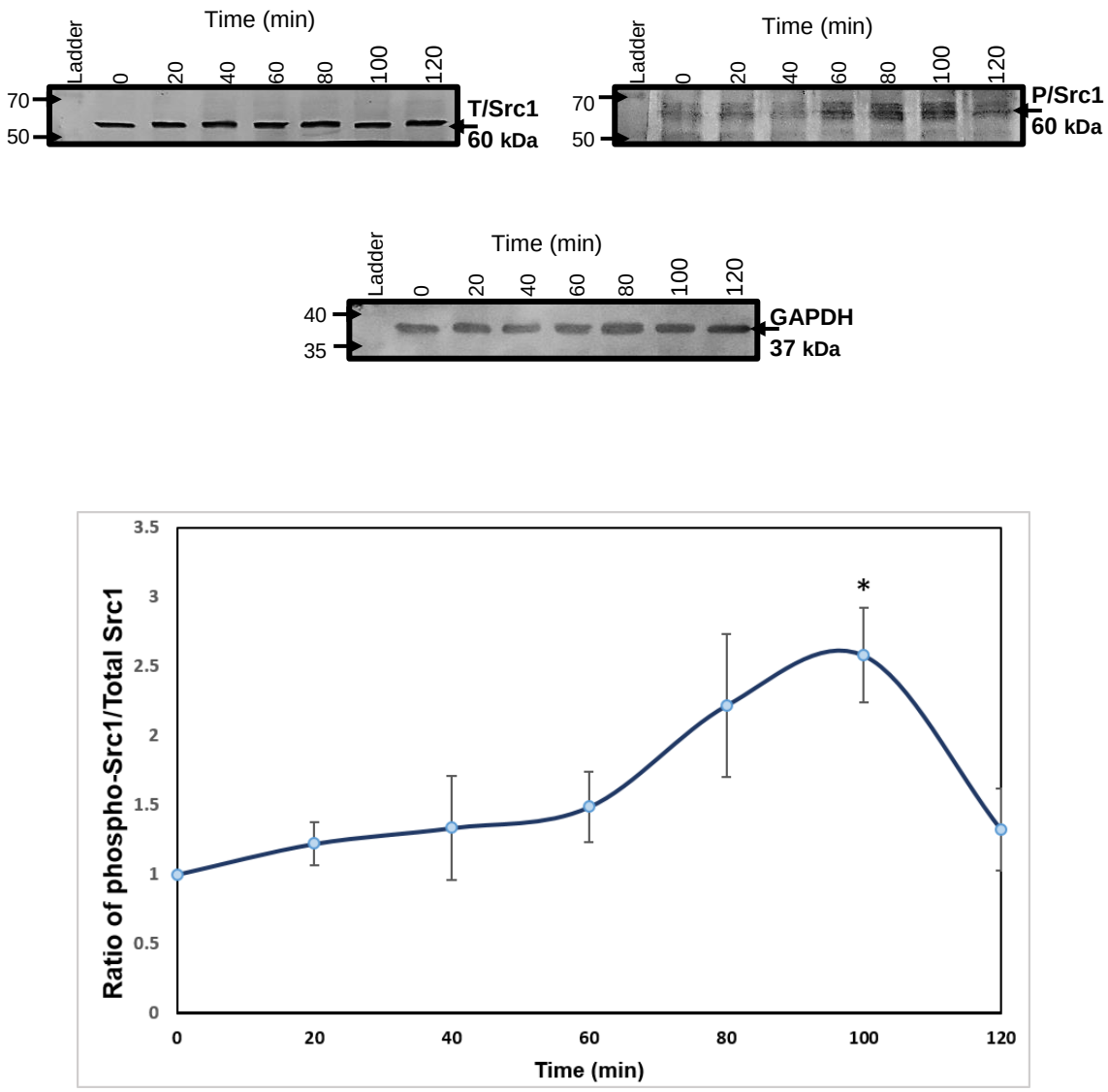

HDBEC (2 × 10^5/well) were transfected with the mutant-form plasmid (TF_{Ala253}-tGFP) and were incubated for 48 h to express the protein. The cells were treated with PAR2-AP (20 μM) for up to 120 min. The cells were then collected at each time point and lysed. The samples were analysed by western blotting using a rabbit anti-human phospho-Src (pTyr416) family antibody and a rabbit anti-human Src antibody. The phospho-Src1 (P/Src1)/total Src1 (T/Src1)/GAPDH ratio was calculated (The data is the average of three independent experiments and expressed as the mean ± SEM; * = P<0.05 vs the untransfected/untreated).

Figure 3.16 Time-course analysis of the phosphorylation of Src1 in HDBEC transfected to express wild-type TF

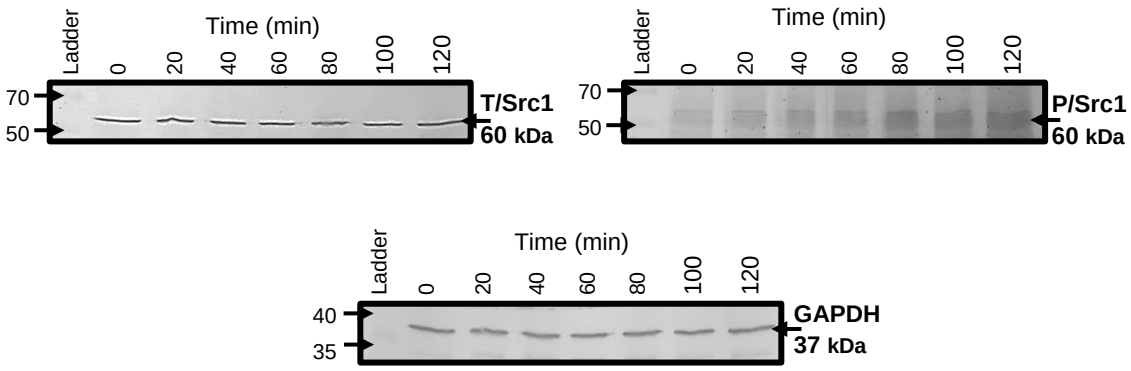

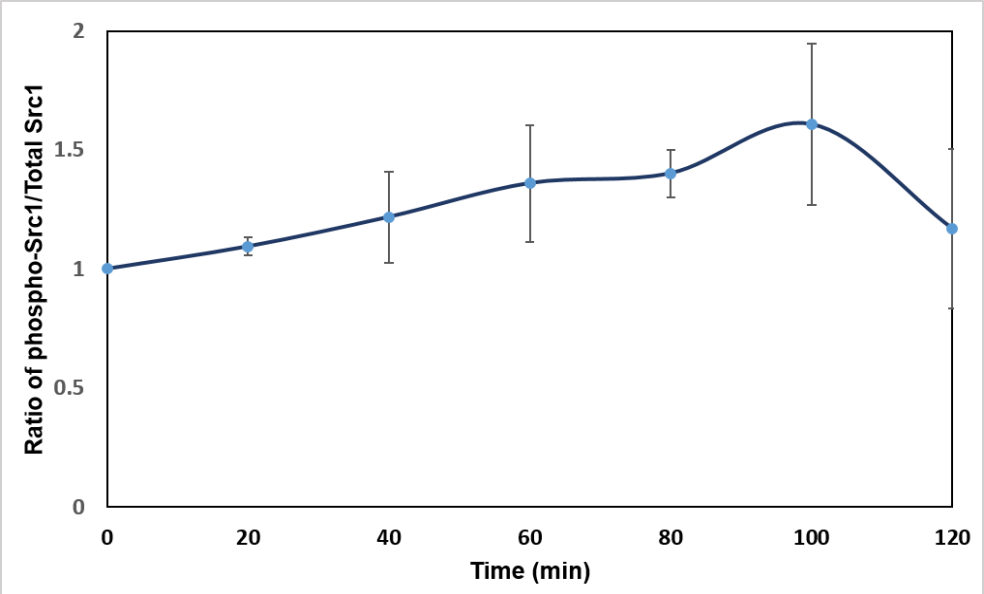

HDBEC (2 × 10^5/well) were transfected with the wild-type pCMV6-AC-TF-tGFP plasmid and incubated for 48 h to express the protein. Then, the cells were treated with PAR2-AP (20 μM) for up to 120 min. The cells were then collected and lysed at each time point. The samples were analysed by western blotting using a rabbit anti-human phospho-Src (pTyr416) family antibody and a rabbit anti-human Src antibody to determine the phospho-Src1 (P/Src1)/total Src1 (T/Src1) ratio (The data is the average of three independent experiments and expressed as the mean ± SEM).

Figure 3.17 Time-course analysis of the phosphorylation of Src1 in HDBEC transfected to express tGFP

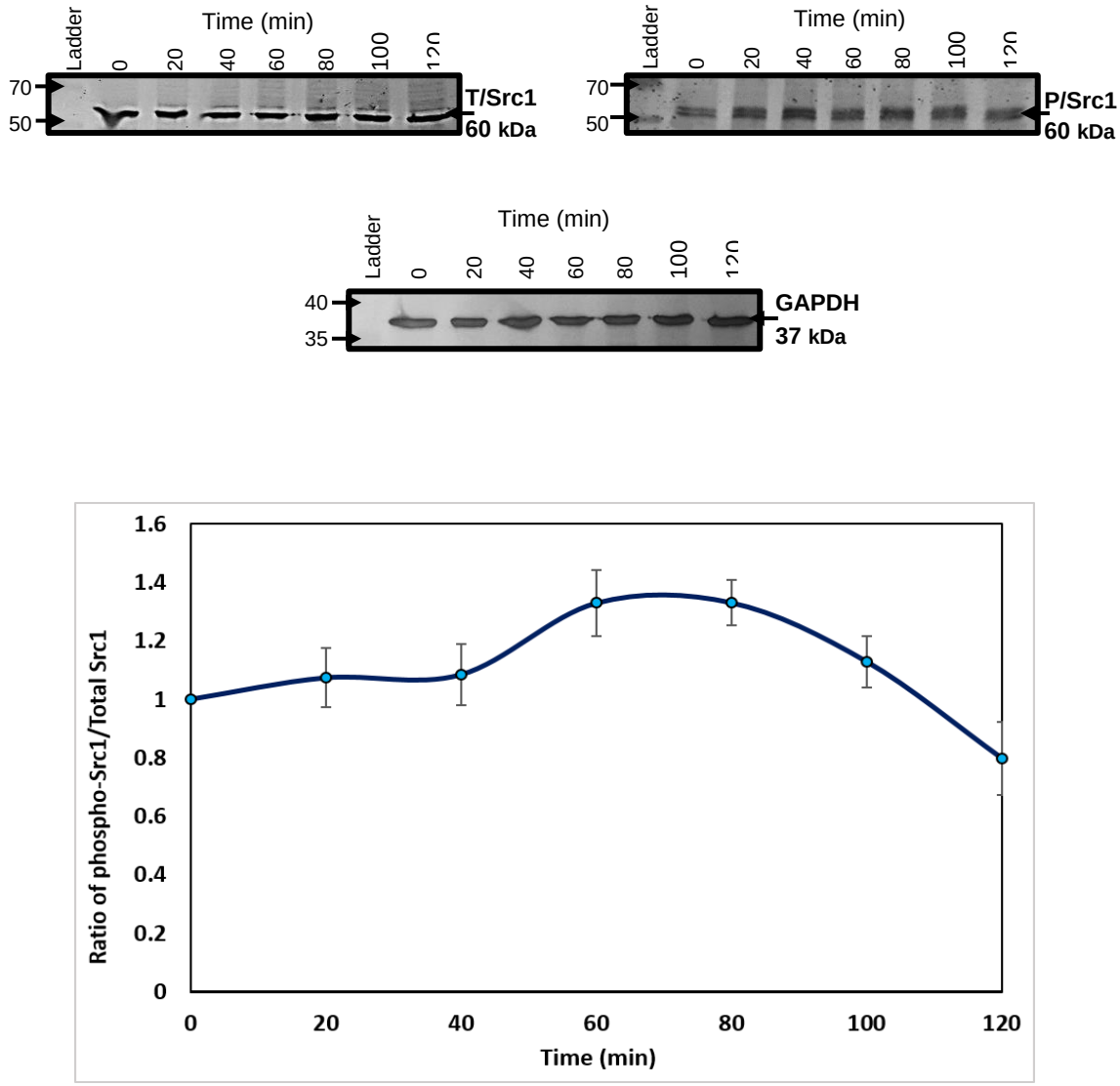

HDBEC (2 × 10^5/well) were transfected with the pCMV6-AC-tGFP plasmid and incubated for 48 h to express the protein. The cells were treated with PAR2-AP (20 μM) for up to 120 min. The cells were then collected at each time point and lysed. The samples were analysed by western blotting using a rabbit anti-human phospho-Src (pTyr416) family antibody and a rabbit anti-human Src antibody and the phospho-Src1 (P/Src1)/total Src1 (T/Src1) ratio calculated (The data is the average of three independent experiments and expressed as the mean ± SEM).

Figure 3.18 Time-course analysis of the phosphorylation of Src1 in untransfected HDBEC

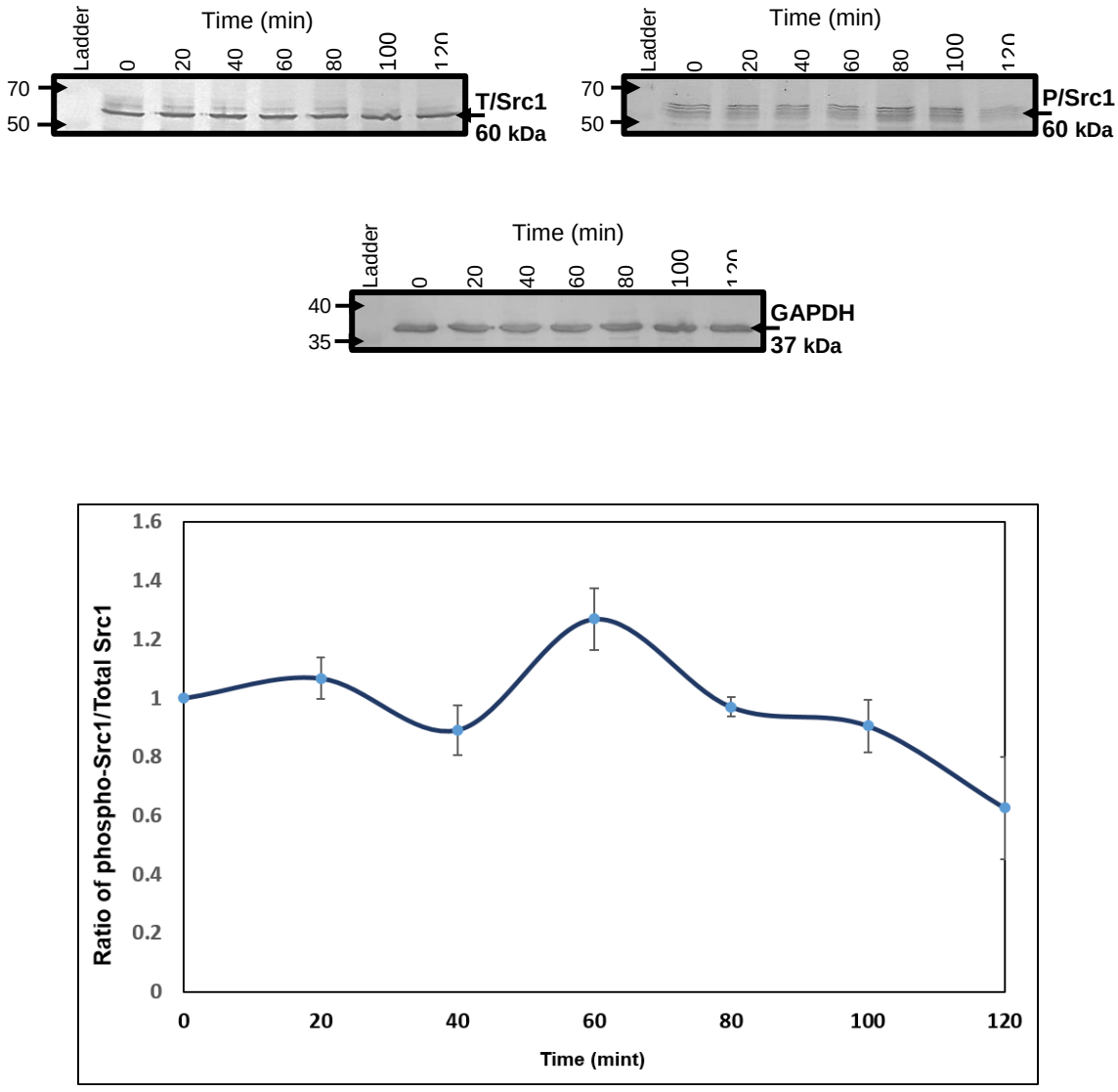

HDBEC (2×10^5/well) were treated with PAR2-AP (20 μM) for up to 120 min. The cells were then collected and lysed at each time point. The samples were analysed by western blotting using a rabbit anti-human phospho-Src (pTyr416) family antibody and a rabbit anti-human Src antibody to determine the phospho-Src1 (P/Src1)/total Src1 (T/Src1) ratio (The data is the average of three independent experiments and expressed as the mean ± SEM).

3.3.6 Examination of Rac1 phosphorylation following PAR2 activation in transfected cells

To assess the effect of TF on the phosphorylation state of Rac1 in HDBEC, four sets of cells were transfected as following plasmids: A) the first set was transfected with the mutant pCMV6-AC-TF_{Ala253}-tGFP plasmid; B) the second set was transfected with the wild-type pCMV6-AC-TF-tGFP plasmid; C) the third set was transfected with the pCMV6-AC-tGFP plasmid; and D) the fourth set was left untransfected. The cells were activated using PAR2-AP (20 µM) for up to 120 min and then lysed. The protein samples were separated by 12% (w/v) SDS-PAGE. The samples were then transferred to a nitrocellulose membrane and probed using anti-phospho-Rac1 and anti-Rac1 antibodies. The bands were quantified using the ImageJ program and the ratio of Rac1 phosphorylation was normalised against the total Rac1 at each interval. The results of the four groups were as follows:

A) Expression of the mutant form of TF in HDBEC resulted in a peak phosphorylation value at 40 and 60 min post-activation with PAR2-AP (Figure 3.19).

B) The second set of cells expressing the wild-type TF showed an increase in the level of phosphorylation value that peaked at 60 min following the activation of PAR2 (Figure 3.20).

C) The third set of cells expressing tGFP showed no clear peak in phosphorylation. The phosphorylation levels rose slightly 20 min after PAR2-AP activation. The phosphorylation remained at this level until 100 min after activation, when it decreased again (Figure 3.21).

D) The fourth untransfected set showed a phosphorylation peak at 60 min following the activation of PAR2 (Figure 3.22).

Figure 3.19 Time-course analysis of the phosphorylation of Rac1 in HDBEC transfected to express TF_{Ala253}-tGFP

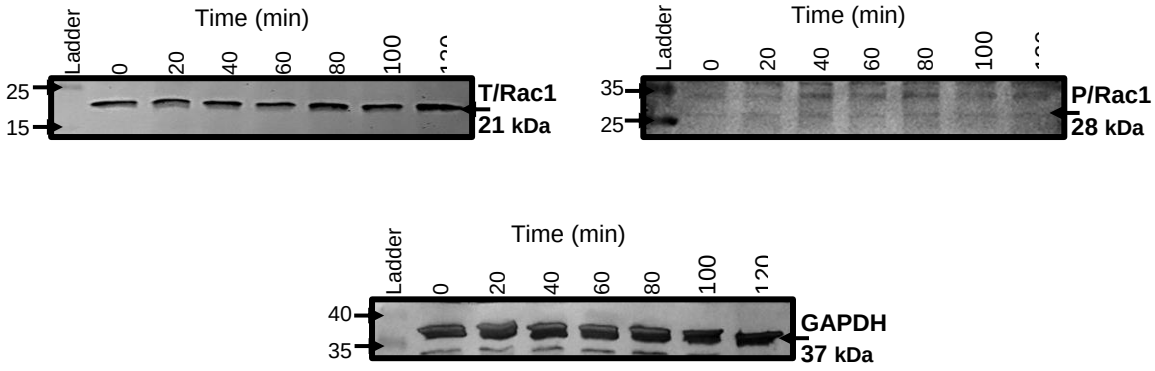

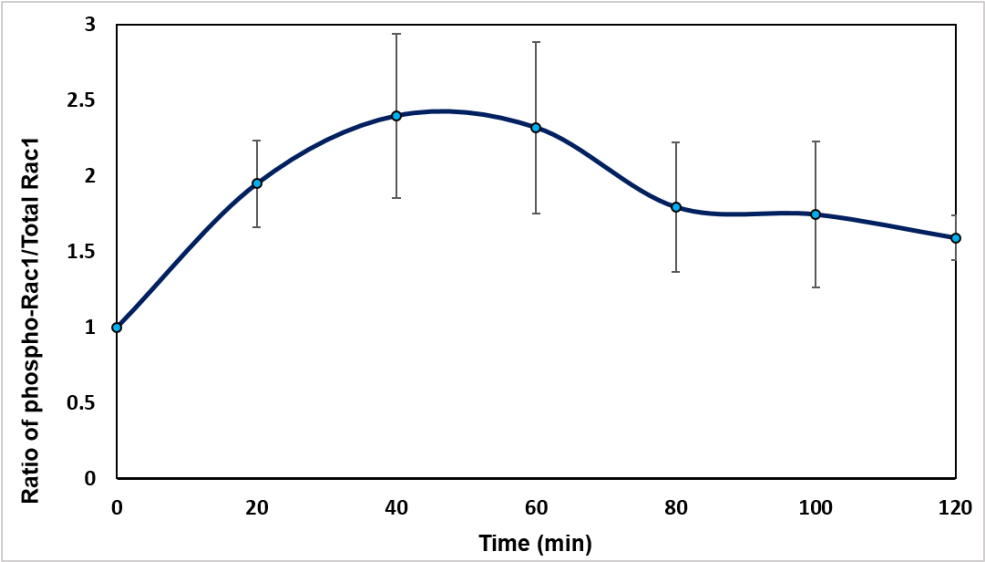

HDBEC (2 × 10^5/well) were transfected with the mutant-form plasmid (TF_{Ala253}-tGFP) and incubated for 48 h to express the protein. The cells were treated with PAR2-AP (20 μM) for up to 120 min. The cells were then collected at each time point and lysed. The samples were analysed by western blotting using a rabbit anti-human phospho-Rac1 antibody and a rabbit anti-human Rac1 antibody and the phospho-Rac1 (P/Rac1)/total Rac1 (T/Rac1) ratio calculated (The data is the average of three independent experiments and expressed as the mean ± SEM).

Figure 3.20 Time-course analysis of the phosphorylation of Rac1 in HDBEC transfected to express wild-type TF

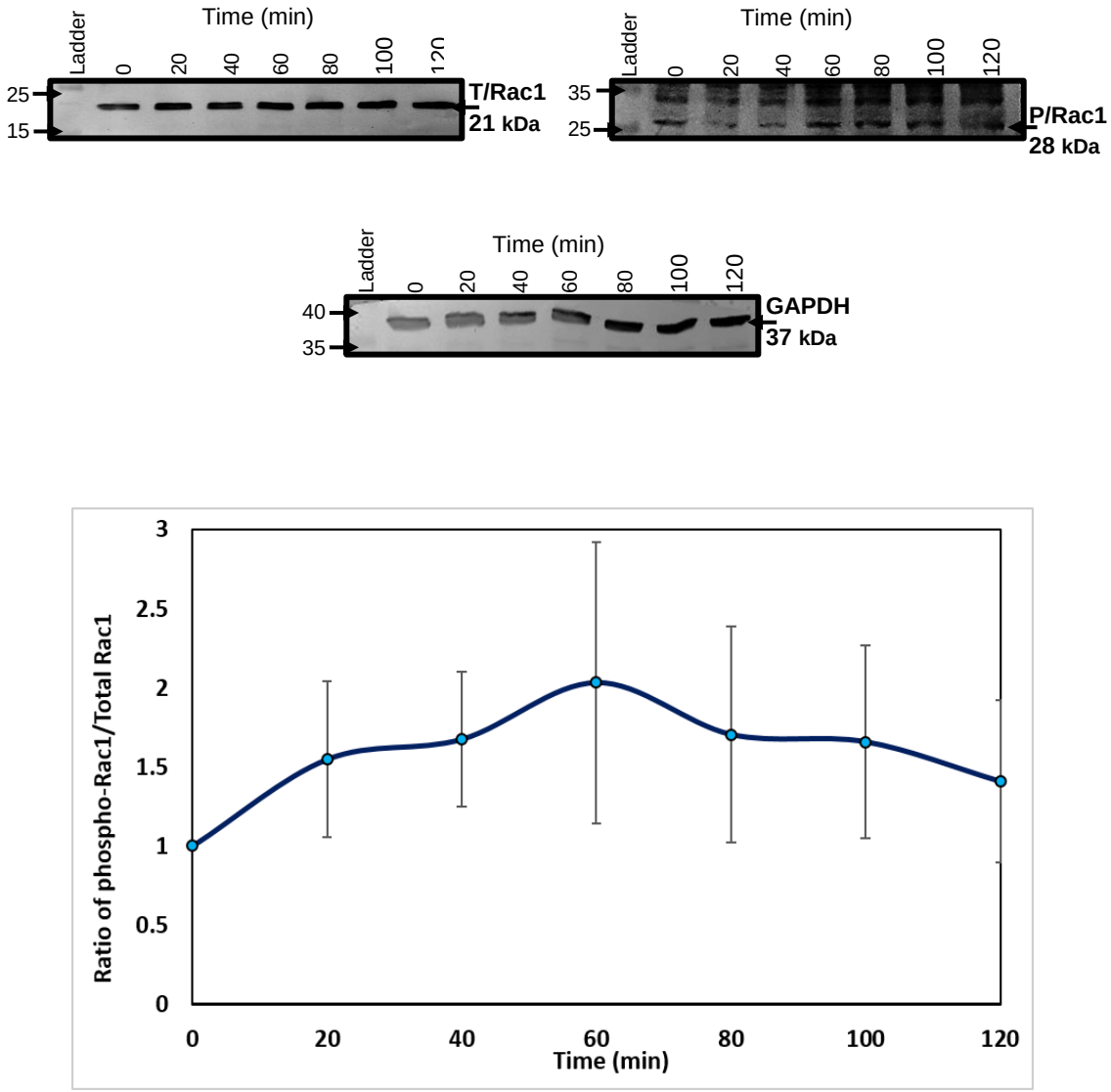

HDBEC (2 × 10^5/well) were transfected with the wild-type pCMV6-AC-TF-tGFP plasmid and incubated for 48 h to express the protein. The cells were treated with PAR2-AP (20 μM) for up to 120 min. The cells were then collected at each time point and lysed. The samples were analysed by western blotting using a rabbit anti-human phospho-Rac1 antibody and a rabbit anti-human Rac1 antibody and the phospho-Rac1 (P/Rac1)/total Rac1 (T/Rac1) ratio calculated (The data is the average of three independent experiments and expressed as the mean ± SEM).

Figure 3.21 Time-course analysis of the phosphorylation of Rac1 in HDBEC transfected to express tGFP

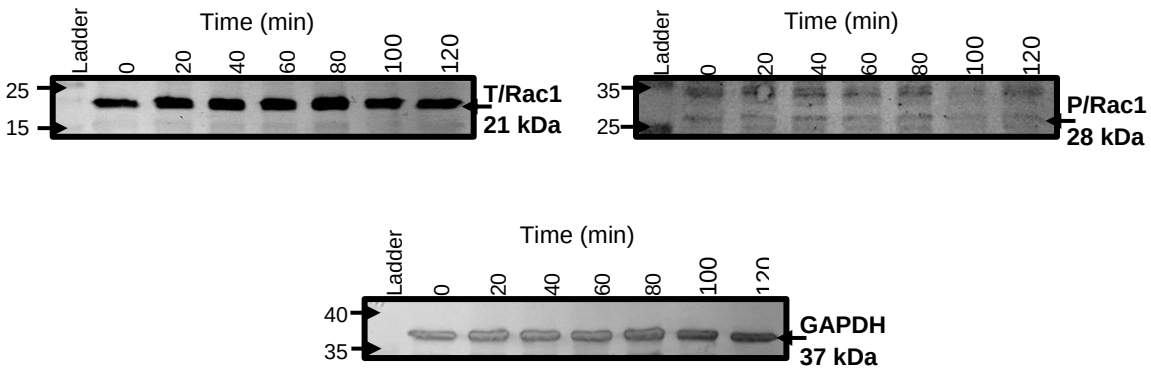

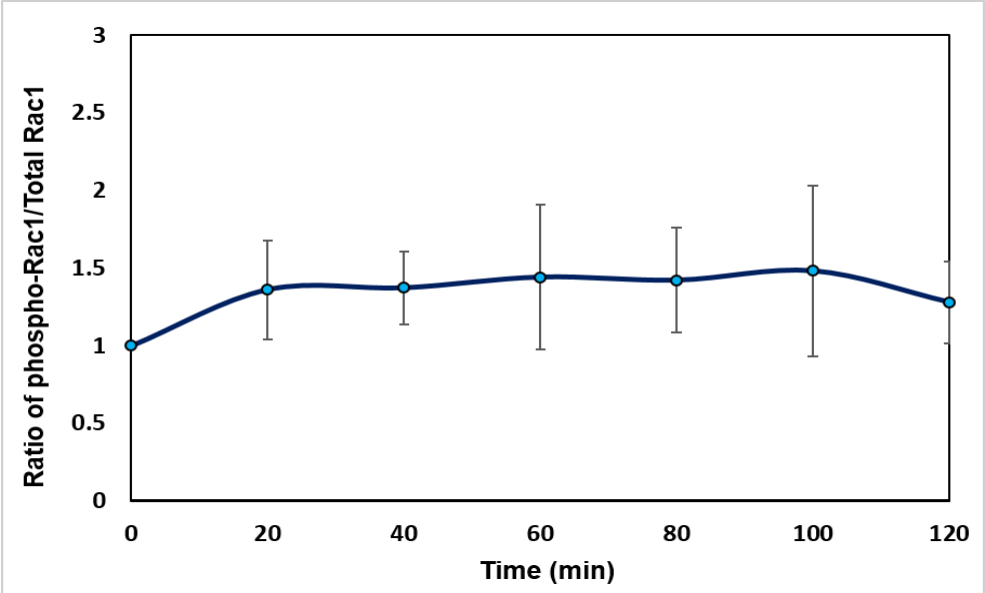

HDBEC (2 × 10^5/well) were transfected with the pCMV6-AC-tGFP plasmid and incubated for 48 h to express the protein. The cells were treated with PAR2-AP (20 μM) for up to 120 min. The cells were then collected at each time point and lysed. The samples were analysed by western blotting using a rabbit anti-human phospho-Rac1 antibody and a rabbit anti-human Rac1 antibody and the phospho-Rac1 (P/Rac1)/total Rac1 (T/Rac1) ratio calculated (The data is the average of three independent experiments and expressed as the mean ± SEM).

Figure 3.22 Time-course analysis of the phosphorylation of Rac1 in untransfected HDBEC

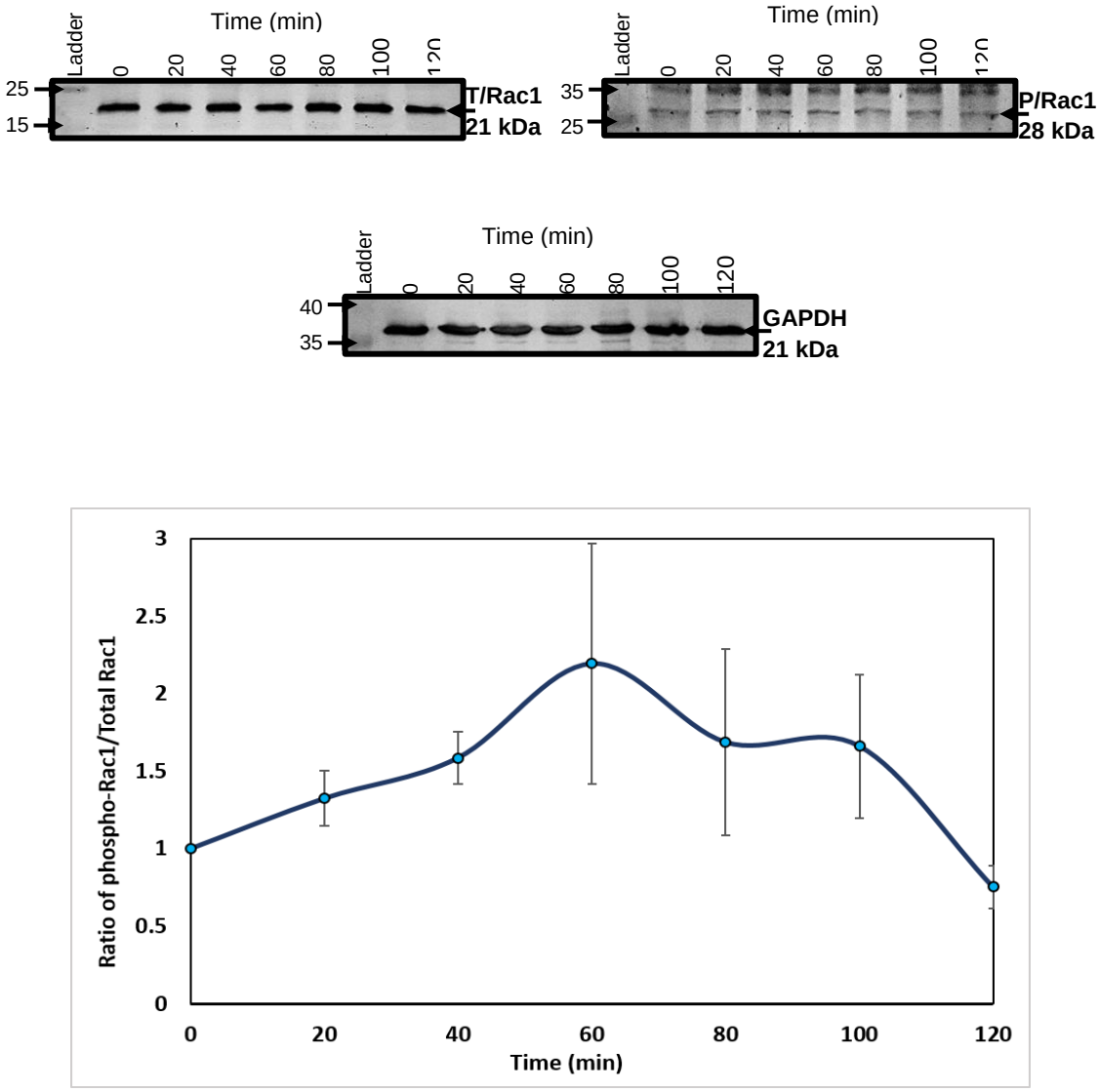

HDBEC (2×10^5/well) were treated with PAR2-AP (20 μM) for up to 120 min. The cells were then collected at each time point and lysed. The samples were analysed by western blotting using a rabbit anti-human phospho-Rac1 antibody and a rabbit anti-human Rac1 antibody and the phospho-Rac1 (P/Rac1)/total Rac1 (T/Rac1) ratio calculated (The data is the average of three independent experiments and expressed as the mean ± SEM).

3.4 Discussion

In addition to its function in coagulation, TF has the ability to regulate cellular processes, such as proliferation and apoptosis through intracellular signalling pathways (Pradier & Ettelaie, 2008; Pyo et al, 2004). TF has been detected in the circulatory system under certain pathophysiological conditions, such as cancer and cardiovascular complications, and following injury (Bach & Moldow, 1997; Giesen et al, 1999; Simak et al, 2006). Recently, it has been reported that the accumulation of TF within endothelial cells can promote cellular apoptosis through mechanisms that are mediated through p38 MAPK signalling (ElKeeb et al, 2015). Proteins including Src1, Rac1 and TAK1 mediate the signals that lead to the activation of p38 MAPK. Therefore, the present study was designed to determine the phosphorylation state of these proteins following the activation of PAR2 in endothelial cells expressing TF, in order to demonstrate a link between TF and p38 MAPK. Endothelial cells were used to investigate the phosphorylation of these proteins following the activation of PAR2, since these cells express PAR2. In addition, these cells do not express TF under normal conditions which may interfere with the signalling from the overexpressed TF-tGFP (Collier & Ettelaie, 2010). The initial objective of the study was to recognise the ability of Src1 to mediate TF-signalling, resulting in the activation of p38 MAPK in HDBEC. Cells transfected to express Ala_{253}-substituted TF (Figure 3.4) were used because this substitution results in the accumulation of TF within the cell which can lead to apoptosis. This model was used as a reproducible mean of investigating the effect of TF accumulation in cells (ElKeeb et al, 2015). The data

were compared to those obtained from cells expressing wild-type TF as well as cells expressing tGFP and also untransfected cells.

To test the role of TF in Src1 activation, the phosphorylation of Src1 was measured. The activation of PAR2 in HDBEC expressing the mutant form of TF (TF_{Ala253}-tGFP) caused the over-activation of Src1, demonstrated by the presence of a second phosphorylation peak with a high magnitude (Figure 3.15) (Figure 3.22A). This phosphorylation peak was absent following the activation of PAR2 in untransfected cells. In the presence of wild-type TF, the second phosphorylation peak was reduced compared to the mutant form of TF (TF_{Ala253}-tGFP), indicating that the increased Src1 activation resulted from the accumulation, rather than the presence of TF. Moreover, although a higher level of Src1 phosphorylation was achieved by the accumulation of TF in cells, this phosphorylation had to be initiated by PAR2 activation. This finding concerning Src1 over-activation, is in line with previous studies which have reported that induction of PAR2 without the release of TF can promote p38 MAPK activation (ElKeeb et al, 2015). Taken together, these results support the hypothesis that Src1 may be a signalling mediator connecting TF to p38 MAPK, leading to cellular apoptosis.

In addition, the possible role of Rac1 in mediating the TF-signalling to the activation of p38 MAPK was examined in HDBEC. Activation of PAR2 in HDBEC resulted in the phosphorylation of Rac1 protein regardless of expression of TF (Figure 3.19). However, previous studies have shown the ability of Src1 to activate Rac1 (Chiariello et al, 2001; Servitja et al, 2003). Also, the importance of Rac1 protein in the regulation of cellular processes including adhesion and apoptosis is well-established (Boissier & Huynh-Do, 2014; Kurdi et al, 2016; Wu et al, 2018). Therefore, Rac1 does not appear to play a role in connecting TF to

p38 MAPK. However, it has been reported that the interaction of TF/FVIIa leads to the activation of Rac1 mediated through Src1 (Versteeg et al, 2000). Therefore, it is possible that Rac1 phosphorylation could occur in response to the activation of PAR2 by the TF/FVIIa complex (Hjortoe et al, 2004)(Figure 3.22B). This also explains the similarity in the phosphorylation patterns which occurred following PAR2 activation, in the presence or absence of TF.

In conclusion, the activation of PAR2 in cells containing high levels of TF can result in the over-activation of Src1 augmenting the magnitude and duration of the resultant signal. In contrast, the activation of Rac1 is initiated by PAR2 and is independent of the levels of cellular TF. Therefore, Src1 appears to be the main connecting protein between TF and p38 MAPK. Finally, the participation of TAK1 as mediator of TF signalling was not tested and therefore, cannot be ruled out. Consequently, by inhibiting Src1 function and through the suppression of Src1 gene expression, the role of Src1 in the relationship between TF accumulation and cellular apoptosis was confirmed.

Figure 3.23 The proposed role of the TF on the activation of Src1 and Rac1

A)

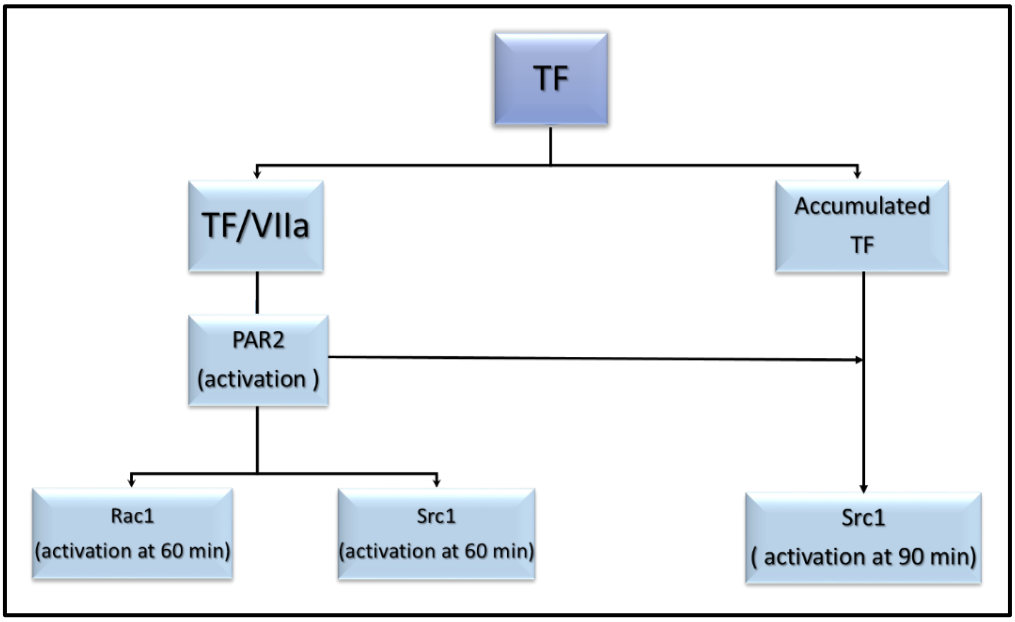

B)

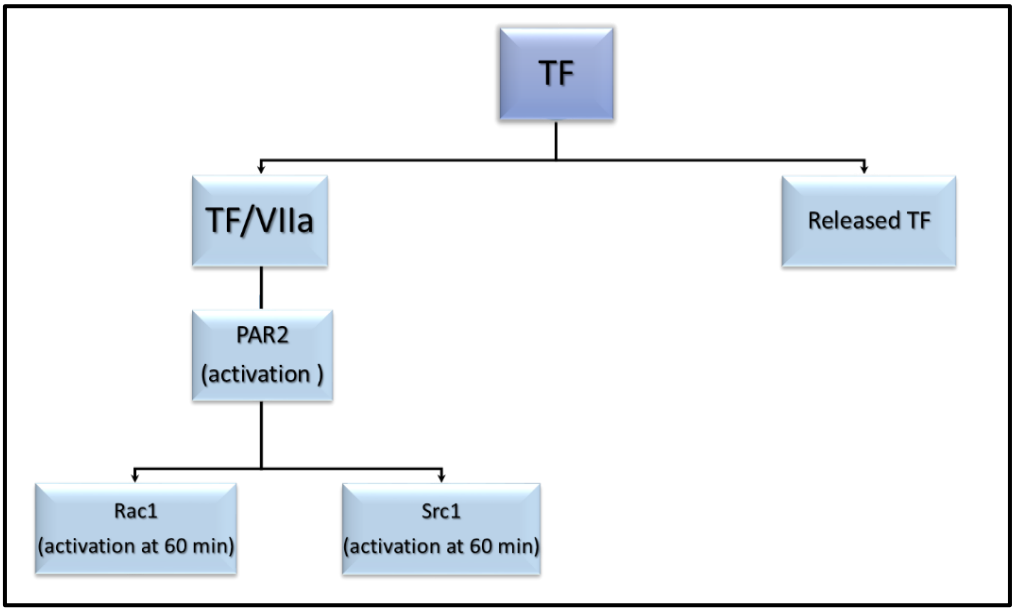

A) The activation of PAR2 following the accumulation of TF in the HDBEC resulting in over-activation of Src1 for 90 min. B) The activation of PAR2 with the presence of low level of TF results in activation of Src1 and Rac1 for 60 min.

Chapter 4

Evaluation of the role of Src1 in TF-mediated cellular apoptosis

4.1 Introduction

It has been established that Src1 protein is involved in the regulation of a number of different cellular functions, including differentiation (Behrens et al, 1993), migration (Altun-Gultekin & Wagner, 1996) and proliferation (Yeatman, 2004). A number of extracellular stimuli such as integrin, can activate Src1 resulting in stimulation of intracellular signalling pathways that induce a cell function such as apoptosis (Sirvent et al, 2012). The data obtained in the previous chapter suggest that the accumulation of tissue factor within the cells results in the over-activation of the Src1 signalling molecules. In addition, it is known that Src1 protein is capable of activating p38 MAPK (Watanabe et al, 2009). Moreover, it has been reported that the activation of p38 MAPK protein can promote cellular apoptosis trigged by TF (ElKeeb et al, 2015). Although Src1 protein plays a vital role in regulating different cellular signalling pathways (Bjorge et al, 2011; Sato et al, 1995) (Figure 4.1), the role of Src1 in the TF- p38 MAPK signalling pathway that results in cellular apoptosis is not yet clear. Therefore, the next series of experiments were designed to determine whether Src1 protein is involved in this signalling pathway by examining its role in cellular apoptosis. To assess this, 1) Src1 activity was inhibited using a specific Src1 inhibitor and 2) the protein expression was suppressed using a specific Src1 siRNA. The phosphorylation of p38 MAPK was measured following the inhibition of Src1 protein.

Figure 4.1 The role of Src1 protein in signalling pathways for different cell types

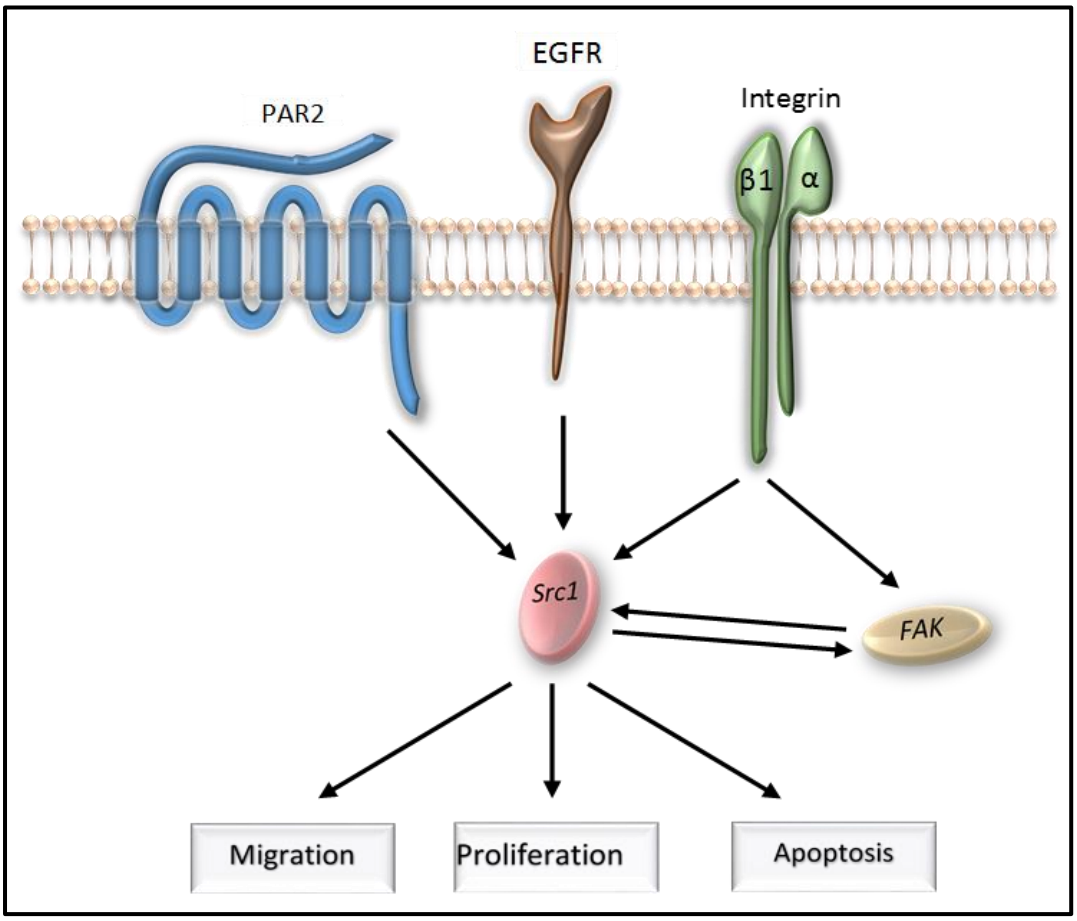

Src1 protein is proposed to regulate many different types of signalling pathways upstream and downstream, resulting in a number of cell functions.

4.1.1 Cellular apoptosis

Apoptosis can broadly be defined as a natural mechanism for programmed cell death and plays a critical role in the maintenance of the cell numbers, tissue size and shape in multicellular organisms (Danial & Korsmeyer, 2004). It is also essential for the clearance of infected or damaged cells and the removal of cells during development (Hipfner & Cohen, 2004). During apoptosis, characteristic changes can be seen in cell features, including cell shrinkage, degradation of the cell cytoskeleton, membrane blebbing, chromatin condensation and DNA fragmentation (Elmore, 2007). These changes occur because of the dimerisation of protease enzymes called caspases (McIlwain et al, 2013). Following the breakdown of DNA, the initial cellular response is the arrest of the cell cycle. This stage allows the cell to repair itself; if this is not possible then the cell undergoes apoptosis. (Hussain & Harris, 1998). Apoptosis is regulated by different cellular signals that control whether cells survive or die (Reed, 2000). It is initiated through one of two pathways: the intrinsic or the extrinsic. In the intrinsic pathway, cell stress induces the cell to kill itself, whereas in the extrinsic pathway, cell death occurs in response to external signals transmitted by other cells. Both pathways induce cellular apoptosis by the activation of cysteine-proteases called caspases and lead to the degradation of cellular proteins (Beurel & Jope, 2006). However, apoptosis is a highly regulated process and once it has started, it cannot be stopped (Beurel & Jope, 2006).

The intrinsic pathway of apoptosis is also known as the mitochondrial pathway and is regulated by intracellular signals (Kroemer & Reed, 2000), which lead to the release of mitochondrial proteins into the cell cytosol (Susin et al, 1999). This release of proteins can occur in response to cell stress such as radiation (Verheij & Bartelink, 2000), heat shock (Stankiewicz et al, 2005), nutrient deprivation

(Braun et al, 2011), hypoxia (Sendoel & Hengartner, 2014), increased levels of intracellular calcium (Uguz et al, 2009) or viral infection (Thomson, 2001). The activation of the intrinsic pathway increases the permeability of the mitochondrial membrane. This increased permeability allows for the release of proteins including cytochrome c and Smac (second mitochondria-derived activators of caspases) into the cytoplasm (Tsujimoto & Shimizu, 2007; Wang, 2001). Smacs bind to apoptosis-inhibiting proteins (IAPs). IAPs bind and inhibit caspases-3, -7 and -9 directly (Deveraux et al, 1998). The binding of Smacs-IAPs results in deactivation of the IAPs, thereby permitting apoptosis to progress (Du et al, 2000). Cytochrome c is also released from mitochondria into the cell cytosol and binds with apoptotic protease activating factor-1 (Apaf-1) and ATP to form the apoptosome (Dejean et al, 2006). Consequently, the apoptosome interacts with and activates procaspase-9, which in turn cleave and activate caspase-3 (Figure 4.2) (Wang, 2001; Zou et al, 1999).

The extrinsic pathway of apoptosis is initiated by the interaction between death activators such as Fas ligand (Fas-L) or tumour necrosis factor α (TNFα) with the corresponding death receptor on the plasma membrane of the cell (Ashkenazi & Dixit, 1998). The engagement of the death activator with its corresponding receptor induces intracellular signals as well as activating caspase-8 and -10 (Donepudi et al, 2003). As a result of this activation, these caspases are released into the cell cytoplasm which then activate caspase-3. (Liu et al, 2005). Caspase-3 cause apoptosis by liberating DNase from the inhibitor of caspase activated DNase (ICAD) as well as degradation of cytoskeleton (Weinberg, 2007).

Defects in the processes involved in cellular apoptosis can interfere with cell biology and are associated with a variety of diseases. For example, the lack of sufficient apoptosis can permit uncontrolled cell proliferation, causing cancer. In

contrast, an increase in the rate of apoptosis may result in the atrophy of the tissue.

4.1.2 The contribution of TF in cellular apoptosis

In addition to its role as the main initiator of the blood coagulation process, TF has been established as a regulator of various cellular processes, including migration and proliferation (Dorfleutner et al, 2004; Hu et al, 2013). The presence of TF in both the acellular and cellular regions of human atherosclerotic plaque within the apoptotic area suggests a possible role for TF in plaque thrombogenicity following the rupture of the plaque (Mallat et al, 1999). Studies have shown different cell responses to exogenous TF depending on the concertation of TF. Low amounts of TF induce cell proliferation, while cellular apoptosis has been reported as a result of exposure to high levels of TF (Ettelaie et al, 2007; Pradier & Ettelaie, 2008). Moreover, it has been shown that the incubation of cardiomyocyte or endothelial cells with a high concentrations of TF causes cell cycle arrest which in turn can result in cellular apoptosis (Frentzou et al, 2010). Following the release of TF-bearing microvesicles into the bloodstream, endothelial cells pick up TF-bearing microvesicles (Dasgupta et al, 2012; Osterud & Bjorklid, 2012). Pathological conditions such as cancer can lead to an accumulation of TF within the endothelial cells. The activation of these cells through inflammation or injury could stimulate pro-apoptotic mechanisms, in the endothelial cells.

Figure 4.2 The role of cytochrome c in mitochondrial pathway of apoptosis

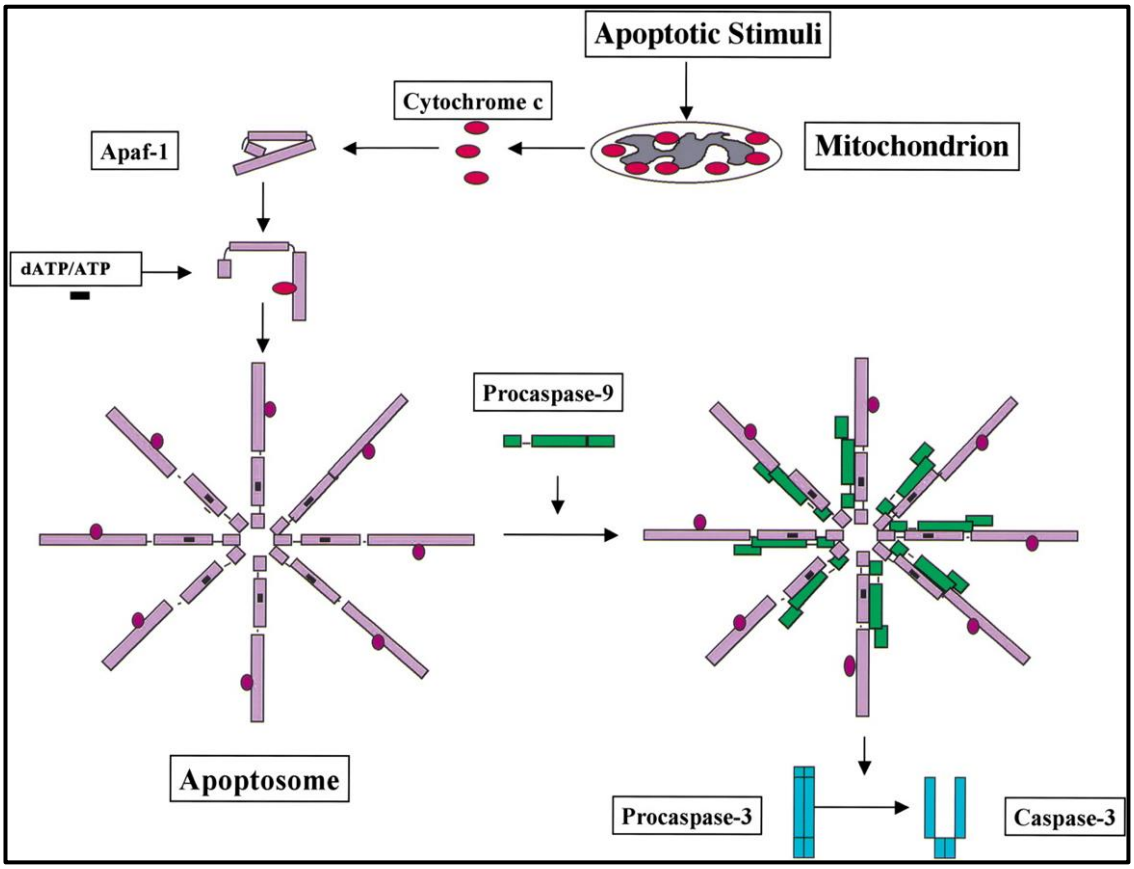

During the intrinsic pathway of apoptosis, cytochrome c is released from mitochondria into the cell cytosol where it binds to apoptotic protease activating factor-1 (Apaf-1) and ATP, to form the apoptosome. The apoptosome interacts with and activates procaspase-9, which in turn cleaves and activates caspase-3 (Wang, 2001).

4.1.3 Aims

The main objectives were to determine the role of Src1 protein in TF-mediated cellular apoptosis by:

- inhibiting the Src1 protein function using a peptide inhibitor ($pp^{60c\text{-}src}$ peptide) and
- suppressing Src1 protein expression using a specific Src1 siRNA to examine the role of Src1 signalling molecules in cellular apoptosis.

4.2 Methods

4.2.1 Examining cellular apoptosis using a TiterTACS™ Colorimetric Apoptosis Detection Kit

Throughout the process of cellular apoptosis, endonucleases cause chromosomal DNA fragmentation. In this study, a quantitative assay to detect cellular apoptosis based on fluorescent labelling of DNA fragments (TUNEL assay) was employed to measure DNA fragmentation using a TiterTACS™ Colorimetric Apoptosis Detection Kit. HDBEC (2 x 10^4/well) were seeded in 96-well plates and incubated overnight. The cells were then washed three times with PBS prior to fixation with 3.7% (v/v) PBS-buffered formaldehyde solution for 7 min each time at room temperature. The cells were then washed twice with PBS and further fixed using pure methanol at room temperature for 20 min. Samples were then washed twice with PBS and incubated with 50 µl of Cytonin solution (provided with the kit) for 15 min at room temperature to permeabilise the cells. The cells were then washed twice with dH2O (200 µl). TACS Nuclease™ Solution (50 µl) containing TACS-Nuclease TM Buffer (50 µl) and TACS-Nuclease TM (1 µl) was added to each positive control well for 30 min at 37°C to degrade cellular DNA to generate a positive control for the kit, while the other samples were covered with PBS. The wells were then washed twice with PBS for 2 min each time and incubated with 200 µl of 3% (v/v) hydrogen peroxide (H_2O_2) solution in methanol solution for 5 min at room temperature. Following a further wash with dH_2O (200 µl), 1X TdT labelling buffer (150 µl) was added to each well and incubated for a 5 min. The buffer was then removed and replaced with 50 µl of labelling reaction solution (1X TdT labelling buffer containing TdT dNTP Mix (0.35 µl), TdT enzyme (0.35 µl) and 50X Mn^{+2} (1 µl)) and incubated for 60 min at 37°C.

To stop the labelling reaction, 150 µl of 1X TdT stop buffer was added and incubated for 5 min. The cells were then washed twice with PBS for 2 min each time and incubated with the provided strep-HRP solution (50 µl) for 10 min at room temperature. The cells were then washed twice with PBS and once more with 200 µl of 0.1% (v/v) Tween 20 PBS solution. Finally, 100 µl of colorimetric substrate (TACS-Sapphire) was added to each well and incubated in the dark for 30 min at room temperature. The reactions were then stopped by adding 100 µl of 0.2 N hydrochloric acid (HCl). The samples (200 µl) were transferred to new 96-well plates and absorption was measured at 450 nm using a plate reader (POLARstar OPTIMA plate reader). Based on the amount of the DNA fragments, the level of cellular apoptosis was determined in differently treated samples. In addition, apoptosis-inducing reagents must be established to generate apoptosis prior to the experiment to be used as a positive control for comparison with treated samples.

4.2.1.1 Determining the concentration of positive control reagents to induce cellular apoptosis

HDBEC (2 x 10^4/well) were seeded in 96-well plates and treated with various reagents to induce cellular apoptosis overnight. These reagents were assessed to establish a positive control for apoptosis to be used for comparison with the treated samples. The analyses were carried out as described previously in 4.2.1. Sets of cells were incubated with cycloheximide (0-100 µg/ml), anisomycin (0-100 µg/ml) or DMSO vehicle. Other sets of cells were deprived of serum overnight to induce apoptosis. In another experiment, HDBEC (4 x 10^4/well) were seeded in 48-well plates and incubated with a different concentrations of H_2O_2 (0-1.6

mM), as H_2O_2 can cause both apoptosis and necrosis (Teramoto et al, 1999). The cells were inspected visually at 6, 16, and 18 h.

4.2.1.2 Determining the optimal incubation time for inducing cellular apoptosis using H_2O_2, TNFα, and IL-1β

To determine the optimal incubation time for inducing cellular apoptosis, HDBEC (4×10^4/well) were seeded in 48-well plates and incubated with H_2O_2 (200 μM) or TNFα (10 ng/ml) and IL-1β (10 ng/ml), as recommended by the manufacturers. Samples were analysed for cellular apoptosis at 16, 18, and 22 h using the TiterTACS™ Colorimetric Apoptosis Detection Kit, as described in section 4.2.1.

4.2.2 Optimising the knockdown of Src1 expression using siRNA

siRNA is synthetic short interfering RNA (iRNA) made of double stranded RNA used to induce the knockdown of protein coding genes in different cell types (Agrawal et al, 2003). To suppress the expression of Src1 protein in endothelial cells, a specific Src1 siRNA (Ambion® Silencer® Select Pre-designed siRNA) (see table 4.1 for details) was employed. Prior to using the Src1 siRNA in an apoptosis assay, the type of siRNA and the concentration of both siRNA and the transfection reagent were optimised.

Furthermore, the siRNA was co-transfected with the plasmid expressing wild-type or mutant form of TF_{Ala253}-tGFP. HDBEC (10^5/well) were cultured in 12-well plates in 1 ml of complete MV medium and incubated overnight. The cells were then washed with 0.5 ml of PBS, and 0.9 ml of complete MV medium was added to the cells and incubated for 1 h at 37ºC. The cells were then transfected with Src1

siRNA. Various transfection reagents were used and the amount used based on the recommendation of the manufacturer to obtain optimal transfection to reach the maximum knockdown of Src1, as follows.

4.2.2.1 Optimising the transfection reagent Lipofectamine® LTX & PLUS™ Reagent, Lipofectamine® 2000 Reagent, Lipofectamine™ 3000 Reagent and Lipofectamine RNAimax

To achieve optimal suppression of Src1 protein, the transfection reagent (Lipofectamine® LTX & PLUS™ Reagent, Lipofectamine® 2000 Reagent, Lipofectamine™ 3000 Reagent or Lipofectamine RNAimax) was mixed with Src1 siRNA complex and prepared as follows

- Plasmid DNA: 0-200 nM of Src1 siRNA concentrations were diluted in Opti-MEM I reduced serum medium (50 µl)
- Reagent solution: 3 µl of one of the transfection reagents was diluted in Opti-MEM I reduced serum medium (50 µl)

Following incubation for 5 min at room temperature, the two solutions were gently mixed and incubated for 10 min at room temperature to produce the siRNA-transfection reagent complex. After incubation, the siRNA-transfection reagent complex was added to the cells and gently shaken. Following incubation of the cells for 48 h at 37°C, cells lysate were collected and boiled for 10 min. The protein samples were then separated by SDS-PAGE and analysed using western blot, as described in section 2.2.8. Quantitative analysis of the western blots was carried out using the ImageJ program. The levels of total Src1 expression were normalised against respective GAPDH.

4.2.2.2 Optimising the Trans IT®-2020 transfection reagent

The Src1 siRNA was also transfected using Trans IT-2020 transfection reagent as described previously in 3.2.2.2 to achieve the maximum suppression of Src1 protein. The samples were incubated with Src1 siRNA at 37°C for 48 h. To examine the transfection efficiency, the protein samples were separated by SDS-PAGE as previously described in 2.2.7, and the level of Src1 protein expression was analysed using western blot as described in section 2.2.8. Quantitative analysis of the western blots was carried out using the ImageJ program. The levels of total Src1 expression were normalised against respective GAPDH.

4.2.3 Investigating cellular apoptosis following the inhibition of Src1 in TF-mediated endothelial cells apoptosis using the TiterTACS™ Colorimetric Apoptosis Detection Kit

To examine the role of Src1 in cellular apoptosis, HDBEC (4 x 10^4/well) were cultured in 48-well plates and incubated overnight. A set of cells were transfected to express a mutant form of TF (TF_{Ala253}-tGFP) or a control plasmid (pCMV6-AC-tGFP). The cells were incubated for 48 h to express the proteins. In addition, sets of untransfected cells were used as a control and adapted to low-serum medium MV containing 2% (v/v) FCS for 60 min. The cells were then treated with or without Src1 inhibitor ($pp^{60c\text{-}src}$ peptide TSTEPQpYQPGENL) (0-900 µM) or Src1 pseudo-inhibitor (TSTEPQWQPGENL) (500 µM) for a further 60 min. Finally, the cells were activated using PAR2-AP (20 µM), following which cellular apoptosis was measured at 24 h, as previously described in section 4.2.1.

Table 4.1 Silencer® Select Pre-designed siRNA information used in Src1 knockdown experiment

Target	Manufacturer	Final concentration	Sequence
Src1 protein (SRC)	Ambion® by Life Technologies™	200nM	GCACAGGACAGACAGGCUAtt
Src1 protein (NCOA1)	Ambion® by Life Technologies™	200nM	GUGUAACCAUCAAAUCGGAtt
Non targeting siRNA	Ambion® by Life Technologies™	200nM	Negative Control siRNA (Confirmed non targeting siRNA)

4.2.4 Evaluating the influence of Src1 knockdown on TF-mediated endothelial cell apoptosis using a TUNEL assay

HDBEC (2 x 10^4/well) were seeded in 96-well plates and incubated overnight. The cells were co-transfected to express a mutant form of TF (TF_{Ala253}-tGFP) together with a specific Src1 siRNA or a control siRNA. In addition, sets of cells were treated with TNFα; an untransfected set was also included. The cells were adapted to low-serum medium MV containing 2% (v/v) FCS for 1 h and then activated using PAR2-AP (20 μM). The level of cellular apoptosis was assessed at 24 h using the TiterTACS™ Colorimetric Apoptosis Detection Kit as described in section 4.2.1.

4.2.5 Evaluating the outcome of Src1 inhibition on p38 MAPK protein phosphorylation

HDBEC (10^5/well) were seeded in 12-well plates and incubated overnight. The cells were transfected to express a mutant form of TF (TF_{Ala253}-tGFP), and untransfected cells were used as a control for comparison. All cells were adapted to low-serum medium MV containing 2% (v/v) FCS for 1 h and then supplemented with a range of concentrations of the Src1 inhibitor ($pp^{60c\text{-}src}$peptide TSTEPQpYQPGENL) (0-500 μM) and incubated for 60 min. The cells were then activated by incubating PAR2-AP (20 μM) for 90 min and then lysed and boiled for 10 min. The protein samples were then separated by SDS-PAGE and analysed using western blot, as described in section 2.2.8 and using specific antibodies (Table 2.1). Quantitative analysis of the western blots was carried out using the ImageJ program, and the amount of phospho p38 MAPK was normalised against total p38 MAPK protein at each interval.

4.3 Results

4.3.1 Analysis of TiterTACS™ Colorimetric Apoptosis Detection Kit and establishing a positive control for the apoptosis assay

Throughout this work, DNA fragmentation due to cellular apoptosis was measured using a TiterTACS™ Colorimetric Apoptosis Detection Kit (TUNEL assay). Consequently, to optimise the use of the kit, a number of apoptosis-inducing reagents were compared, and the duration of the incubation with cells was determined for effective apoptosis. Artificial degradation of the DNA using the provided TACS Nuclease Solution prior to analyses produced apoptosis.

4.3.1.1 Establishing the concentration of the reagents required for optimal induction of cellular apoptosis

Initially, the ability of a range of concentrations of potential apoptosis-inducing reagents to induce apoptosis in endothelial cells was evaluated. HDBEC (2 x 10^4/well) were seeded in 96-well plates, incubated overnight and then incubated with cycloheximide (0-100 µg/ml) for 24 h (Figure 4.3). The second part of the experiment focused on the use of anisomycin (0-100 µg/ml) for 24 h to promote cellular apoptosis (Figure 4.4). Incubation of cells with either cycloheximide (0-100 µg/ml) or anisomycin (0-100 µg/ml) did not induce any measurable increase in cellular apoptosis.

In addition to treatment with cycloheximide and anisomycin, an attempt was made to induce cellular apoptosis in endothelial cells by the withdrawal of serum. However, overnight incubation of cells with the serum-free medium MV did not

result in increased cellular apoptosis for the duration of the experiment (Figure 4.5).

It has previously been shown that incubating cells with H_2O_2 can cause both apoptosis and necrosis, depending on the concentration of H_2O_2 (Teramoto et al, 1999). To examine the effect of H_2O_2, HDBEC (4 x 10^4/well) were cultured in 48-well plates, incubated with H_2O_2 (0-1.6 mM) and inspected at 6, 16 and 18 h to assess the induction of apoptosis and/or necrosis. Treatment of cells with H_2O_2 (0.8-1.6 mM) for 6 h caused a noticeable reduction in cell numbers, which suggests cell necrosis (Figure 4.6A). Furthermore, treatment for 16 h and 18 h with concentrations of 0.4 mM or higher also caused cell perturbation, as shown in Figure 4.6B and C.

4.3.1.2 Establishing the incubation time required for optimal induction of cellular apoptosis

To establish the incubation time of the apoptosis-inducing reagents, HDBEC (4 x 10^4/well) were cultured in 48-well plates. The cells were incubated with TNFα (10 ng/ml), IL-1β (10 ng/ml) for 16, 18, or 22 h or with H_2O_2 (200 μM) for 18 h. The incubation of cells with H_2O_2 (200 μM) for 18 h (Figure 4.7), TNFα (10 ng/ml) for 22 h and IL-1β (10 ng/ml) for 16-22 h (Figure 4.8) produced a maximal amount of apoptosis. Analyses was carried out using an apoptosis detection kit.

Figure 4.3 Optimisation of the induction of cellular apoptosis using cycloheximide

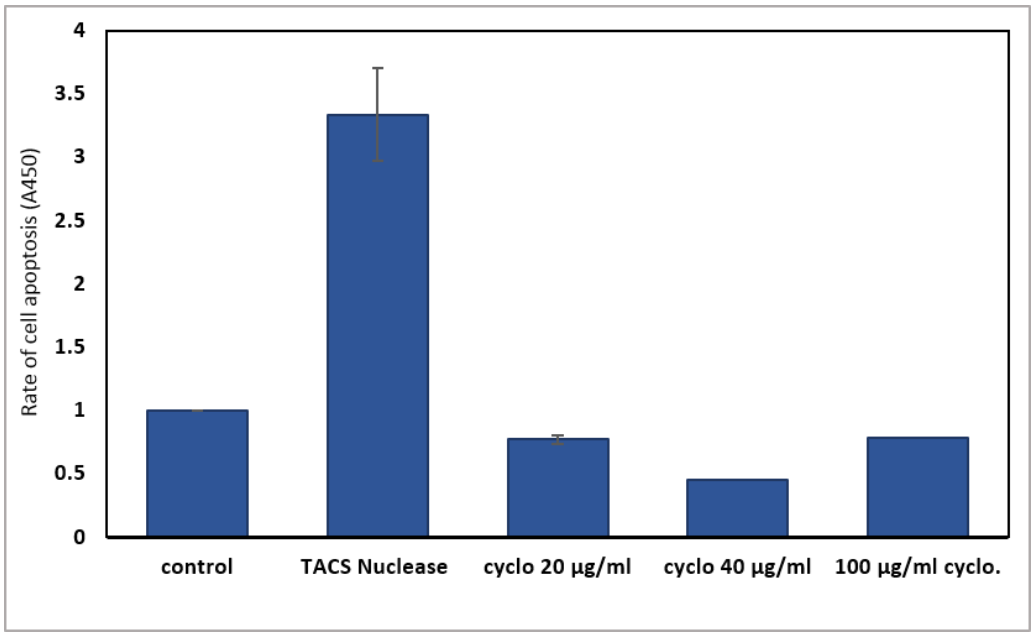

HDBEC (2 x 10^4/well) were seeded in 96-well plates and treated with (0-100 µg/ml) of cycloheximide (cyclo) for 24 h. Sets of cells were treated with TACS Nuclease Solution to degrade cellular DNA or used untreated cells and used to determine the maximum and minimum value. Cellular apoptosis was measured after 24 h using a colorimetric TUNEL assay (The data is the average of two independent experiments and expressed as ± SD).

Figure 4.4 Optimisation of the induction of cellular apoptosis using anisomycin

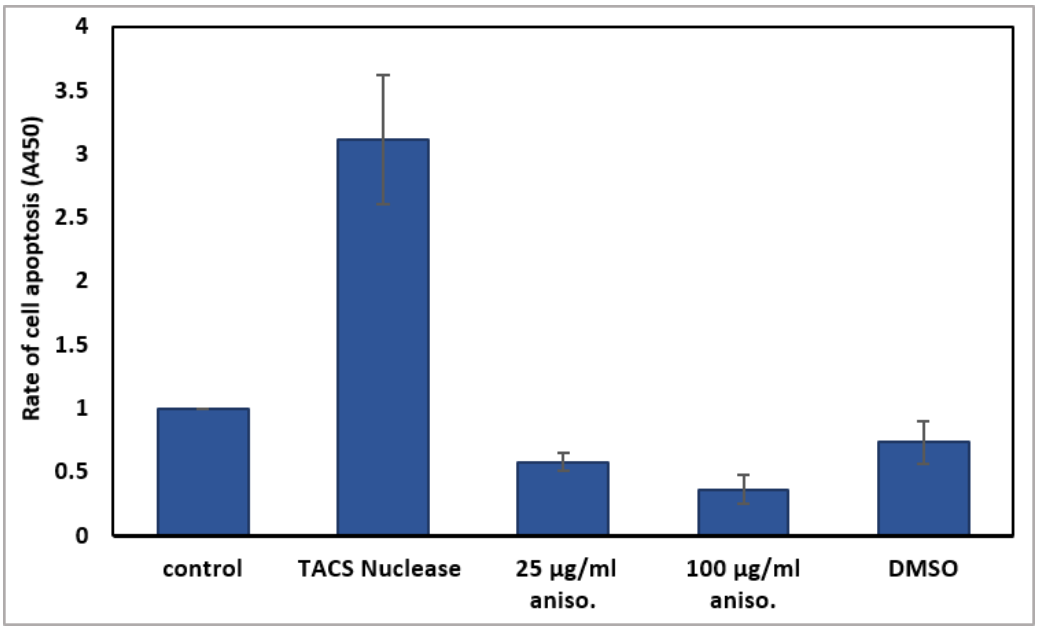

HDBEC (2 x 10^4/well) were seeded in 96-well plates and treated with (0-100 µg/ml) of anisomycin (aniso.), DMSO as a vehicle control overnight. Sets of cells were treated with TACS Nuclease Solution to degrade cellular DNA or used untreated cells and used to determine the maximum and minimum value. Cellular apoptosis was measured after 24 h using a colorimetric TUNEL assay (The data is the average of two independent experiments and expressed as ± SD).

Figure 4.5 Optimisation of the induction of cellular apoptosis using serum-free medium

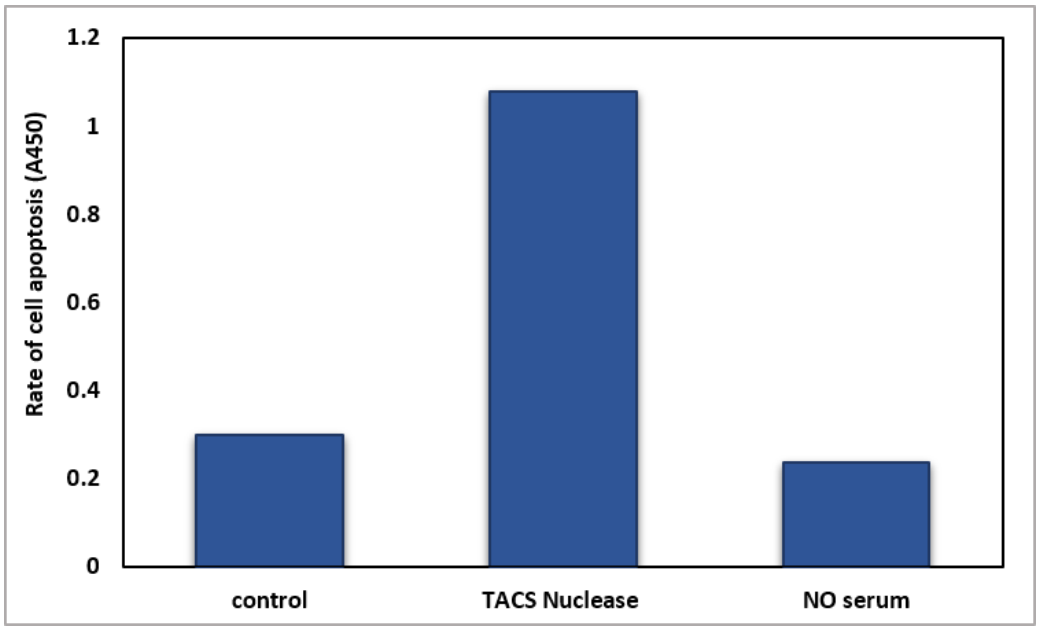

HDBEC (2 x 10^4/well) were seeded in 96-well plates and incubated overnight. Parallel set of cells were then incubated with serum-free medium. Sets of cells were treated with TACS Nuclease Solution to degrade cellular DNA or used untreated cells and used to determine the maximum and minimum value. Cellular apoptosis was measured after 24 h incubation and measured using a colorimetric TUNEL assay (n=1 independent experiment).

Figure 4.6 Examination of the induction of cellular apoptosis and necrosis using H_2O_2

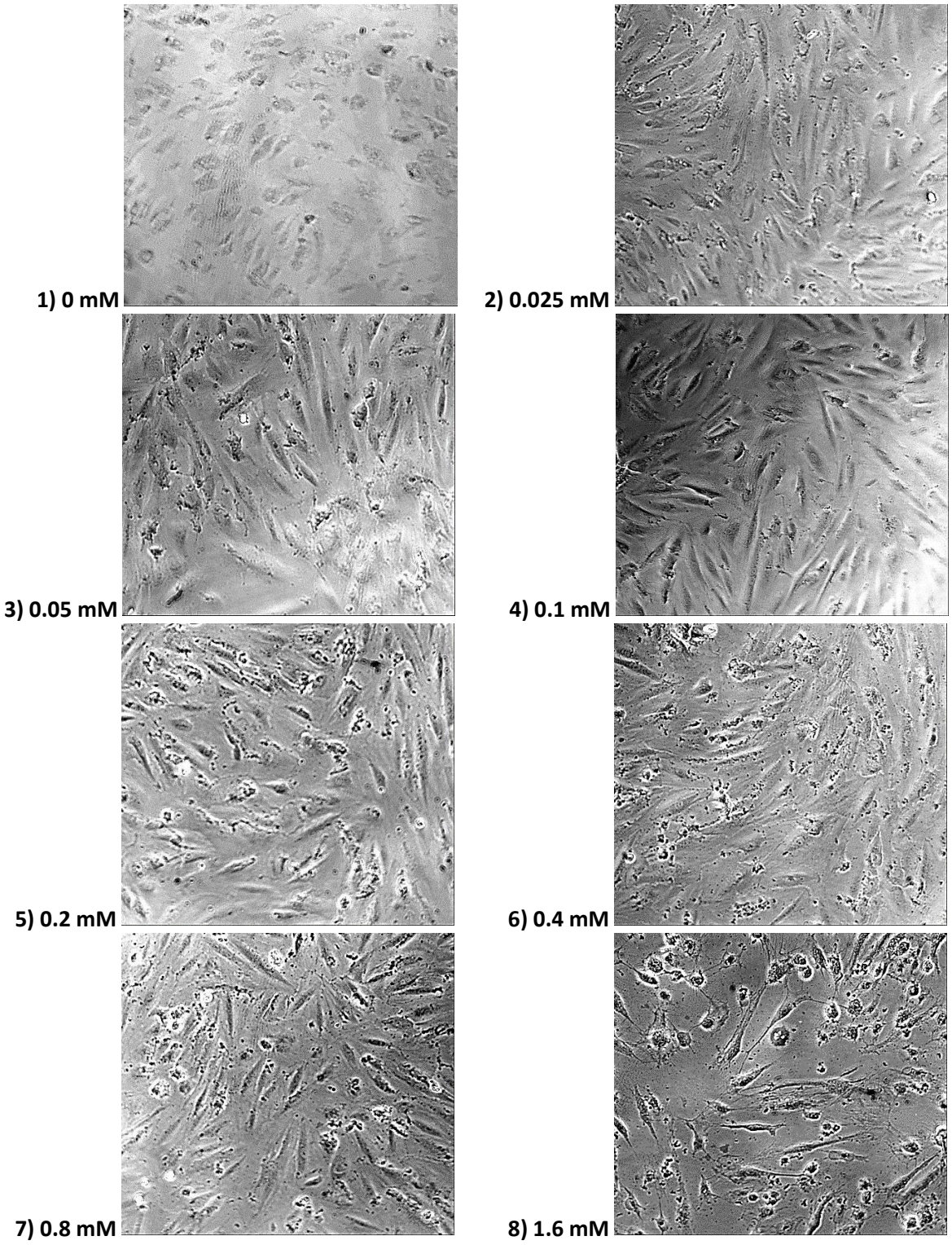

A) 6 hours

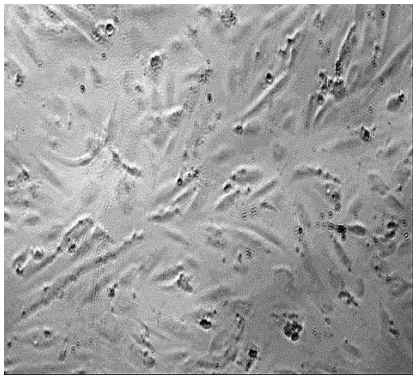

1) 0 mM

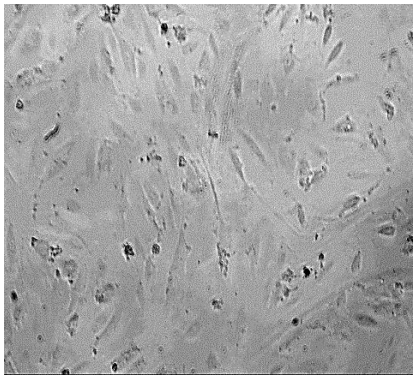

2) 0.025 mM

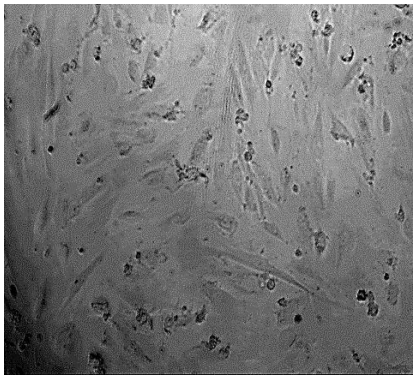

3) 0.05 mM

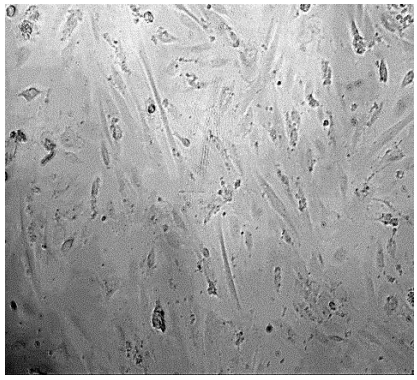

4) 0.1 mM

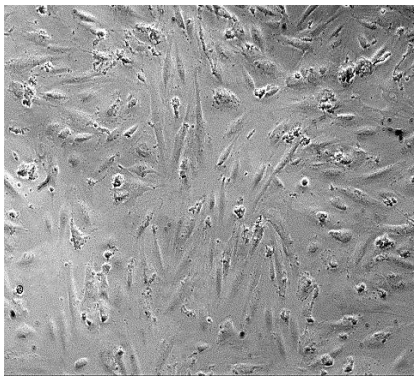

5) 0.2 mM

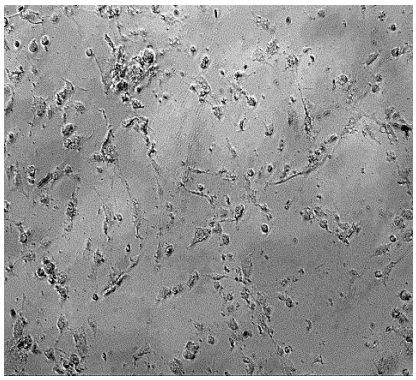

6) 0.4 mM

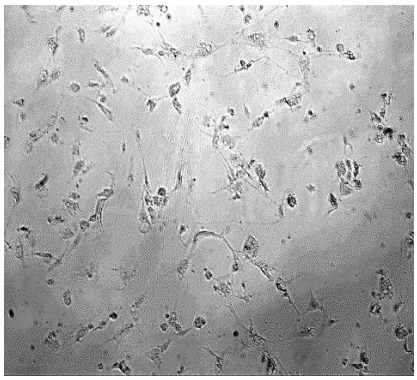

7) 0.8 mM

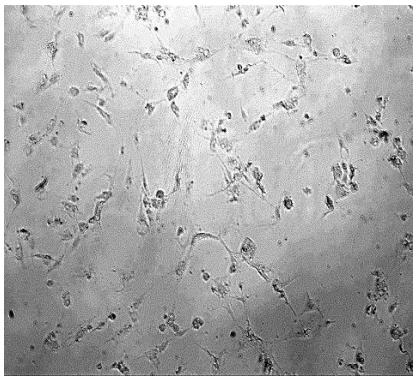

8) 1.6 mM

B) 16 hours

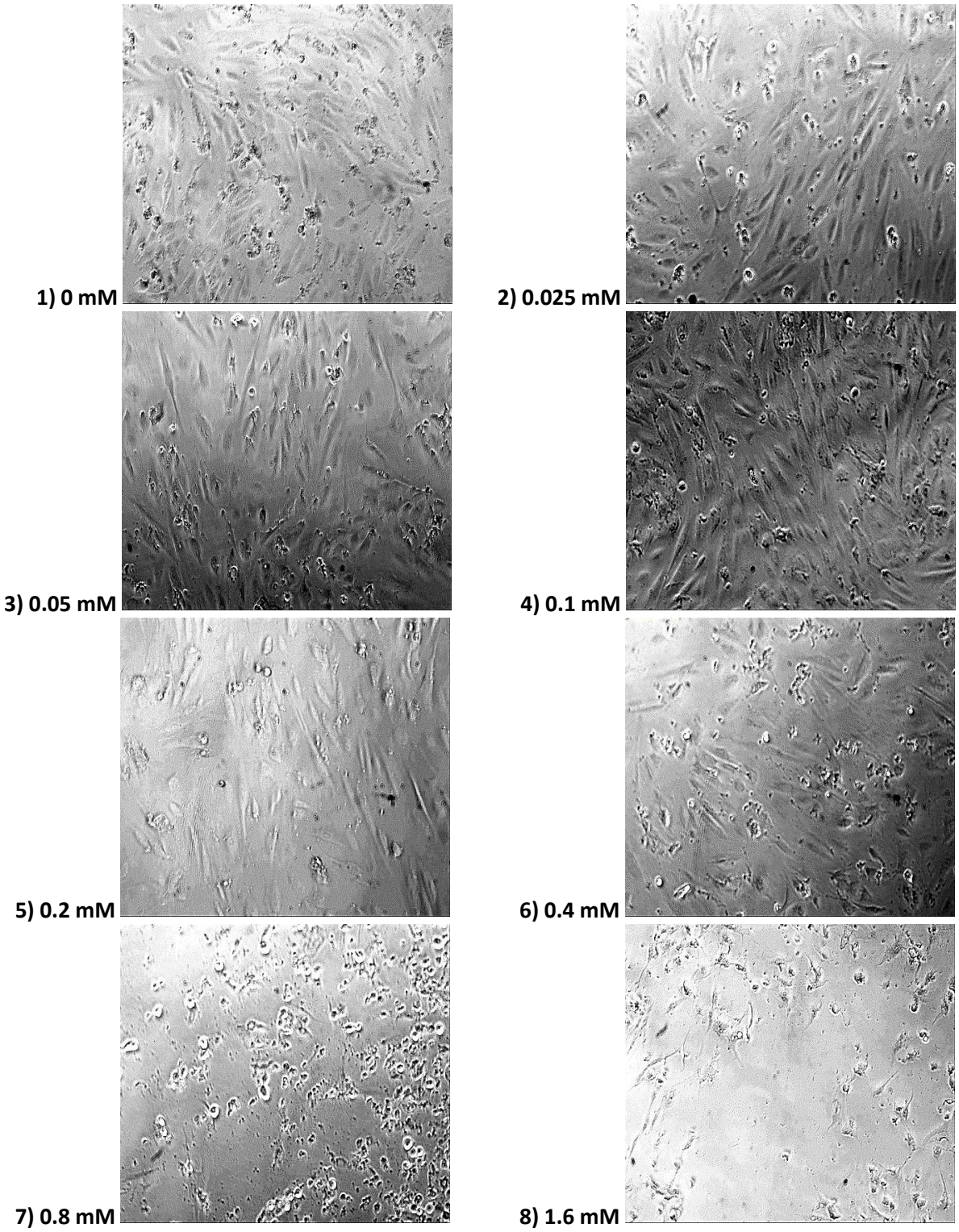

C) 18 hours

HDBEC (4 x 10^4/well) were cultured in 48-well plates and then exposed to H_2O_2 (0-1.6 mM) for A) 6 h, B) 16 h and C) 18 h. Cell morphology was investigated by examining cell integrity, shape, graininess and apparent density using a light microscope.

Figure 4.7 Cellular apoptosis induction using H_2O_2

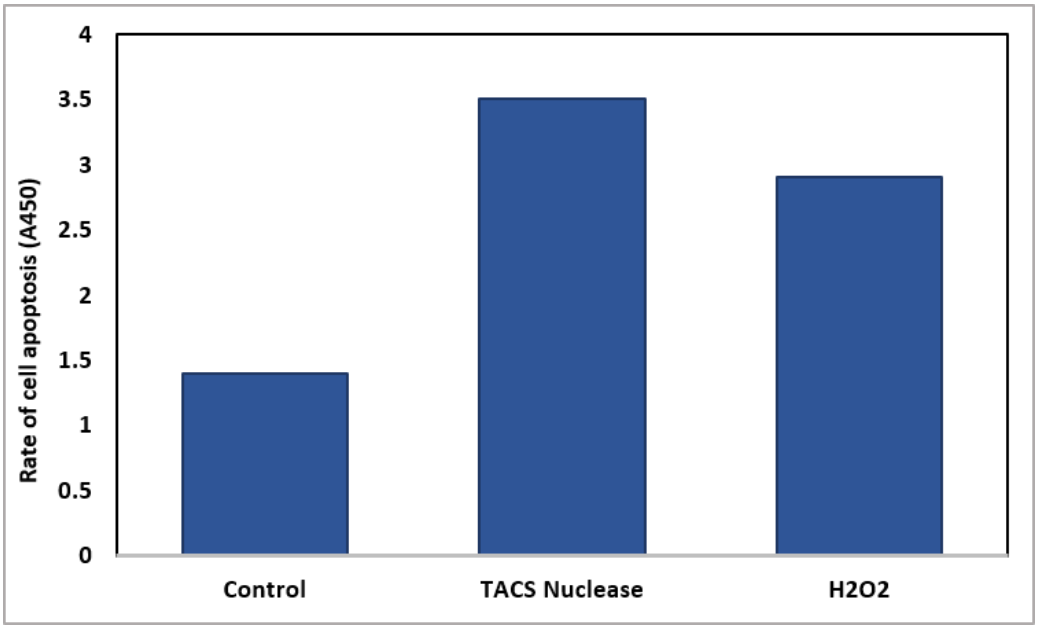

HDBEC (4 x 10^4/well) were seeded in 48-well plates. They were then incubated with H2O2 (200 µM) for 18 h. Sets of cells were treated with TACS Nuclease Solution to degrade cellular DNA or used untreated cells and used to determine the maximum and minimum value. Cellular apoptosis was measured using a colorimetric TUNEL assay (n=1 independent experiment).

Figure 4.8 Apoptosis induction using TNFα (10 ng/ml), IL-1β (10 ng/ml)

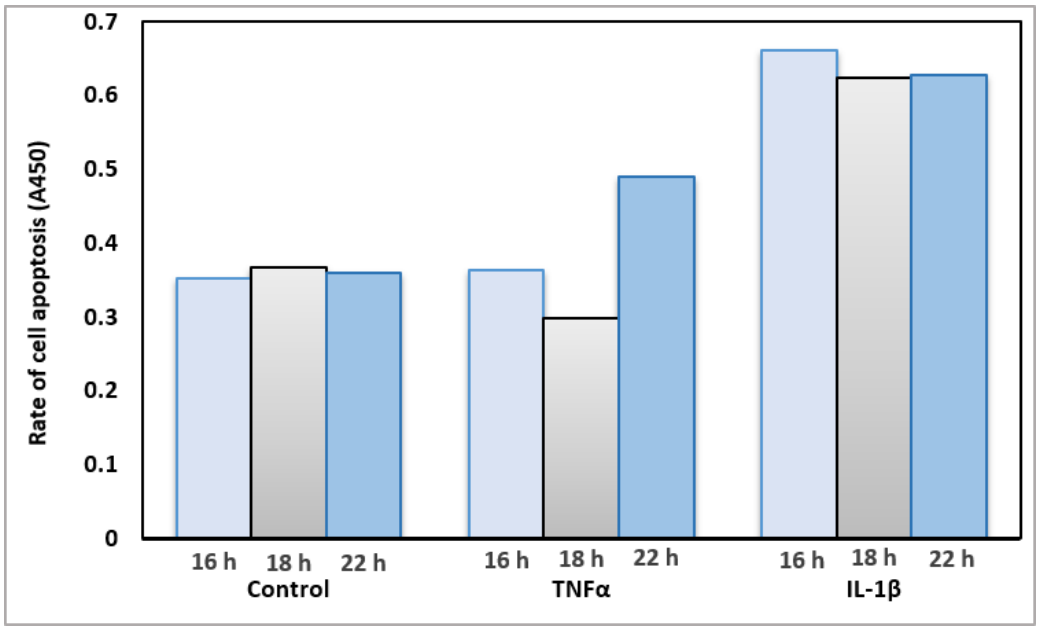

HDBEC (4 x 10^4/well) were cultured in 48-well plates. They were then incubated with TNFα (10 ng/ml) or IL-1β (10 ng/ml), for 16 h, 18 h and 22 h. An untreated set of cells was used as a control. Cellular apoptosis was measured using a colorimetric TUNEL assay (n=1).

4.3.2 Optimising silencing of Src1 expression by siRNA transfection

siRNA was designed to reduce the expression of a specific protein. To knock down the targeted protein Src1, sets of HDBEC (10^5/well) were seeded in 12-well plates and incubated overnight. New media was added, and various transfection reagents were tested in an attempt to transfect the cells with a specific Src1 siRNA. Following the transfection, the cells were incubated for 48 h, and the expression of Src1 protein was examined using western blot. The membranes were analysed using the ImageJ program, and the amount of total Src1 protein was normalised against GAPDH in each sample.

The first sets of experiments were done using 3 µl of Lipofectamine 3000, Lipofectamine LTX together with PLUS™ and Lipofectamine 2000 transfection reagents. The cells were transfected with Src1 siRNA (NCOA1) (5 nM with Lipofectamine 3000, 5 nM with Lipofectamine LTX together with PLUS and 150 nM with Lipofectamine 2000 separately). In these transfections, no evidence of a significant reduction in the amount of Src1 protein was found. Figure 4.9 shows a slight reduction in Src1 expression compared to the control.

An assessment of Src1 knockdown using Lipofectamine RNAimax showed a possible reduction when using 2.5 nM of siRNA (NCOA1) (Figure 4.10A). On further examination over a range of (0-2 nM), a better level of gene silencing was obtained at 2 nM (Figure 4.10B). However, even with the optimal concentration, only marginal levels of Src1 knockdown were observed.

Figure 4.9 Assessment of Src1 siRNA (NCOA1) transfection efficiency using Lipofectamine 3000, Lipofectamine LTX & PLUS and Lipofectamine 2000

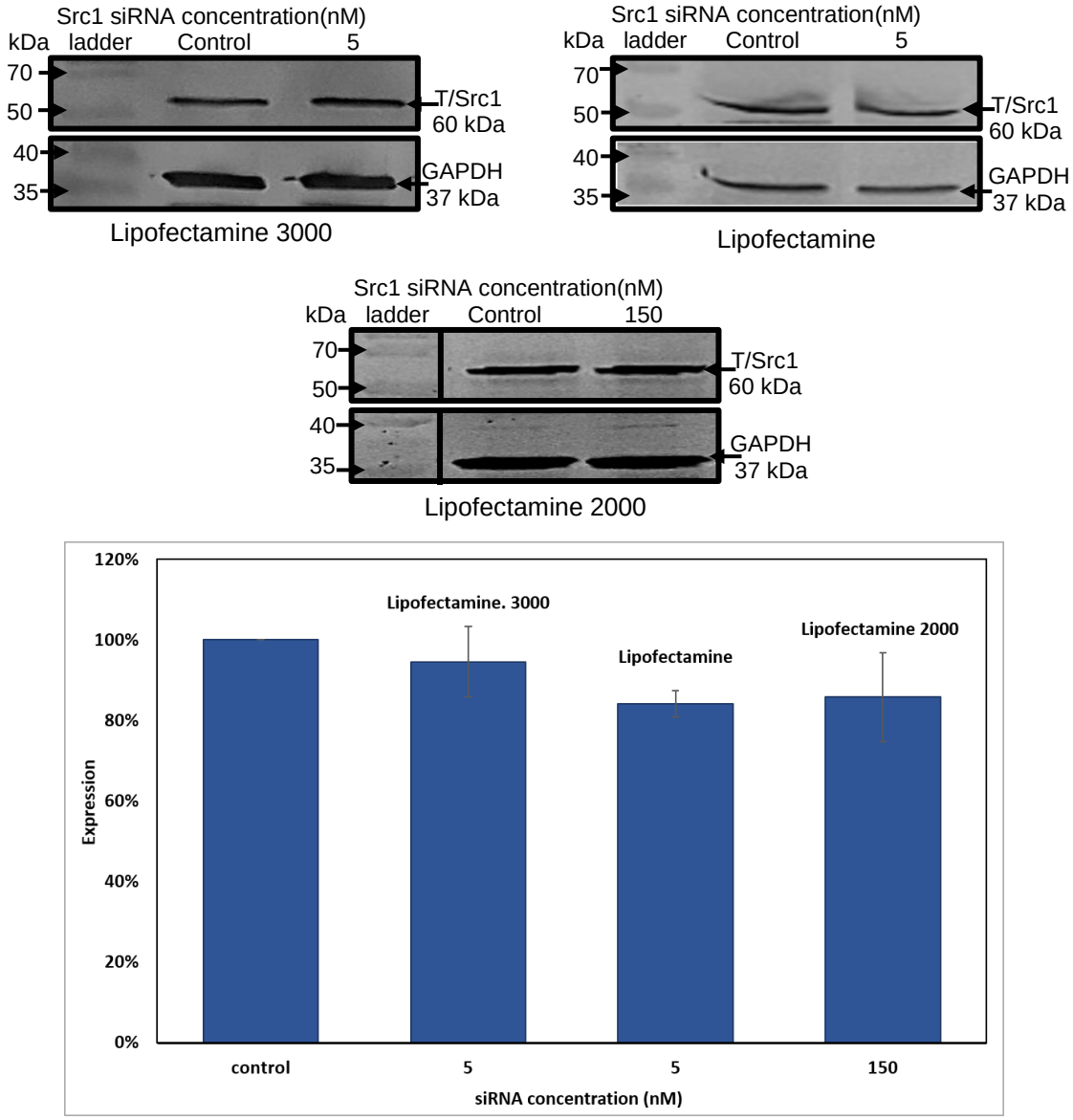

HDBEC (10^5/well) were transfected with 0-150 nM of specific Src1 siRNA (NCOA1) using 3 µl of Lipofectamine™ 3000, Lipofectamine LTX & PLUS and Lipofectamine 2000 transfection reagent and incubated for 48 h. The expression of Src1 protein was examined using western blot and the amount of total Src1 (T/Src1) protein was normalised against GAPDH using ImageJ program analyses (The data is the average of three independent experiments and expressed as the mean ± SEM).

Figure 4.10 Assessment of Src1 siRNA (NCOA1) transfection efficiency using Lipofectamine RNAimax transfection Reagent

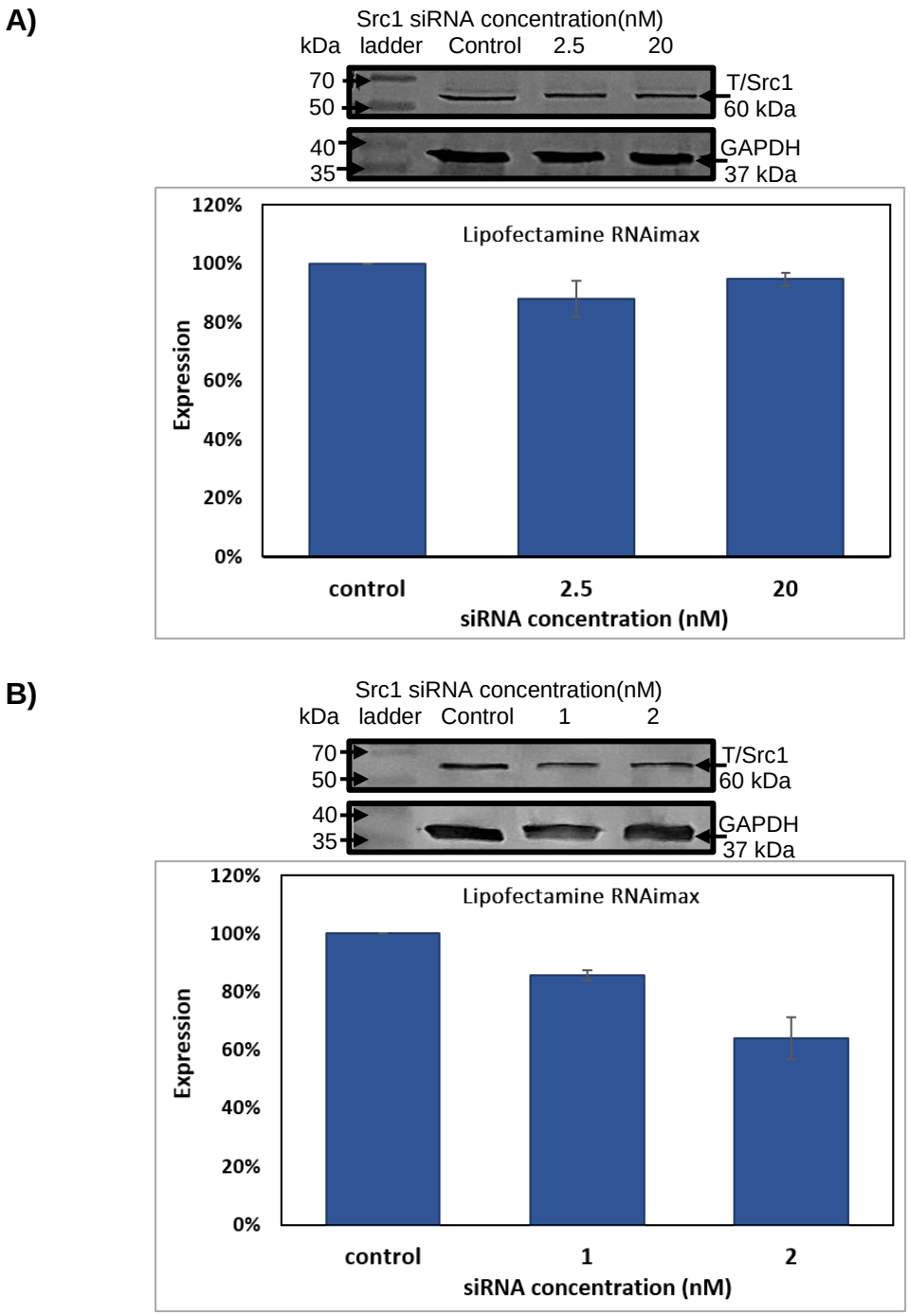

HDBEC (10^5/well) were transfected with A) 0-20 nM or B) 0-2 nM of specific Src1 siRNA (NCOA1) using 3 µl of Lipofectamine RNAimax transfection reagent and incubated for 48 h. The expression of Src1 protein was examined using western blot and the amount of total Src1 protein (T/Src1) was normalised against GAPDH using ImageJ program analyses (The data is the average of two independent experiments and expressed as ± SD).

Because none of the used reagents achieved a significant Src1 knockdown, TransIT-2020 transfection reagent (3 µl) was used to transfect a set of HDBEC with two series of concentrations of Src1 siRNA (NCOA1) (0-10 and 0-150 nM). Figure 4.11A shows a slight reduction in the Src1 expression, and the reduction was about 35% at 150 nM (Figure 4.11B). However, the results in Figure 4.11 show that the decrease in the expression of Src1 protein is still less than required to have the proposed effect on the molecular signalling pathway.

Following the establishment of TransIT-2020 transfection reagent as a suitable transfection reagent for the siRNA-mediated knockdown of Src1, a second siRNA (SRC) was tested and the effective concentrations examined. Sets of HDBEC were transfected with a series of concentrations of Src1 siRNA (SRC) (0-200 nM) using the TransIT-2020 transfection reagent (3 µl). An examination of the expression of Src1 protein by western blot indicated a 77.12% reduction in Src1 protein expression following transfection with 200 nM of SRC siRNA (Figure 4.12).

4.3.3 Examining the role of Src1 in TF-induced endothelial cell apoptosis by inhibiting Src1

To determine the optimal concentration of the Src1 inhibitor, HDBEC (4 x 10^4/well) were seeded in 48-well plates and transfected to express a mutant form of TF (TF_{Ala253}-tGFP). Following the incubation of the cells for 48 h, the cells were adapted to low-serum medium MV containing 2% (v/v) FCS for 60 min and then treated with (0-900 µM) of Src1 inhibitor ($pp^{60c\text{-}src}$peptide) for a further 60 min.

Subsequently, the samples were activated using PAR2-AP (20 μM) to induce cellular apoptosis and measured after 24 h using a TiterTACS™ Colorimetric Apoptosis Detection Kit. Pre-incubation of cells with $pp^{60c\text{-}src}$ (0-500 μM) reduced the TF-induced cellular apoptosis in a concentration-dependent manner (Figure 4.13). However, significant levels of cellular apoptosis were detected at higher concentrations of $pp^{60c\text{-}src}$ (700-900 μM).

Figure 4.11 Assessment of Src1 siRNA (NCOA1) transfection efficiency using TransIT-2020 transfection reagent

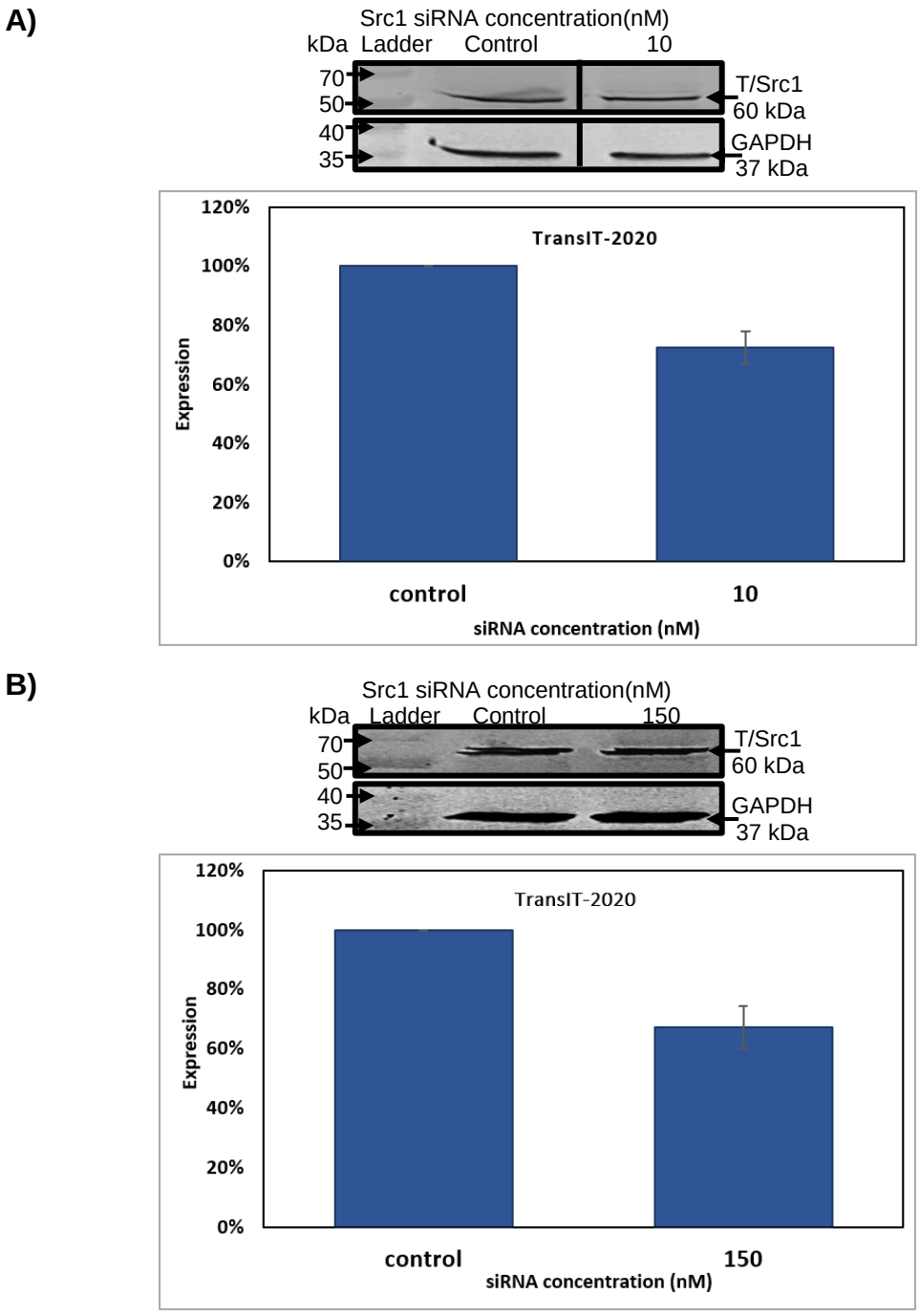

HDBEC (10^5/well) were transfected with A) 0-10 nM or B) 0-150 nM of Src1 siRNA (NCOA1) using 3 µl TransIT-2020 Transfection Reagent and incubated for 48 h. The expression of Src1 protein was examined using western blot, and the amount of total Src1 protein (T/Src1) was normalised against GAPDH using ImageJ program analyses (The data is the average of three independent experiments and expressed as the mean ± SEM).

Figure 4.12 Assessment of Src1 siRNA (SRC) transfection efficiency using TransIT-2020 transfection reagent

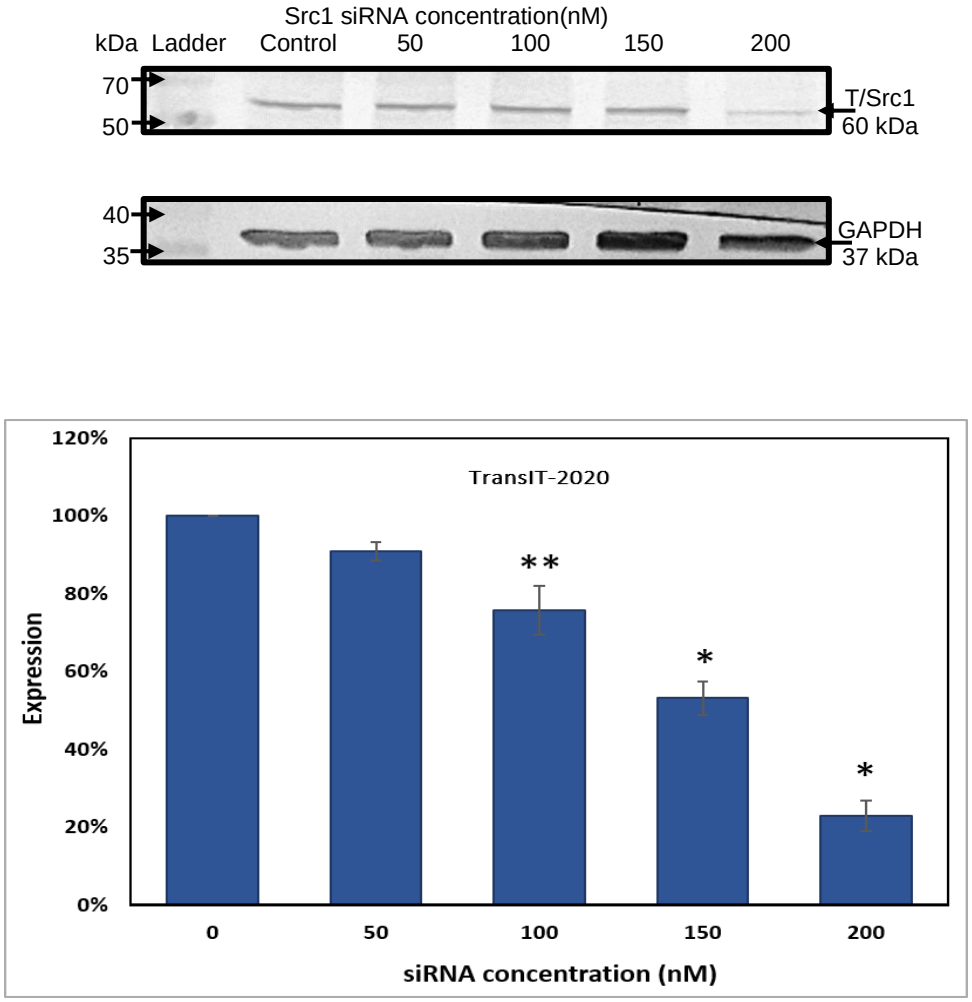

HDBEC (10^5/well) were transfected with 0-200 nM of specific Src1 siRNA (SRC) using 3 µl of TransIT-2020 transfection reagent and incubated for 48 h. The expression of Src1 protein was examined using western blot, and the amount of total Src1 protein (T/Src1) was normalised against GAPDH using ImageJ program analyses (The data is the average of two independent experiments and expressed as the SD; * = P<0.01, ** = P<0.05 vs no inhibitor).

Figure 4.13 The effect of $pp^{60c\text{-}src}$ on TF-induced endothelial cellular apoptosis

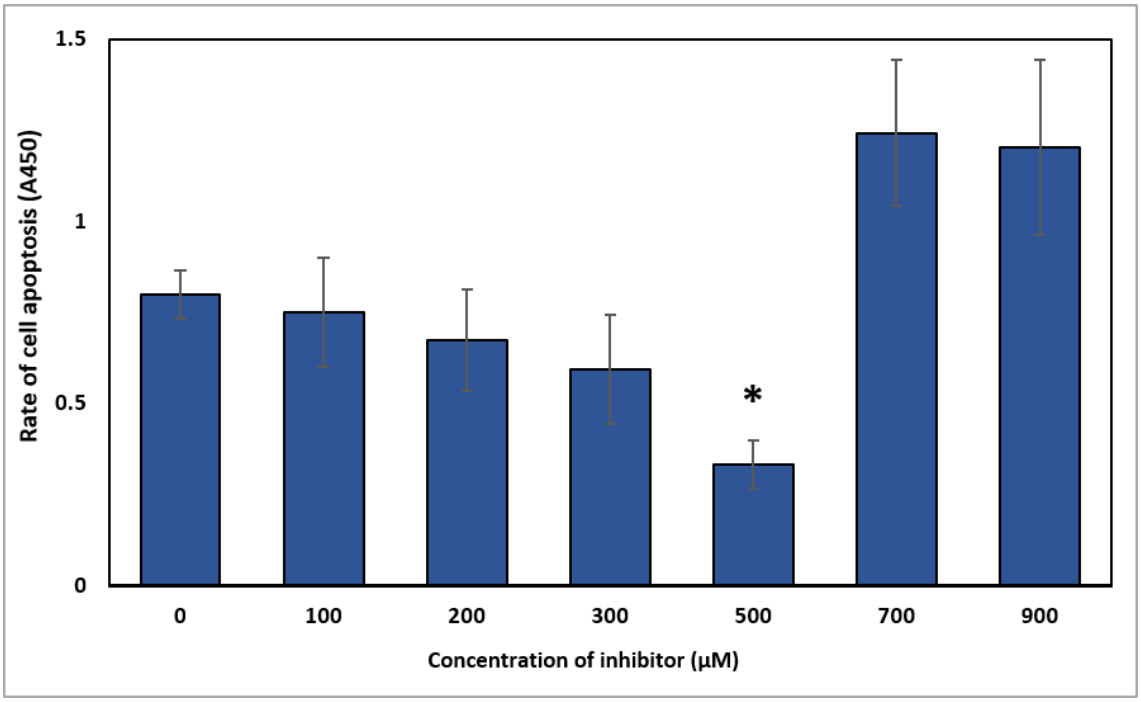

HDBEC (4×10^4) were cultured and transfected with TF_{Ala253}-tGFP plasmid. Following 48 h of incubation, the cells were adapted to low-serum medium MV containing 2% (v/v) FCS for 60 min and incubated with (0-900 μM) of Src1 inhibitor ($pp^{60c\text{-}src}$peptide TSTEPQpYQPGENL) for a further 60 min. Cellular apoptosis was measured after 24 h post-activation with PAR2-AP (20 μM) using a colorimetric TUNEL assay (The data is the average of four independent experiments and expressed as the mean ± SEM; * = $P<0.05$ vs. no inhibitor).

To assess the role of Src1 in TF-mediated endothelial cell apoptosis, HDBEC (4 x 10^4/well) were seeded in 48-well plates and transfected to express a mutant form of TF (TF_{Ala253}-tGFP). Following 48 h of incubation, the cells were adapted to low-serum medium MV containing 2% (v/v) FCS for 60 min. The cells were then incubated with or without Src1 inhibitor ($pp^{60c\text{-}src}$peptide TSTEPQpYQPGENL) (500 µM) or Src1 pseudo-inhibitor (TSTEPQWQPGENL) (500 µM) for a further 60 min before activation with PAR2-AP (20 µM). Sets of cells were also transfected to express control tGFP or used untreated. In addition, sets of cells were treated with IL-1β to be used as a positive control. The level of cellular apoptosis was measured after 24 h using a TiterTACS™ Colorimetric Apoptosis Detection Kit. The activation of PAR2 in cells expressing a mutant form of TF (TF_{Ala253}-tGFP) resulted in increased cellular apoptosis compared to untreated cells (control) (Figure 4.14). Furthermore, the induction of apoptosis was dependent on the expression of TF_{Ala253}-tGFP and also, was induced following PAR2 activation. However, pre-incubation of the cells expressing a mutant form of TF with Src1 inhibitor prior to activation with PAR2-AP significantly decreased the level of apoptosis, while the high level of apoptosis remained unchanged in cells pre-incubated with the pseudo-inhibitor (Figure 4.15).

4.3.4 Examining the role of Src1 in TF-mediated endothelial cells apoptosis through Src1 gene silencing

To assess the role of Src1 signalling molecules in cellular apoptosis triggered by the presence of TF, HDBEC (2 x 10^4/well) were cultured in 96-well plates and co-transfected to express a mutant form of TF (TF_{Ala253}-tGFP) together with either

Src1 siRNA (SRC) or a control silencer siRNA. The cells were adapted to low-serum medium MV containing 2% (v/v) FCS for 1 h prior to activation using PAR2-AP (20 µM). Sets of cells were also examined untransfected or treated with TNFα to induce apoptosis. Cellular apoptosis levels were analysed in all samples after 24 h. Cellular apoptosis was induced following the activation of PAR2 in cells expressing a mutant form of TF (TF_{Ala253}-tGFP). The level of apoptosis was significantly decreased due to Src1 silencing in activated cells expressing a mutant form of TF, which indicates that cellular apoptosis triggered by TF is dependent on Src1 signalling molecules (Figure 4.16).

Figure 4.14 TF-induced endothelial cellular apoptosis

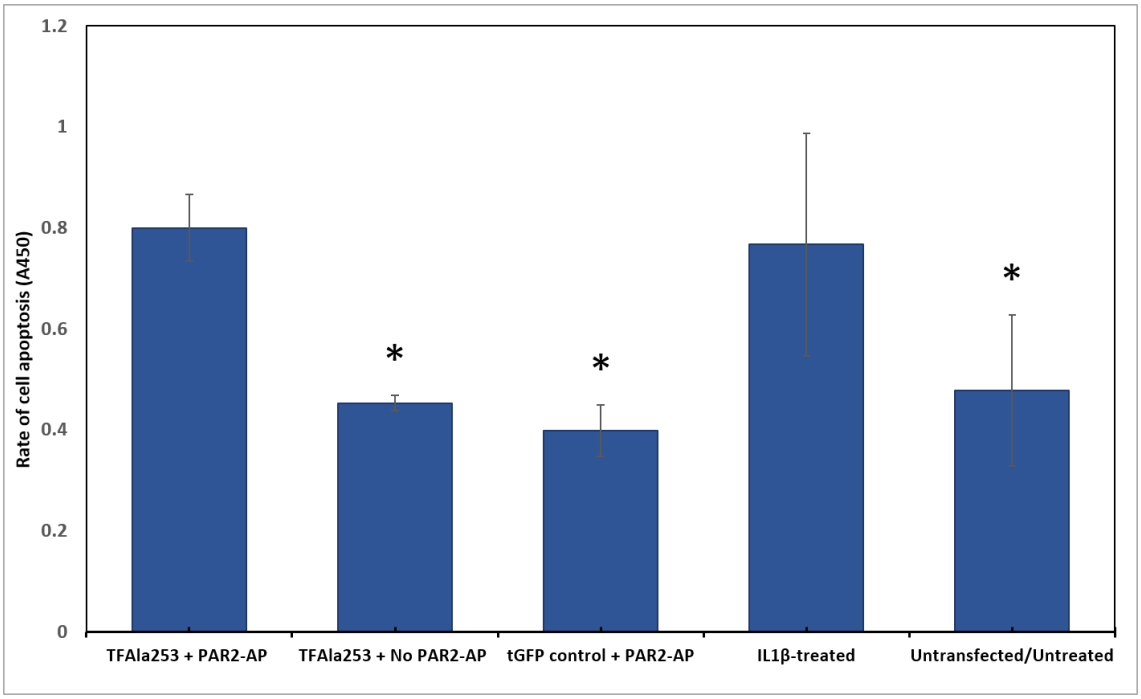

HDBEC (4 x 10^4/well) were seeded in 48-well plates, incubated overnight and transfected with TF_{Ala253}-tGFP, tGFP plasmid. Following 48 h of incubation, the cells were adapted to low-serum medium MV containing 2% (v/v) FCS for 60 min. The cells were then activated using PAR2-AP (20 µM). Sets of cells were treated with IL-1β to be used as a positive control or used untreated. Cellular apoptosis was measured after 24 h post-activation using a colorimetric TUNEL assay (The data is the average of four independent experiments and expressed as the mean ± SEM; * = P<0.05 vs. PAR2 activated cells expressing TF_{Ala253}-tGFP).

Figure 4.15 Endothelial cellular apoptosis following the inhibition of Src1

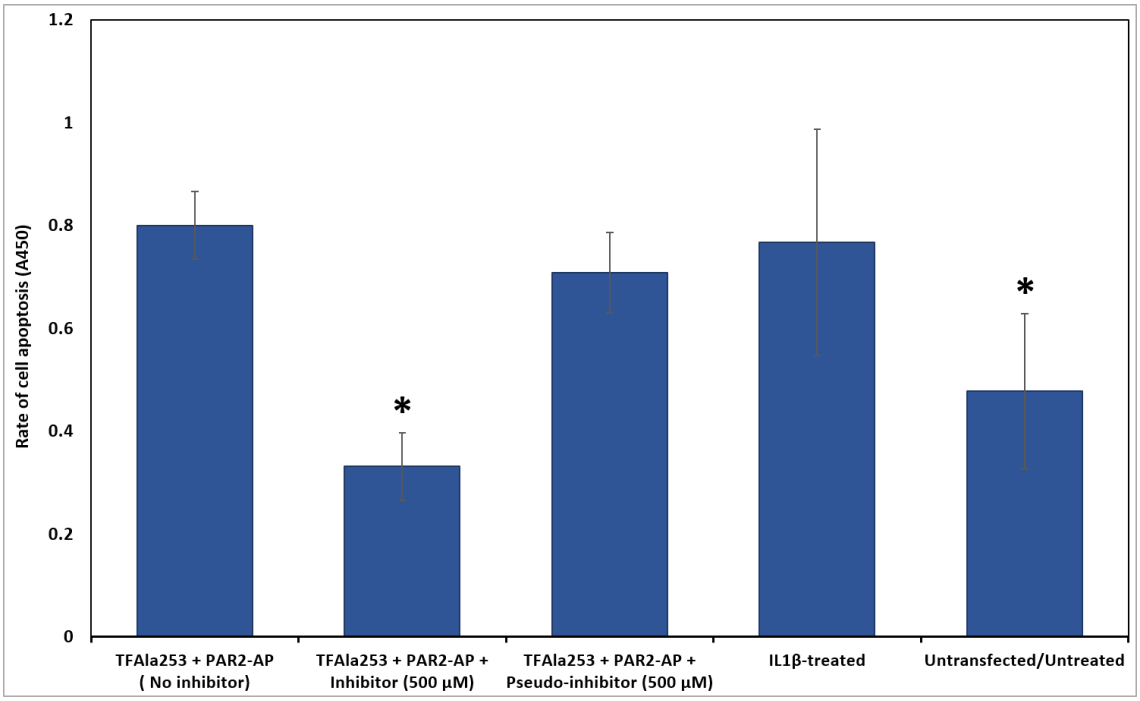

HDBEC (4 x 10^4/well) were seeded in 48-well plates, incubated overnight and transfected with TF_{Ala253}-tGFP plasmid. Following 48 h of incubation, the cells were adapted to low-serum medium MV containing 2% (v/v) FCS for 60 min. The cells were pre-incubated with Src1 inhibitor or pseudo-inhibitor peptides (500 µM) for a further 60 min prior to activation with PAR2-AP (20 µM). Sets of cells were treated with IL-1β to be used as a positive control or used untreated. Cell apoptosis was measured after 24 h post-activation using a colorimetric TUNEL assay (The data is the average of four independent experiments and expressed as the mean ± SEM; * = $P<0.05$ vs. no inhibitor).

4.3.5 Examining the role of Src1 inhibitor on TF-mediated p38 MAPK protein phosphorylation

To examine the role of Src1 as a signalling mediator connecting TF and p38 MAPK, the outcome of Src1 inhibition on p38 MAPK phosphorylation was examined. HDBEC (10^5/well) were seeded in 12-well plates and either transfected to express a mutant form of TF (TF_{Ala253}-tGFP) or used untransfected. The samples were adapted to serum-free medium and then incubated with a range of concentrations of Src1 inhibitor ($pp^{60c\text{-}src}$peptide TSTEPQpYQPGENL) (0-500 µM) for 60 min. The cells were activated using PAR2-AP (20 µM) for 90 min and lysed in Laemmli electrophoresis buffer. p38 MAPK phosphorylation was then assessed by western blot. Analyses of the protein bands showed a dose-dependent reduction in p38 MAPK phosphorylation with increasing concentrations of Scr1 inhibitor (Figure 4.17).

Figure 4.16 The influence of Src1 silencing on TF-mediated endothelial cell apoptosis

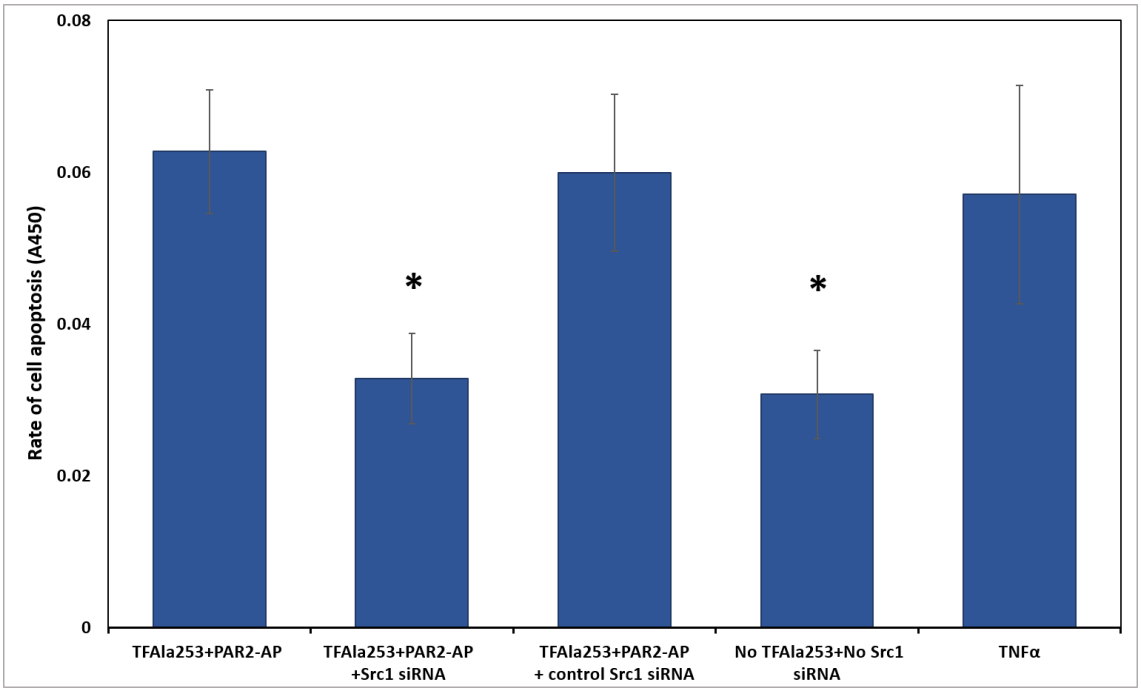

HDBEC (3 x 10^4/well) were co-transfected to express a mutant form of TF together with Src1 siRNA or alternatively a control siRNA. The cells were adapted to low-serum medium MV containing 2% (v/v) FCS for 1 h prior to activation using PAR2-AP (20 µM). For comparison, another set of cells was treated with TNFα or used untreated samples. Cellular apoptosis was measured after 24 h post-activation using a colorimetric TUNEL assay (The data is the average of four independent experiments and expressed as the mean ± SEM; *= P<0.05 vs. no siRNA).

Figure 4.17 Influence of Src1 inhibitor on phosphorylation of P38 MAPK following PAR2 activation

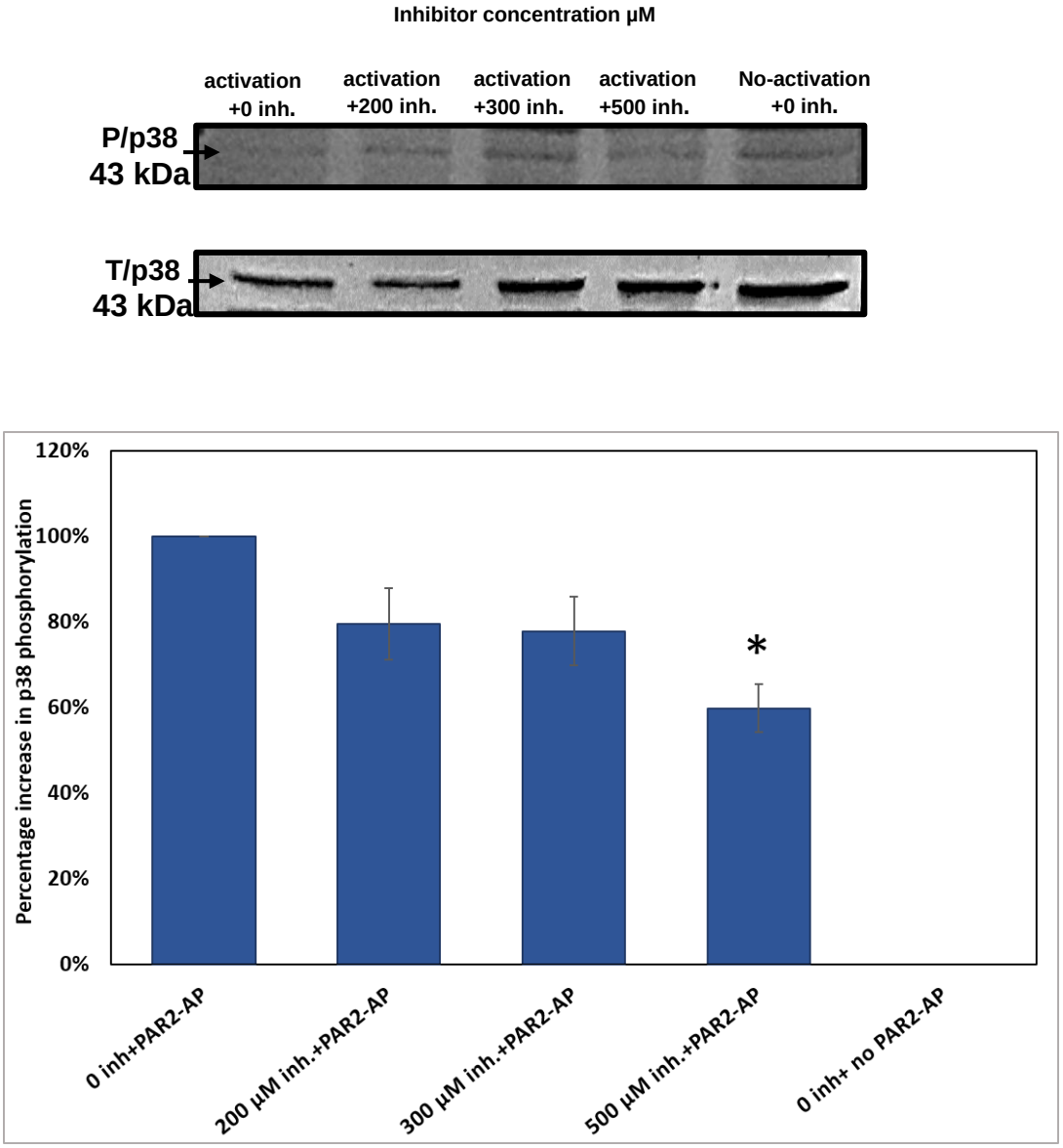

HDBEC (10^5/well) were transfected with TF_{Ala253}-tGFP plasmid and incubated for 48 h. The cells were then incubated with Src1 inhibitor (0-500 µM) for 60 min and then incubated for a further 90 min with PAR2-AP (20 µM). The cells were then lysed in Laemmli buffer and analysed by western blot using mouse anti-human phospho-p38 and rabbit anti-human p38 antibodies. The ratios of phospho-p38 (P/p38)/total p38 (T/p38) were analysed (The data is the average of four independent experiments and expressed as the mean ± SEM; * = $P<0.05$ vs. no inhibitor).

4.4 Discussion

Src1 is involved in the regulation of a number of cellular processes such as differentiation (Biscardi et al, 2000; Zhang et al, 2014) and apoptosis (Hofmeister et al, 2000). Additionally, the activation of Src1 leads to downstream signalling via the p38 MAPK protein (Watanabe et al, 2006; Watanabe et al, 2009). Previously it was reported that the activation of the p38 MAPK protein can promote cellular apoptosis in response to TF accumulation (ElKeeb et al, 2015). However, the signalling mediators linking TF and p38 MAPK have not been identified. The results presented in chapter 3 indicated that the accumulation of TF within cells results in the over-activation of the Src1 protein. Therefore, the present study attempted to confirm the role of Src1 as an intermediary between high levels of cellular TF, and induction of apoptosis.

A quantitative assay for the detection of cellular apoptosis, based on fluorescent labelling of DNA fragments (TUNEL assay) was used to measure DNA degradation. Apoptosis-inducing reagents were examined to generate apoptosis prior to the experiment. These reagents were then used as a positive controls for comparison against treated samples. Incubation of HDBEC with cycloheximide did not induce a measurable increase in cellular apoptosis although previous studies have demonstrated that cycloheximide is capable of inducing apoptosis (Alessenko et al, 1997). However, cycloheximide has been reported to either induce or inhibit apoptosis depending on the cell type treated (Collins et al, 1991; Lemaire et al, 1999; Tessitore et al, 1999). The incubation of the cells with anisomycin also did not produce apoptosis. Again, this finding is contrary to previous studies, which report that the incubation of cells with anisomycin increases the level of cellular apoptosis (Croons et al, 2009). Finally, incubation

of cells with H_2O_2 can induce both apoptosis or necrosis, depending on the concentration of H_2O_2 applied (Teramoto et al, 1999). The analysis of DNA-degradation by TUNEL assay in this study, indicated that the incubation of cells with 0.2 mM of H_2O_2 for 18 h induced apoptosis. However, although there was a reduction in cell numbers, the risk of induction of necrosis could not be ruled out, and therefore the use of H_2O_2 as a means of promoting apoptosis was not pursued further. In devising a more physiological method, an attempt was made to determine the optimal incubation time of the induction of apoptosis using the cytokines TNFα and IL-1β. Incubation of cells with TNFα (10 nM) for 22 h or, with IL-1β (10 nM) for 16-22 h caused apoptosis and were consistent with those suggested by Grunnet et al (2009). Therefore, incubation of the cells with TNFα or IL-1β for 22 h was employed to induce apoptosis in samples and was used as a positive control in the experiments.

The main section of the study aimed to confirm the participation of Src1 in TF-mediated cellular apoptosis. The activation of PAR2 in cells expressing the mutant form of TF (TF_{Ala253}-tGFP) significantly increased cellular apoptosis compared to untreated (control) cells. These data are also in agreement with observations reporting that the incubation of cells with high levels of TF can induce cellular apoptosis (Frentzou et al, 2010; Pradier & Ettelaie, 2008). In addition, pre-incubation of the cells expressing TF_{Ala253}-tGFP with the Src1 inhibitor ($pp^{60c\text{-}src}$peptide; 500 μM) prior to PAR2 activation, significantly reduced the rate of apoptosis (Figure 4.15). In contrast, the level of apoptosis remained unaltered in cells which were pre-incubated with the pseudo-inhibitor. In parallel to the observations in section 3.3.5, the highest level of Src1 phosphorylation occurred following PAR2 activation in cells expressing the mutant form of TF (TF_{Ala253}-tGFP). Taken together, these results define an important role for Src in

cellular apoptosis triggered by TF. This also agrees with a previous study, which showed that the inhibition of Src reduced cellular apoptosis (Hofmeister et al, 2000). Furthermore, although the high levels of apoptosis arose from the accumulation of TF in HDBEC, PAR2 activation was essential in triggering this signal.

Since peptide inhibitors can block the function of a number of proteins within the Src family, in the next part of the experiment the expression of Src1 specifically was suppressed using siRNA knock-down. Following the reduction of Src1 expression, the levels of apoptosis were significantly decreased following the PAR2 activation, in HDBEC expressing TF_{Ala253}-tGFP. This suggests that cellular apoptosis is triggered by TF as well as requiring the induction of PAR2 and is specifically dependent on Src1 signalling protein (Figure 4.18).

The study in this chapter focused on clarifying the role of Src1 as a signalling mediator connecting TF and p38 MAPK proteins. The role of Src1 protein in activating p38 MAPK is well-established (Kim et al, 2008; Tan et al, 2016). In support of this, the inhibition of Src1 resulted in a significant reduction in p38 MAPK phosphorylation. A similar result was obtained by Limami et al (2012) who reported that the phosphorylation of Src1 increased the activity of p38 MAPK and also induced cellular apoptosis. Finally, the complete suppression of cellular apoptosis, following the inhibition of Src1 appears to indicate that TAK1 is not involved in TF-p38 MAPK signalling which can lead to cellular apoptosis.

The activation of PAR2 in cells containing high levels of TF promotes apoptosis in endothelial cells. The study in this chapter confirms that Src1 mediates TF-induction of p38 MAPK activation, promoting cellular apoptosis. And has identified a further step in the mechanism by which TF can induce cellular

apoptosis. Therefore, the possible roles of FAK and β1-integrin in regulating the Src1-signalling mechanisms were examined next.

Figure 4.18 The role of Src1 in regulating p38 MAPK activation and TF-induced cellular apoptosis

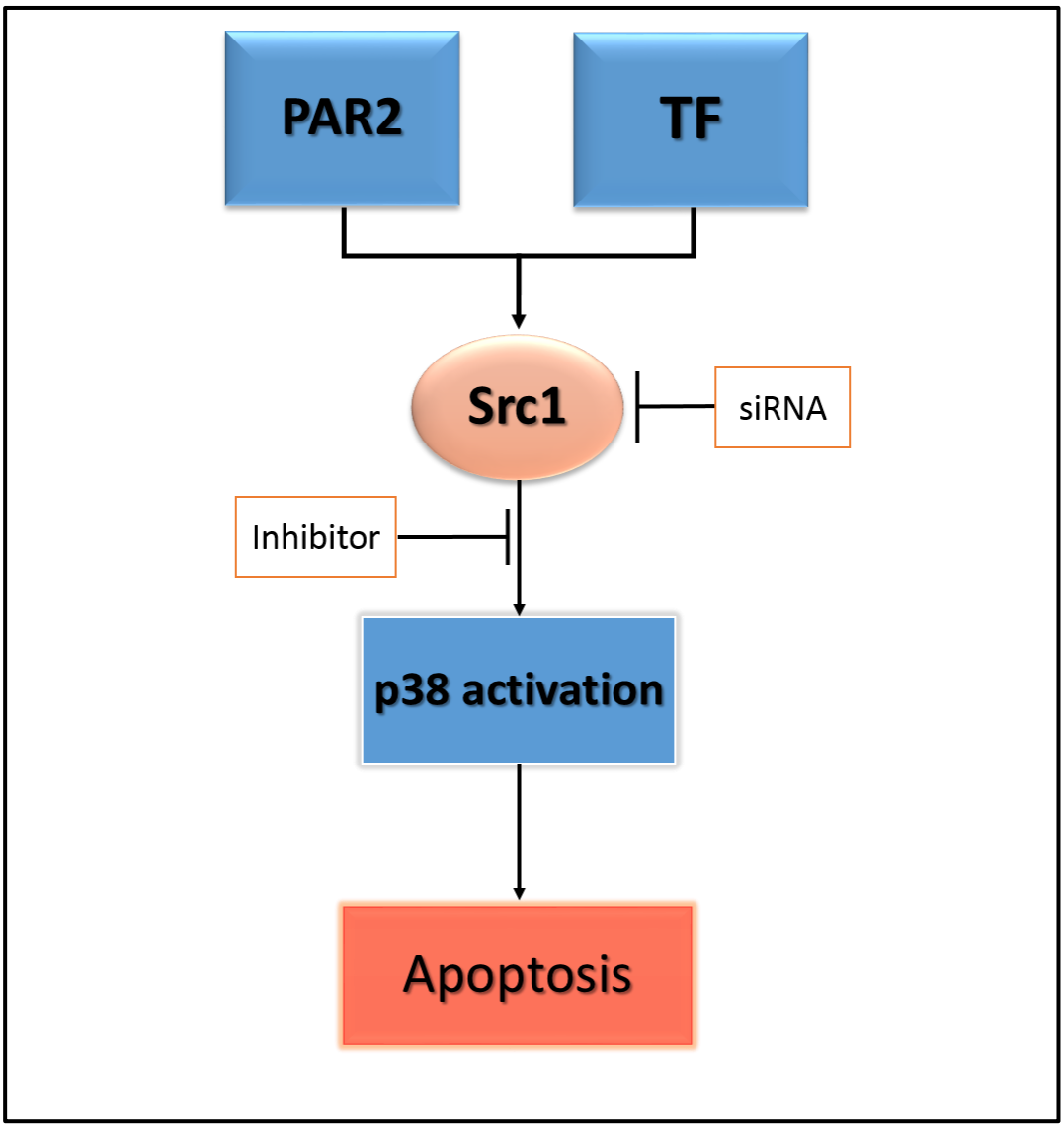

Src1 mediates TF-induced activation of p38 MAPK leading to subsequent cellular apoptosis. The inhibition of Src function, or the suppression of Src1 gene expression resulted in reduction of p38 MAPK activation and prevented cellular apoptosis.

Chapter 5

The influence of FAK and beta1 integrin proteins on the activity of Src1 protein

5.1 Introduction

There have been a number of studies which suggest that TF is capable of affecting different cellular processes through binding to β1-integrin (Collier & Ettelaie, 2010; Collier et al, 2008; Versteeg et al, 2008). Also, many intracellular signalling pathways are known to be initiated by the interaction of integrins with other receptors on the cell membrane (Brizzi et al, 2012; Hynes, 1992; 2002; Shen et al, 2012). These signals are transduced into the cell by the recruitment of intracellular proteins by the cytoplasmic domain of integrins. One such cytoplasmic protein is the focal adhesion kinase (FAK). FAK is a non-receptor tyrosine kinase which is considered a key mediator in transmitting signals from integrins (Mitra & Schlaepfer, 2006; Parsons, 2003). FAK is auto-phosphorylated at Tyr397 which allows it to bind to the SH2 domain of Src1. This interaction results in the activation of Src1 (Harburger & Calderwood, 2009; Playford & Schaller, 2004) (Figure 5.1). In this section of the study, it was hypothesized that β1-integrin and FAK act as intermediates regulating Src1 activity within the pro-apoptotic TF signalling pathway.

5.1.1 Focal adhesion kinase

Focal adhesion kinase (FAK) is also referred to as protein tyrosine kinase 2 (PTK2), cell adhesion kinase β (CAKβ) or related adhesion focal tyrosine kinase (RAFTK) (Avraham et al, 1995; Lev et al, 1995; Sasaki et al, 1995). FAK is a nonreceptor protein tyrosine kinase with a molecular weight 125 kDa and a member of the focal adhesion kinase family (Schaller et al, 1992; Yu et al, 1996). It has been reported that FAK is expressed in the cells of some of the lower eukaryotes such as zebrafish and *Drosophila* as well as in mammals.(Fox et al,

1999; Henry et al, 2001; Zhang et al, 1995). FAK is expressed in many organs, including the liver, lungs, brain and bones (Batista et al, 2014; Burgaya & Girault, 1996). Moreover, the expression of FAK is observed in endothelial cells (Weis et al, 2008) and cancer cells (Golubovskaya et al, 2009).

FAK consists of three distinguishable domains: a large N-terminal (erythrocyte band four.1-ezrin-radixin-moesin; FERM) domain, a central kinase (catalytic) domain and a C-terminal non-catalytic domain (Figure 5.2). β1-integrin interacts with FAK through the N-terminal region (Salmela et al, 2017). This domain contains the FAK auto-phosphorylation site (Tyr397) which interacts with the SH2 domain in Src1 (Schaller et al, 1994). The C-terminal domain includes a number of sites for interaction with other proteins such as Src1, Paxillin and Cas (Parsons, 2003).

Previous studies have shown that the interaction of β1-integrin with FAK causes FAK auto-phosphorylation at Tyr397 (Calalb et al, 1995; Schwartz et al, 1995). Evidence indicates that FAK phosphorylation at Tyr397 as well as the phosphorylation of Tyr576 and Tyr577 within the kinase domain are associated with an increase in the kinase activity of FAK (Calalb et al, 1995; Lipfert et al, 1992; Owen et al, 1999). Maximal activation of FAK is achieved by the phosphorylation of Tyr397, Tyr576 and Tyr577 enhancing the subsequent downstream signalling (Calalb et al, 1996; Owen et al, 1999). The integrin-promoted FAK auto-phosphorylation at Tyr397 generates a binding site with the SH2 domain of the Src1 protein (Calalb et al, 1995; Schaller et al, 1994). This Src1-FAK interaction can induce Src1-mediated signalling (Schlaepfer et al, 2004).

Figure 5.1 The interaction between Src1 and FAK proteins and the subsequent cellular outcomes

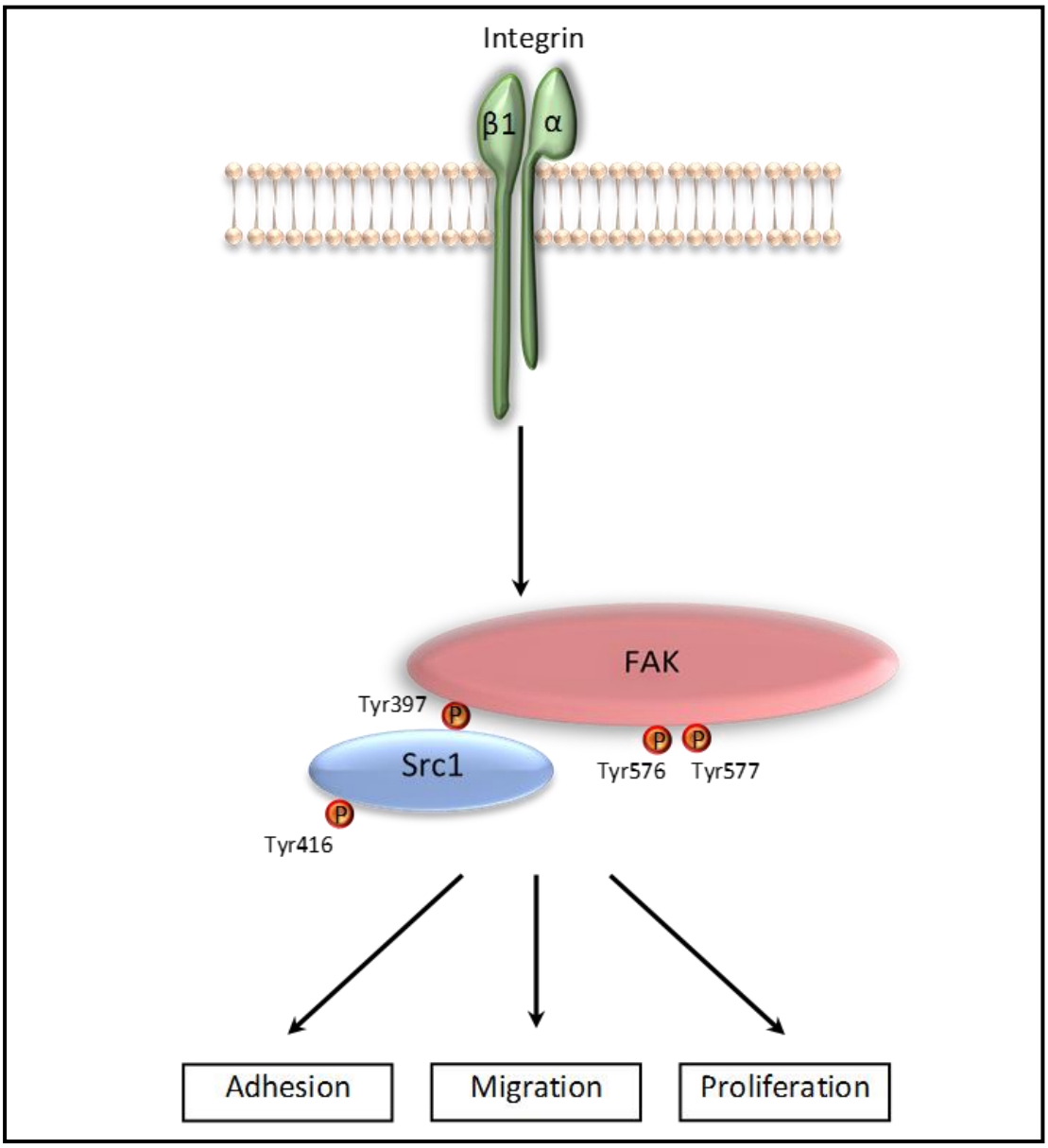

FAK and Src1 proteins cooperate to transmit signals from integrin receptors, and to regulate different cellular processes. Src1 is auto-phosphorylated on tyrosine 416 (Tyr416). FAK is activated by auto-phosphorylation on Tyr397. The auto-phosphorylation provides a binding site with Src1 on the SH2 domain. SH3 domain of Src1 enhances the phosphorylation of other tyrosine residues (576,577) of FAK. The Src1-FAK interaction is involved in the regulation of different cell processes. α subunit may refer to α2, α3, α4 or α5.

Evidence suggests that FAK is mediating the signalling initiated by integrins and other cell membrane receptors, such as the epidermal growth factor receptor (EGFR) (Lu et al, 2001; Maa et al, 1995). FAK is also involved in signalling cancer and cardiovascular disease (Yoon et al, 2015; Zhang et al, 2017a). Consequently, FAK has been suggested to be a promising therapeutic target for diseases associated with apoptosis, especially in cancer and cardiovascular disease (Cheng et al, 2012; Infusino & Jacobson, 2012).

5.1.2 β integrins

Integrins are transmembrane adhesion proteins which form heterodimers which are comprised of an α and a β subunit. The receptors are formed from 18 α-subunits and 8 β-subunits (Nakayamada et al., 2007). The α and β-subunits of integrins consist of a large extracellular domain, a transmembrane domain and a small cytoplasmic domain. Integrins act as a receptor for binding to the extracellular matrix and link to the cytoskeleton. The cytoplasmic domain recruits to adaptor proteins, which in turn interact with the cell cytoskeleton (Barczyk et al, 2010; Brakebusch & Fassler, 2005). This connection transduces a signals from the extracellular ligand into the cells and results in the activation of pathways such as p38 MAPK (Aikawa et al, 2002). In addition, integrins have the ability to transmit intracellular signals by mechanisms called inside-out signalling. This mechanisms can change the binding affinity of integrins for the extracellular matrix. The activation of inside-out signalling regulates different cellular processes including migration and adhesion (Brakebusch & Fassler, 2005; Geiger et al, 2009). It has been shown that the extracellular domain of integrins can interact with different components of the extracellular matrix such as

vitronectin (Bergmann et al, 2009), laminin (Takizawa et al, 2017) and fibronectin (Missirlis et al, 2016).

A number of studies have reported the ability of TF to induce cellular signalling through binding to different complexes of α and β1 subunits of integrin such as α4β1 (Rothmeier et al, 2017) and α3β1 (Dorfleutner et al, 2004), although other complexes including α2β1 and α5β1 cannot be ruled out. In addition, it has been shown that the interaction of TF with β1-integrin requires the formation of a complex with factor VIIa which can then activate PAR2, leading to subsequent pro-angiogenic and pro-migratory signals (Rothmeier et al, 2018). Moreover, activation of p38 MAPK by TF is thought to involve integrins (Kocaturk & Versteeg, 2013). Integrins have been shown to promote apoptosis through the activation of Src1 (Sirvent et al, 2012). The inhibition of β1-integrin results in reduction in Src1 activation (Arias-Salgado et al, 2005; Huveneers et al, 2007). The interaction between FAK and Src1 is known to be capable of transmitting cellular signals initiated by β1-integrin (Oktay et al, 1999; Schlaepfer & Hunter, 1996). Therefore, it is possible that the interaction between TF and β1-integrin may induce Src1 activation.

Figure 5.2 Structural domains of FAK protein

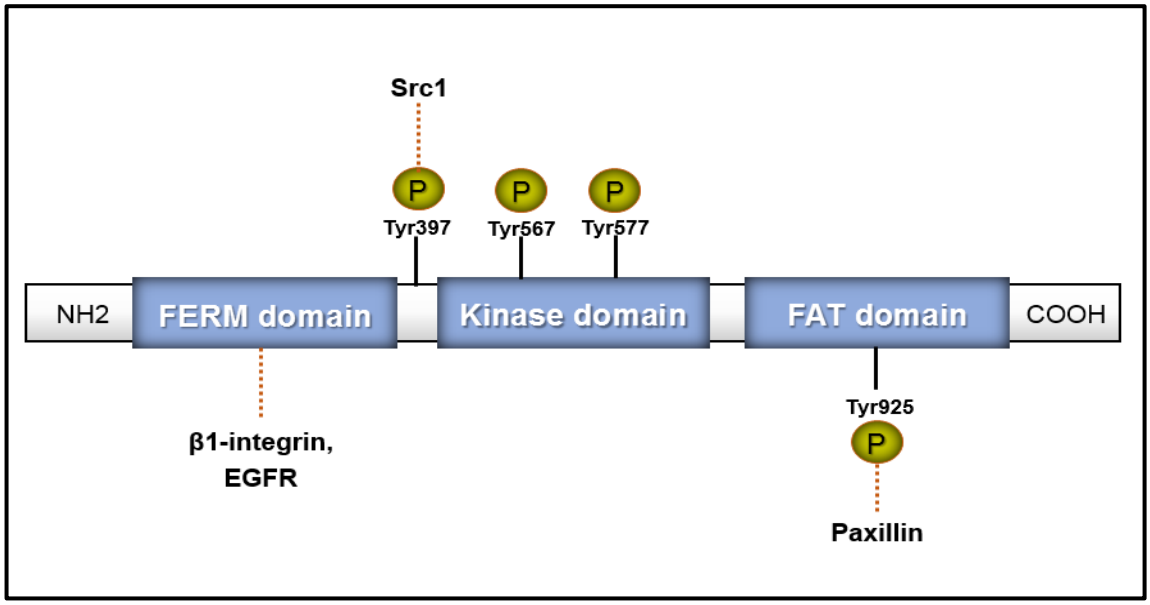

FAK protein is composed of three domains: FAT (focal adhesion targeting), kinase and FERM domains. FERM domain is the binding site with β1-integrin and epidermal growth factor receptor. FAK-β1-integrin binding induces Tyr397 phosphorylation (auto-phosphorylation site). The phosphorylation of Tyr397 creates a binding site with Src1 protein. Kinase (catalytic) domain include Tyr 567 and Tyr577. Phosphorylation of these residues provides the maximal phosphorylation of FAK. The FAT (focal adhesion targeting) domain contains the Tyr925 binding site for the Paxillin protein.

5.1.3 Aims

The results in chapter 3 and 4 have demonstrated that the accumulation of TF within endothelial cells results in cellular apoptosis through a mechanism involving the over-activation of Src1 protein. Furthermore, the level of cellular apoptosis is reduced following the inhibition of Src1 protein. However, the specific mechanisms by which Src1 activity regulates apoptosis have not been studied.

Hypothesis- FAK protein and β1-integrin act as regulators in the signalling mechanisms that allow Src1 to mediate cellular apoptosis following the activation of TF.

The objectives of the study aimed to:

- Examine the influence of FAK protein inhibition on the activation of Src1 in cells expressing TF.
- Examine the influence of β1-integrin inhibition on the activation of Src1 in cells expressing TF.

5.2 Methods

5.2.1 Src1 tyrosine kinase activity assay

The ProFluor® Src-family kinase assay was used to quantify the Src1 enzymatic activity in cells. The kit measured the tyrosine kinase activity of Src1 by its ability to catalyse the phosphorylation of a commercial substrate molecule (Src-Family Kinase rhodamine 110; R110 Substrate provided with the kit). The amount of the released fluorescence substrate depends on the amount of the protein activity.

HDBEC (10^5/well) were seeded in 12-well plates and incubated overnight. Sets of cells were transfected to express a mutant form of TF (TF_{Ala253}-tGFP), wild-type TF or tGFP, as a control (pCMV6-AC-tGFP). The cells were incubated for 48 h to express the proteins. Sets of untransfected cells were used as control in every experiment. All the cells were adapted to low-serum medium MV containing 2 % (v/v) FCS for 60 min. The cells were then activated using PAR2-AP (20 µM) for a further 90 min before being lysed using PhosphoSafe™ Extraction Reagent (PhosphoSafe buffer). Finally, the Src1 activity of the cell lysate for each sample was analysed using the activity assay, as follows.

The solutions for the reaction were prepared as described in Table 5.1 prior to perform the assay.

1- Each sample (cell lysate; 5 µl) was placed in separate well in opaque-walled 96-well plates.
2- Kinase peptide substrate solution (20 µl) was added to the wells
3- ATP solution (25 µl) was added to start the reaction and incubated with shaking for exactly 60 min at room temperature.
4- Protease solution (25 µl) was added and incubated for 60 min at 22-25°C.
5- Stabiliser solution (25 µl) was added to stop the reaction.
6- The fluorescence intensity was measured as follows:

i. Ex 485 nm Em 530 nm Rhodamine

ii . Ex 355 nm Em 460 nm AMC

Table 5.1 Preparation of the reagents used in Src1 activity assay

Kinase Solution	**96-well**
5X Reaction Buffer A	600 µl
Control AMC Substrate	3 µl
Src-Family Kinase R110 Substrate	3 µl
$MnCl_2$, 300 mM	20µl
Sodium Vanadate, 100mM	6 µl
NANOpure® water to a volume of	**3 ml**
ATP Solution	
5X Reaction Buffer A	400 µl
ATP 10mM	20 µl
NANOpure® water to a volume of	**2 ml**
Protease Solution	
5X Termination Buffer A	600 µl
Protease Reagent	120 µl
NANOpure® water to a volume of	**3 ml**
Stabilizer Solution	
5X Termination Buffer A	600µl
Stabilizer Reagent	3 µl
NANOpure® water to a volume of	**3 ml**

5.2.1.1 Estimation of Src1 activity

In order to quantify the Src1 activity in the cell lysate, a standard curve was prepared using serial dilutions of the kinase solution (Table 5.1) covering average of concentration (0-4 µM) in kinase diluent solution (5X reaction buffer A (200 µl), control AMC substrate (1 µl), $MnCl_2$, 300 mM (6.7µl), sodium vanadate, 100 mM (2 µl), and made up to a volume of 1 ml with pure water). PhosphoSafe buffer (5 µl) was added to each well and the fluorescence intensity of the standards was measured (Ex 485 nm, Em 530 nm for rhodamine and Ex 355 nm, Em 460 nm for AMC) as described in 5.2.1. The Src1 protein concentrations of the samples were determined using the following equation derived from the standard curve (Figure 5.3):

Protein concentration (µM) = y/194.68

5.2.2 Estimation of the dilution of cell lysate for measuring Src1 kinase activity

In order to establish the optimum dilution of the cell lysate for the determination of kinase activity, HDBEC (10^5/well) were seeded out in 12-well plates and incubated overnight. The cells were lysed in PhosphoSafe buffer and the lysate collected. PhosphoSafe buffer was used in a separate well as control. The cell lysates from each sample were diluted 0-5 times and the Src1 activity analysed by as described in 5.2.1.

Figure 5.3 Standard curve for the activity assay

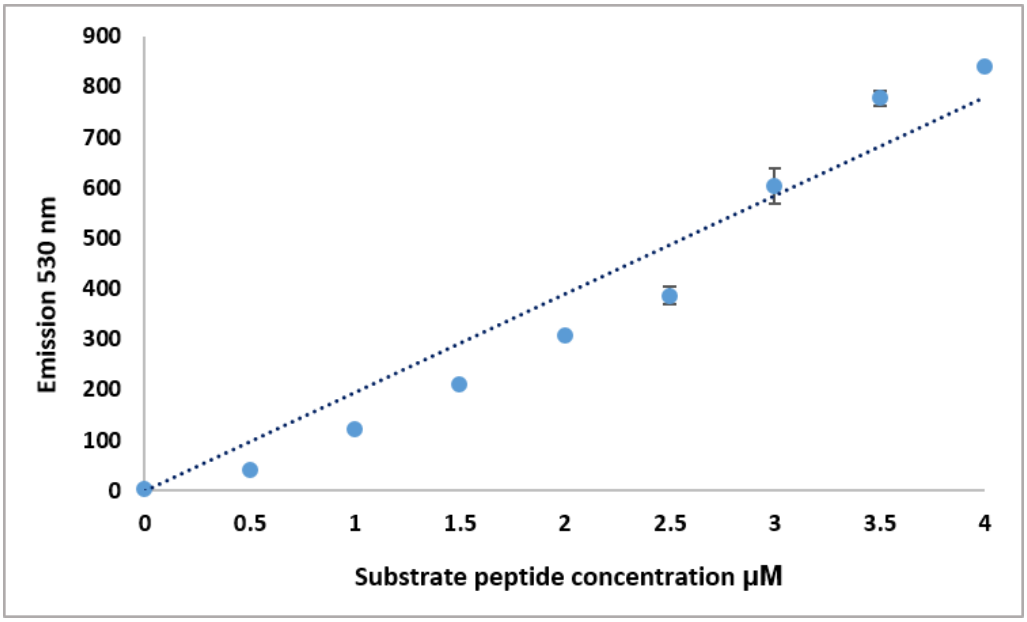

A range of kinase standards was prepared by serially diluting the kinase peptide substrate (0-4 µM) in kinase diluent. PhosphoSafe buffer (5 µl/well) was placed in a 96-well plates and mixed with 20 µl of each standard sample. Protease solution (25 µl/well) was then added and the plate incubated at 22-25°C for 60 min. Finally, 25 µl of the stabiliser solution was added and the fluorescence was measured (Ex 485 nm, Em 530 nm for rhodamine and Ex 355 nm, Em 460 nm for AMC). Data represent the mean value of the three separate experiments.

5.2.3 Optimisation of FAK inhibitor incubation time

Tyr397 is the unique site of auto-phosphorylation in FAK protein (Xing et al, 1994) and is needed for the activation of Src1 through binding with the SH2 domain (Schaller et al, 1994). FAK inhibitor-14 (1,2,4,5-benzenetetraamine tetrahydrochloride) acts by blocking the phosphorylation of FAK at Tyr397. In order to determine the optimal incubation time for maximal inhibition of FAK, HDBEC (10^5/well) were seeded out in 12-well plates and incubated overnight. The cells were treated with the FAK inhibitor (100 µM) for up to 6 h. The cells were then lysed using PhosphoSafe buffer. The protein samples were separated by SDS-PAGE and analysed using western blot as described in section 2.2.8 using specific antibodies as in Table 2.1. Quantitative analysis of the western blots was carried out using ImageJ program and the amount of phospho FAK was normalised against total FAK protein. Also, the amount of phospho Src1 was normalised against total Src1 protein at each interval.

5.2.4 Evaluation of the outcome of FAK inhibition on Src1 phosphorylation in HDBEC expressing TF

In order to assess the effect of FAK inhibition on the phosphorylation of Src1, HDBEC (10^5/well) were seeded out in 12-well plates and incubated overnight. Sets of cells were transfected to express a mutant form of TF (TF_{Ala253}-tGFP), wild-type TF, or a tGFP. The cells were incubated for 48 h to allow protein expression. In addition, a set of untransfected cells was used as a control. All the sets were adapted to low-serum medium MV containing 2 % (v/v) FCS and treated with the FAK inhibitor (100 µM) for 90 min or used untreated. Additionally, a parallal set of cells was incubated with the FAK inhibitor for 24 h, since it has

been reported that total inhibition of the FAK requires 24 h incubation (Hochwald et al, 2009). The cells were then activated using PAR2-AP (20 μM) for a further 90 min after which, the cells were lysed using a PhosphoSafe buffer, collected and boiled for 10 min. The protein samples were separated by SDS-PAGE and analysed using western blot as described in section 2.2.8 using specific antibody for FAK and Src1 proteins (Table 2.1). Quantitative analysis of the western blots was carried out using ImageJ program and the amount of phospho Src1 was normalised against total Src1 protein. Also, the amount of phospho FAK was normalised against total FAK protein at each interval.

5.2.5 Evaluation of the outcome of FAK inhibition on Src1 kinase activity in HDBEC expressing TF

In order to examine the influence of the inhibition of FAK on Src1 kinase activity during the accumulation of TF within the cell, HDBEC were prepared in the presence and absence of FAK inhibitor as described in the previous section (5.2.4). Src1 tyrosine kinase activity was then measured before and after PAR2 activation using the ProFluor® Src-family kinase assay, as described in 5.2.1.

5.2.6 Evaluation of the outcome of blocking of β1-integrin on Src1 protein phosphorylation in HDBEC expressing TF

In order to assess the level of Src1 phosphorylation following the inhibition of β1-integrin, HDBEC (10^5/well) were seeded out in 12-well plates and incubated overnight. A set of cells was transfected to express a mutant form of TF (TF_{Ala253}-tGFP), wild-type TF, or a tGFP. The cells were incubated for 48 h to allow the

expression of the proteins. In addition, a set of untransfected cells was used as a control. All sets were adapted to low-serum medium MV containing 2 % (v/v) FCS. Selected sets were treated with a blocking anti-β1-integrin antibody, (AIIB2; 10 µg/ml) for 60 min. The concentration of the blocking antibody was previously optimised (Maya-Mendoza et al, 2016; Tohidpour et al, 2017; Verma et al, 2016). The cells were activated using PAR2-AP (20 µM) for a further 90 min, and then lysed using a PhosphoSafe buffer. The lysate was boiled for 10 min and the protein samples were separated by SDS-PAGE. The membranes were then analysed by western blot as described in section 2.2.8 using specific antibody for Src1 and FAK proteins (Table 2.1). Quantitative analysis of the western blots was carried out using ImageJ program and the amount of phospho Src1 was normalised against total Src1 protein Also, the amount of phospho FAK was normalised against total FAK protein at each interval.

5.2.7 Evaluation of the outcome of blocking of β1-integrin on Src1 kinase activity in HDBEC expressing TF

In order to examine the influence of the inhibition of β1-integrin on Src1 kinase activity during the accumulation of TF within the cell, HDBEC were prepared in the presence and absence of β1-integrin inhibitor as described in the previous section (5.2.6). Src1 tyrosine kinase activity was then measured before and after PAR2 activation using the ProFluor® Src-family kinase assay, as described in 5.2.1.

5.3 Results

5.3.1 Optimisation of the dilution of the cell lysates for the determination of Src1 kinase activity

In order to determine the optimal dilution of the cell lysates, three dilution of the samples were examined using the ProFluor® Src-family kinase assay. The undiluted and two times diluted samples were found to produce comparable measurements (Figure 5.4). However, duo to high level of auto-fluorescence, the undiluted samples lysate produced spurious results which often saturated and exceeded the limit of the instrument. Therefore, the two times dilution was adopted as part of the procedure.

5.3.2 Establishment of the optimal incubation time for the inhibition of FAK activity

In order to determine the optimal incubation time for inhibiting FAK activity, cells were treated with the FAK inhibitor (100 μM) for up to 6 h. The phosphorylation of FAK was then assessed by western blot. Analyses of the protein bands showed that a maximal reduction in the FAK phosphorylation was obtained following 3 h incubation with the inhibitor (Figure 5.5). However, examination of Src1 showed that the maximal inhibition in Src1 phosphorylation was obtained after 2 h incubation with the FAK inhibitor (Figure 5.6).

Figure 5.4 Analyses of Src1 kinase activity using different dilutions of the cell lysate

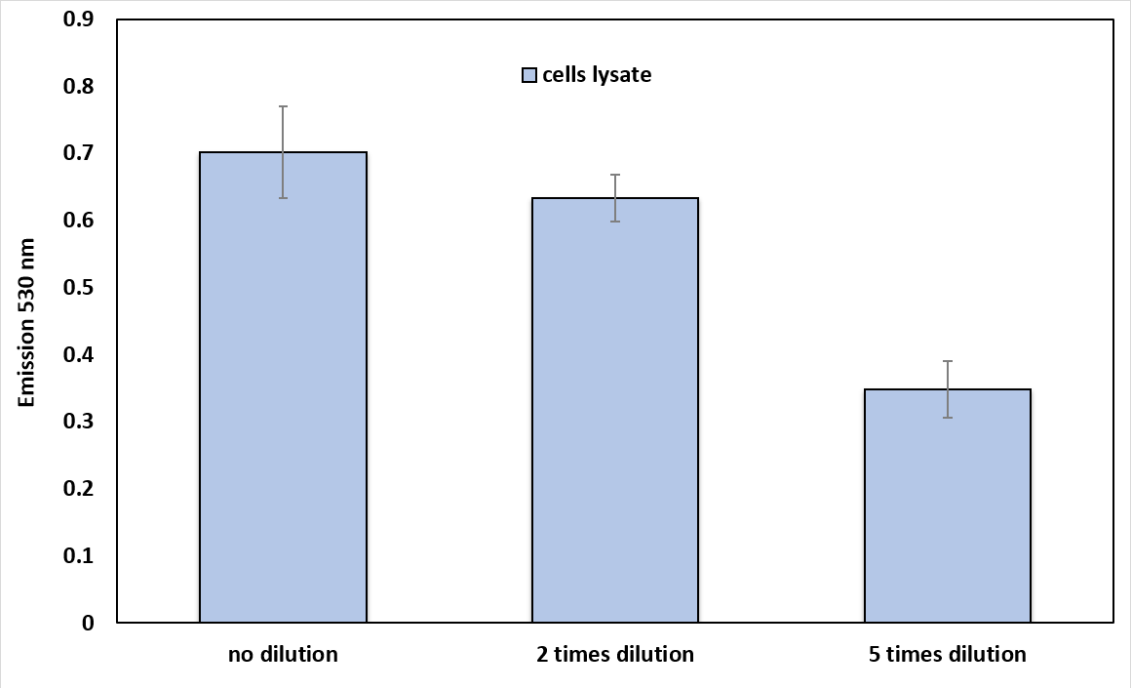

HDBEC (10^5/well) were seeded out in 12-well plates and incubated overnight. The samples were then diluted 5x, 2x or used undiluted. Src1 activity was then analysed using ProFluor® Src-family kinase assay (The data is the average of three independent experiments and expressed as the mean ± SEM).

Figure 5.5 Determnation of the optimal incubation time for the maximal FAK inhibition

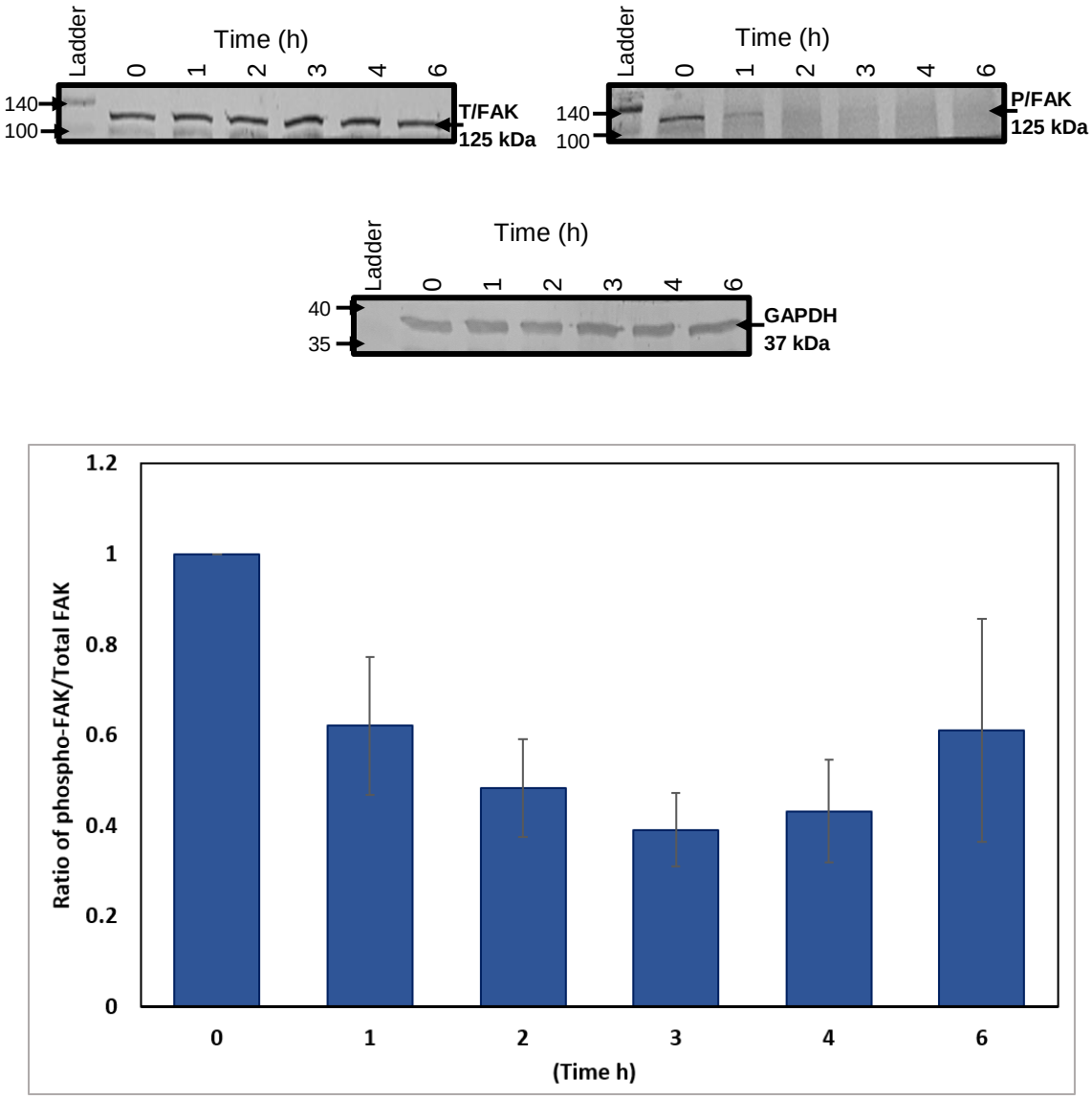

HDBEC (10^5/well) were seeded out in 12-well plates and incubated overnight. The cells were treated with the FAK inhibitor (100 µM) for up to 6 h. The cells were then lysed, collected and analysed by western blot using a rabbit anti-human phospho-FAK antibody and a rabbit anti-human total FAK antibody. Quantitative analysis was carried out using ImageJ program to determine the phospho-FAK (P/FAK)/Total FAK (T/FAK) ratio at each time interval (The data is the average of three independent experiments and expressed as the mean ± SEM).

Figure 5.6 Examination of Src1 phosphorylation following incubation of cells with FAK inhibitor

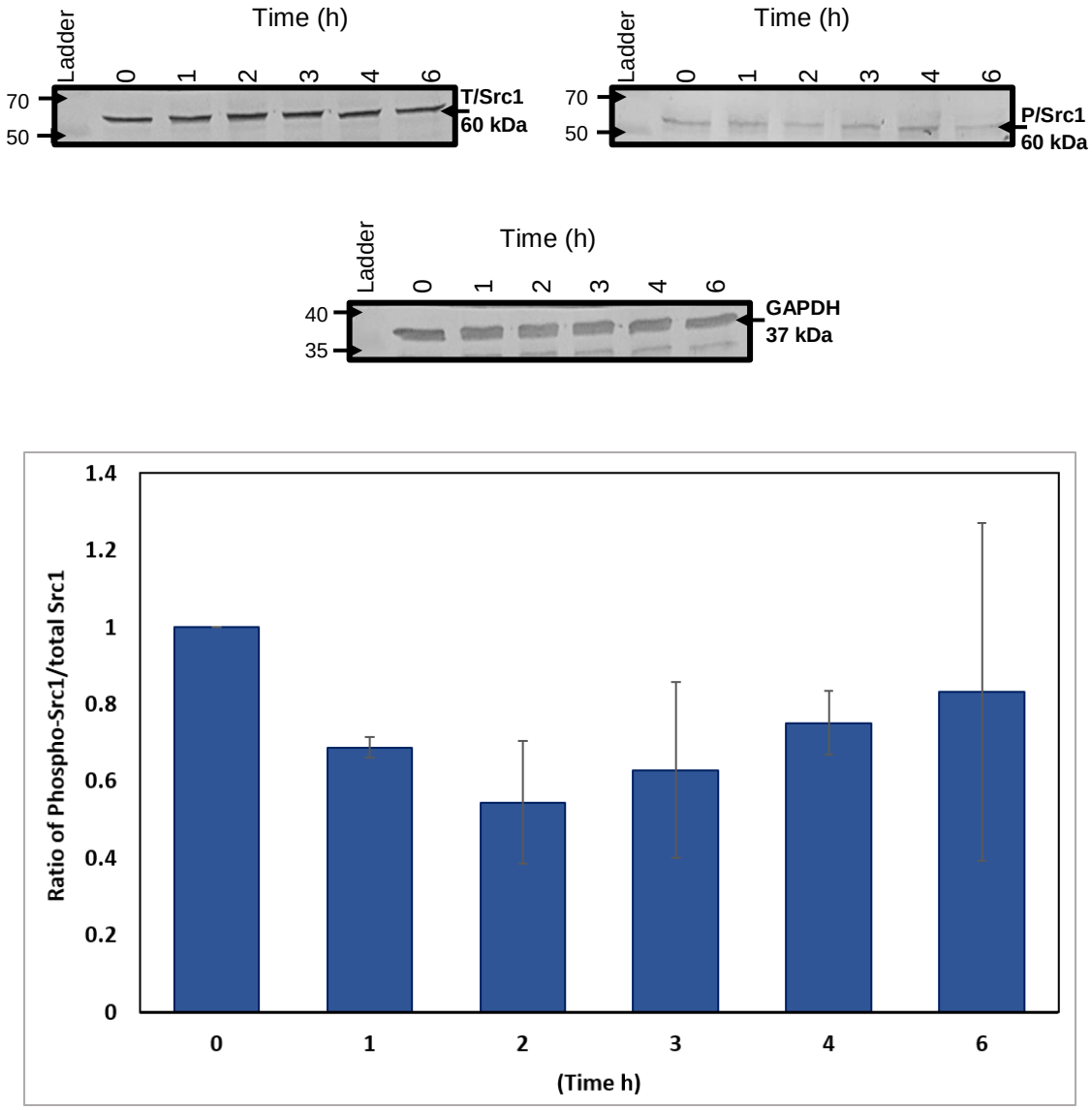

HDBEC (10^5/well) were seeded out in 12-well plates and incubated overnight. The cells were treated with the FAK inhibitor (100 μM) for up to 6 h. The cells were then lysed, collected and analysed by western blot using a rabbit anti-human phospho-Src family antibody and a rabbit anti-human total Src antibody. Quantitative analysis was carried out using ImageJ program to determine the phospho-Src1 (P/Src1)/total Src1 (T/Src1) ratio at each time interval (The data is the average of three independent experiments and expressed as the mean ± SEM).

5.3.3 Examination of the role of FAK on TF-mediated Src1 phosphorylation

In order to evaluate the role of FAK as a signalling mediator connecting TF and Src1, the outcome of FAK inhibition on Src1 phosphorylation was examined. HDBEC (10^5/well) expressing a mutant form of TF (TF_{Ala253}-tGFP), wild-type TF, tGFP or untransfected were treated with the FAK inhibitor (100 μM) for 24 h. Another set of cells was as above but incubated with FAK inhibitor for 90 min. The cells were then activated using PAR2-AP (20 μM) for a further 90 min, lysed in PhosphoSafe buffer and Src1 phosphorylation assessed by western blot. Before measuring the effect of FAK inhibition on Src1 phosphorylation, Src1 phosphorylation following PAR2 activation was measured. Western blot analyses of Src1 seemed to show a marginal increase in the phosphorylation status following PAR2 activation in transfected cells compared to non-transfected cells. This apparent increase in phosphorylation is particularly evident in the samples expressing the mutant form of TF (Figure 5.7). In contrast to the relatively small difference in Src1 phosphorylation, there was a significant reduction in FAK phosphorylation in all sets of cells following incubation with the inhibitor for 90 min (Figure 5.8). However, Analyses of the protein bands showed that incubation of the cells with the FAK inhibitor for 24 h resulted in a reduction in cell numbers as indicated by lower amount of GAPDH in addition to a reduction in the expression of Src1 protein (Figure 5.9). Moreover, incubation of the cells with the inhibitor for 90 min resulted in significant reduction in Src1 phosphorylation (Figure 5.10) compared with the untransfected cells. However, activation of PAR2 in transfected HDBEC did not result in alteration in the level of FAK phosphorylation (Figure 5.11).

5.3.4 Examination of the role of FAK inhibition in Src1 kinase activity in endothelial cells

In order to examine any outcome of FAK inhibition on Src1 kinase activity, HDBEC were prepared as previously described in 5.2.4 and assessed using the ProFluor® Src-family kinase assay as described in 5.2.1. Activation of PAR2 in HDBEC expressing the mutant form of TF resulted in increased Src1 activity. Furthermore, the pre-incubation of cells with the FAK inhibitor only marginally seemed to reduce the Src1 activity (Figure 5.12).

Figure 5.7 Assessment of Src1 phosphorylation following activation of PAR2 in HDBEC

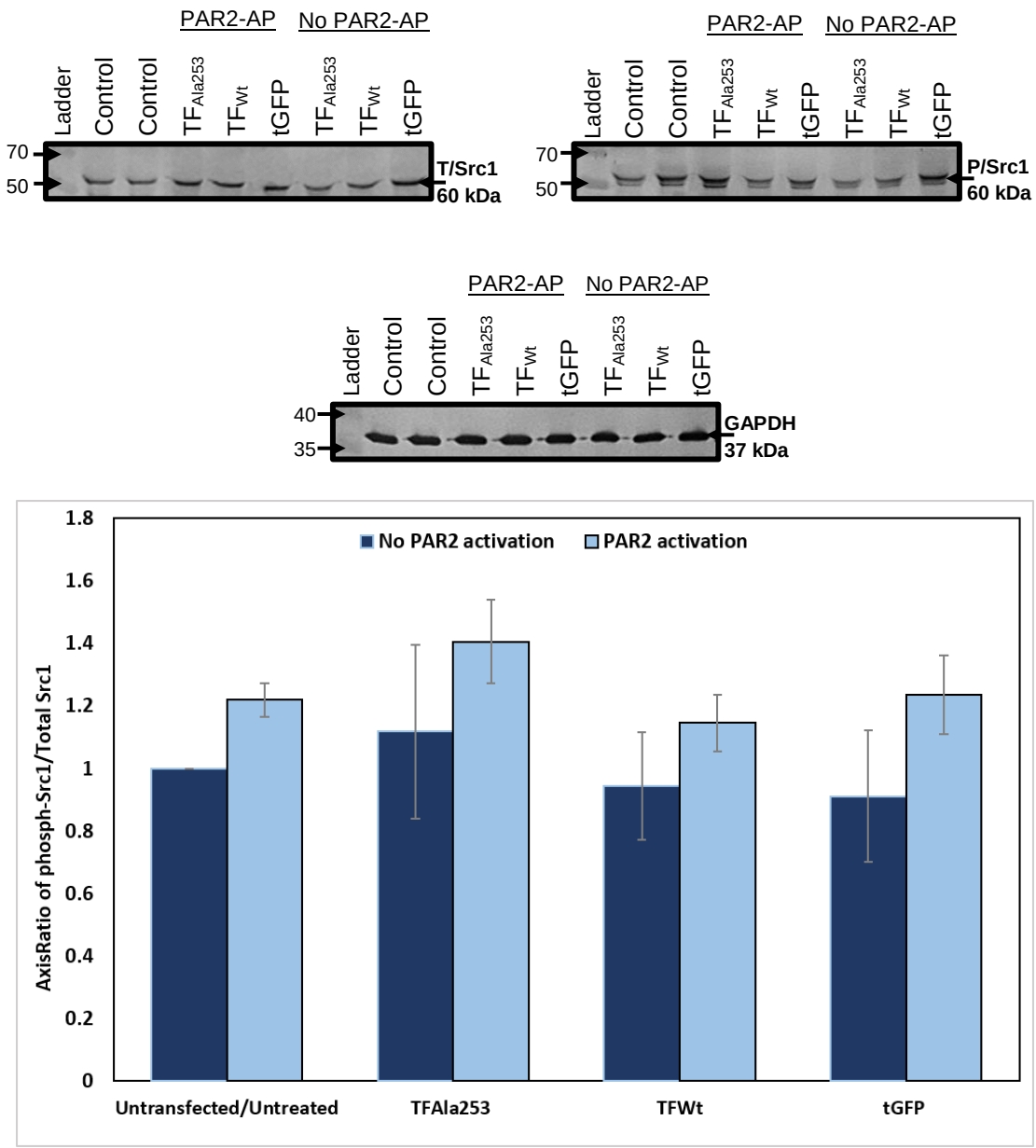

HDBEC (10^5/well) were cultured in 12-well plates and transfected to express TF_{Ala253}-tGFP, wild-type TF, tGFP or were used untransfected and incubated for 48 h to express the proteins. The cells were treated with or without with PAR2-AP (20 µM) for 90 min. The samples were lysed in PhosphoSafe buffer and analysed by western blot using a rabbit anti-human phospho-Src family antibody and a rabbit anti-human total Src antibody. Quantitative analysis was carried out using ImageJ program to determine the phospho-Src1 (P/Src1)/total Src1 (T/Src1) ratio (The data is the average of three independent experiments and expressed as the mean ± SEM).

Figure 5.8 Confirmation of inhibition of FAK phosphorylation by FAK inhibitor

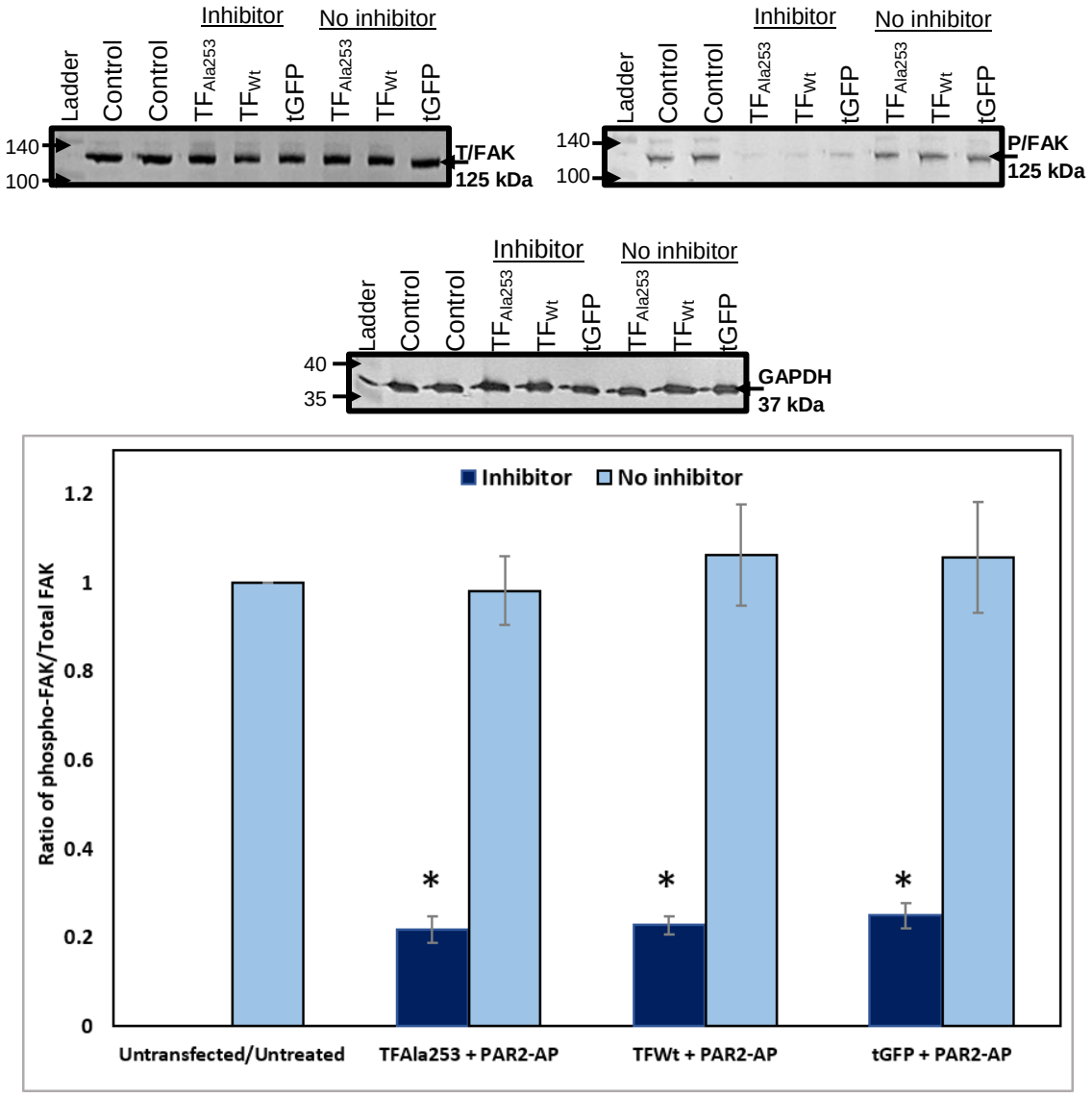

HDBEC (10^5/well) were cultured in 12-well plates and transfected to express TF_{Ala253}-tGFP, wild-type TF, tGFP or were used untransfected and incubated for 48 h to express the proteins. The cells were pre-incubated with the FAK inhibitor (100 µM) for 90 min prior to activation with PAR2-AP (20 µM) for a further 90 min. The samples were lysed in PhosphoSafe buffer and analysed by western blot using a rabbit anti-human phospho-FAK antibody and a rabbit anti-human total FAK antibody. Quantitative analysis was carried out using ImageJ program to determine the phospho-FAK (P/FAK)/total FAK (T/FAK) ratio (The data is the average of three independent experiments and expressed as the mean ± SEM; * = P<0.01 vs respective sample without inhibitor).

Figure 5.9 Examination of the effect of FAK inhibitor on Src1 phosphorylation at 24 h

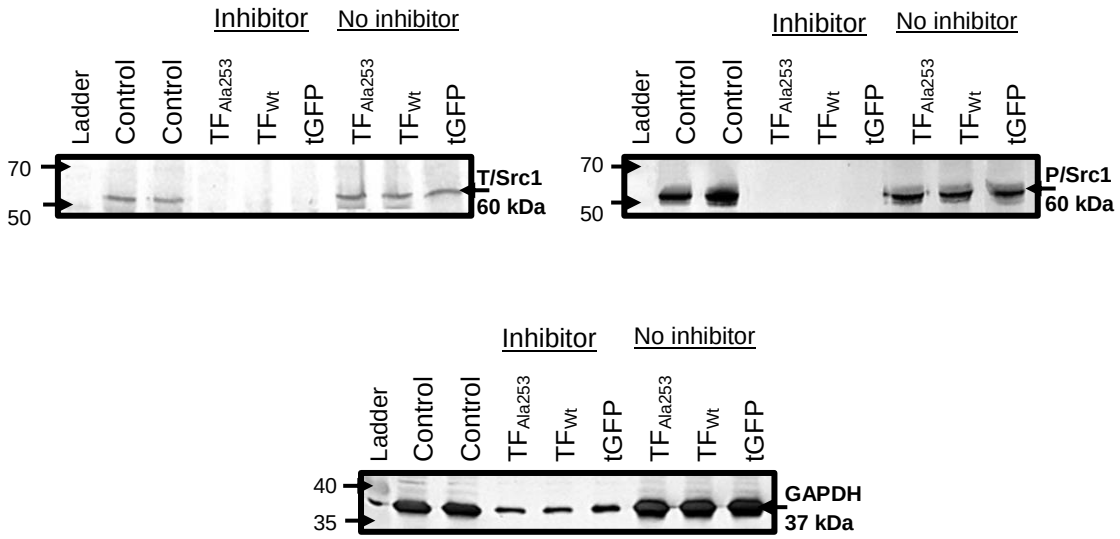

HDBEC (10^5/well) were cultured in 12-well plates and transfected to express TF_{Ala253}-tGFP, wild-type TF, tGFP or were used untransfected and incubated for 48 h to express the proteins. The cells were pre-incubated with FAK inhibitor (100 µM) for 24 h prior to activation with PAR2-AP (20 µM) for a further 90 min. The samples were lysed in PhosphoSafe buffer and analysed by western blot using a rabbit anti-human phospho-Src family antibody and a rabbit anti-human Src antibody. Quantitative analysis was carried out using ImageJ program to determine the phospho-Src1 (P/Src1)/total Src1 (T/Src1) ratio (The data is the average of three independent experiments).

Figure 5.10 Examination of the effect of FAK inhibitor on Src1 phosphorylation at 90 min

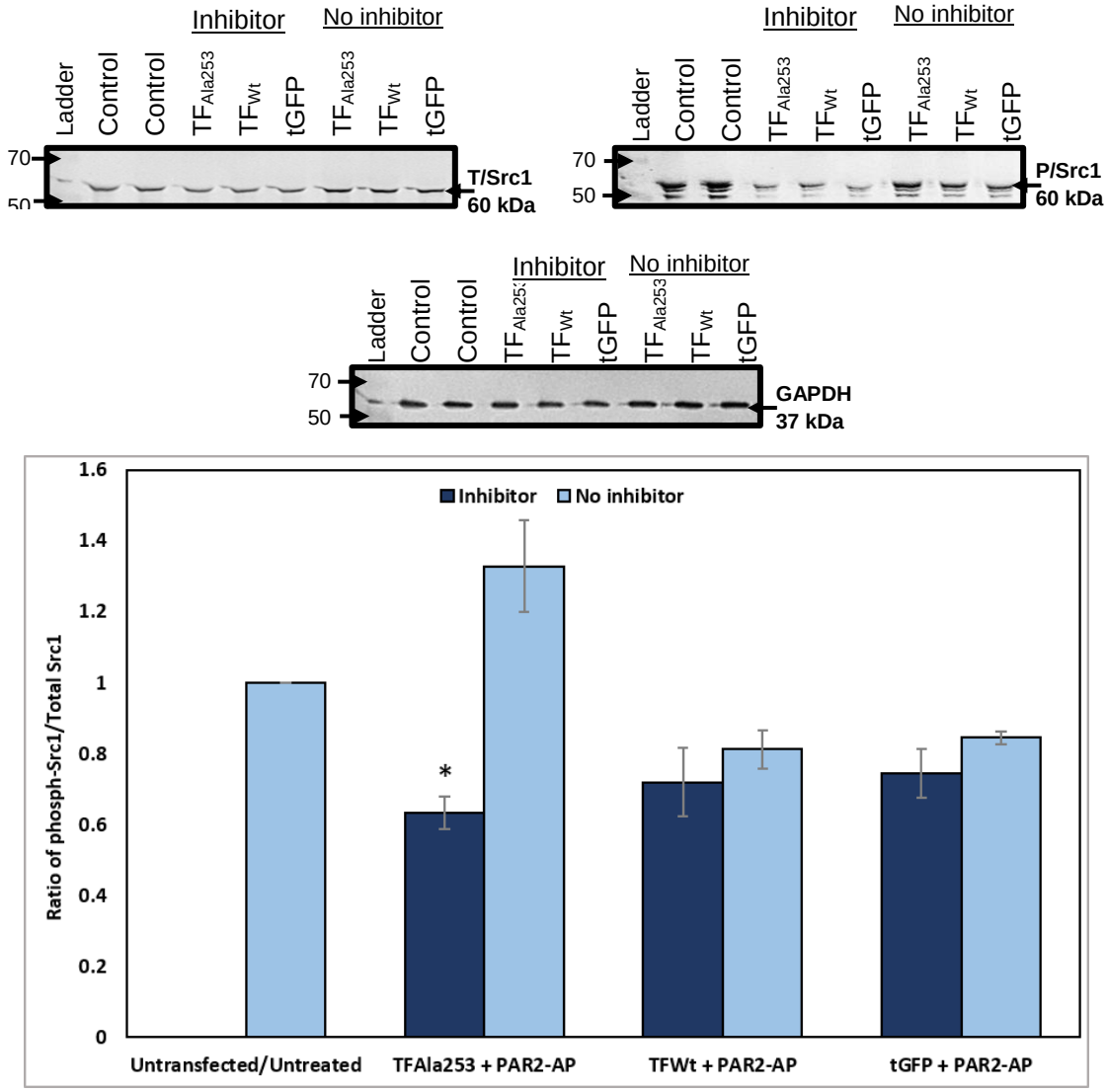

HDBEC (10^5/well) were cultured in 12-well plates and transfected to express TFAla253-tGFP, wild-type TF, tGFP or were used untransfected and incubated for 48 h to express the proteins. The cells were pre-incubated with FAK inhibitor (100 µM) for 90 min prior to activation with PAR2-AP (20 µM) for a further 90 min. The samples were lysed in PhosphoSafe buffer and analysed by western blot using a rabbit anti-human phospho-Src family antibody and a rabbit anti-human total Src antibody. Quantitative analysis was carried out using ImageJ program to determine the phospho-Src1 (P/Src1)/total Src1 (T/Src1) ratio (The data is the average of three independent experiments and expressed as the mean ± SEM; * = P<0.01 vs respective sample without inhibitor).

Figure 5.11 Assessment of FAK phosphorylation following activation of PAR2 in HDBEC

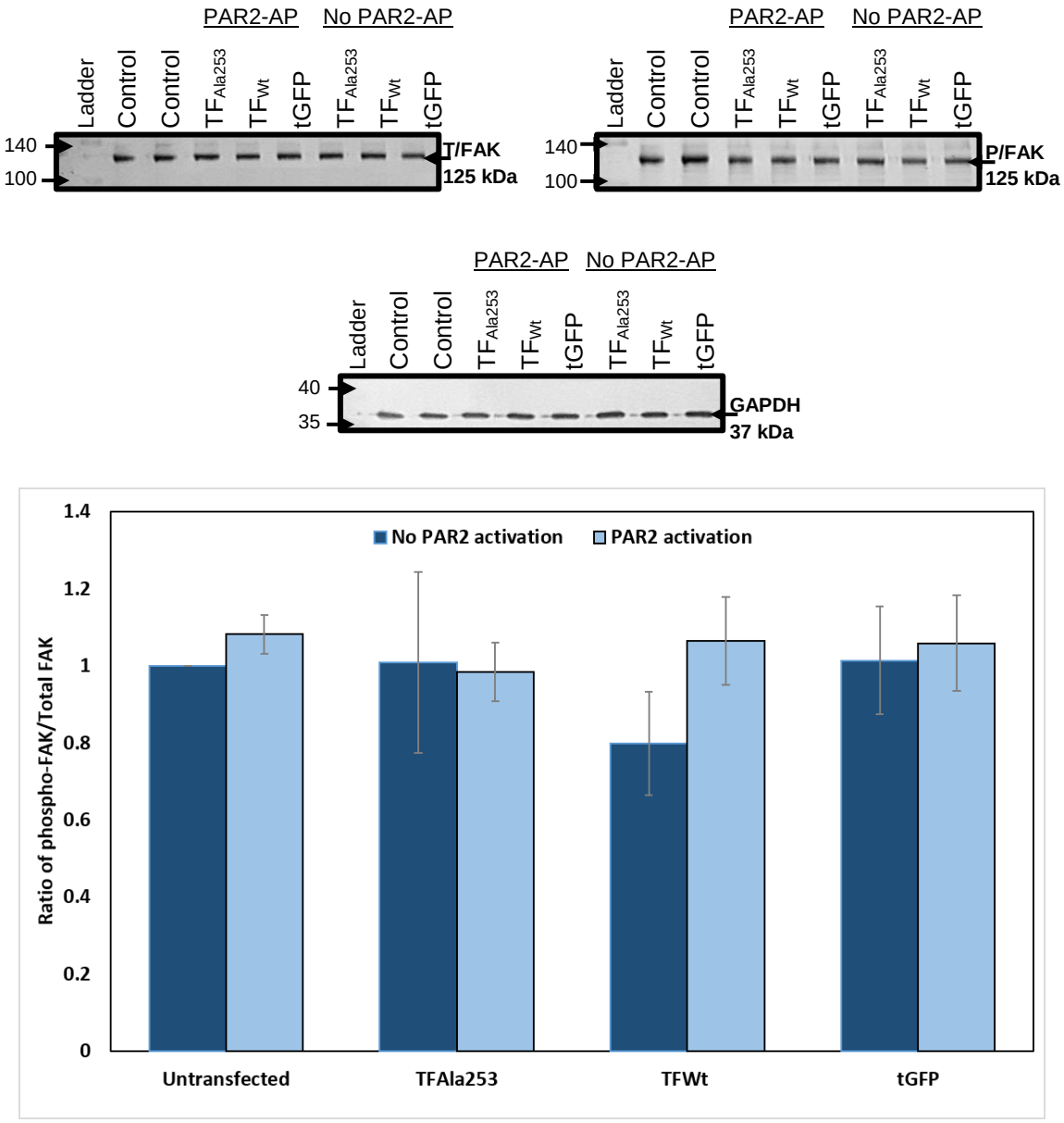

HDBEC (10^5/well) were cultured in 12-well plates and transfected to express TF_{Ala253}-tGFP, wild-type TF, tGFP or were used untransfected and incubated for 48 h to express the proteins. The cells were treated with or without PAR2-AP (20 µM) for 90 min. The samples were lysed in PhosphoSafe buffer and analysed by western blot using a rabbit anti-human phospho-FAK antibody and a rabbit anti-human total FAK antibody. Quantitative analysis was carried out using ImageJ program to determine the phospho-FAK (P/FAK)/total FAK (T/FAK) ratio (The data is the average of three independent experiments and expressed as the mean ± SEM).

Figure 5.12 The influence of FAK inhibition on Src1 kinase activity in HDBEC

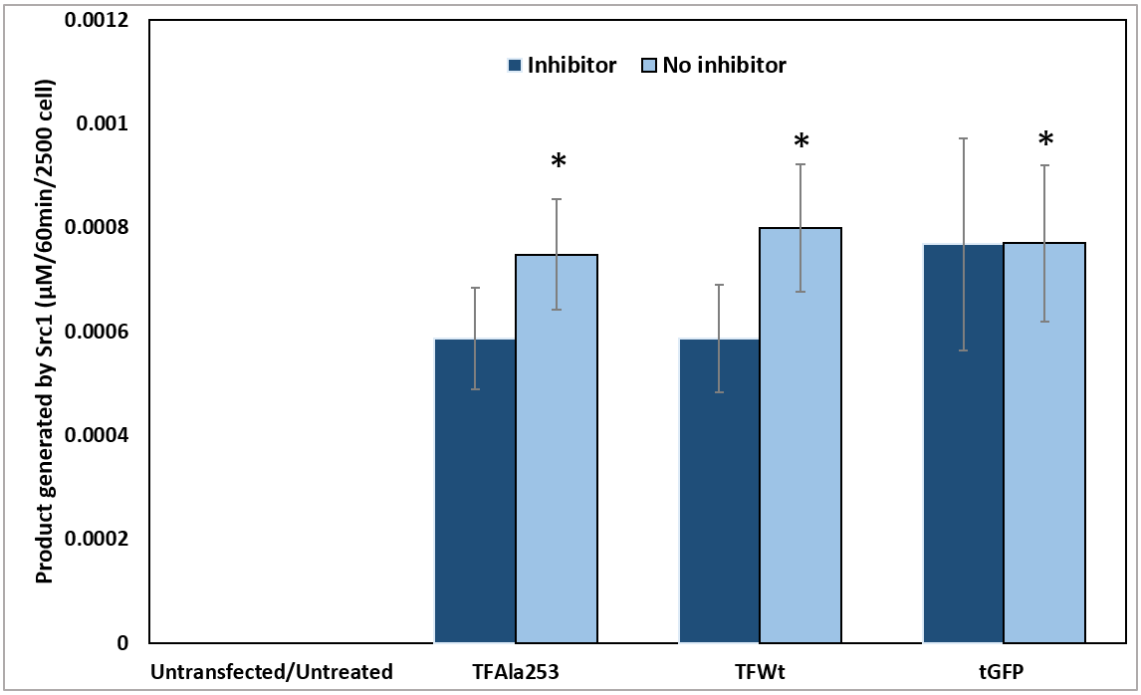

HDBEC (10^5/well) were seeded in 12-well plates and transfected to express TF_{Ala253}-tGFP, wild-type TF, tGFP or used untransfected and incubated for 48 h to express the proteins. The cells were pre-incubated with the FAK inhibitor (100 µM) for 90 min prior to activation with PAR2-AP (20 µM) for a further 90 min. The samples were lysed in PhosphoSafe buffer and Src1 activity was measured using a Src-kinase activity assay kit (The data is the average of four independent experiments and expressed as the mean ± SEM; * = P<0.05 vs the untransfected/untreated).

5.3.5 Examination of the influence of blocking of β1-integrin on TF-mediated Src1 phosphorylation

In this section the role of β1-integrin in the activation of Src1, in cells overexpressing TF was evaluated. HDBEC (10^5/well) expressing the mutant form of TF (TF_{Ala253}-tGFP), wild-type TF, a control plasmid (tGFP) plus an untransfected sample were blocked with anti-β1-integrin antibody, AIIB2 (10 µg/ml) for 60 min. The cells were then activated using PAR2-AP (20 µM) for a further 90 min, lysed in PhosphoSafe buffer and the phosphorylation of Src1 and FAK assessed by western blot. Analyses of the protein bands showed that the blocking of β1-integrin using antibody, only marginally seemed to reduce the level of Src1 phosphorylation in cells expressing TF_{Ala253}-tGFP (Figure 5.13). However, FAK phosphorylation remained unaltered in these cells (Figure 5.14).

5.3.6 Examination of the role of β1-integrin on Src1 kinase activity in endothelial cells

Cells were prepared as described in 5.2.6 and Src1 kinase activity measured using ProFluor® Src-family kinase assay in samples where β1-integrin was blocked as described above in section 5.3.5. Analyses of Src1 tyrosine kinase activity showed a significant increase in Src1 activity following the activation of PAR2 in transfected HDBEC than the untransfected control cells. Furthermore, inhibition of β1-integrin in HDBEC resulted in the reduction in Src1 kinase activity following PAR2 activation in all cells but was significant in cells expressing the mutant TF (Figure 5.15).

Figure 5.13 Assessment of Src1 phosphorylation following incubation of cells with the anti-β1-integrin inhibitor (AIIB2)

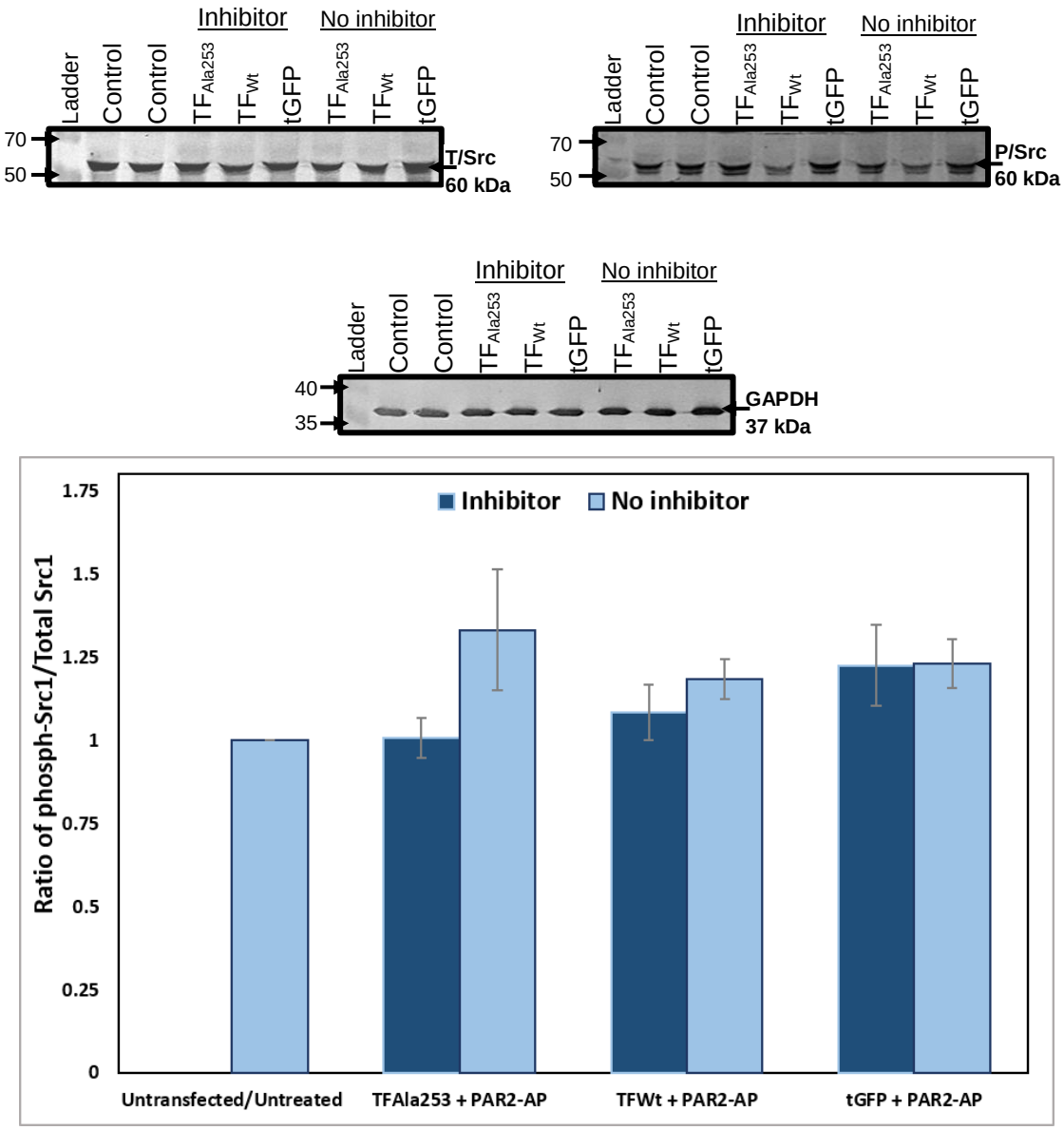

HDBEC (10^5/well) were cultured in 12-well plates and transfected to express TF_{Ala253}-tGFP, wild-type TF, tGFP or were used untransfected. All cells were incubated for 48 h to express the proteins. The cells were then pre-incubated with an inhibitory anti-β1-integrin antibody (AIIB2; 10 µg/ml) for 60 min, prior to activation with PAR2-AP (20 µM) for a further 90 min. The samples were lysed in PhosphoSafe buffer and analysed by western blot using a rabbit anti-human phospho-Src family antibody and a rabbit anti-human total Src antibody. Quantitative analysis was carried out using ImageJ program to determine the phospho-Src1 (P/Src1)/total FAK (T/Src1) ratio (The data is the average of three independent experiments and expressed as the mean ± SEM).

Figure 5.14 Assessment of FAK phosphorylation following incubation of cells with the inhibitory anti-β1-integrin antibody

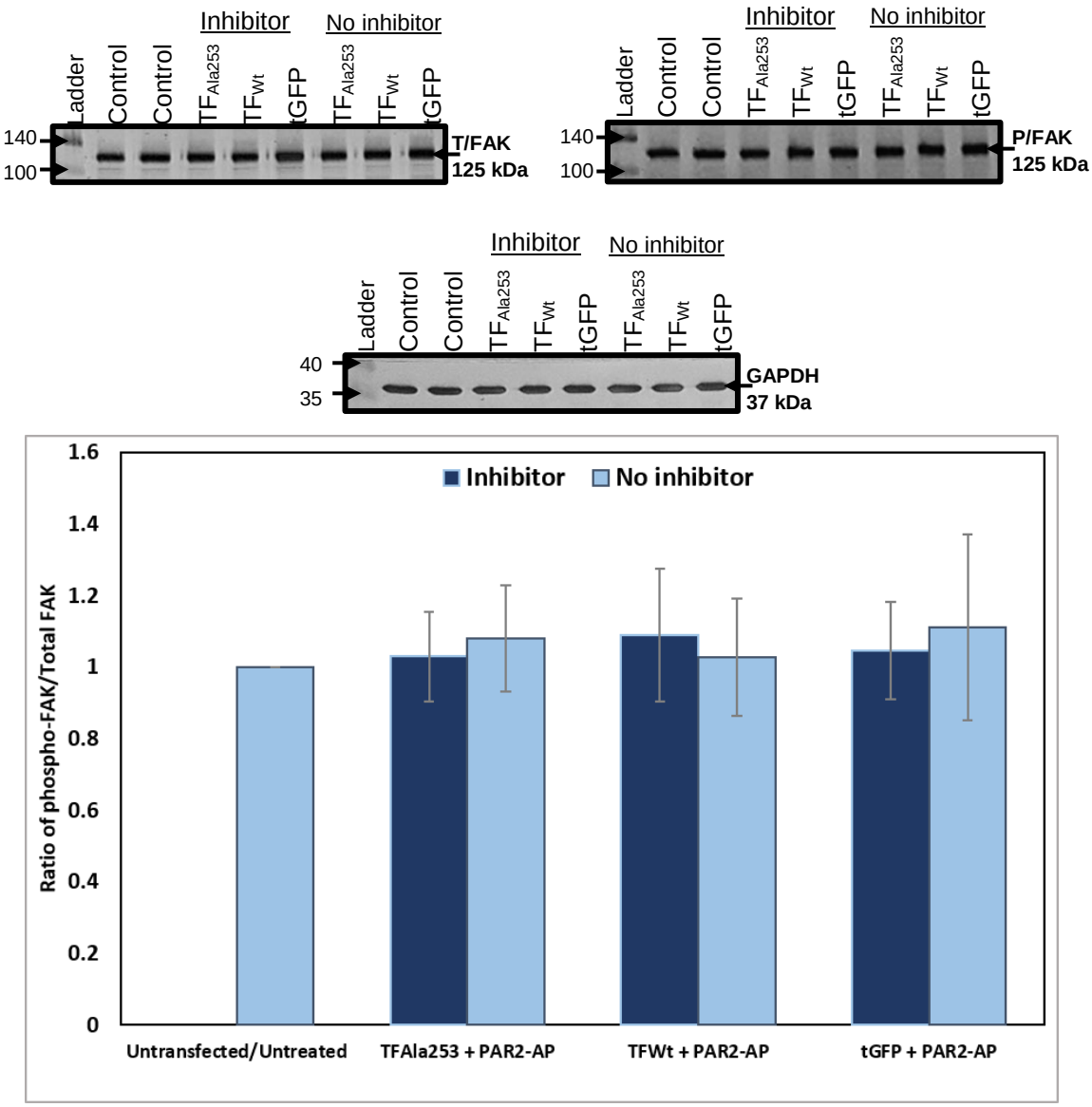

HDBEC (10^5/well) were cultured in 12-well plates and transfected to express TF_{Ala253}-tGFP, wild-type TF, tGFP or were used untransfected. All cells were incubated for 48 h to express the proteins. The cells were then pre-incubated with an inhibitory anti-β1-integrin antibody (AIIB2; 10 µg/ml) for 60 min, prior to activation with PAR2-AP (20 µM) for a further 90 min. The samples were lysed in PhosphoSafe buffer and analysed by western using a rabbit anti-human phospho-FAK antibody and a rabbit anti-human total FAK antibody. Quantitative analysis was carried out using ImageJ program to determine the phospho-FAK (P/FAK)/total FAK (T/FAK) ratio (The data is the average of four independent experiments and expressed as the mean ± SEM).

Figure 5.15 Assessment of the influence of β1-integrin blocking on Src1 kinase activity in HDBEC

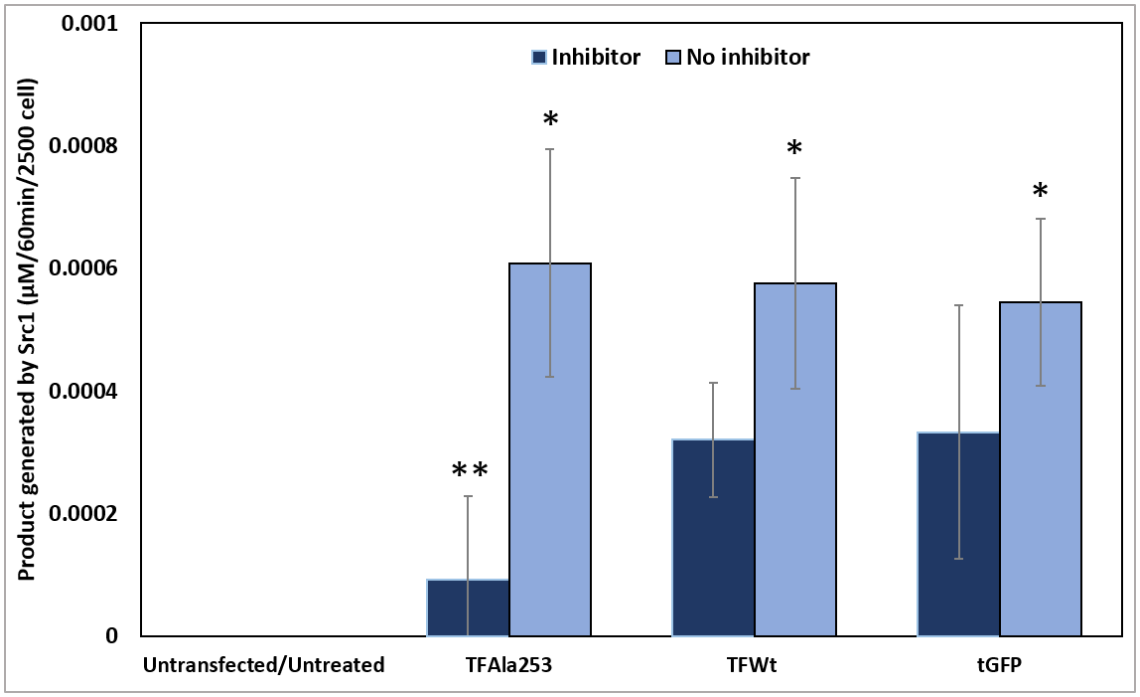

HDBEC (10^5/well) were cultured in 12-well plates and transfected to express TF_{Ala253}-tGFP, wild-type TF, tGFP or were used untransfected. The cells were incubated for 48 h to express the proteins. The cells were then pre-incubated with anti-β1-integrin inhibitory antibody (AIIB2; 10 µg/ml) for 60 min, prior to activation with PAR2-AP (20 µM) for a further 90 min. The samples were lysed using a PhosphoSafe buffer and Src1 activity was measured by a Src-kinase activity assay kit (n=6 independent experiments; * = P<0.05 vs the untransfected/untreated, ** = P<0.05 vs respective sample without the inhibition).

5.4 Discussion

Previous studies have reported the ability of TF to induce cellular signalling through binding with the β1-integrin (Collier & Ettelaie, 2010; Kocaturk et al, 2013; Kocaturk & Versteeg, 2013). Furthermore, the interaction between FAK and Src1 is known to be capable of transmitting cellular signals initiated by β1-integrin (Oktay et al, 1999; Schlaepfer & Hunter, 1996). The results presented in chapter 4 indicated that Src1 is a mediator of p38 MAPK activation following the cellular accumulation of TF. The activation of p38 MAPK can promote cellular apoptosis in endothelial cells (ElKeeb et al, 2015). Therefore, the aim of this section of the study was to examine the ability of β1-integrin and FAK to mediate the over-activation of Src1 following the accumulation of TF as observed in chapter 4. In order to prevent the release of TF, HDBEC was transfected to express a mutant form of TF_{Ala253}-tGFP which is not released by the cells. In addition, cells expressing wild-type TF, tGFP and untreated (untransfected) were used for comparison.

First, this study attempted to determine the involvement of FAK in TF-induced Src1 activation in HDBEC. It has been reported that incubation of cells with the FAK inhibitor-14 for 24 h can achieve full inhibition of FAK at Tyr397 (Hochwald et al, 2009). However, the incubation of the cells with the FAK inhibitor resulted in reduction of number of cells and as indicated by the lower level of GAPDH (Figure 5.9).It is likely that incubation of the cells with the FAK inhibitor for 24 h caused cell detachment and/or anoikis. However, incubation of the cells with the FAK inhibitor for 3 h inhibited FAK phosphorylation without causing a reduction of cell number (Figure 5.5). However, 90 min incubation time of the FAK inhibitor produced sufficient inhibition of FAK phosphorylation in transfected cells

(Figure 5.8). In addition, a 2 h incubation with the FAK inhibitor produced the maximal reduction in Src1 phosphorylation (Figure 5.6).

In agreement with our earlier observations in 3.3.5, highest level of Src1 phosphorylation was observed following PAR2 activation of cells expressing TF_{Ala253}-tGFP (Figure 5.7). Following the inhibition of FAK, phosphorylation of Tyr416 in Src1 was shown to be reduced in PAR2-activated HDBEC (Figure 5.10). These results further support the hypothesis that inhibition of Tyr397 phosphorylation in FAK, prevents the formation of Src1-FAK complex, which is essential for the phosphorylation of Tyr416 in Src1. In agreement with these results, previous studies have reported that integrin-promoted FAK auto-phosphorylation at Tyr397. The phosphorylation of Tyr397 generates a binding site with the SH2 domain of Src1 protein (Calalb et al, 1995; Schaller et al, 1994). As a result of this binding, the intramolecular interaction between the SH2 domain and the phospho Tyr527 in the C-terminal of Src1 is disrupted (Thomas & Brugge, 1997). The removal of the negative regulatory C-terminal creates an active conformation resulting in increased catalytic activity of Src1 (Schlaepfer et al, 1994). Subsequently, the activation loop is exposed which allows the phosphorylation of Src1 at Tyr416 (Guarino, 2010; Kleinschmidt & Schlaepfer, 2017). Therefore, the interaction of Src1 and FAK can induce Src1-mediated signalling (Schlaepfer et al, 2004).

In addition to Src1 phosphorylation, significant increases in Src1 activity was observed in all transfected cell samples following PAR2 activation compared to the untransfected cells. However, only a very marginal reduction in Src1 activity was detected (if at all) following the inhibition of FAK in cells expressing the mutant or wild-type of TF (Figure 5.12). Furthermore, the level of Src1 activity was found to be high even in the samples treated with the FAK inhibitor. These

findings are consistent with previous data which suggest that FAK inhibition is not sufficient to completely supress Src1 activity. Therefore, the lack of Tyr397 phosphorylation in FAK alone, is not sufficient for preventing Src1 activation (Horton et al, 2016). It has been suggested that Src1 may become activated by mechanism that are independent of FAK (Horton et al, 2016). Alternatively, some Src1 activity may arise from the persistence of activated Src1, prior to the addition of the FAK inhibitor (Sen & Johnson, 2011). Several studies have reported that in inactive Src1, Tyr527 is phosphorylated and binds the SH2 domain, while Tyr416 remains unphosphorylated. This produces a closed configuration with no kinase activity (Brown & Cooper, 1996; Johnson et al, 1996; Xu et al, 1999). Following the binding of FAK to the SH2 domain in Src1, the displaced phosphorylated Tyr527 becomes dephosphorylated. The subsequent phosphorylation of Tyr416 creates an active Src1 protein (Figure 1.6) (Frame, 2002; Mitra & Schlaepfer, 2006; Thomas & Brugge, 1997). However, in our study no significant decrease in Src1 activity was detected despite a reduction in Tyr416 phosphorylation, following the inhibition of FAK. Moreover, These results are in agreement with the findings of others, who reported that phosphorylation of Tyr416 is not needed for Src1 activity (Cary et al, 2002).in contrast, (Stover et al, 1994) reported that both Tyr416 and Tyr527 may be phosphorylated in the same Src1 molecule. The replacement of phospho Tyr527 at the C-terminal with a high affinity phospho-tyrosine from FAK results in the exposure of the SH3 domain in Src1 which interacts with the FERM domain within FAK and leads to the stabilisation of the Src1-FAK complex (Brown & Cooper, 1996).

Overall, our findings indicate that, although blocking of the Src1-FAK binding site prevents FAK-induced Src1 activation, the Src1 protein may become activated by mechanisms independent of FAK. In agreement with these results, previous

studies have reported that the α4β1-integrin is capable of activating Src1 independently of FAK (Hsia et al, 2005) through mechanism involving other members of the focal adhesion complex such as Paxillin and vinculin, which were reported as binding proteins of Src1 at SH3 (Figure 5.16) (Weng et al, 1993).

The second part of this study aimed to determine the possible role of β1-integrin in TF-induced Src1 activation in HDBEC. It has been reported that the influence of β1-integrin on Src1 is mediated through activation of FAK-Src1 complex. (Giancotti, 2000; Huveneers & Danen, 2009; Meves et al, 2011). The blocking of β1-integrin using an inhibitory antibody (AIIB2) has been shown to suppress FAK phosphorylation at Tyr397 (Eke et al, 2012). Since the phosphorylation of Tyr397 on FAK is required for Src1 activation, the lack of phosphorylation of FAK should inhibit the activation of Src1 by β1-integrin. The highest level of Src1 phosphorylation was observed in HDBEC expressing TF_{Ala253}-tGFP following PAR2 activation. However, the phosphorylation of Src1 was reduced following the blocking of β1-integrin with AIIB2 antibody (Figure 5.13). These results are in agreement with those reported by (Zhao et al, 1998), who suggested that prevention of FAK phosphorylation at Tyr397 prevents the binding of Src1 and is required to stop integrin-induced signalling. However, analysis of FAK phosphorylation using western blot, in cells pre-incubated with β1-integrin blocking antibody did not show a reduction in FAK phosphorylation (Figure 5.14). Therefore, It has been suggested that Src1 may become activated by mechanism that are independent of FAK (Horton et al, 2016). Alternatively, some Src1 activity may arise from the persistence of activated Src1, prior to the addition of the FAK inhibitor (Sen & Johnson, 2011). Therefore, the observed decrease in Src1 phosphorylation, following the blocking of β1-integrin appears to involve reduced the recruitment of Src1 protein to the focal adhesion complex, possibly by

preventing the interaction of other protein components. In addition, a higher level of Src1 activity was detected in transfected HDBEC than the untransfected control cells. Inhibition of β1-integrin in HDBEC resulted in the reduction in Src1 kinase activity following PAR2 activation in all cells but was highest in cells expressing the mutant TF protein (Figure 5.15). A direct binding site between the cytoplasmic tail of β3-integrin and the SH3 domain of Src1 has been identified (Arias-Salgado et al, 2005). Furthermore, the blocking antibody used in the study (AIIB2) prevents the clustering of integrin which is essential for the maximal activation of Src1 (Arias-Salgado et al, 2005; Huveneers et al, 2007). However, partial activation of Src1 by mechanisms involving the integrin cannot be ruled out (Kaminsky et al, 2012). For example, studies have reported that αvβ3-integrin is capable of inducing FAK phosphorylation in both tumour and normal cells which in turn activates Src1 (Kuphal et al, 2005).

In conclusion, a high level of Src1 activation occurs as a result of accumulation of TF in cells and in response to activation of PAR2. β1-integrin mediates TF induced Src1 activation through clustering of integrin with the focal adhesion complex which is essential for activation of Src1 in PAR2 activated cells. In addition, the phosphorylation of Src1 is enhanced by FAK activity although the Src1 activity is not only dependent on FAK activity. Therefore, this study demonstrates a mechanism by which TF can induce cell apoptosis mediated through β1-integrin and Src1 signalling.

Figure 5.16 Proposed signalling mechanism connecting β1-integrin to Src1

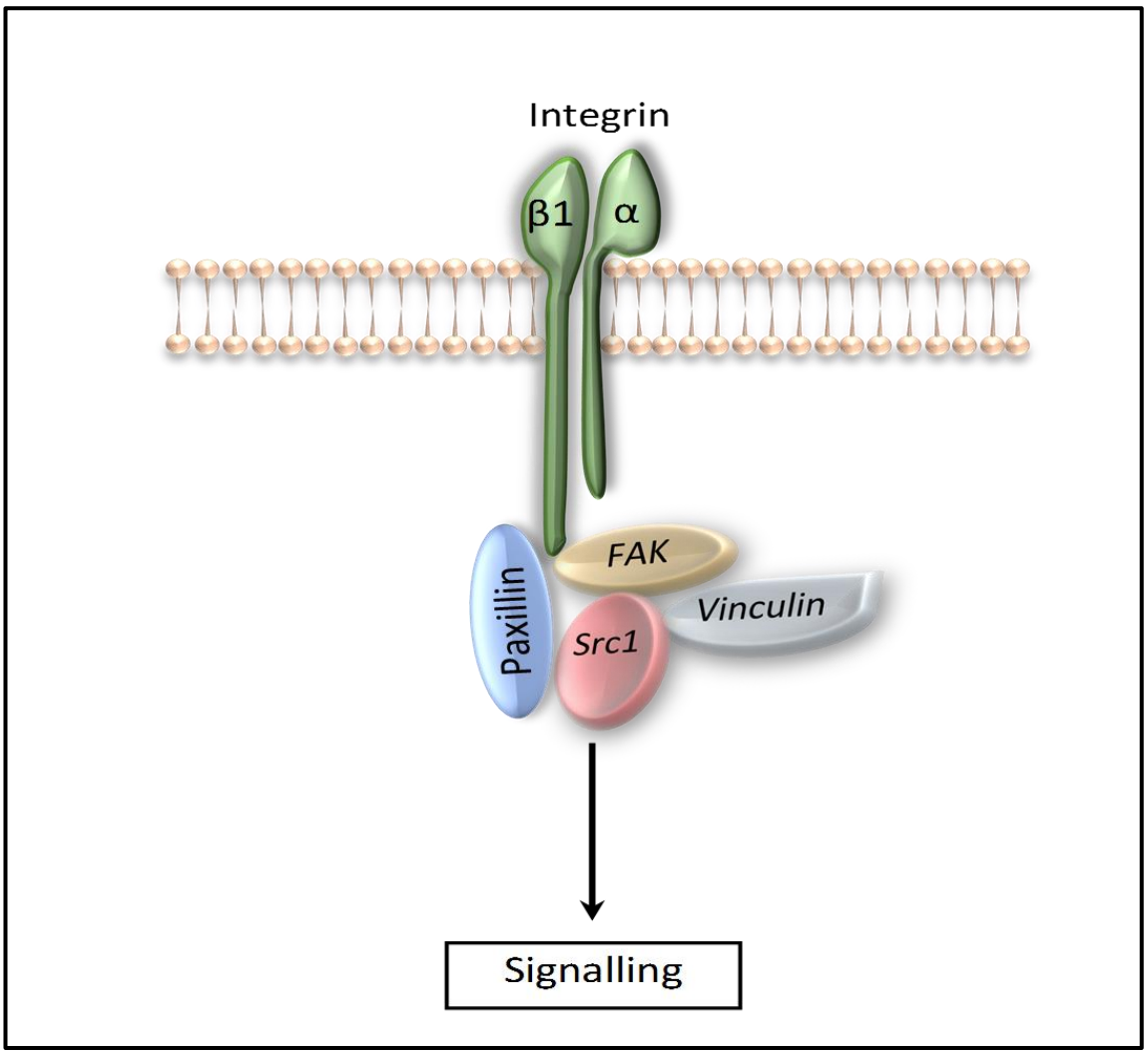

Different members of focal adhesion complex (FAK, Paxillin and Vinculin) were suggested to intermediate β1-integrin induced Src1-activation to regulate cell signalling.

Chapter 6

Discussion

6.1 General discussion

The aim of this study was to identify the signalling intermediaries that connect the signal initiated by TF to p38 MAPK activation, giving rise to subsequent endothelial cell apoptosis which occurs during inflammatory conditions such as cancer and vascular disease (Morel et al, 2005; Morel et al, 2006; Muller et al, 2000). Following trauma or injury, endothelial cells can produce and release TF-bearing microvesicles into the bloodstream (Aird, 2007; Yau et al, 2015). Moreover, endothelial cells have the ability to take up TF carried by circulating microvesicles from other sources (Collier et al, 2013; Osterud & Bjorklid, 2012) which can lead to cellular dysfunction (Widlansky et al, 2003). In addition to its function in coagulation, TF has the ability to regulate cellular processes including migration and proliferation through intracellular signalling pathways (Ettelaie et al, 2008; Pradier & Ettelaie, 2008; Pyo et al, 2004). Moreover, the role of TF as an initiator of cellular apoptosis has now been confirmed (Ettelaie et al, 2007; Frentzou et al, 2010). Recently, it was reported that the accumulation of TF within endothelial cells either through increased expression, or by acquiring TF from the bloodstream, can promote cellular apoptosis through mechanisms mediated by p38 MAPK (ElKeeb et al, 2015). TF-induced p38 MAPK activation was hypothesized to be mediated by one or more signalling molecules. It has also been suggested that one or more member of the Src kinase family can act as mediators in connecting TF and p38 MAPK (Versteeg et al, 2000). In addition, p38 MAPK activation by TF is thought to involve integrins (Kocaturk & Versteeg, 2013). Therefore, this study aimed to elucidate the signalling intermediaries associating increased cellular levels of TF, with p38 MAPK activation and

subsequent apoptosis. Therefore, Src1, Rac1 and/or TAK1 were examined as candidates for the signals that lead to the activation of p38 MAPK following PAR2 activation, in a mechanism that was also dependent on the level of TF. Previously, it was shown that the expression of Ala_{253}-substituted TF in cells prevented the release of TF, following the activation of PAR2 (ElKeeb et al, 2015). In the first section of the study, expression of wild-type TF in HDBEC was shown to lengthen the duration of Src1 phosphorylation up to 100 min. In addition, the retention of TF in cells expressing the mutant form of TF (TF_{Ala253}-TGFP) resulted in Src1 over-activation, demonstrated by the increase in the rate and duration of Src1 phosphorylation (up to 100 min) and a greater magnitude. These findings indicate that the accumulation of TF within cells further augments the activation of Src1 following PAR2 signalling. Moreover, the induction of PAR2 in HDBEC was shown to cause Rac1 phosphorylation which peaked at 60 min regardless of the presence TF. Therefore, Rac1 does not appear to play a role in connecting TF accumulation to p38 MAPK activation. However, it has been reported that the interaction of TF/FVIIa leads to the activation of Rac1 which itself is mediated through Src1 (Versteeg et al, 2000). Furthermore, it is possible that Rac1 phosphorylation could occur in response to the proteolytic activation of PAR2 by the TF/FVIIa complex (Hjortoe et al, 2004). Therefore, Src1 but not Rac1 appears to be the mediator of TF-induced activation of p38 MAPK, which subsequently leads to cellular apoptosis in endothelial cells. Finally, since TAK1 phosphorylation could not be examined in HDBEC, it was not possible to continue the examination of the any contribution that this protein may have.

Both inhibition of Src1 using $pp^{60c\text{-}src}$peptide, and suppression of Src1 expression were used to confirm the role of Src1 as the intermediary between high levels of cellular TF, and induction of apoptosis. The activation of PAR2 following the

accumulation of TF in cells resulted in a significant increase in cellular apoptosis. This cellular apoptosis was dependent on the accumulation of TF, and also was induced following PAR2 activation. These data are in agreement with observations reporting that the incubation of cells with high levels of TF can induce cellular apoptosis (Frentzou et al, 2010; Pradier & Ettelaie, 2008). Pre-incubation of cells expressing the mutant form of TF (TF_{Ala253}-tGFP) with the Src inhibitor ($pp^{60c\text{-}src}$peptide; 500 μM) prior to PAR2 activation significantly decreased the level of apoptosis in a concentration-dependent manner. In addition, the inhibition of Src was used to confirm the participation of Src as a signalling mediator connecting TF and the p38 MAPK protein. The inhibition of Src was concurrent with a dose-dependent reduction in p38 MAPK phosphorylation. Therefore, these findings further confirm that Src is involved in TF-p38 MAPK signalling pathway. However, Src inhibitors may block the function of other members of the Src family. Therefore, Src1 knockdown was used to further assess the role of Src1 specifically. Suppression of the Src1 gene expression using Src1-siRNA in cells expressing the mutant form of TF (TF_{Ala253}-tGFP) was shown to prevent apoptosis in HDBEC on PAR2 activation. Therefore, these results define an important role for Src1 in cellular apoptosis triggered by TF and also agree with a previous study, which showed that the inhibition of Src reduced cellular apoptosis (Hofmeister et al, 2000).

The signalling mechanism connecting the accumulation of TF to the activation of Src1 was examined next. The role of TF in different cellular processes through interaction of TF/FVIIa complex with β1-integrin has been established (Collier & Ettelaie, 2010; Collier et al, 2008; Versteeg et al, 2008). Integrin has been shown to activate Src1, resulting in stimulation of intracellular signalling pathways that alter cellular functions such as apoptosis (Sirvent et al, 2012). A recent study has

shown that the interaction of TF with β1-integrin requires complex formation with factor VIIa and can promote PAR2 activation leading to subsequent pro-angiogenic and pro-migratory signals (Rothmeier et al, 2018). In addition, it has been suggested that cellular migration is regulated by TF/FVIIa and involves Src1 (Siegbahn et al, 2008). Therefore, it has been suggested that the TF-induced Src1 activation could be mediated through β1-integrin. The blocking of β1-integrin using an antibody (AIIB2) reduced the kinase activity of Src1 following PAR2 activation in HDBEC expressing TF_{Ala253}-tGFP. In contrast, the release of TF from cells expressing wild-type TF following PAR2 activation did not show detectable alteration in the level of Src1 activity. In addition, blocking of β1-integrin reduced the phosphorylation of Src1 at Tyr416. Therefore, β1-integrin appears to mediate TF induced Src1 activation. These findings are consistent with previous data which suggest that the blocking of β1-integrin using the inhibitory antibody (AIIB2) prevents the clustering of integrin which is essential for the maximal activation of Src1 (Arias-Salgado et al, 2005; Huveneers et al, 2007). In summary, these findings suggest a mechanism by which TF accumulation and activation of PAR2 can induce cellular apoptosis mediated through β1-integrin and Src1 signalling.

Integrins are known to regulate different cellular signalling pathways mediated by different members of the focal adhesion complex (Li et al, 2018a; Mitra & Schlaepfer, 2006; Parsons, 2003). The interaction between FAK and Src1 is known to be capable of transmitting cellular signals initiated by β1-integrin (Oktay et al, 1999; Schlaepfer & Hunter, 1996) (Figure 6.1). Therefore, the study also examined the roles of FAK as a possible signalling intermediary between high levels of TF and Src1 over-activation, and the induction of apoptosis. Blocking of the Src1 binding site on FAK, at Tyr397 was carried out using FAK inhibitor-14 and resulted in significant reduction in Src1 phosphorylation following the

activation of PAR2 in cells expressing mutant form of TF (TF_{Ala253}-tGFP). In contrast, no detectable reduction in Src1 activity was shown following the inhibition of FAK. These findings are in agreement with recent studies which suggest that FAK inhibition is not sufficient to completely supress Src1 activity. Therefore, the lack of Tyr397 phosphorylation in FAK alone, is not sufficient for preventing Src1 activation (Horton et al, 2016). It is therefore possible that Src1 is activated by mechanisms independent of FAK (Horton et al, 2016) which may involve the participation of other members of the focal adhesion complex.

The release of TF into the bloodstream during inflammatory conditions has been well-documented. High levels of circulating TF have been detected particularly during pathophysiological conditions including cancer and cardiovascular disease (Peshkova et al, 2017). Consequently, TF may accumulate within endothelial cells in the vasculature. In addition, cancer cells are capable of secreting trypsin-like proteases that induce the PAR2 activation (Nystedt et al, 1995) which can activate the endothelial cells. Throughout this study HDBEC was transfected to express a mutant form of TF_{Ala253}-tGFP which is not released following the activation of the cells. This model was used as a reproducible mean of investigating the effect of TF accumulation in activated cells. The accumulation of TF and the activation of PAR2 in endothelium within the vasculature could suggest an explanation for the mechanism of TF-induced cellular apoptosis during cancer. This may also explain the erosion of endothelial cells that occurs during cardiovascular disease.

This study has demonstrated that the presence of high levels of TF within the cells increases the activation of Src1 protein. This increase in Src1 activation results in an increase in the rate of cellular apoptosis. It is known that Src1 protein has the ability to activate p38 MAPK (Watanabe et al, 2009). Therefore, it was

suggested that Src1 plays an essential role in TF-induced p38 MAPK activation and subsequent apoptosis since p38 MAPK was reported to induce cellular apoptosis triggered by TF. Under normal physiological conditions, TF-bearing microvesicles are not detected within blood circulation (Nemerson, 1988; Steffel et al, 2006). However, microvesicles with a high level of procoagulant activity have been reported to be released from cancer cell lines, particularly pancreatic and breast cancers (Gerotziafas et al, 2012; Zhang et al, 2017b). The procoagulant activity of these microvesicles is dependent on the presence of TF on the membrane of microvesicles (Davila et al, 2008). Additionally, TF may be detected within the circulation during various pathophysiological conditions such as cancer and cardiovascular complications and following injury and trauma (Bach & Moldow, 1997; Giesen et al, 1999; Simak et al, 2006; Thaler et al, 2012). The high levels of microvesicle-associated TF within the bloodstream can promote blood coagulation (Kopec et al, 2018). It has been demonstrated that endothelial cells respond to the presence of TF-containing microvesicles by taking up the microvesicles (Collier et al, 2013; Osterud & Bjorklid, 2012). The accumulation of these microvesicles can results in endothelial impairment and damage. In addition, the incubation of the cells with high levels of TF can cause apoptosis. However, at lower levels, TF can induce cell proliferation (Ettelaie et al, 2007; Pradier & Ettelaie, 2008). Moreover, the release of TF in normal physiological conditions has been reported to participate in wound healing (Xu et al, 2010). Also, a previous study showed that the inhibition of Src1 can reduce cellular apoptosis (Hofmeister et al, 2000). In agreement with our findings, the release of TF following the activation of PAR2 in cells expressing wild-type TF did not induce over-activation of Src1 and subsequent apoptosis. Therefore, this

study defines an important role for Src1 activity in cellular apoptosis triggered by TF

In conclusion, this study has identified a crucial role for Src1 in mediating TF signalling, resulting in the activation of p38 MAPK and subsequent apoptosis in HDBEC. In addition, β1-integrin was shown to act as signalling intermediary associating increased cellular levels of TF with the over-activation of Src1. Therefore, this study has identified a further step in the mechanism of TF-induced apoptosis which occurs during inflammatory conditions such as cancer and vascular disease.

Figure 6.1 Proposed mechanism for the regulation of TF-p38 MAPK induced cellular apoptosis

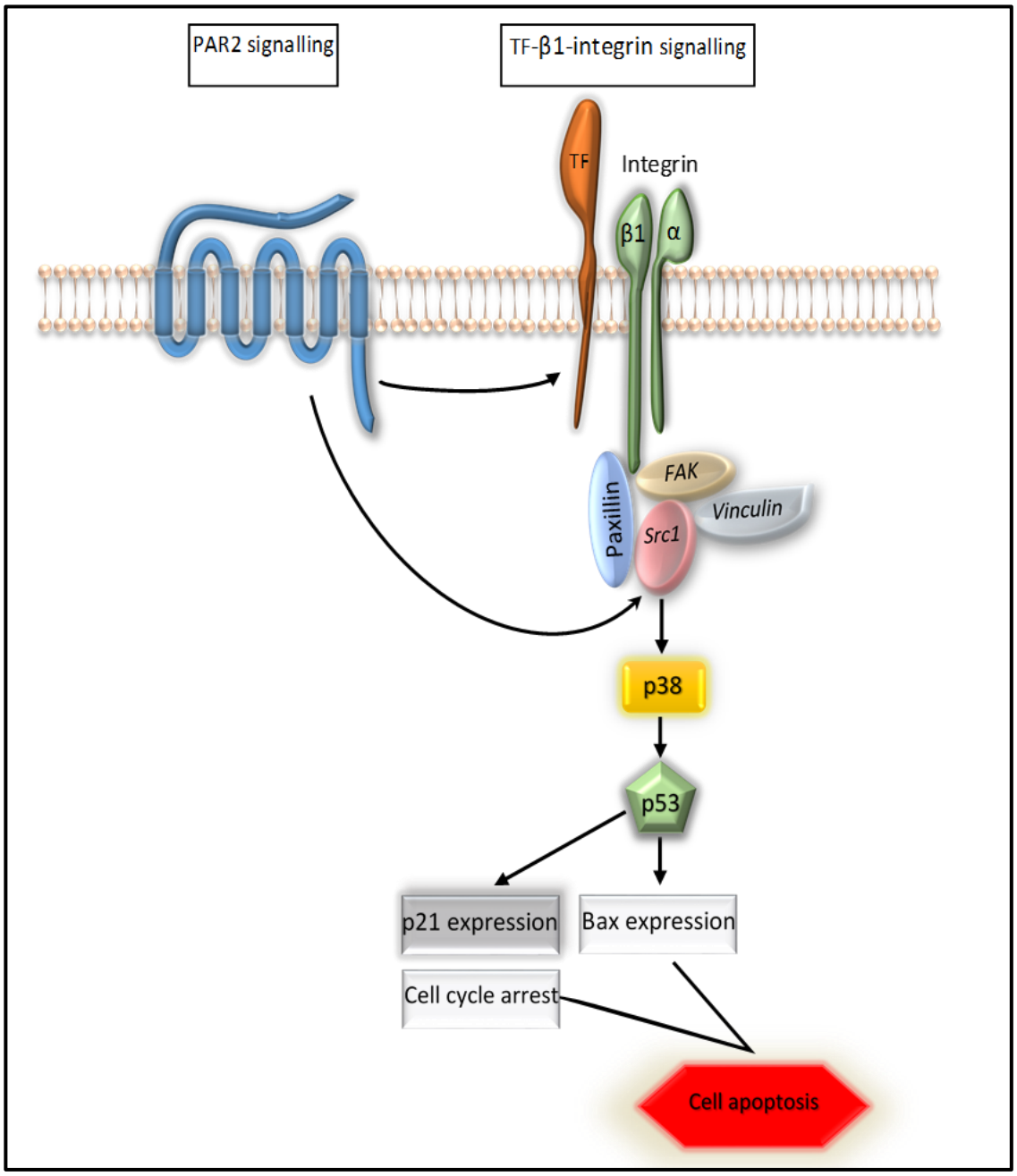

The accumulation of TF within the cells and induction of PAR2 results in activation of p38 MAPK protein and subsequent cellular apoptosis through a mechanism which is mediated by β1-integrin. In addition, β1-integrin may be capable of inducing of activation of focal adhesion complex resulting in the over-activation of Src1.

Chapter 7

References

References

Adams, M. N., Ramachandran, R., Yau, M.-K., Suen, J. Y., Fairlie, D. P., Hollenberg, M. D. & Hooper, J. D. (2011) Structure, function and pathophysiology of protease activated receptors. *Pharmacology & Therapeutics*, 130(3), 248-282.

Agrawal, N., Dasaradhi, P. V., Mohmmed, A., Malhotra, P., Bhatnagar, R. K. & Mukherjee, S. K. (2003) RNA interference: biology, mechanism, and applications. *Microbiol Mol Biol Rev*, 67(4), 657-85.

Ahamed, J. & Ruf, W. (2004) Protease-activated receptor 2-dependent phosphorylation of the tissue factor cytoplasmic domain. *J Biol Chem*, 279(22), 23038-44.

Aikawa, R., Nagai, T., Kudoh, S., Zou, Y., Tanaka, M., Tamura, M., Akazawa, H., Takano, H., Nagai, R. & Komuro, I. (2002) Integrins play a critical role in mechanical stress-induced p38 MAPK activation. *Hypertension*, 39(2), 233-8.

Aird, W. C. (2007) Phenotypic heterogeneity of the endothelium: I. Structure, function, and mechanisms. *Circ Res*, 100(2), 158-73.

Alessenko, A. V., Boikov, P. Y., Filippova, G. N., Khrenov, A. V., Loginov, A. S. & Makarieva, E. D. (1997) Mechanisms of cycloheximide-induced apoptosis in liver cells. *FEBS Letters*, 416(1), 113-116.

Altun-Gultekin, Z. F. & Wagner, J. A. (1996) Src, ras, and rac mediate the migratory response elicited by NGF and PMA in PC12 cells. *J Neurosci Res*, 44(4), 308-27.

Arias-Salgado, E. G., Lizano, S., Shattil, S. J. & Ginsberg, M. H. (2005) Specification of the direction of adhesive signaling by the integrin beta cytoplasmic domain. *J Biol Chem*, 280(33), 29699-707.

Ashkenazi, A. & Dixit, V. M. (1998) Death receptors: signaling and modulation. *Science*, 281(5381), 1305-8.

Aspenstrom, P., Fransson, A. & Saras, J. (2004) Rho GTPases have diverse effects on the organization of the actin filament system. *Biochem J*, 377(Pt 2), 327-37.

Avraham, S., London, R., Fu, Y., Ota, S., Hiregowdara, D., Li, J., Jiang, S., Pasztor, L. M., White, R. A., Groopman, J. E. & et al. (1995) Identification and characterization of a novel related adhesion focal tyrosine kinase (RAFTK) from megakaryocytes and brain. *J Biol Chem*, 270(46), 27742-51.

Bach, R. R. & Moldow, C. F. (1997) Mechanism of tissue factor activation on HL-60 cells. *Blood*, 89(9), 3270-6.

Bachli, M. D. E. (2000) Historical review. *British Journal of Haematology*, 110(2), 248-255.

Banfi, C., Brioschi, M., Barbieri, S. S., Eligini, S., Barcella, S., Tremoli, E., Colli, S. & Mussoni, L. (2009) Mitochondrial reactive oxygen species: a common pathway for PAR1- and PAR2-mediated tissue factor induction in human endothelial cells. *Journal of Thrombosis and Haemostasis*, 7(1), 206-216.

Barczyk, M., Carracedo, S. & Gullberg, D. (2010) Integrins. *Cell Tissue Res*, 339(1), 269-80.

Bastida, E., Ordinas, A., Escolar, G. & Jamieson, G. A. (1984) Tissue factor in microvesicles shed from U87MG human glioblastoma cells induces coagulation, platelet aggregation, and thrombogenesis. *Blood*, 64(1), 177-84.

Batista, S., Maniati, E., Reynolds, L. E., Tavora, B., Lees, D. M., Fernandez, I., Elia, G., Casanovas, O., Lo Celso, C., Hagemann, T. & Hodivala-Dilke, K. (2014) Haematopoietic focal adhesion kinase deficiency alters haematopoietic homeostasis to drive tumour metastasis. *Nat Commun*, 5, 5054.

Bazan, J. F. (1990) Structural design and molecular evolution of a cytokine receptor superfamily. *Proceedings of the National Academy of Sciences of the United States of America*, 87(18), 6934-6938.

Behrens, J., Vakaet, L., Friis, R., Winterhager, E., Van Roy, F., Mareel, M. M. & Birchmeier, W. (1993) Loss of epithelial differentiation and gain of invasiveness correlates with tyrosine phosphorylation of the E-cadherin/beta-catenin complex

in cells transformed with a temperature-sensitive v-SRC gene. *J Cell Biol*, 120(3), 757-66.

Berckmans, R. J., Nieuwland, R., Boing, A. N., Romijn, F. P., Hack, C. E. & Sturk, A. (2001) Cell-derived microparticles circulate in healthy humans and support low grade thrombin generation. *Thromb Haemost*, 85(4), 639-46.

Bergmann, S., Lang, A., Rohde, M., Agarwal, V., Rennemeier, C., Grashoff, C., Preissner, K. T. & Hammerschmidt, S. (2009) Integrin-linked kinase is required for vitronectin-mediated internalization of Streptococcus pneumoniae by host cells. *J Cell Sci*, 122(Pt 2), 256-67.

Beurel, E. & Jope, R. S. (2006) The paradoxical pro- and anti-apoptotic actions of GSK3 in the intrinsic and extrinsic apoptosis signaling pathways. *Progress in Neurobiology*, 79(4), 173-189.

Biscardi, J. S., Ishizawar, R. C., Silva, C. M. & Parsons, S. J. (2000) Tyrosine kinase signalling in breast cancer: epidermal growth factor receptor and c-Src interactions in breast cancer. *Breast Cancer Res*, 2(3), 203-10.

Bjorge, J. D., Pang, A. S., Funnell, M., Chen, K. Y., Diaz, R., Magliocco, A. M. & Fujita, D. J. (2011) Simultaneous siRNA targeting of Src and downstream signaling molecules inhibit tumor formation and metastasis of a human model breast cancer cell line. *PLoS One*, 6(4), e19309.

Boggon, T. J. & Eck, M. J. (2004) Structure and regulation of Src family kinases. *Oncogene*, 23(48), 7918-27.

Boissier, P. & Huynh-Do, U. (2014) The guanine nucleotide exchange factor Tiam1: A Janus-faced molecule in cellular signaling. *Cellular Signalling*, 26(3), 483-491.

Boureux, A., Vignal, E., Faure, S. & Fort, P. (2007) Evolution of the Rho family of ras-like GTPases in eukaryotes. *Mol Biol Evol*, 24(1), 203-16.

Brakebusch, C. & Fassler, R. (2005) beta 1 integrin function in vivo: adhesion, migration and more. *Cancer Metastasis Rev*, 24(3), 403-11.

Braun, F., Bertin-Ciftci, J., Gallouet, A. S., Millour, J. & Juin, P. (2011) Serum-nutrient starvation induces cell death mediated by Bax and Puma that is counteracted by p21 and unmasked by Bcl-x(L) inhibition. *PLoS One*, 6(8), e23577.

Brizzi, M. F., Tarone, G. & Defilippi, P. (2012) Extracellular matrix, integrins, and growth factors as tailors of the stem cell niche. *Current Opinion in Cell Biology*, 24(5), 645-651.

Brown, M. T. & Cooper, J. A. (1996) Regulation, substrates and functions of src. *Biochim Biophys Acta*, 1287(2-3), 121-49.

Burgaya, F. & Girault, J. A. (1996) Cloning of focal adhesion kinase, pp125FAK, from rat brain reveals multiple transcripts with different patterns of expression. *Brain Res Mol Brain Res*, 37(1-2), 63-73.

Byeon, S. E., Yi, Y. S., Oh, J., Yoo, B. C., Hong, S. & Cho, J. Y. (2012) The role of Src kinase in macrophage-mediated inflammatory responses. *Mediators Inflamm*, 2012, 512926.

Calalb, M. B., Polte, T. R. & Hanks, S. K. (1995) Tyrosine phosphorylation of focal adhesion kinase at sites in the catalytic domain regulates kinase activity: a role for Src family kinases. *Mol Cell Biol*, 15(2), 954-63.

Calalb, M. B., Zhang, X., Polte, T. R. & Hanks, S. K. (1996) Focal adhesion kinase tyrosine-861 is a major site of phosphorylation by Src. *Biochem Biophys Res Commun*, 228(3), 662-8.

Camerer, E., Huang, W. & Coughlin, S. R. (2000) Tissue factor- and factor X-dependent activation of protease-activated receptor 2 by factor VIIa. *Proc Natl Acad Sci U S A*, 97(10), 5255-60.

Camussi, G., Deregibus, M. C., Bruno, S., Cantaluppi, V. & Biancone, L. (2010) Exosomes/microvesicles as a mechanism of cell-to-cell communication. *Kidney International*, 78(9), 838-848.

Carmeliet, P., Mackman, N., Moons, L., Luther, T., Gressens, P., Van Vlaenderen, L., Demunck, H., Kasper, M., Breier, G., Evrard, P., Müller, M.,

Risau, W., Edgington, T. & Collen, D. (1996) Role of tissue factor in embryonic blood vessel development. *Nature*, 383, 73.

Cary, L. A., Klinghoffer, R. A., Sachsenmaier, C. & Cooper, J. A. (2002) SRC catalytic but not scaffolding function is needed for integrin-regulated tyrosine phosphorylation, cell migration, and cell spreading. *Mol Cell Biol*, 22(8), 2427-40.

Chen, Y., Li, G. & Liu, M. L. (2018) Microvesicles as Emerging Biomarkers and Therapeutic Targets in Cardiometabolic Diseases. *Genomics Proteomics Bioinformatics*, 16(1), 50-62.

Cheng, X., Peuckert, C. & Wölfl, S. (2017) Essential role of mitochondrial Stat3 in p38MAPK mediated apoptosis under oxidative stress. *Scientific Reports*, 7(1), 15388.

Cheng, Z., DiMichele, L. A., Hakim, Z. S., Rojas, M., Mack, C. P. & Taylor, J. M. (2012) Targeted FAK activation in cardiomyocytes protects the heart from ischemia/reperfusion injury. *Arteriosclerosis, thrombosis, and vascular biology*, 32(4), 924-933.

Cheung, P. C., Nebreda, A. R. & Cohen, P. (2004) TAB3, a new binding partner of the protein kinase TAK1. *Biochem J*, 378(Pt 1), 27-34.

Chiariello, M., Marinissen, M. J. & Gutkind, J. S. (2001) Regulation of c-myc expression by PDGF through Rho GTPases. *Nat Cell Biol*, 3(6), 580-6.

Chu, A. J. (2011) Tissue factor, blood coagulation, and beyond: an overview. *Int J Inflam*, 2011, 367284.

Collier, M. E. & Ettelaie, C. (2010) Induction of endothelial cell proliferation by recombinant and microparticle-tissue factor involves beta1-integrin and extracellular signal regulated kinase activation. *Arterioscler Thromb Vasc Biol*, 30(9), 1810-7.

Collier, M. E. & Ettelaie, C. (2011) Regulation of the incorporation of tissue factor into microparticles by serine phosphorylation of the cytoplasmic domain of tissue factor. *J Biol Chem*, 286(14), 11977-84.

Collier, M. E., Li, C. & Ettelaie, C. (2008) Influence of exogenous tissue factor on estrogen receptor alpha expression in breast cancer cells: involvement of beta1-integrin, PAR2, and mitogen-activated protein kinase activation. *Mol Cancer Res*, 6(12), 1807-18.

Collier, M. E., Mah, P. M., Xiao, Y., Maraveyas, A. & Ettelaie, C. (2013) Microparticle-associated tissue factor is recycled by endothelial cells resulting in enhanced surface tissue factor activity. *Thromb Haemost*, 110(5), 966-76.

Collins, R. J., Harmon, B. V., Souvlis, T., Pope, J. H. & Kerr, J. F. (1991) Effects of cycloheximide on B-chronic lymphocytic leukaemic and normal lymphocytes in vitro: induction of apoptosis. *Br J Cancer*, 64(3), 518-22.

Combes, V., Simon, A. C., Grau, G. E., Arnoux, D., Camoin, L., Sabatier, F., Mutin, M., Sanmarco, M., Sampol, J. & Dignat-George, F. (1999) In vitro generation of endothelial microparticles and possible prothrombotic activity in patients with lupus anticoagulant. *J Clin Invest*, 104(1), 93-102.

Cook-Mills, J. M. & Deem, T. L. (2005) Active participation of endothelial cells in inflammation. *J Leukoc Biol*, 77(4), 487-95.

Coso, O. A., Chiariello, M., Yu, J. C., Teramoto, H., Crespo, P., Xu, N., Miki, T. & Gutkind, J. S. (1995) The small GTP-binding proteins Rac1 and Cdc42 regulate the activity of the JNK/SAPK signaling pathway. *Cell*, 81(7), 1137-46.

Coughlin, S. R. (2000) Thrombin signalling and protease-activated receptors. *Nature*, 407(6801), 258-64.

Coughlin, S. R. & Camerer, E. (2003) PARticipation in inflammation. *Journal of Clinical Investigation*, 111(1), 25-27.

Croons, V., Martinet, W., Herman, A. G., Timmermans, J. P. & De Meyer, G. R. (2009) The protein synthesis inhibitor anisomycin induces macrophage apoptosis in rabbit atherosclerotic plaques through p38 mitogen-activated protein kinase. *J Pharmacol Exp Ther*, 329(3), 856-64.

Cuenda, A. & Rousseau, S. (2007) p38 MAP-Kinases pathway regulation, function and role in human diseases. *Biochimica et Biophysica Acta (BBA) - Molecular Cell Research*, 1773(8), 1358-1375.

Dai, L., Aye Thu, C., Liu, X. Y., Xi, J. & Cheung, P. C. (2012) TAK1, more than just innate immunity. *IUBMB Life*, 64(10), 825-34.

Danial, N. N. & Korsmeyer, S. J. (2004) Cell death: critical control points. *Cell*, 116(2), 205-19.

Dasgupta, S. K., Le, A., Chavakis, T., Rumbaut, R. E. & Thiagarajan, P. (2012) Developmental endothelial locus-1 (Del-1) mediates clearance of platelet microparticles by the endothelium. *Circulation*, 125(13), 1664-72.

Davila, M., Amirkhosravi, A., Coll, E., Desai, H., Robles, L., Colon, J., Baker, C. H. & Francis, J. L. (2008) Tissue factor-bearing microparticles derived from tumor cells: impact on coagulation activation. *J Thromb Haemost*, 6(9), 1517-24.

Dejean, L. M., Martinez-Caballero, S. & Kinnally, K. W. (2006) Is MAC the knife that cuts cytochrome c from mitochondria during apoptosis? *Cell Death Differ*, 13(8), 1387-95.

Deveraux, Q. L., Roy, N., Stennicke, H. R., Van Arsdale, T., Zhou, Q., Srinivasula, S. M., Alnemri, E. S., Salvesen, G. S. & Reed, J. C. (1998) IAPs block apoptotic events induced by caspase-8 and cytochrome c by direct inhibition of distinct caspases. *The EMBO Journal*, 17(8), 2215-2223.

Didsbury, J., Weber, R. F., Bokoch, G. M., Evans, T. & Snyderman, R. (1989) rac, a novel ras-related family of proteins that are botulinum toxin substrates. *J Biol Chem*, 264(28), 16378-82.

Diehl, P., Aleker, M., Helbing, T., Sossong, V., Germann, M., Sorichter, S., Bode, C. & Moser, M. (2011) Increased platelet, leukocyte and endothelial microparticles predict enhanced coagulation and vascular inflammation in pulmonary hypertension. *Journal of Thrombosis and Thrombolysis*, 31(2), 173-179.

Distler, J. H. W., Huber, L. C., Hueber, A. J., Reich, C. F., Gay, S., Distler, O. & Pisetsky, D. S. (2005) The release of microparticles by apoptotic cells and their effects on macrophages. *Apoptosis*, 10(4), 731-741.

Donepudi, M., Mac Sweeney, A., Briand, C. & Grutter, M. G. (2003) Insights into the regulatory mechanism for caspase-8 activation. *Molecular Cell*, 11(2), 543-549.

Dorfleutner, A., Hintermann, E., Tarui, T., Takada, Y. & Ruf, W. (2004) Cross-talk of integrin alpha3beta1 and tissue factor in cell migration. *Mol Biol Cell*, 15(10), 4416-25.

Drake, T. A., Morrissey, J. H. & Edgington, T. S. (1989) Selective cellular expression of tissue factor in human tissues. Implications for disorders of hemostasis and thrombosis. *Am J Pathol*, 134(5), 1087-97.

Du, C., Fang, M., Li, Y., Li, L. & Wang, X. (2000) Smac, a mitochondrial protein that promotes cytochrome c-dependent caspase activation by eliminating IAP inhibition. *Cell*, 102(1), 33-42.

Dvorak, H. F., Quay, S. C., Orenstein, N. S., Dvorak, A. M., Hahn, P., Bitzer, A. M. & Carvalho, A. C. (1981) Tumor shedding and coagulation. *Science*, 212(4497), 923-4.

Egorina, E. M., Sovershaev, M. A. & Osterud, B. (2008) Regulation of tissue factor procoagulant activity by post-translational modifications. *Thromb Res*, 122(6), 831-7.

Eisenreich, A. & Rauch, U. (2010) Regulation and differential role of the tissue factor isoforms in cardiovascular biology. *Trends Cardiovasc Med*, 20(6), 199-203.

Eke, I., Deuse, Y., Hehlgans, S., Gurtner, K., Krause, M., Baumann, M., Shevchenko, A., Sandfort, V. & Cordes, N. (2012) β(1) Integrin/FAK/cortactin signaling is essential for human head and neck cancer resistance to radiotherapy. *The Journal of Clinical Investigation*, 122(4), 1529-1540.

El-Daly, M., Saifeddine, M., Mihara, K., Ramachandran, R., Triggle, C. R. & Hollenberg, M. D. (2014) Proteinase-activated receptors 1 and 2 and the regulation of porcine coronary artery contractility: a role for distinct tyrosine kinase pathways. *Br J Pharmacol*, 171(9), 2413-25.

ElKeeb, A. M., Collier, M. E., Maraveyas, A. & Ettelaie, C. (2015) Accumulation of tissue factor in endothelial cells induces cell apoptosis, mediated through p38 and p53 activation. *Thromb Haemost*, 114(2), 364-78.

Elmore, S. (2007) Apoptosis: a review of programmed cell death. *Toxicol Pathol*, 35(4), 495-516.

Enjoji, S., Ohama, T. & Sato, K. (2014) Regulation of epithelial cell tight junctions by protease-activated receptor 2. *J Vet Med Sci*, 76(9), 1225-9.

Erlich, J., Fearns, C., Mathison, J., Ulevitch, R. J. & Mackman, N. (1999) Lipopolysaccharide induction of tissue factor expression in rabbits. *Infect Immun*, 67(5), 2540-6.

Esmon, C. T., Owen, W. G. & Jackson, C. M. (1974) The conversion of prothrombin to thrombin. V. The activation of prothrombin by factor Xa in the presence of phospholipid. *J Biol Chem*, 249(24), 7798-807.

Ettelaie, C., Collier, M. E. W., Featherby, S., Benelhaj, N. E., Greenman, J. & Maraveyas, A. (2016) Analysis of the potential of cancer cell lines to release tissue factor-containing microvesicles: correlation with tissue factor and PAR2 expression. *Thrombosis Journal*, 14, 2.

Ettelaie, C., Fountain, D., Collier, M. E., Beeby, E., Xiao, Y. P. & Maraveyas, A. (2011) Low molecular weight heparin suppresses tissue factor-mediated cancer cell invasion and migration in vitro. *Exp Ther Med*, 2(2), 363-367.

Ettelaie, C., Li, C., Collier, M. E., Pradier, A., Frentzou, G. A., Wood, C. G., Chetter, I. C., McCollum, P. T., Bruckdorfer, K. R. & James, N. J. (2007) Differential functions of tissue factor in the trans-activation of cellular signalling pathways. *Atherosclerosis*, 194(1), 88-101.

Ettelaie, C., Su, S., Li, C. & Collier, M. E. (2008) Tissue factor-containing microparticles released from mesangial cells in response to high glucose and AGE induce tube formation in microvascular cells. *Microvasc Res*, 76(3), 152-60.

Faust, D., Schmitt, C., Oesch, F., Oesch-Bartlomowicz, B., Schreck, I., Weiss, C. & Dietrich, C. (2012) Differential p38-dependent signalling in response to cellular

stress and mitogenic stimulation in fibroblasts. *Cell Communication and Signaling : CCS*, 10, 6-6.

Fleck, R. A., Rao, L. V., Rapaport, S. I. & Varki, N. (1990) Localization of human tissue factor antigen by immunostaining with monospecific, polyclonal anti-human tissue factor antibody. *Thromb Res*, 59(2), 421-37.

Fox, G. L., Rebay, I. & Hynes, R. O. (1999) Expression of DFak56, a Drosophila homolog of vertebrate focal adhesion kinase, supports a role in cell migration in vivo. *Proc Natl Acad Sci U S A*, 96(26), 14978-83.

Frame, M. C. (2002) Src in cancer: deregulation and consequences for cell behaviour. *Biochim Biophys Acta*, 1602(2), 114-30.

Frentzou, A. G., Collier, M. E., Seymour, A. M. & Ettelaie, C. (2010) Differential induction of cellular proliferation, hypertrophy and apoptosis in H9c2 cardiomyocytes by exogenous tissue factor. *Mol Cell Biochem*, 345(1-2), 119-30.

Fujita, S., Ota, E., Sasaki, C., Takano, K., Miyake, M. & Miyake, J. (2007) Highly efficient reverse transfection with siRNA in multiple wells of microtiter plates. *Journal of Bioscience and Bioengineering*, 104(4), 329-333.

Galley, H. F. & Webster, N. R. (2004) Physiology of the endothelium. *Br J Anaesth*, 93(1), 105-13.

Garcia-Gomez, C., Parages, M. L., Jimenez, C., Palma, A., Mata, M. T. & Segovia, M. (2012) Cell survival after UV radiation stress in the unicellular chlorophyte Dunaliella tertiolecta is mediated by DNA repair and MAPK phosphorylation. *J Exp Bot*, 63(14), 5259-74.

Geiger, B., Spatz, J. P. & Bershadsky, A. D. (2009) Environmental sensing through focal adhesions. *Nat Rev Mol Cell Biol*, 10(1), 21-33.

Gerotziafas, G. T., Galea, V., Mbemba, E., Khaterchi, A., Sassi, M., Baccouche, H., Prengel, C., van Dreden, P., Hatmi, M., Bernaudin, J. F. & Elalamy, I. (2012) Tissue factor over-expression by human pancreatic cancer cells BXPC3 is related to higher prothrombotic potential as compared to breast cancer cells MCF7. *Thromb Res*, 129(6), 779-86.

Giancotti, F. G. (2000) Complexity and specificity of integrin signalling. *Nature Cell Biology*, 2, E13.

Giesen, P. L., Rauch, U., Bohrmann, B., Kling, D., Roque, M., Fallon, J. T., Badimon, J. J., Himber, J., Riederer, M. A. & Nemerson, Y. (1999) Blood-borne tissue factor: another view of thrombosis. *Proc Natl Acad Sci U S A*, 96(5), 2311-5.

Goedert, M., Cuenda, A., Craxton, M., Jakes, R. & Cohen, P. (1997) Activation of the novel stress-activated protein kinase SAPK4 by cytokines and cellular stresses is mediated by SKK3 (MKK6); comparison of its substrate specificity with that of other SAP kinases. *The EMBO Journal*, 16(12), 3563-3571.

Golubovskaya, V. M., Kweh, F. A. & Cance, W. G. (2009) Focal adhesion kinase and cancer. *Histol Histopathol*, 24(4), 503-10.

Grunnet, L. G., Aikin, R., Tonnesen, M. F., Paraskevas, S., Blaabjerg, L., Storling, J., Rosenberg, L., Billestrup, N., Maysinger, D. & Mandrup-Poulsen, T. (2009) Proinflammatory cytokines activate the intrinsic apoptotic pathway in beta-cells. *Diabetes*, 58(8), 1807-15.

Gu, J. & Gu, X. (2003) Natural history and functional divergence of protein tyrosine kinases. *Gene*, 317(1-2), 49-57.

Guarino, M. (2010) Src signaling in cancer invasion. *J Cell Physiol*, 223(1), 14-26.

Gyorgy, B., Modos, K., Pallinger, E., Paloczi, K., Pasztoi, M., Misjak, P., Deli, M. A., Sipos, A., Szalai, A., Voszka, I., Polgar, A., Toth, K., Csete, M., Nagy, G., Gay, S., Falus, A., Kittel, A. & Buzas, E. I. (2011) Detection and isolation of cell-derived microparticles are compromised by protein complexes resulting from shared biophysical parameters. *Blood*, 117(4), e39-48.

Habersberger, J., Strang, F., Scheichl, A., Htun, N., Bassler, N., Merivirta, R. M., Diehl, P., Krippner, G., Meikle, P., Eisenhardt, S. U., Meredith, I. & Peter, K. (2012) Circulating microparticles generate and transport monomeric C-reactive protein in patients with myocardial infarction. *Cardiovasc Res*, 96(1), 64-72.

Hall, A. (1994) Small GTP-binding proteins and the regulation of the actin cytoskeleton. *Annu Rev Cell Biol*, 10, 31-54.

Han, J., Lee, J., Bibbs, L. & Ulevitch, R. (1994) A MAP kinase targeted by endotoxin and hyperosmolarity in mammalian cells. *Science*, 265(5173), 808-811.

Harburger, D. S. & Calderwood, D. A. (2009) Integrin signalling at a glance. *Journal of Cell Science*, 122(2), 159-163.

Hellum, M., Ovstebo, R., Troseid, A. M., Berg, J. P., Brandtzaeg, P. & Henriksson, C. E. (2012) Microparticle-associated tissue factor activity measured with the Zymuphen MP-TF kit and the calibrated automated thrombogram assay. *Blood Coagul Fibrinolysis*, 23(6), 520-6.

Henry, C. A., Crawford, B. D., Yan, Y. L., Postlethwait, J., Cooper, M. S. & Hille, M. B. (2001) Roles for zebrafish focal adhesion kinase in notochord and somite morphogenesis. *Dev Biol*, 240(2), 474-87.

Hinz, M., Stilmann, M., Arslan, S. C., Khanna, K. K., Dittmar, G. & Scheidereit, C. (2010) A cytoplasmic ATM-TRAF6-cIAP1 module links nuclear DNA damage signaling to ubiquitin-mediated NF-kappaB activation. *Mol Cell*, 40(1), 63-74.

Hipfner, D. R. & Cohen, S. M. (2004) Connecting proliferation and apoptosis in development and disease. *Nature Reviews Molecular Cell Biology*, 5, 805.

Hjortoe, G. M., Petersen, L. C., Albrektsen, T., Sorensen, B. B., Norby, P. L., Mandal, S. K., Pendurthi, U. R. & Rao, L. V. (2004) Tissue factor-factor VIIa-specific up-regulation of IL-8 expression in MDA-MB-231 cells is mediated by PAR-2 and results in increased cell migration. *Blood*, 103(8), 3029-37.

Hochwald, S. N., Nyberg, C., Zheng, M., Zheng, D., Wood, C., Massoll, N. A., Magis, A., Ostrov, D., Cance, W. G. & Golubovskaya, V. M. (2009) A novel small molecule inhibitor of FAK decreases growth of human pancreatic cancer. *Cell Cycle*, 8(15), 2435-43.

Hofmeister, J. K., Cooney, D. & Coggeshall, K. M. (2000) Clustered CD20 induced apoptosis: src-family kinase, the proximal regulator of tyrosine

phosphorylation, calcium influx, and caspase 3-dependent apoptosis. *Blood Cells Mol Dis*, 26(2), 133-43.

Horton, E. R., Humphries, J. D., Stutchbury, B., Jacquemet, G., Ballestrem, C., Barry, S. T. & Humphries, M. J. (2016) Modulation of FAK and Src adhesion signaling occurs independently of adhesion complex composition. *The Journal of Cell Biology*, 212(3), 349-364.

Hron, G., Kollars, M., Weber, H., Sagaster, V., Quehenberger, P., Eichinger, S., Kyrle, P. A. & Weltermann, A. (2007) Tissue factor-positive microparticles: cellular origin and association with coagulation activation in patients with colorectal cancer. *Thromb Haemost*, 97(1), 119-23.

Hsia, D. A., Lim, S. T., Bernard-Trifilo, J. A., Mitra, S. K., Tanaka, S., den Hertog, J., Streblow, D. N., Ilic, D., Ginsberg, M. H. & Schlaepfer, D. D. (2005) Integrin alpha4beta1 promotes focal adhesion kinase-independent cell motility via alpha4 cytoplasmic domain-specific activation of c-Src. *Mol Cell Biol*, 25(21), 9700-12.

Hu, L., Xia, L., Zhou, H., Wu, B., Mu, Y., Wu, Y. & Yan, J. (2013) TF/FVIIa/PAR2 promotes cell proliferation and migration via PKCalpha and ERK-dependent c-Jun/AP-1 pathway in colon cancer cell line SW620. *Tumour Biol*, 34(5), 2573-81.

Hugel, B., Martinez, M. C., Kunzelmann, C. & Freyssinet, J. M. (2005) Membrane microparticles: two sides of the coin. *Physiology (Bethesda)*, 20(1), 22-7.

Hunter, T. & Sefton, B. M. (1980) Transforming gene product of Rous sarcoma virus phosphorylates tyrosine. *Proc Natl Acad Sci U S A*, 77(3), 1311-5.

Hussain, S. P. & Harris, C. C. (1998) Molecular epidemiology of human cancer: contribution of mutation spectra studies of tumor suppressor genes. *Cancer Res*, 58(18), 4023-37.

Huth, H. W., Santos, D. M., Gravina, H. D., Resende, J. M., Goes, A. M., de Lima, M. E. & Ropert, C. (2017) Upregulation of p38 pathway accelerates proliferation and migration of MDA-MB-231 breast cancer cells. *Oncol Rep*, 37(4), 2497-2505.

Huveneers, S. & Danen, E. H. (2009) Adhesion signaling - crosstalk between integrins, Src and Rho. *J Cell Sci*, 122(Pt 8), 1059-69.

Huveneers, S., van den Bout, I., Sonneveld, P., Sancho, A., Sonnenberg, A. & Danen, E. H. (2007) Integrin alpha v beta 3 controls activity and oncogenic potential of primed c-Src. *Cancer Res*, 67(6), 2693-700.

Hynes, R. O. (1992) Integrins: versatility, modulation, and signaling in cell adhesion. *Cell*, 69(1), 11-25.

Hynes, R. O. (2002) Integrins: bidirectional, allosteric signaling machines. *Cell*, 110(6), 673-87.

Imamura, T., Sugiyama, T., Cuevas, L. E., Makunde, R. & Nakamura, S. (2002) Expression of tissue factor, the clotting initiator, on macrophages in Plasmodium falciparum-infected placentas. *J Infect Dis*, 186(3), 436-40.

Infusino, G. A. & Jacobson, J. R. (2012) Endothelial FAK as a therapeutic target in disease. *Microvasc Res*, 83(1), 89-96.

Irie, T., Muta, T. & Takeshige, K. (2000) TAK1 mediates an activation signal from toll-like receptor(s) to nuclear factor-kappaB in lipopolysaccharide-stimulated macrophages. *FEBS Lett*, 467(2-3), 160-4.

Ishitani, T., Takaesu, G., Ninomiya-Tsuji, J., Shibuya, H., Gaynor, R. B. & Matsumoto, K. (2003) Role of the TAB2-related protein TAB3 in IL-1 and TNF signaling. *EMBO J*, 22(23), 6277-88.

Jansen, F., Yang, X., Hoelscher, M., Cattelan, A., Schmitz, T., Proebsting, S., Wenzel, D., Vosen, S., Franklin, B. S., Fleischmann, B. K., Nickenig, G. & Werner, N. (2013) Endothelial microparticle-mediated transfer of MicroRNA-126 promotes vascular endothelial cell repair via SPRED1 and is abrogated in glucose-damaged endothelial microparticles. *Circulation*, 128(18), 2026-38.

Johnson, L. N., Noble, M. E. & Owen, D. J. (1996) Active and inactive protein kinases: structural basis for regulation. *Cell*, 85(2), 149-58.

Kaminsky, P. M., Keiser, N. W., Yan, Z., Lei-Butters, D. C. & Engelhardt, J. F. (2012) Directing integrin-linked endocytosis of recombinant AAV enhances productive FAK-dependent transduction. *Mol Ther*, 20(5), 972-83.

Kim, J. Y., Kajino-Sakamoto, R., Omori, E., Jobin, C. & Ninomiya-Tsuji, J. (2009) Intestinal epithelial-derived TAK1 signaling is essential for cytoprotection against chemical-induced colitis. *PLoS One*, 4(2), e4561.

Kim, M. J., Byun, J. Y., Yun, C. H., Park, I. C., Lee, K. H. & Lee, S. J. (2008) c-Src-p38 mitogen-activated protein kinase signaling is required for Akt activation in response to ionizing radiation. *Mol Cancer Res*, 6(12), 1872-80.

Kim, S. I. & Choi, M. E. (2012) TGF-β-activated kinase-1: New insights into the mechanism of TGF-β signaling and kidney disease. *Kidney Research and Clinical Practice*, 31(2), 94-105.

Kishimoto, K., Matsumoto, K. & Ninomiya-Tsuji, J. (2000) TAK1 mitogen-activated protein kinase kinase kinase is activated by autophosphorylation within its activation loop. *Journal of Biological Chemistry*, 275(10), 7359-7364.

Kleinschmidt, E. G. & Schlaepfer, D. D. (2017) Focal adhesion kinase signaling in unexpected places. *Curr Opin Cell Biol*, 45, 24-30.

Kocaturk, B., Van den Berg, Y. W., Tieken, C., Mieog, J. S., de Kruijf, E. M., Engels, C. C., van der Ent, M. A., Kuppen, P. J., Van de Velde, C. J., Ruf, W., Reitsma, P. H., Osanto, S., Liefers, G. J., Bogdanov, V. Y. & Versteeg, H. H. (2013) Alternatively spliced tissue factor promotes breast cancer growth in a beta1 integrin-dependent manner. *Proc Natl Acad Sci U S A*, 110(28), 11517-22.

Kocaturk, B. & Versteeg, H. H. (2013) Tissue factor-integrin interactions in cancer and thrombosis: every Jack has his Jill. *J Thromb Haemost*, 11 Suppl 1, 285-93.

Kopec, A. K., Spada, A. P., Contreras, P. C., Mackman, N. & Luyendyk, J. P. (2018) Caspase Inhibition Reduces Hepatic Tissue Factor-Driven Coagulation In Vitro and In Vivo. *Toxicol Sci*, 162(2), 396-405.

Kroemer, G. & Reed, J. C. (2000) Mitochondrial control of cell death. *Nat Med*, 6(5), 513-9.

Kuphal, S., Bauer, R. & Bosserhoff, A.-K. (2005) Integrin signaling in malignant melanoma. *Cancer and Metastasis Reviews*, 24(2), 195-222.

Kurdi, A. T., Bassil, R., Olah, M., Wu, C., Xiao, S., Taga, M., Frangieh, M., Buttrick, T., Orent, W., Bradshaw, E. M., Khoury, S. J. & Elyaman, W. (2016) Tiam1/Rac1 complex controls Il17a transcription and autoimmunity. *Nature Communications*, 7, 13048.

Kwon, T., Kwon, D. Y., Chun, J., Kim, J. H. & Kang, S. S. (2000) Akt protein kinase inhibits Rac1-GTP binding through phosphorylation at serine 71 of Rac1. *J Biol Chem*, 275(1), 423-8.

Lemaire, C., Andreau, K., Souvannavong, V. & Adam, A. (1999) Specific dual effect of cycloheximide on B lymphocyte apoptosis: involvement of CPP32/caspase-3. *Biochem Pharmacol*, 58(1), 85-93.

Leone, D. P., Srinivasan, K., Brakebusch, C. & McConnell, S. K. (2010) The rho GTPase Rac1 is required for proliferation and survival of progenitors in the developing forebrain. *Dev Neurobiol*, 70(9), 659-78.

Lev, S., Moreno, H., Martinez, R., Canoll, P., Peles, E., Musacchio, J. M., Plowman, G. D., Rudy, B. & Schlessinger, J. (1995) Protein tyrosine kinase PYK2 involved in Ca(2+)-induced regulation of ion channel and MAP kinase functions. *Nature*, 376(6543), 737-45.

Li, L., Dong, X., Peng, F. & Shen, L. (2018a) Integrin beta1 regulates the invasion and radioresistance of laryngeal cancer cells by targeting CD147. *Cancer Cell Int*, 18, 80.

Li, P., Chen, D., Cui, Y., Zhang, W., Weng, J., Yu, L., Chen, L., Chen, Z., Su, H., Yu, S., Wu, J., Huang, Q. & Guo, X. (2018b) Src Plays an Important Role in AGE-Induced Endothelial Cell Proliferation, Migration, and Tubulogenesis. *Front Physiol*, 9(765), 765.

Limami, Y., Pinon, A., Leger, D. Y., Pinault, E., Delage, C., Beneytout, J. L., Simon, A. & Liagre, B. (2012) The P2Y2/Src/p38/COX-2 pathway is involved in the resistance to ursolic acid-induced apoptosis in colorectal and prostate cancer cells. *Biochimie*, 94(8), 1754-63.

Lipfert, L., Haimovich, B., Schaller, M. D., Cobb, B. S., Parsons, J. T. & Brugge, J. S. (1992) Integrin-dependent phosphorylation and activation of the protein tyrosine kinase pp125FAK in platelets. *J Cell Biol*, 119(4), 905-12.

Liu, H., Chang, D. W. & Yang, X. (2005) Interdimer processing and linearity of procaspase-3 activation: A unifying mechanism for the activation of initiator and effector caspases. *Journal of Biological Chemistry*, 280(12), 11578-11582.

Loyer, X., Vion, A. C., Tedgui, A. & Boulanger, C. M. (2014) Microvesicles as cell-cell messengers in cardiovascular diseases. *Circ Res*, 114(2), 345-53.

Lu, Z., Jiang, G., Blume-Jensen, P. & Hunter, T. (2001) Epidermal growth factor-induced tumor cell invasion and metastasis initiated by dephosphorylation and downregulation of focal adhesion kinase. *Mol Cell Biol*, 21(12), 4016-31.

Maa, M. C., Leu, T. H., McCarley, D. J., Schatzman, R. C. & Parsons, S. J. (1995) Potentiation of epidermal growth factor receptor-mediated oncogenesis by c-Src: implications for the etiology of multiple human cancers. *Proc Natl Acad Sci U S A*, 92(15), 6981-5.

Macfarlane, S. R., Seatter, M. J., Kanke, T., Hunter, G. D. & Plevin, R. (2001) Proteinase-activated receptors. *Pharmacol Rev*, 53(2), 245-82.

Mackman, N. (2004) Role of tissue factor in hemostasis, thrombosis, and vascular development. *Arterioscler Thromb Vasc Biol*, 24(6), 1015-22.

Mackman, N. (2009) The role of tissue factor and factor VIIa in hemostasis. *Anesth Analg*, 108(5), 1447-52.

Mackman, N., Morrissey, J. H., Fowler, B. & Edgington, T. S. (1989) Complete sequence of the human tissue factor gene, a highly regulated cellular receptor that initiates the coagulation protease cascade. *Biochemistry*, 28(4), 1755-62.

Major, C. D., Santulli, R. J., Derian, C. K. & Andrade-Gordon, P. (2003) Extracellular mediators in atherosclerosis and thrombosis: lessons from thrombin receptor knockout mice. *Arterioscler Thromb Vasc Biol*, 23(6), 931-9.

Mallat, Z., Hugel, B., Ohan, J., Leseche, G., Freyssinet, J. M. & Tedgui, A. (1999) Shed membrane microparticles with procoagulant potential in human

atherosclerotic plaques: a role for apoptosis in plaque thrombogenicity. *Circulation*, 99(3), 348-53.

Martin, S. E., Wu, Z. H., Gehlhaus, K., Jones, T. L., Zhang, Y. W., Guha, R., Miyamoto, S., Pommier, Y. & Caplen, N. J. (2011) RNAi screening identifies TAK1 as a potential target for the enhanced efficacy of topoisomerase inhibitors. *Curr Cancer Drug Targets*, 11(8), 976-86.

Mause, S. F. & Weber, C. (2010) Microparticles: protagonists of a novel communication network for intercellular information exchange. *Circ Res*, 107(9), 1047-57.

Maya-Mendoza, A., Bartek, J., Jackson, D. A. & Streuli, C. H. (2016) Cellular microenvironment controls the nuclear architecture of breast epithelia through beta1-integrin. *Cell Cycle*, 15(3), 345-56.

McCoy, A. M., Collins, M. L. & Ugozzoli, L. A. (2010) Using the gene pulser MXcell electroporation system to transfect primary cells with high efficiency. *J Vis Exp*(35).

McIlwain, D. R., Berger, T. & Mak, T. W. (2013) Caspase functions in cell death and disease. *Cold Spring Harb Perspect Biol*, 5(4), a008656.

Melisi, D., Xia, Q., Paradiso, G., Ling, J., Moccia, T., Carbone, C., Budillon, A., Abbruzzese, J. L. & Chiao, P. J. (2011) Modulation of pancreatic cancer chemoresistance by inhibition of TAK1. *J Natl Cancer Inst*, 103(15), 1190-204.

Mesri, M. & Altieri, D. C. (1999) Leukocyte microparticles stimulate endothelial cell cytokine release and tissue factor induction in a JNK1 signaling pathway. *J Biol Chem*, 274(33), 23111-8.

Meves, A., Geiger, T., Zanivan, S., DiGiovanni, J., Mann, M. & Fassler, R. (2011) Beta1 integrin cytoplasmic tyrosines promote skin tumorigenesis independent of their phosphorylation. *Proc Natl Acad Sci U S A*, 108(37), 15213-8.

Michiels, C. (2003) Endothelial cell functions. *J Cell Physiol*, 196(3), 430-43.

Minden, A., Lin, A., Claret, F. X., Abo, A. & Karin, M. (1995) Selective activation of the JNK signaling cascade and c-Jun transcriptional activity by the small GTPases Rac and Cdc42Hs. *Cell*, 81(7), 1147-57.

Missirlis, D., Haraszti, T., Scheele, C., Wiegand, T., Diaz, C., Neubauer, S., Rechenmacher, F., Kessler, H. & Spatz, J. P. (2016) Substrate engagement of integrins alpha5beta1 and alphavbeta3 is necessary, but not sufficient, for high directional persistence in migration on fibronectin. *Sci Rep*, 6, 23258.

Mitra, S. K. & Schlaepfer, D. D. (2006) Integrin-regulated FAK-Src signaling in normal and cancer cells. *Curr Opin Cell Biol*, 18(5), 516-23.

Morel, O., Jesel, L., Freyssinet, J. M. & Toti, F. (2005) Elevated levels of procoagulant microparticles in a patient with myocardial infarction, antiphospholipid antibodies and multifocal cardiac thrombosis. *Thromb J*, 3, 15.

Morel, O., Toti, F., Hugel, B., Bakouboula, B., Camoin-Jau, L., Dignat-George, F. & Freyssinet, J. M. (2006) Procoagulant microparticles: disrupting the vascular homeostasis equation? *Arterioscler Thromb Vasc Biol*, 26(12), 2594-604.

Moriguchi, T., Kuroyanagi, N., Yamaguchi, K., Gotoh, Y., Irie, K., Kano, T., Shirakabe, K., Muro, Y., Shibuya, H., Matsumoto, K., Nishida, E. & Hagiwara, M. (1996) A novel kinase cascade mediated by mitogen-activated protein kinase kinase 6 and MKK3. *J Biol Chem*, 271(23), 13675-9.

Morrison, S. A. & Jesty, J. (1984) Tissue factor-dependent activation of tritium-labeled factor IX and factor X in human plasma. *Blood*, 63(6), 1338-47.

Muller, D. N., Mervaala, E. M. A., Dechend, R., Fiebeler, A., Park, J. K., Schmidt, F., Theuer, J., Breu, V., Mackman, N., Luther, T., Schneider, W., Gulba, D., Ganten, D., Haller, H. & Luft, F. C. (2000) Angiotensin II (AT(1)) receptor blockade reduces vascular tissue factor in angiotensin II-induced cardiac vasculopathy. *American Journal of Pathology*, 157(1), 111-122.

Munoz-Sanjuan, I., Bell, E., Altmann, C. R., Vonica, A. & Brivanlou, A. H. (2002) Gene profiling during neural induction in Xenopus laevis: regulation of BMP signaling by post-transcriptional mechanisms and TAB3, a novel TAK1-binding protein. *Development*, 129(23), 5529-40.

Nemerson, Y. (1988) Tissue factor and hemostasis. *Blood*, 71(1), 1-8.

Ninomiya-Tsuji, J., Kishimoto, K., Hiyama, A., Inoue, J., Cao, Z. & Matsumoto, K. (1999) The kinase TAK1 can activate the NIK-I kappaB as well as the MAP kinase cascade in the IL-1 signalling pathway. *Nature*, 398(6724), 252-6.

Nomura, S., Niki, M., Nisizawa, T., Tamaki, T. & Shimizu, M. (2015) Microparticles as Biomarkers of Blood Coagulation in Cancer. *Biomark Cancer*, 7, 51-6.

Nystedt, S., Emilsson, K., Larsson, A. K., Strombeck, B. & Sundelin, J. (1995) Molecular cloning and functional expression of the gene encoding the human proteinase-activated receptor 2. *Eur J Biochem*, 232(1), 84-9.

Oktay, M., Wary, K. K., Dans, M., Birge, R. B. & Giancotti, F. G. (1999) Integrin-mediated activation of focal adhesion kinase is required for signaling to Jun NH2-terminal kinase and progression through the G1 phase of the cell cycle. *J Cell Biol*, 145(7), 1461-9.

Ono, K., Ohtomo, T., Sato, S., Sugamata, Y., Suzuki, M., Hisamoto, N., Ninomiya-Tsuji, J., Tsuchiya, M. & Matsumoto, K. (2001) An evolutionarily conserved motif in the TAB1 C-terminal region is necessary for interaction with and activation of TAK1 MAPKKK. *J Biol Chem*, 276(26), 24396-400.

Osterud, B. & Bjorklid, E. (2012) Tissue factor in blood cells and endothelial cells. *Front Biosci (Elite Ed)*, 4, 289-99.

Owen, J. D., Ruest, P. J., Fry, D. W. & Hanks, S. K. (1999) Induced focal adhesion kinase (FAK) expression in FAK-null cells enhances cell spreading and migration requiring both auto- and activation loop phosphorylation sites and inhibits adhesion-dependent tyrosine phosphorylation of Pyk2. *Mol Cell Biol*, 19(7), 4806-18.

Pan, Q., Liu, H., Zheng, C., Zhao, Y., Liao, X., Wang, Y., Chen, Y., Zhao, B., Lazartigues, E., Yang, Y. & Ma, X. (2016) Microvesicles Derived from Inflammation-Challenged Endothelial Cells Modulate Vascular Smooth Muscle Cell Functions. *Front Physiol*, 7, 692.

Parsons, J. T. (2003) Focal adhesion kinase: the first ten years. *J Cell Sci*, 116(Pt 8), 1409-16.

Parsons, S. J. & Parsons, J. T. (2004) Src family kinases, key regulators of signal transduction. *Oncogene*, 23(48), 7906-9.

Peshkova, A. D., Le Minh, G., Tutwiler, V., Andrianova, I. A., Weisel, J. W. & Litvinov, R. I. (2017) Activated Monocytes Enhance Platelet-Driven Contraction of Blood Clots via Tissue Factor Expression. *Sci Rep*, 7(1), 5149.

Peterson, D. B., Sander, T., Kaul, S., Wakim, B. T., Halligan, B., Twigger, S., Pritchard, K. A., Oldham, K. T. & Ou, J.-S. (2008) Comparative proteomic analysis of PAI-1 and TNF-alpha-derived endothelial microparticles. *Proteomics*, 8(12), 2430-2446.

Playford, M. P. & Schaller, M. D. (2004) The interplay between Src and integrins in normal and tumor biology. *Oncogene*, 23(48), 7928-46.

Pober, J. S. (2002) Endothelial activation: intracellular signaling pathways. *Arthritis Research*, 4(Suppl 3), S109-S116.

Pober, J. S. & Cotran, R. S. (1990) Cytokines and endothelial cell biology. *Physiol Rev*, 70(2), 427-51.

Pradier, A. & Ettelaie, C. (2008) The influence of exogenous tissue factor on the regulators of proliferation and apoptosis in endothelial cells. *J Vasc Res*, 45(1), 19-32.

Preston, R. A., Jy, W., Jimenez, J. J., Mauro, L. M., Horstman, L. L., Valle, M., Aime, G. & Ahn, Y. S. (2002) Effects of severe hypertension on endothelial and platelet microparticles. *Hypertension*, 41(2), 211-217.

Puls, A., Eliopoulos, A. G., Nobes, C. D., Bridges, T., Young, L. S. & Hall, A. (1999) Activation of the small GTPase Cdc42 by the inflammatory cytokines TNF(alpha) and IL-1, and by the Epstein-Barr virus transforming protein LMP1. *J Cell Sci*, 112 (Pt 17), 2983-92.

Pyo, R. T., Sato, Y., Mackman, N. & Taubman, M. B. (2004) Mice deficient in tissue factor demonstrate attenuated intimal hyperplasia in response to vascular

injury and decreased smooth muscle cell migration. *Thromb Haemost*, 92(3), 451-8.

Raingeaud, J., Gupta, S., Rogers, J. S., Dickens, M., Han, J., Ulevitch, R. J. & Davis, R. J. (1995) Pro-inflammatory cytokines and environmental stress cause p38 mitogen-activated protein kinase activation by dual phosphorylation on tyrosine and threonine. *J Biol Chem*, 270(13), 7420-6.

Rallapalli, P. M., Orengo, C. A., Studer, R. A. & Perkins, S. J. (2014) Positive selection during the evolution of the blood coagulation factors in the context of their disease-causing mutations. *Mol Biol Evol*, 31(11), 3040-56.

Reed, J. C. (2000) Mechanisms of apoptosis. *Am J Pathol*, 157(5), 1415-30.

Rezaie, A. R. (2014) Protease-activated receptor signalling by coagulation proteases in endothelial cells. *Thromb Haemost*, 112(5), 876-82.

Riewald, M., Kravchenko, V. V., Petrovan, R. J., O'Brien, P. J., Brass, L. F., Ulevitch, R. J. & Ruf, W. (2001) Gene induction by coagulation factor Xa is mediated by activation of protease-activated receptor 1. *Blood*, 97(10), 3109-16.

Riewald, M. & Ruf, W. (2001) Mechanistic coupling of protease signaling and initiation of coagulation by tissue factor. *Proc Natl Acad Sci U S A*, 98(14), 7742-7.

Riewald, M. & Ruf, W. (2003) Science review: Role of coagulation protease cascades in sepsis. *Critical Care*, 7(2), 123-129.

Roskoski, R., Jr. (2004) Src protein-tyrosine kinase structure and regulation. *Biochem Biophys Res Commun*, 324(4), 1155-64.

Rothmeier, A. S., Liu, E., Chakrabarty, S., Disse, J., Mueller, B. M., Østergaard, H. & Ruf, W. (2018) Identification of the integrin-binding site on coagulation factor VIIa required for proangiogenic PAR2 signaling. *Blood*, 131(6), 674-685.

Rothmeier, A. S., Marchese, P., Langer, F., Kamikubo, Y., Schaffner, F., Cantor, J., Ginsberg, M. H., Ruggeri, Z. M. & Ruf, W. (2017) Tissue Factor Prothrombotic Activity Is Regulated by Integrin-arf6 Trafficking. *Arterioscler Thromb Vasc Biol*, 37(7), 1323-1331.

Rothmeier, A. S. & Ruf, W. (2012) Protease-activated receptor 2 signaling in inflammation. *Seminars in Immunopathology*, 34(1), 133-149.

Ruf, W. & Edgington, T. S. (1994) Structural biology of tissue factor, the initiator of thrombogenesis in vivo. *The FASEB Journal*, 8(6), 385-390.

Ruf, W. & Mueller, B. M. (1999) Tissue factor signaling. *Thromb Haemost*, 82(2), 175-82.

Ruf, W., Rehemtulla, A., Morrissey, J. H. & Edgington, T. S. (1991) Phospholipid-independent and -dependent interactions required for tissue factor receptor and cofactor function. *J Biol Chem*, 266(4), 2158-66.

Sabatier, F., Darmon, P., Hugel, B., Combes, V., Sanmarco, M., Velut, J. G., Arnoux, D., Charpiot, P., Freyssinet, J. M., Oliver, C., Sampol, J. & Dignat-George, F. (2002) Type 1 and type 2 diabetic patients display different patterns of cellular microparticles. *Diabetes*, 51(9), 2840-5.

Sakurai, H., Miyoshi, H., Mizukami, J. & Sugita, T. (2000) Phosphorylation-dependent activation of TAK1 mitogen-activated protein kinase kinase kinase by TAB1. *FEBS Lett*, 474(2-3), 141-5.

Sakurai, H., Miyoshi, H., Toriumi, W. & Sugita, T. (1999) Functional interactions of transforming growth factor beta-activated kinase 1 with IkappaB kinases to stimulate NF-kappaB activation. *J Biol Chem*, 274(15), 10641-8.

Salmela, M., Jokinen, J., Tiitta, S., Rappu, P., Cheng, R. H. & Heino, J. (2017) Integrin α2β1 in nonactivated conformation can induce focal adhesion kinase signaling. *Scientific Reports*, 7(1), 3414.

Sasaki, H., Nagura, K., Ishino, M., Tobioka, H., Kotani, K. & Sasaki, T. (1995) Cloning and characterization of cell adhesion kinase beta, a novel protein-tyrosine kinase of the focal adhesion kinase subfamily. *J Biol Chem*, 270(36), 21206-19.

Sato, K., Sato, A., Aoto, M. & Fukami, Y. (1995) Site-specific association of c-Src with epidermal growth factor receptor in A431 cells. *Biochem Biophys Res Commun*, 210(3), 844-51.

Schaffner, F., Versteeg, H. H., Schillert, A., Yokota, N., Petersen, L. C., Mueller, B. M. & Ruf, W. (2010) Cooperation of tissue factor cytoplasmic domain and PAR2 signaling in breast cancer development. *Blood*, 116(26), 6106-6113.

Schaller, M. D., Borgman, C. A., Cobb, B. S., Vines, R. R., Reynolds, A. B. & Parsons, J. T. (1992) pp125FAK a structurally distinctive protein-tyrosine kinase associated with focal adhesions. *Proceedings of the National Academy of Sciences*, 89(11), 5192-5196.

Schaller, M. D., Hildebrand, J. D., Shannon, J. D., Fox, J. W., Vines, R. R. & Parsons, J. T. (1994) Autophosphorylation of the focal adhesion kinase, pp125FAK, directs SH2-dependent binding of pp60src. *Molecular and Cellular Biology*, 14(3), 1680-1688.

Schlaepfer, D. D., Hanks, S. K., Hunter, T. & van der Geer, P. (1994) Integrin-mediated signal transduction linked to Ras pathway by GRB2 binding to focal adhesion kinase. *Nature*, 372(6508), 786-91.

Schlaepfer, D. D. & Hunter, T. (1996) Evidence for in vivo phosphorylation of the Grb2 SH2-domain binding site on focal adhesion kinase by Src-family protein-tyrosine kinases. *Molecular and Cellular Biology*, 16(10), 5623-5633.

Schlaepfer, D. D., Mitra, S. K. & Ilic, D. (2004) Control of motile and invasive cell phenotypes by focal adhesion kinase. *Biochim Biophys Acta*, 1692(2-3), 77-102.

Scholz, T., Temmler, U., Krause, S., Heptinstall, S. & Losche, W. (2002) Transfer of tissue factor from platelets to monocytes: role of platelet-derived microvesicles and CD62P. *Thromb Haemost*, 88(6), 1033-8.

Schwartz, M. A., Schaller, M. D. & Ginsberg, M. H. (1995) Integrins: emerging paradigms of signal transduction. *Annu Rev Cell Dev Biol*, 11, 549-99.

Sen, B. & Johnson, F. M. (2011) Regulation of SRC family kinases in human cancers. *J Signal Transduct*, 2011, 865819.

Sendoel, A. & Hengartner, M. O. (2014) Apoptotic cell death under hypoxia. *Physiology (Bethesda)*, 29(3), 168-76.

Servitja, J. M., Marinissen, M. J., Sodhi, A., Bustelo, X. R. & Gutkind, J. S. (2003) Rac1 function is required for Src-induced transformation. Evidence of a role for Tiam1 and Vav2 in Rac activation by Src. *J Biol Chem*, 278(36), 34339-46.

Shai, E. & Varon, D. (2011) Development, cell differentiation, angiogenesis--microparticles and their roles in angiogenesis. *Arterioscler Thromb Vasc Biol*, 31(1), 10-4.

Shen, B., Delaney, M. K. & Du, X. (2012) Inside-out, outside-in, and inside–outside-in: G protein signaling in integrin-mediated cell adhesion, spreading, and retraction. *Current Opinion in Cell Biology*, 24(5), 600-606.

Shibuya, H., Yamaguchi, K., Shirakabe, K., Tonegawa, A., Gotoh, Y., Ueno, N., Irie, K., Nishida, E. & Matsumoto, K. (1996) TAB1: an activator of the TAK1 MAPKKK in TGF-beta signal transduction. *Science*, 272(5265), 1179-82.

Siegbahn, A., Johnell, M., Nordin, A., Aberg, M. & Velling, T. (2008) TF/FVIIa transactivate PDGFRbeta to regulate PDGF-BB-induced chemotaxis in different cell types: involvement of Src and PLC. *Arterioscler Thromb Vasc Biol*, 28(1), 135-41.

Simak, J., Gelderman, M. P., Yu, H., Wright, V. & Baird, A. E. (2006) Circulating endothelial microparticles in acute ischemic stroke: a link to severity, lesion volume and outcome. *J Thromb Haemost*, 4(6), 1296-302.

Singh, A., Sweeney, M. F., Yu, M., Burger, A., Greninger, P., Benes, C., Haber, D. A. & Settleman, J. (2012) TAK1 (MAP3K7) inhibition promotes apoptosis in KRAS-dependent colon cancers. *Cell*, 148(4), 639-650.

Sirvent, A., Benistant, C. & Roche, S. (2012) Oncogenic signaling by tyrosine kinases of the SRC family in advanced colorectal cancer. *Am J Cancer Res*, 2(4), 357-71.

Smith, C. C., Lee, K. S., Li, B., Laing, J. M., Hersl, J., Shvartsbeyn, M. & Aurelian, L. (2012) Restored expression of the atypical heat shock protein H11/HspB8 inhibits the growth of genetically diverse melanoma tumors through activation of novel TAK1-dependent death pathways. *Cell Death & Disease*, 3(8), e371.

Soh, U. J., Dores, M. R., Chen, B. & Trejo, J. (2010) Signal transduction by protease-activated receptors. *Br J Pharmacol*, 160(2), 191-203.

Spicer, E. K., Horton, R., Bloem, L., Bach, R., Williams, K. R., Guha, A., Kraus, J., Lin, T. C., Nemerson, Y. & Konigsberg, W. H. (1987) Isolation of cDNA clones coding for human tissue factor: primary structure of the protein and cDNA. *Proc Natl Acad Sci U S A*, 84(15), 5148-52.

Stankiewicz, A. R., Lachapelle, G., Foo, C. P., Radicioni, S. M. & Mosser, D. D. (2005) Hsp70 inhibits heat-induced apoptosis upstream of mitochondria by preventing Bax translocation. *J Biol Chem*, 280(46), 38729-39.

Steffel, J., Luscher, T. F. & Tanner, F. C. (2006) Tissue factor in cardiovascular diseases: molecular mechanisms and clinical implications. *Circulation*, 113(5), 722-31.

Stepien, E., Stankiewicz, E., Zalewski, J., Godlewski, J., Zmudka, K. & Wybranska, I. (2012) Number of microparticles generated during acute myocardial infarction and stable angina correlates with platelet activation. *Arch Med Res*, 43(1), 31-5.

Stover, D. R., Liebetanz, J. & Lydon, N. B. (1994) Cdc2-mediated modulation of pp60c-src activity. *J Biol Chem*, 269(43), 26885-9.

Su, S., Li, Y., Luo, Y., Sheng, Y., Su, Y., Padia, R. N., Pan, Z. K., Dong, Z. & Huang, S. (2009) Proteinase-activated receptor 2 expression in breast cancer and its role in breast cancer cell migration. *Oncogene*, 28(34), 3047-57.

Suen, J. Y., Cotterell, A., Lohman, R. J., Lim, J., Han, A., Yau, M. K., Liu, L., Cooper, M. A., Vesey, D. A. & Fairlie, D. P. (2014) Pathway-selective antagonism of proteinase activated receptor 2. *Br J Pharmacol*, 171(17), 4112-24.

Susin, S. A., Lorenzo, H. K., Zamzami, N., Marzo, I., Brenner, C., Larochette, N., Prevost, M. C., Alzari, P. M. & Kroemer, G. (1999) Mitochondrial release of caspase-2 and -9 during the apoptotic process. *J Exp Med*, 189(2), 381-94.

Takaesu, G., Kishida, S., Hiyama, A., Yamaguchi, K., Shibuya, H., Irie, K., Ninomiya-Tsuji, J. & Matsumoto, K. (2000) TAB2, a novel adaptor protein,

mediates activation of TAK1 MAPKKK by linking TAK1 to TRAF6 in the IL-1 signal transduction pathway. *Mol Cell*, 5(4), 649-58.

Takizawa, M., Arimori, T., Taniguchi, Y., Kitago, Y., Yamashita, E., Takagi, J. & Sekiguchi, K. (2017) Mechanistic basis for the recognition of laminin-511 by alpha6beta1 integrin. *Sci Adv*, 3(9), e1701497.

Tan, B. S., Kwek, J., Wong, C. K., Saner, N. J., Yap, C., Felquer, F., Morris, M. B., Gardner, D. K., Rathjen, P. D. & Rathjen, J. (2016) Src Family Kinases and p38 Mitogen-Activated Protein Kinases Regulate Pluripotent Cell Differentiation in Culture. *PLoS One*, 11(10), e0163244.

Teramoto, S., Tomita, T., Matsui, H., Ohga, E., Matsuse, T. & Ouchi, Y. (1999) Hydrogen peroxide-induced apoptosis and necrosis in human lung fibroblasts: protective roles of glutathione. *Jpn J Pharmacol*, 79(1), 33-40.

Tesselaar, M. E., Romijn, F. P., Van Der Linden, I. K., Prins, F. A., Bertina, R. M. & Osanto, S. (2007) Microparticle-associated tissue factor activity: a link between cancer and thrombosis? *J Thromb Haemost*, 5(3), 520-7.

Tessitore, L., Tomasi, C. & Greco, M. (1999) Fasting-induced apoptosis in rat liver is blocked by cycloheximide. *Eur J Cell Biol*, 78(8), 573-9.

Thaler, J., Ay, C., Mackman, N., Bertina, R. M., Kaider, A., Marosi, C., Key, N. S., Barcel, D. A., Scheithauer, W., Kornek, G., Zielinski, C. & Pabinger, I. (2012) Microparticle-associated tissue factor activity, venous thromboembolism and mortality in pancreatic, gastric, colorectal and brain cancer patients. *Journal of Thrombosis and Haemostasis*, 10(7), 1363-1370.

Thery, C., Ostrowski, M. & Segura, E. (2009) Membrane vesicles as conveyors of immune responses. *Nat Rev Immunol*, 9(8), 581-93.

Thomas, S. M. & Brugge, J. S. (1997) Cellular functions regulated by Src family kinases. *Annu Rev Cell Dev Biol*, 13, 513-609.

Thomson, B. J. (2001) Viruses and apoptosis. *International Journal of Experimental Pathology*, 82(2), 65-76.

Tohidpour, A., Gorrell, R. J., Roujeinikova, A. & Kwok, T. (2017) The Middle Fragment of Helicobacter pylori CagA Induces Actin Rearrangement and Triggers Its Own Uptake into Gastric Epithelial Cells. *Toxins (Basel)*, 9(8).

Tsujimoto, Y. & Shimizu, S. (2007) Role of the mitochondrial membrane permeability transition in cell death. *Apoptosis*, 12(5), 835-40.

Uguz, A. C., Naziroglu, M., Espino, J., Bejarano, I., Gonzalez, D., Rodriguez, A. B. & Pariente, J. A. (2009) Selenium modulates oxidative stress-induced cell apoptosis in human myeloid HL-60 cells through regulation of calcium release and caspase-3 and -9 activities. *J Membr Biol*, 232(1-3), 15-23.

van den Berg, Y. W., van den Hengel, L. G., Myers, H. R., Ayachi, O., Jordanova, E., Ruf, W., Spek, C. A., Reitsma, P. H., Bogdanov, V. Y. & Versteeg, H. H. (2009) Alternatively spliced tissue factor induces angiogenesis through integrin ligation. *Proc Natl Acad Sci U S A*, 106(46), 19497-502.

Verheij, M. & Bartelink, H. (2000) Radiation-induced apoptosis. *Cell Tissue Res*, 301(1), 133-42.

Verma, R., Venkatareddy, M., Kalinowski, A., Patel, S. R. & Garg, P. (2016) Integrin Ligation Results in Nephrin Tyrosine Phosphorylation In Vitro. *PLoS One*, 11(2), e0148906.

Versteeg, H. H., Hoedemaeker, I., Diks, S. H., Stam, J. C., Spaargaren, M., van Bergen En Henegouwen, P. M., van Deventer, S. J. & Peppelenbosch, M. P. (2000) Factor VIIa/tissue factor-induced signaling via activation of Src-like kinases, phosphatidylinositol 3-kinase, and Rac. *J Biol Chem*, 275(37), 28750-6.

Versteeg, H. H., Schaffner, F., Kerver, M., Petersen, H. H., Ahamed, J., Felding-Habermann, B., Takada, Y., Mueller, B. M. & Ruf, W. (2008) Inhibition of tissue factor signaling suppresses tumor growth. *Blood*, 111(1), 190-199.

Wang, J., Chen, S., Ma, X., Cheng, C., Xiao, X., Chen, J., Liu, S., Zhao, B. & Chen, Y. (2013) Effects of endothelial progenitor cell-derived microvesicles on hypoxia/reoxygenation-induced endothelial dysfunction and apoptosis. *Oxid Med Cell Longev*, 2013, 572729.

Wang, W., Zhou, G., Hu, M. C., Yao, Z. & Tan, T. H. (1997) Activation of the hematopoietic progenitor kinase-1 (HPK1)-dependent, stress-activated c-Jun N-terminal kinase (JNK) pathway by transforming growth factor beta (TGF-beta)-activated kinase (TAK1), a kinase mediator of TGF beta signal transduction. *J Biol Chem*, 272(36), 22771-5.

Wang, X. (2001) The expanding role of mitochondria in apoptosis. *Genes Dev*, 15(22), 2922-33.

Watanabe, T., Tsuda, M., Makino, Y., Ichihara, S., Sawa, H., Minami, A., Mochizuki, N., Nagashima, K. & Tanaka, S. (2006) Adaptor molecule Crk is required for sustained phosphorylation of Grb2-associated binder 1 and hepatocyte growth factor-induced cell motility of human synovial sarcoma cell lines. *Mol Cancer Res*, 4(7), 499-510.

Watanabe, T., Tsuda, M., Tanaka, S., Ohba, Y., Kawaguchi, H., Majima, T., Sawa, H. & Minami, A. (2009) Adaptor protein Crk induces Src-dependent activation of p38 MAPK in regulation of synovial sarcoma cell proliferation. *Mol Cancer Res*, 7(9), 1582-92.

Weinberg, R. A. (2007) *The biology of cancer*, 1 vols. New York: Garland Science.

Weis, S. M., Lim, S. T., Lutu-Fuga, K. M., Barnes, L. A., Chen, X. L., Gothert, J. R., Shen, T. L., Guan, J. L., Schlaepfer, D. D. & Cheresh, D. A. (2008) Compensatory role for Pyk2 during angiogenesis in adult mice lacking endothelial cell FAK. *J Cell Biol*, 181(1), 43-50.

Weng, Z., Taylor, J. A., Turner, C. E., Brugge, J. S. & Seidel-Dugan, C. (1993) Detection of Src homology 3-binding proteins, including paxillin, in normal and v-Src-transformed Balb/c 3T3 cells. *J Biol Chem*, 268(20), 14956-63.

Widlansky, M. E., Gokce, N., Keaney, J. F., Jr. & Vita, J. A. (2003) The clinical implications of endothelial dysfunction. *J Am Coll Cardiol*, 42(7), 1149-60.

Wu, J.-C., Chen, Y.-C., Kuo, C.-T., Wenshin Yu, H., Chen, Y.-Q., Chiou, A. & Kuo, J.-C. (2015) Focal adhesion kinase-dependent focal adhesion recruitment

of SH2 domains directs SRC into focal adhesions to regulate cell adhesion and migration. *Scientific Reports*, 5, 18476.

Wu, N., Ren, D., Li, S., Ma, W., Hu, S., Jin, Y. & Xiao, S. (2018) RCC2 over-expression in tumor cells alters apoptosis and drug sensitivity by regulating Rac1 activation. *BMC Cancer*, 18, 67.

Xiao, Z., Liu, L., Tao, W., Pei, X., Wang, G. & Wang, M. (2018) Clostridium Tyrobutyricum Protect Intestinal Barrier Function from LPS-Induced Apoptosis via P38/JNK Signaling Pathway in IPEC-J2 Cells. *Cell Physiol Biochem*, 46(5), 1779-1792.

Xing, Z., Chen, H. C., Nowlen, J. K., Taylor, S. J., Shalloway, D. & Guan, J. L. (1994) Direct interaction of v-Src with the focal adhesion kinase mediated by the Src SH2 domain. *Mol Biol Cell*, 5(4), 413-21.

Xu, W., Doshi, A., Lei, M., Eck, M. J. & Harrison, S. C. (1999) Crystal structures of c-Src reveal features of its autoinhibitory mechanism. *Mol Cell*, 3(5), 629-38.

Xu, Z., Xu, H., Ploplis, V. A. & Castellino, F. J. (2010) Factor VII deficiency impairs cutaneous wound healing in mice. *Mol Med*, 16(5-6), 167-76.

Yang, L., Ma, Y., Han, W., Li, W., Cui, L., Zhao, X., Tian, Y., Zhou, Z., Wang, W. & Wang, H. (2015) Proteinase-activated receptor 2 promotes cancer cell migration through RNA methylation-mediated repression of miR-125b. *J Biol Chem*, 290(44), 26627-37.

Yasuda, S., Sugiura, H., Tanaka, H., Takigami, S. & Yamagata, K. (2011) p38 MAP kinase inhibitors as potential therapeutic drugs for neural diseases. *Cent Nerv Syst Agents Med Chem*, 11(1), 45-59.

Yau, J. W., Teoh, H. & Verma, S. (2015) Endothelial cell control of thrombosis. *BMC Cardiovascular Disorders*, 15, 130.

Yeatman, T. J. (2004) A renaissance for SRC. *Nature Reviews Cancer*, 4, 470.

Yoon, H., Dehart, J. P., Murphy, J. M. & Lim, S. T. (2015) Understanding the roles of FAK in cancer: inhibitors, genetic models, and new insights. *J Histochem Cytochem*, 63(2), 114-28.

Yu, H., Li, X., Marchetto, G. S., Dy, R., Hunter, D., Calvo, B., Dawson, T. L., Wilm, M., Anderegg, R. J., Graves, L. M. & Earp, H. S. (1996) Activation of a novel calcium-dependent protein-tyrosine kinase. Correlation with c-Jun N-terminal kinase but not mitogen-activated protein kinase activation. *J Biol Chem*, 271(47), 29993-8.

Zhang, J., Fan, G., Zhao, H., Wang, Z., Li, F., Zhang, P., Zhang, J., Wang, X. & Wang, W. (2017a) Targeted inhibition of Focal Adhesion Kinase Attenuates Cardiac Fibrosis and Preserves Heart Function in Adverse Cardiac Remodeling. *Sci Rep*, 7, 43146.

Zhang, X., Li, Q., Zhao, H., Ma, L., Meng, T., Qian, J., Jin, R., Shen, J. & Yu, K. (2017b) Pathological expression of tissue factor confers promising antitumor response to a novel therapeutic antibody SC1 in triple negative breast cancer and pancreatic adenocarcinoma. *Oncotarget*, 8(35), 59086-59102.

Zhang, X., Simerly, C., Hartnett, C., Schatten, G. & Smithgall, T. E. (2014) Src-family tyrosine kinase activities are essential for differentiation of human embryonic stem cells. *Stem Cell Res*, 13(3 Pt A), 379-89.

Zhang, X., Wright, C. V. E. & Hanks, S. K. (1995) Cloning of a Xenopus laevis cDNA encoding focal adhesion kinase (FAK) and expression during early development. *Gene*, 160(2), 219-222.

Zhao, J. H., Reiske, H. & Guan, J. L. (1998) Regulation of the cell cycle by focal adhesion kinase. *J Cell Biol*, 143(7), 1997-2008.

Zhou, B., Zhou, H., Ling, S., Guo, D., Yan, Y., Zhou, F. & Wu, Y. (2011) Activation of PAR2 or/and TLR4 promotes SW620 cell proliferation and migration via phosphorylation of ERK1/2. *Oncol Rep*, 25(2), 503-11.

Ziauddin, J. & Sabatini, D. M. (2001) Microarrays of cells expressing defined cDNAs. *Nature*, 411, 107.

Zioncheck, T. F., Roy, S. & Vehar, G. A. (1992) The cytoplasmic domain of tissue factor is phosphorylated by a protein kinase C-dependent mechanism. *Journal of Biological Chemistry*, 267(6), 3561-3564.

Zou, H., Li, Y., Liu, X. & Wang, X. (1999) An APAF-1.cytochrome c multimeric complex is a functional apoptosome that activates procaspase-9. *J Biol Chem*, 274(17), 11549-56.

Zwicker, J. I., Liebman, H. A., Neuberg, D., Lacroix, R., Bauer, K. A., Furie, B. C. & Furie, B. (2009) Tumor-derived tissue factor-bearing microparticles are associated with venous thromboembolic events in malignancy. *Clin Cancer Res*, 15(22), 6830-40.